Downloaded from orbit.dtu.dk on: May 05, 2023

DTU Library

Potassium Capture by Kaolin and Coal Fly Ash

Wang, Guoliang

Publication date:
2018

Document Version
Publisher's PDF, also known as Version of record

Link back to DTU Orbit

Citation (APA):
Wang, G. (2018). *Potassium Capture by Kaolin and Coal Fly Ash*. Technical University of Denmark.

General rights
Copyright and moral rights for the publications made accessible in the public portal are retained by the authors and/or other copyright owners and it is a condition of accessing publications that users recognise and abide by the legal requirements associated with these rights.

- Users may download and print one copy of any publication from the public portal for the purpose of private study or research.
- You may not further distribute the material or use it for any profit-making activity or commercial gain
- You may freely distribute the URL identifying the publication in the public portal

If you believe that this document breaches copyright please contact us providing details, and we will remove access to the work immediately and investigate your claim.

Potassium Capture by Kaolin and Coal Fly Ash

Guoliang Wang

PhD Thesis

April 2018

DTU Chemical Engineering
Department of Chemical and Biochemical Engineering

Potassium Capture by Kaolin and Coal Fly Ash

Guoliang Wang

PhD thesis

16th April, 2018

Supervisors: Peter Arendt Jensen (DTU Chemical engineering)

Hao Wu (DTU Chemical engineering)

Peter Glarborg (DTU Chemical engineering)

Flemming Jappe Frandsen (DTU Chemical engineering)

Bo Sander (Ørsted Bioenergy & Energy Thermal Power A/S)

DTU Chemical Engineering
Department of Chemical and Biochemical Engineering

Preface and Acknowledgements

This dissertation is written to fulfill the partial requirement of obtaining a Ph.D. degree at Technical University of Denmark (DTU). This Ph.D. work is a part of the project, 'Flexible use of Biomass on PF Fired Power Plants', funded by Energinet.dk, through the ForskEL program, Ørsted and DTU. This work was conducted from October 2014 to April 2018 at the CHEC (Combustion and Harmful Emission Control) research center at the Department of Chemical and Biochemical Engineering, Technical University of Denmark, under the supervision of Senior Researcher Peter Arendt Jensen, Assistant Professor Hao Wu, Professor Peter Glarborg, Associate Professor Flemming Jappe Frandsen, and Lead Process Chemistry Specialist Bo Sander.

A number of people have in various ways contributed to this work and their support is gratefully acknowledged. Firstly, I would like to express my sincere gratitude to my supervisors.

Grateful thanks to Peter Arendt for his continuous support, fruitful discussion and constructive suggestions for my research work though out the whole project.

Sincere thanks to Hao, for a lot practical help for my experimental work as well as very valuable comments and suggestions for all my reports, posters and manuscripts.

Sincere thanks to Peter Glarborg for being always inspiring me and motivating me on research. I benefited greatly from his innovative ideas and suggestion on this project.

I am also grateful to Flemming. His excellent, interesting ash course and Doctoral Thesis provide almost all the knowledge needed for being an ash pro.

Many thanks to Bo for providing helpful knowledge closely related to industry, and for his travelling across half Denmark for every supervisor meeting in the past three years.

I am grateful to the CHEC technicians and the technicians from the workshop, especially Nikolaj, Søren, Jens, and Ivan, for their invaluable and swift support on the monster-size EFR in the pilot hall.

I would like to thank the PhD students from CHEC, especially, Yashasvi, Bozidar-Tianci, Burak, Xueting, Guofeng, Hadi, Lars, Sonia, Nezam, Andrea, Gerard and Victor for bringing so much fun to my life in DTU. Thanks also to all the other people whom I did not mentioned but have contributed to this work directly or indirectly.

Above all, I would like to thank my parents, my sister, my brother for their continued support and understanding over the past three years. Great thanks to my wife Yuan, for not only the three years support but also her taking care of our son by herself and allow me to focus on my work during the busiest time. Thanks to my baby son Yichen, who came to our life during my Ph.D., bringing us a lot of joy, also making home piled with diapers. Thanks also go to my master supervisor Changdong Sheng, who opened the door to research for me eight years ago.

Guoliang Wang

16th April, 2018, Lyngby, Denmark

Summary

Combustion is an important way for bio-energy production. Suspension-firing boilers, also called pulverized fuel combustion boilers (PF-boilers) are increasingly used for production of power and heat from biomass. Combustion of biomass in suspension-fired boilers can produce renewable, CO_2-neutral electricity with a higher electrical efficiency compared with that of grate-fired boilers. However, during the combustion of biomass, significant amount of K-species are released to gas phase in the boiler chamber, as KOH, KCl and K_2SO_4, consequently leading to deposit formation, corrosion as well as de-activation of SCR (Selective Catalytic Reduction) catalysts. One option to tackle these ash-related problems is to use additives to capture gaseous alkali species in flue gas. Kaolin and coal fly ash are two effective Al-Si based additives to capture alkali species. The mechanisms and kinetics of alkali capture by kaolin and coal fly ash have previously been investigated in several studies published in the open literature. However, most of these studies were conducted in fixed bed reactors where kaolin or coal fly ash pellets or flakes were utilized. In suspension fired boilers, kaolin and coal fly ash particles are well dispersed in flue gas, with a total residence time of a few seconds and the controlling mechanisms could be considerably different from that in fixed bed reactors. In this Ph.D. project, the reaction between gaseous potassium species (KOH, K_2CO_3, KCl and K_2SO_4) and different Al-Si based additives (kaolin, mullite and coal fly ash) under well-controlled suspension-fired conditions was investigated by performing experiments in the DTU entrained flow reactor (EFR). The K-capture level of additives C_K (g K/(g additive)) and K-conversion X_K (%) were quantified by analyzing the solid products (C_K is the mass of potassium captured by 1 g of additive; X_K is the percentage of fed potassium captured by additive). The impact of different parameters, such as K-concentration in flue gas (50-1000 ppmv), molar ratio of K/(Al+Si) in reactants (0.048-0.961), reaction temperature (800-1450 °C), gas residence time (0.6-1.9 s), additive particle size as well as the type of coal fly ashes on the K-capture reaction was studied. Corresponding equilibrium calculations were carried out using the equilibrium module of FactSage 7.0, to shed light upon how far the EFR reaction system is from the equilibrium and provide information for understanding the EFR experimental results.

The results of the K-capture experiments using kaolin at 1100 °C or 1300 °C showed that for all the four K-species, KOH, K_2CO_3, KCl and K_2SO_4, the K-capture level (C_K) increased considerably when the K-concentration in the flue gas changed from 50 ppmv to 500 ppmv (molar ratio of K/(Al+Si) in reactants varied from 0.048 to 0.481). However, no obvious

increase of C_K was observed when the K-concentration increased further to 750 ppmv and 1000 ppmv (molar ratio of K/(Al+Si) in reactants was 0.721 and 0.961). This is probably because all kaolin Si has been consumed forming K-aluminosilicates at 500 ppmv.

Results of K-capture experiments using kaolin at different temperatures show that, for KOH, KCl and K_2CO_3, the K-capture level (C_K) and K-conversion (X_K) by kaolin generally followed the equilibrium predictions at 1100 °C and above, when using a kaolin particle size of D_{50} = 5.47 μm and a gas residence time of 1.2 s. This reveals that a nearly full conversion of kaolin to K-aluminosilicates was achieved without kinetic or diffusion limitations under the applied conditions. At 800 °C and 900 °C, the measured conversions were lower than the equilibrium predictions, indicating that the reactions were either kinetically or diffusion controlled. For K_2SO_4, the measured C_K was obviously lower than the equilibrium predictions. Kaliophilite ($KAlSiO_4$) was predicted by the equilibrium calculations; however, the XRD analysis results revealed that leucite ($KAlSi_2O_6$) was actually formed.

Results of KOH capture experiments by kaolin of different particle sizes showed that, fine kaolin powder (D_{50} = 3.51 μm) and normal kaolin powder (D_{50} = 5.47 μm) behaved similarly, while coarse kaolin (D_{50} = 13.48 μm) showed a smaller K-capture level (C_K) at 1100 and 1300 °C. This is probably because KOH diffusion into the kaolin particles became a limiting factor for the coarse kaolin at 1100 °C and above. At 900 °C the difference was smaller, probably because the reaction is more kinetically controlled and the additive particle size did not influence the reaction significantly at 900 °C.

Results of KOH capture by kaolin at different residence times showed that the K-capture reaction reached equilibrium at 1300 and 1450 °C, with a gas residence time of 1.2 s and a kaolin particle size of D_{50} = 5.47 μm. However, at 800 °C, C_K is obviously far away from the equilibrium even with a longer residence time of 1.9 s, showing that the reaction is more kinetically or diffusion controlled. Similar results were observed for KCl capture by kaolin.

Results of K-capture experiments by kaolin using different K-species show that, for KOH and K_2CO_3, leucite ($KAlSi_2O_6$) was formed at low K-concentration of 250 ppmv, while at higher K-concentration (500-1000 ppmv), kaliophilite ($KAlSiO_4$) was detected in the products. But in the experiments with KCl and K_2SO_4, only leucite ($KAlSi_2O_6$) was detected by XRD analysis. Another difference was that the C_K of K_2CO_3 was comparable to that of KOH, while C_K of KCl and K_2SO_4 by kaolin were both relatively lower.

The results of K-capture experiments using coal fly ash showed that the behaviors of the studied four K-species were similar to what was observed when using kaolin. C_K and X_K

increased when K-concentration increased from 50 ppmv to 500 ppmv (molar ratio of K/(Al+Si) in reactants varied from 0.048 to 0.481), and they did not increase further at K-concentration of 750 ppmv and 1000 ppmv (molar ratio of K/(Al+Si) in reactants was 0.721 and 0.961). One difference observed was that at 250 ppmv K and above, the measured C_K and X_K of coal fly ash was lower than the equilibrium predictions. In addition, compared with kaolin, although the types of formed K-aluminosilicates agreed with that of kaolin, coal fly ash captured the K-species less effectively at a K-concentration higher than 250 ppmv (molar ratio of K/(Al+Si) in reactants changed from 0.240 to 0.961).

Results of K-capture experiments by coal fly ash at different temperatures showed that, at 800 °C, the KOH-capture reaction was kinetically controlled. At 900-1300 °C, the reaction was both diffusion and kinetically influenced. At 1450 °C the reaction was equilibrium and diffusion influence. Results of 500 ppmv KOH capture by coal fly ash (with a molar ratio K/(Al+Si) = 0.481 in the reactants) showed that, C_K of coal fly ash generally increased when the temperature increased from 800 °C to 1450 °C, but the C_K of coal fly ash was lower than that of kaolin through the whole temperature range studied. At 50 ppmv KOH (K/(Al+Si) = 0.048) which is comparable to the K-concentration under practical full-scale wood combustion conditions, C_K of the coal fly ash was comparable both to the equilibrium data and to the C_K of kaolin. Results on C_K of KOH-capture by coal fly ash of different particle sizes showed that decreasing the coal fly ash particle size could increase the K-capture level.

Comparison of KOH-capture by kaolin, mullite and coal fly ashes at 500 ppmv KOH showed that kaolin is the most effective additive for alkali capture followed by mullite and coal fly ashes. However, no obvious difference was observed between the three additives at 50 ppmv KOH. In addition, when the reaction temperature was varied from 800 to 1450 °C, C_K of kaolin firstly increased then decreased, reaching peak at 1300 °C. C_K of mullite and coal fly generally increased with increasing temperatures from 800 to 1450 °C.

Dansk Resumé

Suspension-fyrede kedler (også kaldet pulverfyrede kedler) bruges i stigende grad til produktion af kraft og varme fra biomasse. Forbrænding af biomasse producerer vedvarende CO_2-neutral elektricitet med højere elektrisk effektivitet end ristfyrede kedler. Under forbrænding af biomasse frigives signifikante mængder af K forbindelser i from af KOH, KCl og K_2SO_4 til gasfasen i fyrrummet, hvilket fører til askebelægningsdannelse, korrosion såvel som deaktivering af SCR (Selektiv Katalytisk Reduktion) katalysatorer. En mulighed for at takle disse aske-relaterede problemer er at bruge additiver til at reagere de gasformige alkalispecier. Kaolin og kul flyveaske er to effektive Al-Si-baserede additiver til der kan reagere med alkali og binde den i stoffer med et højt smeltepunkt. Mekanismerne og kinetikken af alkaliindfangning med kaolin og kul flyveaske er tidligere blevet undersøgt i og er beskrevet i den åbne litteratur. Imidlertid blev de fleste af disse undersøgelser udført i fixed bed reaktorer, hvor kaolin eller kul flyveaskepiller eller flager blev anvendt. I suspensionsfyrede kedler er kaolin og kulflyveaskepartikler godt dispergeret i røggassen med en samlet opholdstid på få sekunder, og de styrende mekanismer kan derfor være væsentligt anderledes end i fixed bed reaktorer.

I dette Ph.d. projekt blev reaktionen mellem gasformige kaliumspecier (KOH, K_2CO_3, KCl og K_2SO_4) og forskellige Al-Si-baserede additiver (kaolin, mullit og kul flyveaske) eksperimentelt undersøgt under velkontrollerede suspensionsforbrændingsbetingelser i DTU's entrained flowreaktor (EFR). K-indfangningsevne for additiverne C_K (g K/(g additiv)) og K-konverterings graden X_K (%) blev kvantificeret ved analyse af de faste produkter (C_K er massen af kalium bundet af 1 g additiv, X_K er procentdelen af indført kalium indbundet af additivet). Indflydelsen på K-indfangningsreaktionen af forskellige parametre, såsom K-koncentration i røggas (50-1000 ppmv), molforhold K/(Al+Si) af reaktanter (0,048-0,961), reaktionstemperatur (800-1450 °C), gas opholdstid (0,6-1,9 s), additiv partikelstørrelse såvel som typen af kul flyveaske blev undersøgt. Tilsvarende blev ligevægtsberegninger udført under anvendelse af ligevægtsmodulet i FactSage 7.0 for at belyse hvor langt EFR-reaktionssystemet er fra ligevægten og forbedre tolkningen af de udførte EFR-forsøg.

Resultaterne af K-indfangningsforsøgene ved anvendelse af kaolin ved 1100 °C eller 1300 °C viste, at K-indfangningsniveauet (C_K) af alle fire K specier KOH, K_2CO_3, KCI og K_2SO_4 steg betydeligt, når K- koncentrationen i røggassen blev ændret fra 50 ppmv til 500 ppmv, svarende til at molforholdet K/(Al+Si) af reaktanter varierede fra 0,048-0,481. Der blev

imidlertid ikke observeret nogen stigning af C_K, når K-koncentrationen steg yderligere til 750 ppmv og 1000 ppmv (molforhold K/(Al+Si) af reaktanter var 0,721 og 0,961). Dette skyldes sandsynligvis, at al kaolin Si blev brugt til dannelse af K-aluminosilikater ved 500 ppmv K.

Resultaterne af K-indfangningsforsøgene ved anvendelse af kaolin ved forskellige temperaturer viste, at for KOH, KCI og K_2CO_3 fulgte K-indfangningsniveauet (C_K) og K-omdannelsen (X_K) af kaolin generelt ligevægtsberegningerne ved og over 1100 °C, når der anvendes en kaolinpartikelstørrelse på D_{50} = 5,47 µm og en gasopholdstid på 1,2 s. Dette viser, at en næsten fuld omdannelse af kaolin til K-aluminosilikater blev opnået uden kinetiske- eller diffusionsbegrænsninger under de anvendte betingelser. Ved 800 °C og 900 °C var de målte omdannelser lavere end ligevægts forudsigelserne, hvilket indikerede, at reaktionerne enten var kinetisk- eller diffusionskontrolleret. For K_2SO_4 var den målte C_K betydeligt lavere end ligevægtsforudsigelserne. Kaliophilite ($KAlSiO_4$) var det termodynamisk stabile produkt ifølge ligevægtsberegningerne, mens XRD-analysen viste, at leucit ($KAlSi_2O_6$) faktisk blev dannet.

Resultaterne af KOH-indfangningsforsøgene med kaolin med forskellige partikelstørrelser viste, at 'fint' kaolinpulver (D_{50} = 3,51 µm) og 'normalt' kaolinpulver (D_{50} = 5,47 µm) reagerede i samme grad, mens grov kaolin (D_{50} = 13,48 µm) viste et lavere K-indfangningsniveau (C_K) ved 1100 og 1300 °C. Dette skyldes sandsynligvis, at KOH-diffusion i kaolinpartiklerne blev en begrænsende faktor for den 'grove' kaolin ved 1100 °C og derover. Ved 900 °C var forskellen mindre, sandsynligvis fordi reaktionen er mere kinetisk styret ved lavere temperature, hvorfor additivpartikelstørrelsen havde en mindre effekt på reaktionen.

Resultaterne af KOH reaktionen med kaolin ved forskellige opholdstider viste, at K-indfangningsreaktionen nåede ligevægt ved 1300 og 1450 °C med en gasopholdstid på 1,2 s og en kaolinpartikelstørrelse på D_{50} = 5,47 µm. Ved 800 °C var C_K imidlertid langt fra ligevægt selv med en længere opholdstid på 1,9 s, hvilket indikerer, at reaktionen er mere kinetisk eller diffusionskontrolleret. Lignende resultater blev observeret for KCl-indfangning med kaolin.

Resultaterne af K-indfangningsforsøgene med kaolin under anvendelse af forskellige K-specier viste, at for KOH og K_2CO_3 blev leucit ($KAlSi_20_6$) dannet ved lav en K-koncentration på 250 ppmv, mens ved højere K-koncentrationer (500-1000 ppmv) blev kaliumililit ($KAlSiO_4$) detekteret i produkterne. Imidlertid blev udelukkende leucit ($KAlSi_20_6$) observeret ved XRD-analyse i eksperimenterne med KCl og K_2SO_4. En anden forskel var, at

C_K for K_2CO_3 var sammenlignelig med den for KOH, mens C_K for KCI og K_2SO_4 var nogenlunde ens men betydeligt laveren end værdien for K_2CO_3 og KOH.

Resultaterne af K-reaktion med kulflyveaske viste, at de relevante fire K-specier reagerede på samme måde som ved brug af kaolin. C_K og X_K steg, når K-koncentrationen steg fra 50 til 500 ppmv, og de steg ikke yderligere ved K-koncentration på 750 ppmv og 1000 ppmv. En observeret forskel var at ved 250 ppmv K og derover var den målte C_K og X_K for kulflyveaske lavere end ligevægtsforudsigelserne. Desuden viste det sig, at selvom typen af de dannede K-aluminosilikater var ens ved brug af kulflyveaske og kaolin, var K-indfangningen mindre effektiv ved brug af kulflyveaske.

Resultater af K-indfangningsforsøg med kulflyveaske ved forskellige temperaturer viste, at ved 800 °C var reaktionen med KOH kinetisk kontrolleret. Ved 900-1300 °C var reaktionen formentlig både diffusions og kinetisk påvirket. Resultater med 500 ppmv KOH reaktion med kulflyveaske (med et molforhold K/(Al+Si) = 0,481 i reaktanterne) viste, at C_K af kulflyveaske generelt steg, når temperaturen steg fra 800 °C til 1450 °C, men at C_K for kulflyveaske var lavere end for kaolin gennem hele det undersøgte temperaturområde. Ved 50 ppmv KOH (K/(Al+Si) = 0,048), som er sammenlignelig med K-koncentrationen observeret under industriel fuldskala træforbrænding, var C_K af kulflyveasken sammenlignelig både med ligevægtsberegningerne og med C_K for kaolin. C_K resultater af KOH reaktionen med kulflyveaske med forskellige partikelstørrelser viste, at K-indfangningsniveauet steg ved mindske kulflyveaskepartikelstørrelsen.

Sammenligning af KOHs reaktion med kaolin, mullit og kulflyveaske ved 500 ppmv KOH viste, at kaolin er det mest effektive additiv til alkaliindfangning efterfulgt af mullit og kulflyveaske, hvorimod der ikke blev observeret nogen åbenbar forskel ved 50 ppmv KOH. Når reaktionstemperaturen blev varieret fra 800 til 1450 °C, steg C_K af kaolin og nåede et maksimum ved 1300 °C, hvorefter det igen faldt. C_K af mullit og kulflyveaske steg generelt med stigende temperaturer fra 800 til 1450 °C.

Introduction to this Thesis

Biomass suspension-combustion has a higher electrical efficiency and load adaption capability compared to traditional grate-fired technology. However, ash-related problems, including deposition, corrosion and SCR catalysts deactivation, may limit the availability of biomass suspension-fired boilers. Using additives to capture gaseous alkali species and transfer them into less problematic compounds with higher melting points is an attractive solution. Kaolin and coal fly ash are effective Al-Si based additives for alkali capture in biomass combustion. They have been studied both in lab-scale and pilot-scale experiments. In addition, coal fly ash has been utilized in full-scale suspension-fired boilers. However, the influence of local parameters on the reaction between additives and potassium species is still not fully understood.

Project objectives

The objective of this project is to get a deep understand of the reaction mechanisms and the influence of local parameters on the reaction of kaolin and coal fly ash with different potassium salt species. It is wanted to investigate the influence of K-concentration, reaction temperature, the composition and particle size of additives, and the type of K-salts. Basing on the experimental results, guidelines for optimal utilization of additives for K-capture at suspension-fired conditions are provided.

Structure of this thesis

Literature Survey

Chapter 1 of this thesis is a literature study, where the alkali-related problems in biomass combustion boilers, including ash-deposition, corrosion and de-activation of SCR (Selective Catalytic Reduction) catalysts are introduced. Corresponding countermeasures, mainly utilizing additives, to deal with ash-related challenges are summarized. Fundamental knowledges on alkali capture using Al-Si based, S based and P/Ca based additives are provided in the literature survey. The focus is put on Al-Si based additives.

Method Development

The experimental setup - an entrained flow reactor (EFR), the analytical technics as well as the equilibrium calculation methods are introduced in Chapter 2. A liquid feeding system was developed to feed a slurry containing K-salts and solid additives to achieve a high

vaporization of K-salts. The amount of potassium captured by solid additives was quantified based on ICP-OES analysis data. In addition, XRD and SEM analysis was utilized for mineralogical and morphology analysis.

Potassium Capture by Kaolin and Coal Flay Ash

Chapter 3 and 4 deal with K-capture by kaolin and mullite. Chapter 5 and 6 deal with K-capture by coal fly ash. The influences of K-concentration in flue gas, molar K/(Al+Si) ratio in reactants, reaction temperature, additive particle size, type of K-species, type of coal fly ash were investigated by conducting EFR experiments at well-controlled suspension-fired conditions. Corresponding equilibrium calculations were performed and the data obtained were compared with experimental results to understand the reaction.

Recommendations for utilizing additives

Basing on data from open literature and the results from this study, recommendations of using additives in PF-fired boilers to capture K-species is provided in Chapter 7. The influence of additive type, fuel type, temperature, additive particle size as well as dosage methods, were considered.

Peer-reviewed Publications

The results presented in this thesis are based on several scientific articles that have been published or submitted to peer-reviewed journals:

Chapter 3 has been published in peer-reviewed journal **Energy & Fuels** as: Wang G., Jensen P.A., Wu H., Frandsen F.J., Sander B., Glarborg P. Potassium Capture by Kaolin, Part 1: KOH. Energy & Fuels, 32(2): 1851-1862. DOI: 10.1021/acs.energyfuels.7b03645

Chapter 4 has been published in peer-review journal **Energy & Fuels** as: Wang G., Jensen P.A., Wu H., Frandsen F.J., Sander B., Glarborg P. Potassium Capture by Kaolin, Part 2: K_2CO_3, KCl and K_2SO_4. Energy & Fuels, 32(3): 3566-3578. DOI: 10.1021/acs.energyfuels. 7b04055.

Chapter 5 has been submitted to peer-reviewed journal **Fuel** as: Wang G., Jensen P.A., Wu H., Laxminarayan, Y., Frandsen F.J., Sander B., Glarborg P. Potassium Capture by Coal Fly Ash, Part 1: KOH.

Chapter 6 has been submitted to peer-reviewed journal **Fuel** as: Wang G., Jensen P.A., Wu H., Frandsen F.J., Laxminarayan, Y., Sander B., Glarborg P. Potassium Capture by Coal Fly Ash, Part 2: K_2CO_3, KCl and K_2SO_4.

Contents

1 Literature Survey

1.1 Global warming and biomass combustion

Information on the composition of earth's atmosphere can be obtained by analyzing the ancient air bubbles trapped in ice. Related studies show that the CO_2 level in atmosphere had never been higher than 300 ppmv throughout the past 771,000 years, as shown in Figure 1-1.[1, 2] However, in 2013, for the first time in recorded history, the CO_2 concentration in atmosphere surpassed 400 ppm.[1] It was predicted that, if not taking any measures, the atmospheric CO_2 concentration will reach 800 ppm by 2100, resulting a global temperature increase of 4.2 ℃.[3]

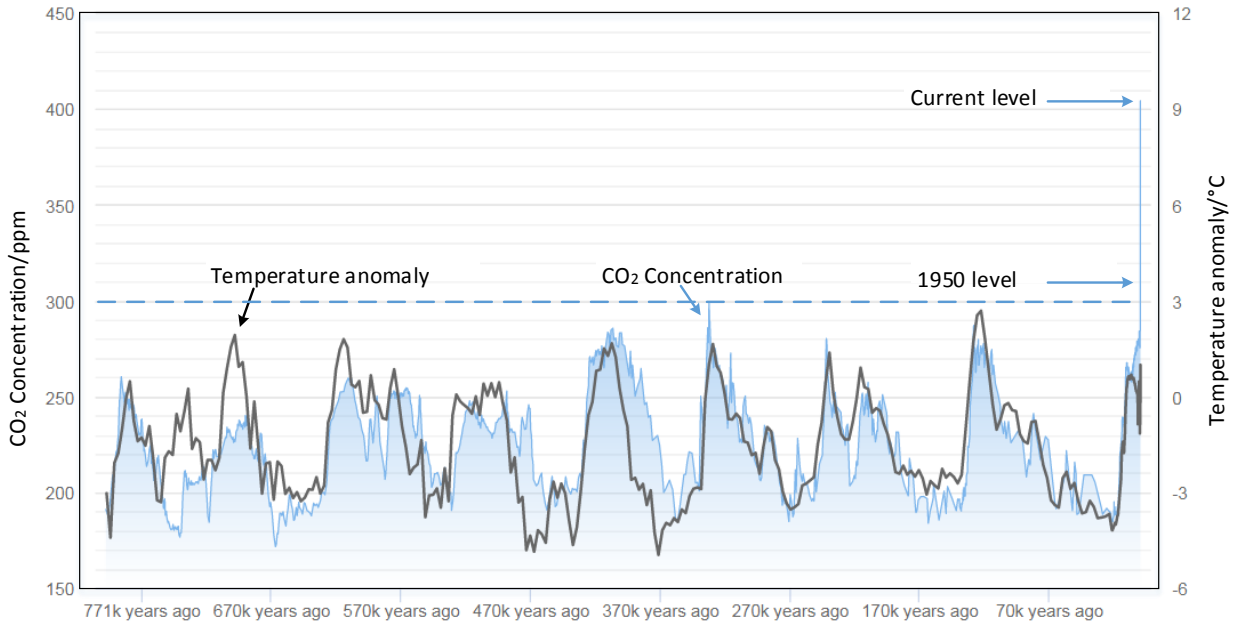

Figure 1-1. CO_2 concentration and temperature anomaly history.[1, 2]

Global warming is strongly linked to the rising concentration of CO_2 and other greenhouse gases in the atmosphere (Figure 1-1).[2, 4] To reduce the CO_2 emission, extensive studies of renewable and green energy sources, including wind energy, solar energy, hydropower, geothermal energy and biomass fuels, for heat or power generation, have been conducted.[5, 6] Among these technologies, biomass combustion is a renewable, high-efficient, CO_2-neutral option, with extra benefit of urban and rural waste disposal. Biomass combustion could be, in a short time scale, utilized widely in existing coal-fired boilers.[4, 5, 7, 8] Combustion is one important way for utilizing bio-energy.[9] Various combustion technologies have been employed for biomass firing, including grate-combustion, fluidized bed combustion and suspension combustion.[9, 10] Grate-firing is the traditional way to burn biomass, while fluidized bed is increasingly used, due to its wide fuel range and flexibility.[4, 11] Suspension firing is also increasingly used for biomass combustion because of its higher efficiency load adaption, and that existing coal fired power plants can be converted to biomass-firing.[12-14]

1.2 Ash related problems in biomass combustion

Different from coal, in which most of the ash forming elements are present in the form of minerals,[9, 15] alkali elements, like K, in biomass exist as salts or associated with organic matrix.

Biomass alkali elements can easily vaporize during combustion, forming gaseous reactive species rich in K, Cl and S, as shown in Figure 1-2.[16-26] When cooling down, aerosols are formed and they may deposit on heat-exchange surfaces, especially super heater and re-heater coils, resulting in fast-growing deposit and accelerated corrosion.[6, 18, 21-23] To avoid excessive corrosion, some biomass-fired plants have to run with a low final steam temperature which resulted in a decrease of electrical efficiency of up to 32-35 %.[4, 27, 28] Efficiency and availability of biomass-fired boilers are significantly decreased due to these ash-related problems. In severe cases, boilers are forced to shut down and costly manual removing of these deposits is required. The alkali species also contribute to the accelerated deactivation of SCR (Selective Catalytic Reduction) catalyst in biomass-fired boilers.[29-31] Details on aerosol formation, deposition and corrosion are discussed in the following sections.

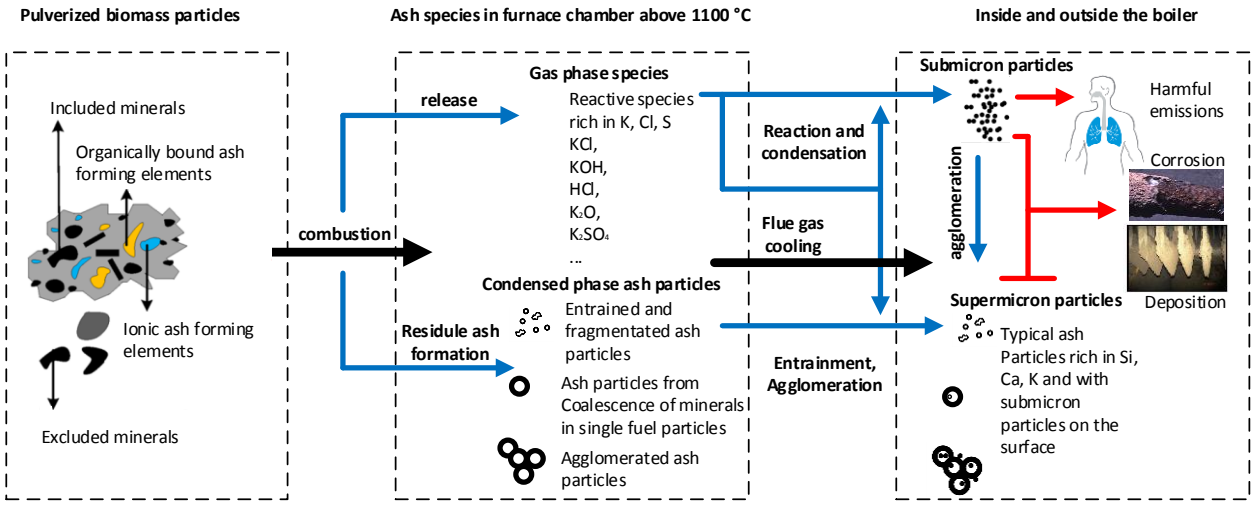

Figure 1-2. Major transformation routes and processes of ash-forming elements during biomass suspension firing.[24]

1.2.1 Aerosol formation and emission

During cooling of the flue gas, chemical reaction and condensation of the volatile inorganic species can take place. If the cooling becomes too fast, or if there is not enough surface available for heterogeneous condensation to occur, there will be an excess of gas molecules, starting to form clusters (i.e. small groups of associated molecules).[4] If these clusters pass a critical size, homogeneous nucleation starts in the flue gas, forming a significant number of small nuclei. These nuclei collide at a high rate, resulting in the formation of aerosols. The mass load of aerosols in flue gas from biomass combustion can be as high as 800-2000 mg/Nm^3.[4] Theses aerosols may pose a threat to the environment and health of human, if they are not appropriately handled. Inorganic aerosols can also induce other challenges in biomass-fired boilers such accelerated deposition, corrosion and deactivation of SCR catalysts as discussed in the following sections.

1.2.2 Ash deposition

The K rich aerosols formed from biomass combustion may cohere on the heat-transfer surfaces and form a sticky layer, which increases the trapping efficiency of impacted large ash particles.[4, 32, 33] In addition, K-species can also coat other refractory ash particles through diffusion, adsorption, thermophoresis, condensation and reactions with inherent SiO_2 in ash particles forming K-silicate with low melting points.[34, 35] A rapid build-up of troublesome deposits on fireside heat-transfer surfaces especially on the super heaters and re-heaters is observed consequently.[11, 36-47]

The deposits on the heat transfer surfaces, especially on super heater surfaces in the convective pass, can hinder the heat transfer to the steam and hence reduce the overall process efficiency.[11, 21, 48-50] In severe cases, it may result in unscheduled shutdown and costly manual cleanup.[47, 50, 51]

1.2.3 Corrosion

Normally, metal alloys utilized in boilers gradually oxidize and form a protective oxide layer on heat transfer surfaces. However, in biomass-fired plants, condensed NaCl or KCl in deposits can react with alloy metals (Cr and Fe) or its oxides forming volatile chlorides, which is continuously released to gas phase. Consequently, the protective oxide scales are destroyed and this resulted in an accelerated corrosion of alloys.[21, 41] A full-scale measuring campaign showed that when the metal temperature is above 520 °C, severe corrosion took place when firing Cl-rich fuels, like straw and waste.[21, 41] To alleviate the ash-related corrosion, the final steam temperature of some biomass-fired boilers has to be kept below 450 °C,[41] which significantly limits the electrical efficiency.[4, 52, 53] If severe corrosion happens in boilers, the plants may have to be shut down and the tubes need to be replaced at high costs.[2, 79, 80]

1.2.4 Deactivation of SCR catalysts

SCR (Selective Catalytic Reduction) is an effective method for reducing NO_x from stationary sources. Commercial SCR catalysts consist of TiO_2 as support, and V_2O_5-WO_3 as the active catalytic component.[54] In the SCR plant, ammonia is injected into the flue gas containing NO_x. When the mixture passes over the SCR catalysts at 300-400 °C, ammonia reduces NO_x to N_2.[30, 55, 56] In Denmark and Sweden, the SCR process is used in power plants burning biomass.[29] However, the experiences from those boilers show that an accelerated deterioration of the SCR catalyst is observed, when they are exposed to flue gas loaded with high concentration of alkali species. The deactivation of the SCR catalysts is because of physical deposition, as well as chemical poisoning caused by K-species, like KCl and K_2SO_4.[31, 45, 57, 58]

1.2.5 Countermeasures for ash-related problems in biomass combustion

To minimize the operational problems caused by ash in biomass combustion, different treatments and processing technologies have been developed, including use of additives,[59] co-combustion,[47, 60] pretreatment of biomass, like washing or ulterior drying,[42, 61, 62] utilization of effective deposit removal techniques,[63] and using anti-corrosion alloys or

coating for super-heater or re-heater tubes.[64-66] Using additives to capture volatile alkali species seems to be an attractive and practical option to minimize the ash-related problems in biomass combustion. At present, various additives have been studied in lab and in full-scale experiments.[4, 14, 49, 67-69]

1.3 Fundamentals of alkali capture by additives

The concept of capturing alkali compounds by additives was developed from scavenging alkali containing hot flue gas from combined-cycle power generation system incorporated with pressurized fluidized-bed combustion (PFBC).[70, 71] Gaseous alkali species in hot flue gases (about 800-900 °C) should be removed to avoid fouling and corrosion of the blades of gas turbines.[69] In 1980s, several US companies and institutes, including Argonne National Laboratory (ANL),[71] General Electric Company (GE),[72] Westinghouse R&D center[73] and University of Arizona[74, 75] carried out a series of research in this area. The tested alkali-capture additives during this period were mainly Al-Si based, including bauxite,[71, 72, 76, 77] kaolinite[76, 78, 79], dolomite,[72] emathlite,[76] diatomaceous earth,[77] silica, [77] silica gel,[71, 77] attapulgus clay,[80] and coal ash[81]. The capturing capability, the mechanisms, the feasibility as well as the preliminary cost were discussed in these works.[71] In all these studies, Na removal received greater emphasis than K because the focus was on coal combustion. In the last two decades, K-capture by additives attracted more attentions due to the increasing utilization of biomass for power and heat production worldwide, and various additives have been studied in literature.

1.3.1 Categorization and mechanisms of additives

According to the main effective elements that are present in the additives, alkali capture additives can be divided into: Al-Si based, S based and P/Ca based additives.[51, 59, 60, 67, 68, 82-87] According to the mechanisms of dealing with ash-related problems, additives can be categorized as reactive additives and non-reactive additives. Reactive additives are additives that can chemically react with volatile alkali species (such as KCl and KOH) forming compounds with higher melting points, like, kaolin, coal fly ash and sulfates.[21, 68, 88] Non-reactive additives address alkali-related problems mainly though physical adsorption or dilution effect, like bauxite and ophite.[66, 80] The mechanisms involved for different alkali capture additives are summarized as below.

- Physical adsorption

Some Al-based additives, like bauxite can capture K-species at low temperature, typically below 800 °C. In cases where regeneration of additives is required, physical adsorption additives could be an option.

- Chemical reaction

The characteristics of alkali capture through chemical reaction are high alkali capturing capability, irreversibility, as well as chemical selectivity. Generally, most Al-Si-based and S-based additives function through chemical reaction. When the release of captured alkali should be avoided, such as in the case where the K concentration fluctuate, an irreversible chemical fixation additive should be applied.

- Diluting effect

Injecting refractory additives can dilute the concentration of volatile elements in deposit, consequently reducing the stickiness of deposit. One example is ophite with the formula of $((Ca,Na)_{2.25}(Mg,Fe,Al)_{5.15}(Si,Al)_8O_{22}(OH)_2)$. It does not react with alkali species, however, it can mitigate biomass ash sintering significantly through the dilution effect.[66]

1.3.2 Additives dosage methods

Alkali-capturing additives can be utilized in different ways, depending on the combustion technology (grate-firing, suspension-firing or fluidized bed combustion), physical and chemical properties of additives, and, the reaction conditions (temperature, gas atmosphere, residence time, gas-solid contact pattern). The different utilization methods of additives are summarized below:

(1) In-situ removal: injecting additives directly into the combustion zone or higher up in freeboard of the furnace, to capture alkali species, as soon as they are released.[4] This method has been utilized in the multi-fuels firing CHP (combined heat and power) plant at Avedøre Power Station Unit 2 (AVV2) in Denmark, owned by Ørsted Bioenergy & Thermal Power A/S.[12, 14] Additives used in this way can either be a powdery material (e.g. coal fly ash)[12, 14] or a solution (e.g. ammonium sulfate).[89]
(2) To premix the additives and fuels, before feeding into combustors. Additives can be introduced into the combustion system by pelletizing biomass fuel with additives together, or by mixing additive with fuel, when fuel is transported to the feeding point by a conveyor. Additives and fuels can be well mixed by this method.[90]
(3) To pass the alkali-containing flue gas through a fixed bed of alkali sorbent. This method can be applied in combined cycle power generation from coal or biomass.[78]

1.4 Commonly studied alkali-capture additives

1.4.1 Al Si-based additives

Al-Si based additives have been proven to be very effective in capturing gaseous alkali species in hot flue gas.[59, 76, 91-95] The principle of Al-Si based additives is that volatile K-species react with additives forming K-aluminosilicates, such as leucite ($KAlSi_2O_6$) and kalsilite ($KAlSiO_4$), with higher melting points, as shown in Figure 1-3.

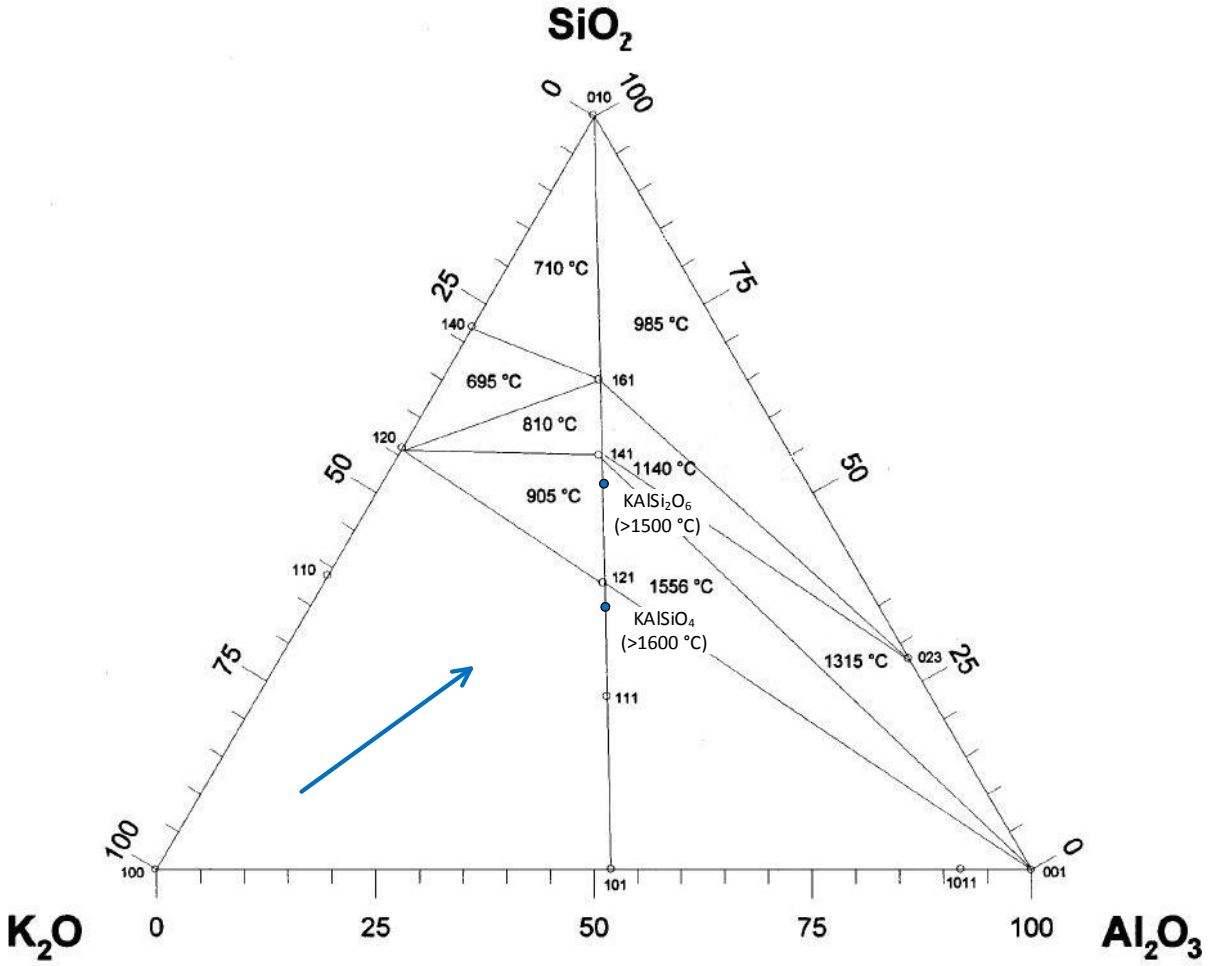

Figure 1-3. K_2O-SiO_2-Al_2O_3 ternary diagram with solidus temperatures.[68, 88]

The K-capture capacity of additives is sensitive to its elemental composition, especially the content of Al and Si. Additives which are only high in either Al or Si, like alumina or silica,[71, 72] are usually less efficient in alkali capturing. Additives with high contents of both Al and Si, are able to capture alkali species more effectively.[93, 96, 97] Commonly studied Al-Si based additives include kaolin,[59, 67, 98] coal ash[12, 93] bauxite,[76] emathlite,[76] bentonite,[51, 59] clay,[51] and

diatomaceous earth. Among these additives, kaolin and coal ash are the most commonly studied. Kaolin has been identified as one of the most effective additives for gas phase alkali metal capture at high temperature,[75, 76] while coal fly ash is the one of the most economical, and effective additives.[12, 93]

1.4.1.1 Kaolin

Kaolin refers to a kind of clay mineral.[99] Its main mineral phase is kaolinite ($Al_2Si_2O_5(OH)_4$), also written as $Al_2O_3{\cdot}2SiO_2{\cdot}2H_2O$. When kaolinite is heated above 450 °C, the hydroxyl bonds are released, and the Al-Si-O lattice is rearranged,[97, 98] forming activated kaolin (metakaolin), as shown in reaction R 1.1. The porosity of metakaolin was observed to increase slightly comparing to parent kaolin.[93, 97] When the temperature is increased to about 980 °C, further reactions and structural changes take place and alumina-silica spinel is formed, as shown in reaction R 1.2. At temperature higher than 1100 °C and sufficient residence time, the formed alumina-silica spinel undergoes an exothermic process and progressively transforms into mullite and amorphous SiO_2, as shown in reaction R 1.3.[93, 97, 100]. Metakaolin is reactive towards alkali species, while mullite is relatively less reactive.[93, 97]

$$Al_2Si_2O_5(OH)_4\ (kaolin) \xrightarrow{450\ ^\circ C} Al_2O_3 \cdot 2SiO_2\ (metakaolin) + 2H_2O\ (g) \qquad \text{(R 1.1)}$$

$$Al_2O_3 \cdot 2SiO_2(metakaolin) \xrightarrow{980\ ^\circ C} Al_2O_3 \cdot SiO_2\ (spinel) + SiO_2(amorphous) \qquad \text{(R 1.2)}$$

$$3\ (Al_2O_3 \cdot SiO_2)\ (spinel) + 3\ SiO_2(amorphous) \xrightarrow{1100\ ^\circ C} 3Al_2O_3 \cdot 2SiO_2\ (mullite) + 4\ SiO_2(amorphous) \qquad \text{(R 1.3)}$$

$$Al_2O_3 \cdot 2SiO_2(metakaolin) + 2KCl + H_2O \rightarrow 2KAlSiO_4(kalsilite/kaliophilite) + 2HCl\ (g) \qquad \text{(R 1.4)}$$

$$Al_2O_3 \cdot 2SiO_2(metakaolin) + 2SiO_2 + 2KCl + H_2O \rightarrow 2KAlSi_2O_6(leucite) + 2HCl\ (g) \qquad \text{(R 1.5)}$$

$$Al_2O_3 \cdot 2SiO_2(metakaolin) + 4SiO_2 + 2KCl + H_2O \rightarrow 2KAlSi_3O_8(sanidine) + 2HCl\ (g) \qquad \text{(R 1.6)}$$

The reaction of Na-capture by kaolin has been studied for its application on removing Na vapor from hot flue gases in Combined Cycle Gas Turbine (CCGT) power plants[76, 79, 101] and for addressing ash-related problems in combustion of Na-rich low rank coals in power plant boilers.[75, 96, 102, 103] Kaolin can capture gaseous Na irreversibly with a maximum of 0.266 g

Na/g kaolin.[74, 104] Kaolin/metakaolin can react with NaCl forming Na-aluminosilicates with Cl being released as HCl. Nephelite ($Na_2Al_2Si_2O_8$),[76, 78, 97] and carnegiete ($Na_2Al_2Si_2O_8$)[76] have been reported to be formed from NaCl-kaolin reactions.

However, when it comes to biomass combustion, K-capture reaction is of greater concern, but it has been studied to a less extent.[98] KCl reacts with kaolin in a similar way as NaCl, as shown in Reactions R 1.4, R 1.5 and R 1.6. Various K-aluminosilicates formed from KCl-kaolin reactions have been reported, such as kalsilite ($KAlSiO_4$), kaliophilite ($KAlSiO_4$), leucite ($KAlSi_2O_6$), sanidine ($KAlSi_3O_8$),[21, 69, 95] microcline ($KAlSi_3O_8$)[105] and muscovite ($KAl_3Si_3O_{10}(OH)_2$).[59]

Due to the complex phase transformation of kaolin at high temperature, the reaction temperature poses an impact on its K-capture level. The K-capture level of kaolin at different temperatures calculated from open literatures[93, 106] are compared in Figure 1-4. The heating mixture data in Figure 1-4 (*), is from a study by Wang,[107] where KCl and kaolin was mixed and heated at 900 and 1000 °C with different residence time of 1 h and 12 h. The K-capture level of kaolin decreased with the reaction temperature. The kaolin pellet results(**) are from a fixed bed study,[93] in which kaolin pellets (diameter of 1.6 mm) were utilized for capturing KCl. The residence time was 1 hour and the KCl concentration was 1000 ppm. A wider temperature range from 900 to 1500 °C was covered. The results reveal that at temperatures below 1300 °C, the K-capture level of kaolin generally decreased. However, at above 1300 °C, it increased with temperature.

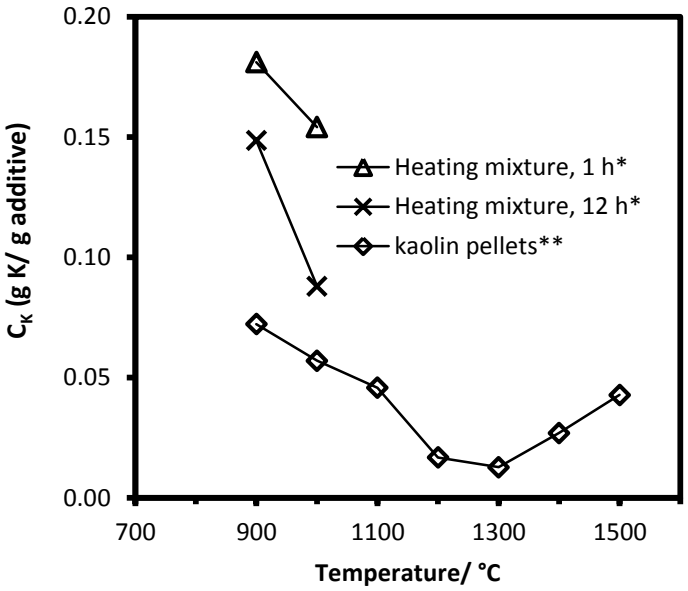

Figure 1-4. K-capture level of kaolin calculated from literatures (*heating KCl and kaolin mixture[107], ** K-capture in fixed bed reactor using kaolin pellets[93]).

Shadman and co-workers carried out a series of studies on sodium and potassium capture by kaolin, aiming at understanding the mechanism and the kinetics of alkali-capture reactions.[74, 76, 78, 79, 108-111] In their work, a thermogravimetric reactor was designed, in which flue gas containing alkali (100-260 ppmv) was passed through kaolin flakes (~0.5 mm thick) at 800 °C and the weight change of kaolin flakes was recorded by a microbalance. The results showed that kaolin can effectively capture gaseous KCl or NaCl from flue gas. The mechanisms depended on the atmospheres. In 100 % nitrogen,[74] NaCl was observed to be captured through physical adsorption, while in simulated flue gas (15 % CO_2, 3 % O_2, 80 % N_2 and 2 % H_2O), NaCl was captured through chemical reaction.[74] Nephelite and carnegieite with the same chemical formula $NaAl_2Si_2O_8$ were detected in the reacted products. The sodium capture reaction was diffusion-influenced at the studied conditions (800 °C, and residence time of 40 hours). A saturation limit of 26.6 % of weight increase of kaolin flakes was observed. Based on the experimental data, a model incorporated both physisorption and chemical reaction was developed.

Tran and co-workers studied the K-capture reaction by kaolin using a fixed bed reactor equipped with a surface ionization detector.[98, 112, 113] Gaseous alkali species (0-1.2 ppm) are generated from KCl, KOH or K_2SO_4, and consequently go through a fixed bed where the kaolin pellets (0.5 - 2.0 mm) was hold, at 750-950 °C. Part of the alkali species are captured by kaolin, while the rest unreacted part was measured by the ionization detector.[98, 112, 113] A series of experiments on alkali capture by kaolin are conducted in this setup. The influence

of atmosphere (oxidizing or reducing), presence of water, temperature, as well as the competition between alkali and heavy metal was studied. It was found that the reducing conditions and the presence of water promoted the K-capture by kaolin and the coexistence of potassium and cadmium promoted the capture of both metals by kaolin. Moreover, it was observed that kaolin captured KCl slightly more efficiently than KOH, and much more effectively than K_2SO_4 under the studied conditions (850 °C and residence time of several hours).[98, 112, 113]

Zheng et al.[93] studied the kinetics of gaseous KCl capture by kaolin pellets (diameter of 1.6 mm) in a fixed bed reactor. The influence of reaction temperature (900-1500 °C), residence time, oxygen and water content, as well as KCl concentration (0-1600 ppm) in flue gas was investigated. The results showed that the KCl-kaolin reaction was dominated by chemical reaction and it was independent from oxygen concentration. However the presence of water could promote the KCl capture reaction. Results at different KCl concentrations showed that the KCl capture capacity of kaolin pellet increased almost linearly with the KCl concentration (900 °C, 0.5 h). In addition, the reaction temperature posed a significant impact on the K-capture reaction at the studied conditions (diameter of kaolin pellets of 1.6 mm, residence time of 1 hour). The potassium capture level of kaolin firstly decreased when temperature increased from 900 to 1300 °C, and then it increased when the temperature increased further to 1500 °C. This is because the reaction was internal-diffusion controlled. The sintering of kaolin pellets was responsible for the decreasing of K-capture level at 900-1300 °C. At 1300-1500 °C, kaolin melted and the liquid diffusion elevated the K-capture level at 1300-1500 °C.

All the studies mentioned above were conducted in fixed bed reactors. The only quantitative study on alkali capture by kaolin under suspension fired conditions, was carried out by Wendt et al.[75, 97] Sodium capture by dispersed kaolin particles was investigated in a down-flow reactor. Sodium hydroxide was utilized to produce sodium vapor. Cl_2 and SO_2 were doped into the reactor to study their influence. The results show that kaolin could capture sodium effectively under suspension-fired conditions, through a chemical reaction between NaOH and metakaolin. 900–1100 °C was the optimum kaolin injection temperature window for obtaining the best sodium capture results. In addition, it was found that the Na-capture reaction was kinetically controlled when using kaolin particles smaller than 3.0 μm. For kaolin particles larger than 3.0 μm, interphase diffusion became the controlling mechanism. Experiments with doping Cl_2 and SO_2 show that the presence of SO_2 and Cl_2 inhibited the Na-capture reaction by kaolin.[75, 97]

Kaolin has also been tested in large CFB boilers (35 MW) as additives to deal with alkali-related problems.[53] With addition of kaolin, the amount of water soluble K and Cl in fly ash was significantly decreased, and bed agglomeration temperature was increased.[53] However, the disadvantage of kaolin is its high cost.[68, 83]

1.4.1.2 Coal ash

The mineralogical composition of coal fly ash is quite complex. The dominant mineral phases include quartz (SiO_2), mullite ($3Al_2O_3{\cdot}2SiO_2$), illite, siderite, etc.[114-118] Reaction between alkali species with coal ash was observed when co-firing biomass and coal.[119-121] The mechanism of capturing alkali species using coal ash is similar as that of kaolin. The aluminosilicate species in coal ash, like mullite, can react with gaseous K or Na, forming alkali-aluminosilicates. Utilizing coal fly ash as additives in biomass combustion process can potentially minimize the ash-related operational problems at a fairly low price. Available results show that the chemical composition of coal ash has a noticeable impact on its alkali capture ability.[93] Generally, bituminous coal fly ash which is rich in oxides of Al, Si shows an effective alkali capture ability, whereas the alkali capture capacity of Ca-Mg rich coal ash generated from low rank coal (lignite) is significantly low.[93]

Coal fly ash has been commercially utilized in full-scale biomass suspension-fired boilers in Denmark.[12, 14] A full-scale boiler measuring campaign conducted by DTU-CHEC investigated the influence of coal fly ash addition on the deposition behaviors, deposit composition[12] and the formation of aerosols.[14] The amount of aerosols formed was greatly suppressed, with the composition of the aerosols changed from K-S-Cl rich to Ca-P-Si rich, when adding coal fly ash.[14] The influence on ash deposition during wood suspension-firing is summarized in Figure 1-5.[12] The amount of K_2SO_4 in inner layer deposit at high temperature flue gas (1300 °C) was significantly reduced, and $KCl/KOH/K_2CO_3$ completely disappeared when adding coal fly ash. The large outer deposit also transferred from K-Ca-Si rich to Si-Al rich, resulting in an easier removal of deposits. In deposits formed at low temperature flue gas (800 °C), KCl disappeared, and the content KOH and K_2CO_3 was significantly decreased. The corrosion risk of the deposit decreased considerably because of the changes of the deposit composition.

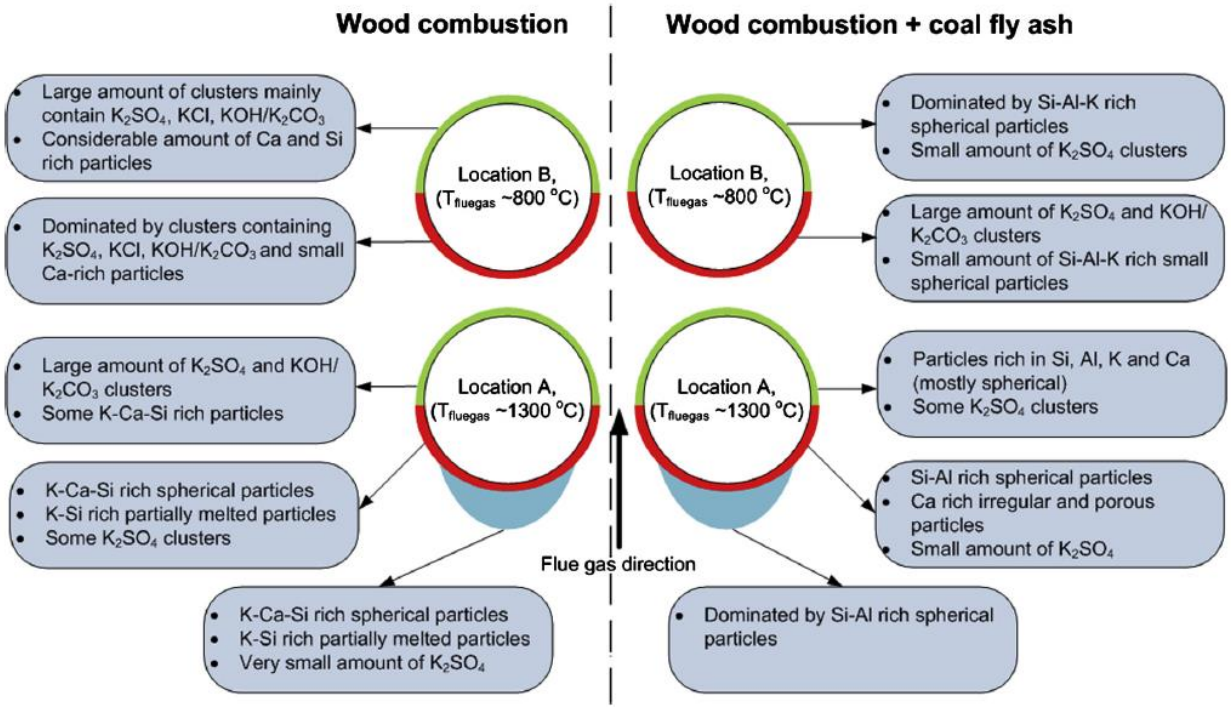

Figure 1-5. Summary of the influences of coal fly ash addition on deposit properties during full-scale pulverized wood combustion.[12]

Lab-scale experiments in a fixed bed reactor have been carried out to study the reaction between coal ash pellets and gaseous KCl.[93, 122] The results suggested that bituminous coal ash rich in Al and Si can capture KCl effectively, while Ca-Mg rich lignite coal ash captured KCl much less effectively. The results also showed that the KCl capture reaction by coal ash pellets was diffusion controlled at studied conditions (900-1500 °C, diameter of coal ash pellets of 1.5 mm, residence time of 1 hour).[93]

In another fixed bed reactor study, Liu et al. investigated the KCl capture reaction utilizing bituminous coal fly ashes (70-100 μm) which were paved in a stainless wires holder.[122] The impact of reaction temperature, KCl-concentration and the reaction atmosphere was investigated. The results indicated that 900 °C was the optimal K-capture temperature for the investigated bituminous coal fly ash. They also observed that a reducing atmosphere and the presence of water vapor promoted the K-capture capability of coal fly ash.[122]

1.4.1.3 Other Al-Si based additives

Apart from kaolin and coal fly ash, various other Al-Si based additives, such as bauxite (Al_2O_3), emathlite (mixture of Al_2SiO_5 and SiO_2) and diatomaceous earth (92% SiO_2 + 5% Al_2O_3), silica gel (SiO_2), silica (SiO_2), and alumina (Al_2O_3) have been tested and studied in open literatures.[59, 67, 73, 93, 98]

Bauxite is an effective alkali-capture additive. Lee[71, 80] studied the alkali (including NaCl, KCl) capture behavior of bauxite in a fixed bed reactor. It was found that physical adsorption was the dominant mechanism for alkali capture by bauxite.[71, 72, 80] However the study by Punjak et al.[76, 78] showed that the adsorption of NaCl by bauxite at 800 °C is a combination of physical sorption and chemical reaction. Nephelite and carnegiete are the products from the part of chemical reaction. For the physical adsorption part, both Na and Cl were observed to be retained in reacted bauxite.[76, 78]

Emathlite can capture NaCl vapor effectively.[73, 109] The alkali capture mechanism of emathlite is through irreversible chemical reaction.[82] Experimental results show, that at 800 °C, crystalline albite ($Na_2O{\cdot}Al_2O_3{\cdot}6SiO_2$) is formed. While at 1000 °C, a glassy Na-containing phase was formed. Comparing to nephelite (melting point 1560 °C) and carnegiete form Na-capture reaction by kaolin and bauxite, the melting point of albite from emathlite capture is obviously lower (1000 °C). Therefore, emathlite is more suitable for lower temperature system, such as in the downstream of combustors or gasifiers.[123] The apparent activation energy for emathlite was found to be very low, indicating that alkali capture by emathlite was not significantly affected by changes of temperature.[73, 76]

Diatomaceous earth is another alkali capture clay mineral mainly composed of silica and alumina co-existing to different extent. It is found that at 800 °C, diatomaceous earth could capture alkali species through chemical reaction. Water-insoluble alkali-silicates was detected in reacted products.[71]

1.4.2 S-based additives

The principle of S based additives is to convert KCl or KOH to K_2SO_4. The global reactions could be described by reaction R 1.7 and R 1.8. Alkali sulfates are less volatile than chlorides and hydroxides,[94] and are less sticky and less problematic with respect to ash deposition and corrosion.[89] Moreover, Cl-induced high temperature corrosion can be mitigated by S-based additives, because the most aggressive element, Cl, is released as HCl (g) through sulfation reaction.

$$2KCl\ (g,l,s) + SO_2 + 0.5\ O_2 + H_2O \rightarrow K_2SO_4(g,l,s) + 2HCl\ (g) \qquad \text{(R 1.7)}$$

$$2KCl\ (g,l,s) + SO_3 + H_2O \rightarrow K_2SO_4(g,l,s) + 2HCl\ (g) \qquad \text{(R 1.8)}$$

For the sulfation reaction, usually SO_3 is favored because it reacted with KOH and KCl significantly faster than SO_2.[124-127] Therefore additives that can produce SO_3, like ammonium

sulfate,[51, 89] ferric sulfate,[82, 128, 129] and aluminum sulfate[128] are usually more effective than SO_2 based additives (elemental sulfur[83, 84] and SO_2[83, 129-132]).

1.4.2.1 Elemental sulfur

The sulfation effect of elemental sulfur has been tested both in pilot-scale reactors and full-scale boilers.[51, 83, 84, 129, 130] In a grate-fired boiler study, Aho studied the sulfation effect of elemental sulfur by mixing fuel (wood chips and corn stover) with sulfur of different dosages and fed into the boiler.[129] To achieve a satisfied result of preventing Cl deposition, a dosage of elemental sulfur of S/Cl (molar) = 3 was required. However, the sulfur addition led to a significant increase of SO_2 emission (2000 mg/Nm^3 with 6% O_2) and need for expensive SO_2 removal from the flue gas.

1.4.2.2 SO_2

Study on the sulfation of KCl or KOH by SO_2 showed that both homogeneous and heterogeneous reactions took place. Iisa studied the KCl sulfation reaction by SO_2 in gas phase and molten phase using an entrained flow reactor (EFR) at 900-1100 °C.[130] A significant faster sulfation reaction was observed in gas phase (100 % conversion at studied conditions). However, in the molten phase only a 0.5-2 % conversion was observed. The study also revealed that in gas phase, the sulfation reaction was limited by the availability of SO_3, while in molten phase the sulfation reaction was diffusion limited.[130]

Sippula et al. studied the impact of the addition of SO_2 on the transformation of alkali metals during wood combustion in an laminar flow reactor.[131] The fine particle number concentration in flue gas was significantly decreased due to the sulfation of KCl by SO_2.

In a laboratory study carried out by Sengeløv,[133] the sulfation of particulate KCl by SO_2 was studied in the temperature range 400-750 °C, by monitoring the formation of HCl and analyzing the solid residual.[133] The results confirmed the reaction proceeds according to a shrinking core model. A rate expression for the sulfation reaction was derived which revealed that only KCl particles smaller than 1 μm is sulfated significantly at the short gas residence times which is typical in suspension combustion systems.

A model of gaseous sulfation of alkali hydroxide and alkali chloride was developed by Glarborg.[125] Detailed reaction mechanisms for the sulfation of alkali metal were proposed. The sulfation reaction was initiated by oxidation of SO_2 to SO_3. Subsequently, SO_3 recombines with alkali hydroxide or alkali chloride to form alkali hydrogen sulfate or alkali oxysulfur chloride, which were finally converted into K_2SO_4.

1.4.2.3 Sulfates

Sulfates are effective additives to convert KCl into less harmful K_2SO_4. The commonly studied sulfates include aluminum sulfate, ferric sulfate and ammonium sulfate.[83, 84, 134] The principle for sulfate additives is that they decompose at high temperature forming SO_3 which subsequently reacts with KCl as shown in Reaction R 1.8.[83, 135]

The yields of SO_3 from the decomposition of sulfates played a key role in the KCl-sulfation reaction. The decomposition behavior of ferric sulfate, aluminum sulfate and ammonium sulfate, as well as the SO_3 yields were studied by Wu et al. using a tube reactor and a faster heating rate TGA.[124, 128] A yield of 85 % SO_3 accompanied by 15 % SO_2 was observed for aluminum sulfate decomposition at 700-900 °C. For ferric sulfate, approximately a yield of 40 % SO_3 was observed at 600-1000 °C. The yield of SO_3 from ammonium sulfate decomposition decreased almost linearly with increasing temperature in the temperature range 600-900 °C. A detailed chemical kinetic model was also developed in his work.[124, 128]

The different sulfates were also tested in pilot and full-scale boilers. Ammonium sulfate addition was tested in a CFB boiler firing a mixture of straw and wood pellets.[136] With the injection of ammonium sulfate, the concentration of gaseous KCl in flue gas was significantly decreased and almost no chlorine was found in the deposit.[136] Vattenfall AB developed a patent named ChlorOut,[89] in which ammonium sulfate injection together with a in-situ chloride monitor was utilized to sulfate KCl as well as monitoring the results online.[89] This concept was tested in a 96 MW_{th} CFB boiler firing bark and Cl-containing waste. The KCl concentration in flue gas was reduced to as low as 2 ppm. Corrosion risk relate to Cl has been significantly reduced and almost a full sulfation of KCl aerosols was achieved.[89]

Sulfation effect of ferric sulfate was tested by spraying its solution into the upper furnace and mixing ferric sulfate with fuels in a grated-fired boiler. It was revealed that the sulfation results were not only depended on the dosage but also the way of feeding. In the case of spraying the ferric sulfate solution, with a dosage of S/Cl = 0.4–0.6, it was observed that the Cl-deposit and corrosion of super heaters was significantly prevented.[129] However, in the case of mixing ferric sulfate with fuels, the sulfation effect was much less effective even with a higher ferric sulfate dosage. One reason is the decomposition of sulfates at high temperature was different for the two different feeding methods.

1.4.3 P/Ca based additives

When firing P rich biofuels, like, grain, bran, and rapeseed cake, K and P originated from fuels is released to gas phase, generating K-phosphate (such as K_3PO_4, KPO_3 and $K_5P_3O_{10}$; see Figure 1-6) with low melting temperature.[86, 137-139] Severe deposition and corrosion was observed in boilers firing P rich biofuels. However, if Ca is present, ternary phosphates of K_2O-CaO-P_2O_5 with melting temperature higher than 1000 °C would be formed, as shown in Figure 1-6.[137, 140, 141] Basing on this, a strategy of using additives with Ca or P has been developed to capture alkali species and thereby mitigate ash-related problems. Additives, like $Ca(OH)_2$,[137] $CaCO_3$,[137] phosphoric acid,[68, 138, 140, 142] Ca-sludge[104] and ammonium phosphate[143] have been studied in open literatures.

$Ca(OH)_2$ and $CaCO_3$ were investigated in experimental study by Wu.[137] Ca-based additives could be used to reduce the release of P and to some extent increase the release of K during grate-firing of bran. The K/P ratio in flue gas was increased by adding Ca-based additives. This effect is observed to be more pronounced in the full-scale grate-fired power plants, where a 5-8 wt. % $CaCO_3$ was added in his study.[137]

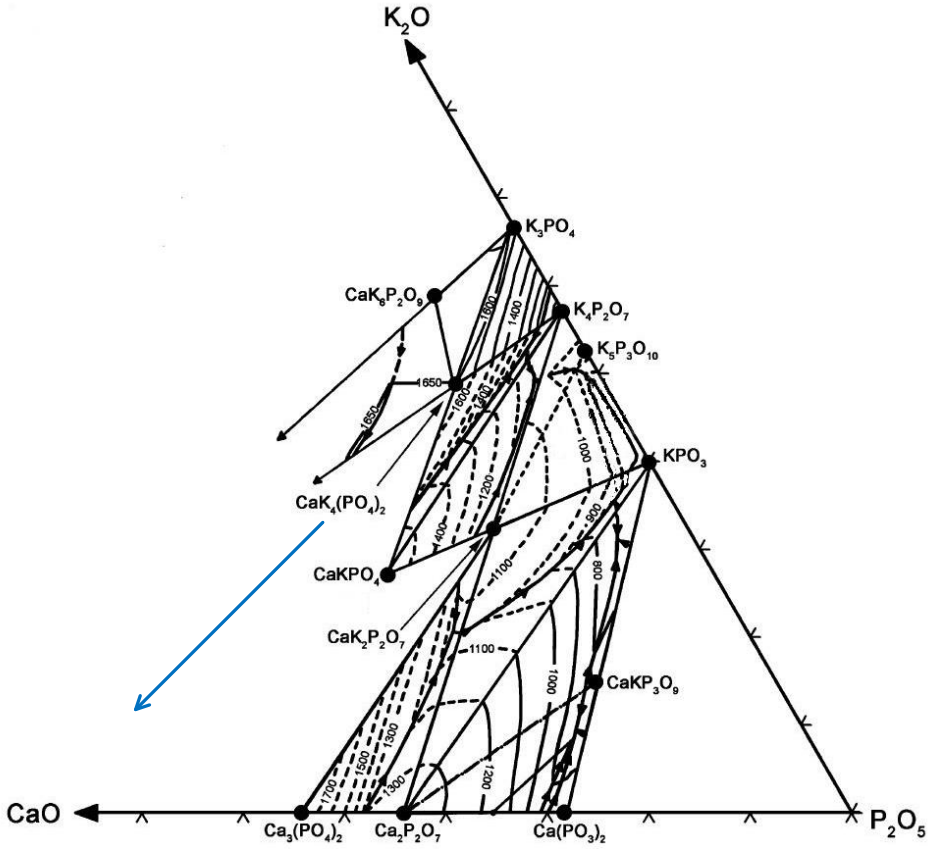

Figure 1-6. K_2O-P_2O_5-CaO ternary diagram showing the influence of P/Ca based additives on ash melting behavior.[68, 137, 141]

Results from another experimental studies[140] conducted in an industrial-scale DTF (drop tube furnace) showed that, by adding optimized dosage of P based additives and Ca based additives, alkali-related fouling could be significantly decreased by converting low-melting temperature alkali oxide, hydroxide or chloride into K/Na-Ca/Mg-phosphate with high melting points.[138-140, 144] However, to achieve a satisfactory result, an optimal P-Ca ratio as well as the feeding method should be well designed.

1.5 Conclusions

The mechanisms of alkali capture by additives to address ash-related problems in biomass combustion are reviewed in this chapter. The commonly studied additives can be divided into: Al-Si base, S based, P/Ca based groups according to the active elements. Kaolin and coal fly ash are the two most effective Al-Si additives. Coal fly ash is the only additive that has been commercially utilized in full-scale suspension fired boilers. S based additives including elemental sulfur, SO_2 and sulfates can alleviate the alkali related problems

through sulfation reaction. P/Ca based additives can significantly reduce deposition and corrosion by forming ternary K-Ca-P phosphates.

Most of the studies available in open literature on K-capture using additives were conducted in fixed bed reactors. However, the reaction conditions in fixed bed reactors are significantly different from that in suspension-fired boilers. The controlling mechanisms at suspension-fired boilers could be significantly different. The influence of local conditions, like reaction temperature, additive particle size, K-concentration on the reaction is still not available. To obtain an optimal result of K-capture using additives, detailed knowledge about the K-capture reaction with additives is still required.

2 Method Development

2.1 Materials

Four different potassium species, including KOH, K_2CO_3, KCl and K_2SO_4, were studied in this work. Kaolin of three different particle sizes, mullite and two coal fly ashes were utilized as the K-capture additives. The characteristics of the solid additives are listed in Table 2-1.

The three kaolin powders are named according to the particle size as normal kaolin (D_{50} = 5.47 μm), fine kaolin (D_{50} = 3.51 μm), and coarse kaolin (D_{50} = 13.48 μm). The normal kaolin was purchased from VWR Chemicals, and the fine kaolin was generated by grinding the normal kaolin in a ball mill. The coarse kaolin was obtained by grinding kaolin stones purchased from Ward's Science. Mullite powder was generated by heat treatment of the normal kaolin (D_{50} = 5.47 μm) at 1100 °C for 24 h.[100] The calcinated mullite sample was re-grinded, to break the agglomerated blocks, and to get a sample with D_{50} = 5.90 μm, which is similar to that of the normal kaolin powder (D_{50} = 5.47 μm).

The two coal fly ashes were from unit 2 of Asnæsværket Power Plant (ASV2), and Amager Power Plant (AMV) in Denmark. They are named as ASV2CFA and AMVCFA, respectively. The coal fly ashes were sieved to 0-32 μm, and 32-45 μm and named as ASV2CFA0-32, ASV2CFA32-45 and AMVCFA0-32 respectively. The median diameter D_{50} of ASV2CFA0-32 was 10.20 μm, and D_{50} of ASV2CFA32-45 was 33.70 μm. In addition, the ASV2CFA0-32 was grinded in a ball mill to get a finer coal ash sample with D_{50} of 6.03 μm, which was comparable with the normal kaolin and mullite powder. The grinded ASV2 coal fly ash was termed as ASV2CFAGR.

The additives were analyzed by ICP-OES (Inductively Coupled Plasma Atomic Emission Spectroscopy) for elemental composition, with results shown in Table 2-1. The elemental composition of kaolin and the two coal fly ashes was different, but they are all rich in Al and Si. The molar (Na+K)/(Si+Al) ratio of the three kaolin samples and three ASV2 coal fly ashes

was around 0.02. For AMVCFA0-32 the molar ratio was slightly higher as 0.07. The molar ratio of (Na+K)/(Al+Si) for all additives were relatively low, indicating that there was a large content of Al and Si available for the K-capture reaction. Generally, the Si content of kaolin and coal fly ash was similar; the Al content of coal fly ash was obviously lower than that of kaolin.

Table 2-1. Characteristics of solid additives (kaolin, mullite and coal fly ash).

	Kaolin and mullite				**Coal fly ash**			
Name	Fine kaolin	Normal kaolin	Coarse kaolin	Mullite	ASV2CF AGR	ASV2CFA 0-32	ASV2CFA 32-45	AMVCFA 0-32
D_{50} (μm)	3.51	5.47	13.48	5.90	6.03	10.20	33.70	8.42
BET surface area (m^2/g)	13.02	12.70	11.83	5.30	9.07	8.04	3.41	3.18
O (wt. %, dry)	56.9	56.9	55.88	56.9	46.60	46.60	45.06	49.92
S (wt. %, dry)	0.02	0.02	0.03	0.02	0.26	0.26	0.21	0.23
Si (wt. %, dry)	22.0	22.0	23.0	24.8	22.00	22.00	21.00	25.00
Al (wt. %, dry)	19.0	19.0	19.0	21.4	14.00	14.00	13.00	11.00
Fe (wt. %, dry)	0.47	0.47	0.46	0.53	2.90	2.90	3.0	4.30
Ca (wt. %, dry)	0.10	0.10	0.10	0.11	4.50	4.50	5.20	4.10
Mg (wt. %, dry)	0.14	0.14	0.12	0.16	0.97	0.97	0.88	1.40
Na (wt. %, dry)	0.10	0.10	0.10	0.10	0.27	0.27	0.20	0.92
K (wt. %, dry)	1.10	1.10	1.20	1.20	0.87	0.87	0.67	2.10
Ti (wt. %, dry)	0.02	0.02	0.01	0.02	0.88	0.88	0.74	0.53
P (wt. %, dry)	0.05	0.05	0.05	0.06	0.64	0.64	0.57	0.30
deformation temperature (°C)	—	—	—	—	1280	1280	—	1200
hemisphere temperature (°C)	—	—	—	—	1390	1390	—	1290
flow temperature (°C)	—	—	—	—	1440	1440	—	1380

One difference between the two types of coal fly ashes was the alkali metal content. The concentration of (K+Na) of AMVCFA is about 3.0 %, while it was slightly lower as 1.1 % for ASV2 coal fly ashes. Another difference is that the Si/Al molar ratio of ASV2CFA0-32 was around 1.5, while the ratio for AMVCFA0-32 was obviously higher as 2.2. Si usually stays in the form of mullite or quartz, or amorphous species in coal ash. Relatively higher Si content or lower Al usually implicates a possible lower content of mullite and thereby a lower K-

capture capability, since mullite is considered the crucial mineral phase in coal ash for K-capture reaction forming K-aluminosilicate.[12, 93, 98]

Generally, alkali elements, like Na and K stay in the form of alkali-aluminosilicates in coal ash. A higher contents of alkali elements in coal ash can usually weak the availability of Al and Si. For the alkaline earth metal elements, the content of Ca of AMV coal fly ash was slightly lower than that of ASV2 coal fly ashes, while Mg is slightly higher. Ca is primarily present in coal fly ash as lime, anhydrite or calcite,[145, 146] and it can also exist together with Mg as Ca-Mg-silicate.[147, 148] Therefore, Ca and Mg may affect the availability of Al and Si to a lower extent. In summary, the lower content of Al and relatively higher content of K and Na are believed to weaken the K-capture ability of AMV coal fly ash. Aside from Al and Si, S is another protective element in coal fly ash, which can react with KCl and transfer it into less corrosive sulfate. The concentration of S in all the four ash samples was very low, at around 0.25 %, and may not play a key role in the K-capture reaction in this study.

The solid additives were also analyzed with XRD. The results showed that kaolinite ($Al_2Si_2O_5(OH)_4$) and quartz (SiO_2) are the main mineral phases in the three kaolin samples. In the mullite sample, mullite ($3Al_2O_3{\cdot}2SiO_2$) and quartz (SiO_2) are detected as the main mineral phases. No kaolinite was detected in the mullite sample, indicating a complete transformation from kaolinite to mullite during heat treatment. XRD analysis of coal fly ash showed that, for all coal fly ash samples, mullite ($3Al_2O_3{\cdot}2SiO_2$) and quartz (SiO_2) are the main crystalline phases, while no crystalline species containing alkali or alkaline earth metal elements was detected in kaolin or coal fly ash samples, implying that the small amount of Na, K, Ca and Mg detected by ICP-OES may stay in the form of amorphous species, or the concentration is too low to be detected.

2.2 Setup

Experiments were conducted in the DTU Entrained Flow Reactor (EFR), as shown in Figure 2-1, which can simulate the conditions in suspension-fired boilers. The EFR consists of a gas supply system, a liquid/slurry feeding system, a gas preheater, a vertical reactor tube, a bottom chamber and a particle and flue gas extraction system. The vertical reactor tube is 2 m long, and the inner diameter is 79 mm. The reactor is electrically heated by 7 heating elements, and can be heated up to 1450 °C. A 0.8 m long preheater is placed above the reactor tube for preheating the secondary gas. The EFR was surrounded with a shell which can capture gas that leaked from the reactor.

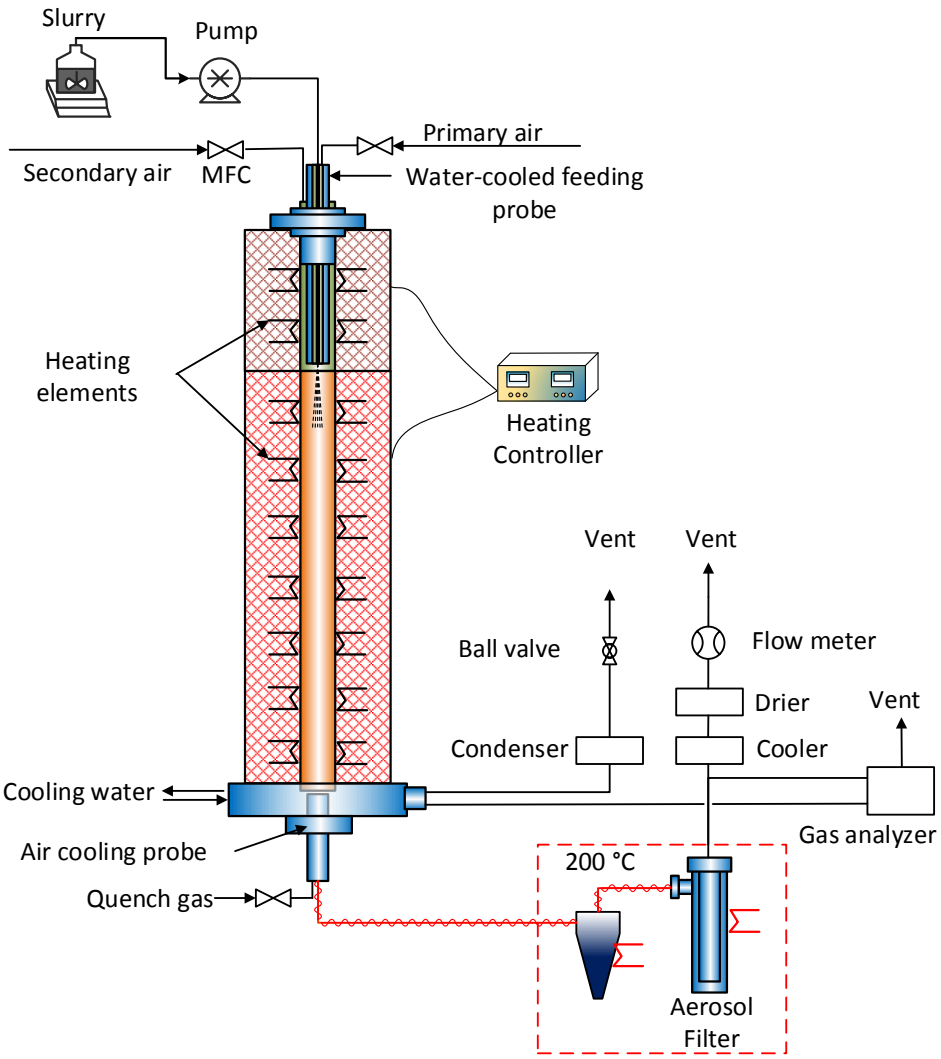

Figure 2-1. Schematic of the Entrained Flow Reactor (EFR).

To obtain a high vaporization degree of K-species and a good contact of K-salt vapor with additives, a slurry containing K-species and solid additives (kaolin, mullite or coal fly ash) was fed into the EFR, instead of feeding solid K-species and solid additives into the reactor directly.[74, 75] The slurry was fed into the reactor, using a peristaltic pump through a water-cooled feeding probe, as shown in Figure 2-2. During each experiment, the slurry was stirred with a magnetic stirrer to keep it homogeneous. A steady feeding could be obtained with this slurry feeding system. Detailed information on developing the liquid feeding system can be found in Appendix A.

The slurry also contained ethanol, which combusted in the reactor producing CO_2. Therefore, the feeding rate can be indirectly monitored by measuring the CO_2 concentration in the flue gas. Slurry fed into the reactor was atomized, at the outlet of the water-cooled feeding probe by a 30 Nl/min primary air flow. The atomized slurry droplets were mixed

with the preheated secondary air and subsequently evaporated. K-species transferred into gas phase and reacted with solid additives in the reactor tube. At the outlet of the reactor tube, the flue gas and the entrained solid samples entered into a water-cooled bottom chamber, where the flue gas was divided into two fractions, with around 50 % going to the sampling probe and subsequently to the solid sampling line, while the remaining 50 % vent to the ventilation, directly. The sampling probe is about 1.5 m long and is air-cooled, keeping the flue gas temperature at around 300 °C. A 10 Nl/min quench gas was introduced at the inlet of the sampling probe, for quenching the flue gas and the reaction. The quenching gas also helped to prevent the deposition of solid samples on the inner wall of the sampling tube. The entrained large solid particles and aerosols were captured, respectively, by a cyclone (with a cut-off diameter of 2.3 μm) and a metal filter (with a pore size of 0.8 μm) in the sampling line. The cyclone and filter were both heated to 200 °C, to avoid condensation of water vapor. Each experiment lasted about 60 min, and the solid samples were collected for further analysis.

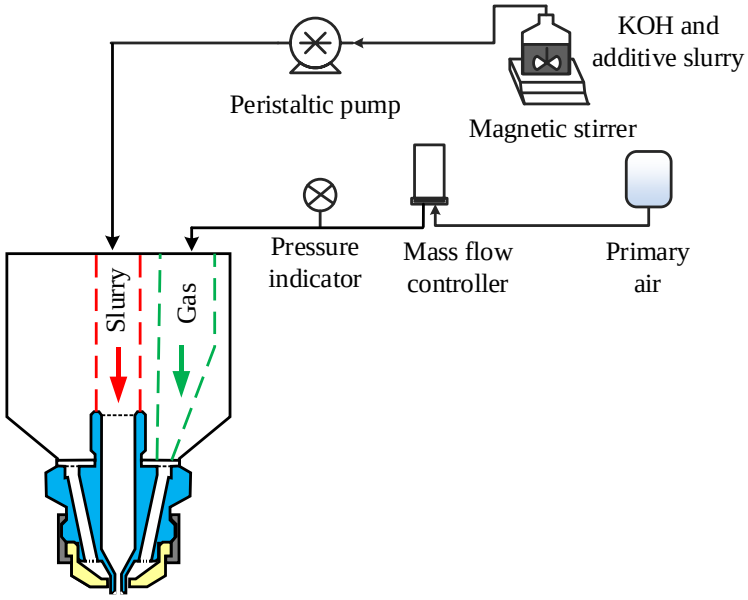

Figure 2-2. Slurry feeding and atomizing system of the DTU Entrained Flow Reactor (EFR).

In order to avoid unexpected air leakage into the EFR, the reactor was operated at a pressure slightly higher (approximately 1.0-3.0 mbar) than the atmospheric pressure, and the possible gas escaping from the reactor was captured by a shell around the reactor and pumped to ventilation.

2.3 Analytical methods

To quantify the amount of potassium captured by additives, the reacted solid samples were analyzed with ICP-OES (Inductively Coupled Plasma Atomic Emission Spectroscopy). The concentration of major elements (Al, Ca, Fe, Mg, P, S, K, Si, Na and Ti) was determined according to the Danish Standard of DS/EN 15290 (Solid Biofuels- Determination of Major Elements). The standard DS/EN ISO 16995 (Solid Biofuels- Determination of water soluble Chloride, Sodium and Potassium) was used to determine the concentration of water-soluble K and Cl. The concentration of total potassium and water-soluble potassium of product samples were both analyzed.

Two parameters were defined for quantifying the amount of potassium captured by additives: the K-conversion (X_K), and the K-capture level (C_K). X_K is defined as the percentage (%) of input K-salt (KOH, KCl, K_2CO_3 and K_2SO_4) chemically captured by solid additives (kaolin/mullite/coal fly ash) forming water-insoluble K-aluminosilicate. C_K is the mass of potassium captured by 1 g of additive (g K/(g additive)).

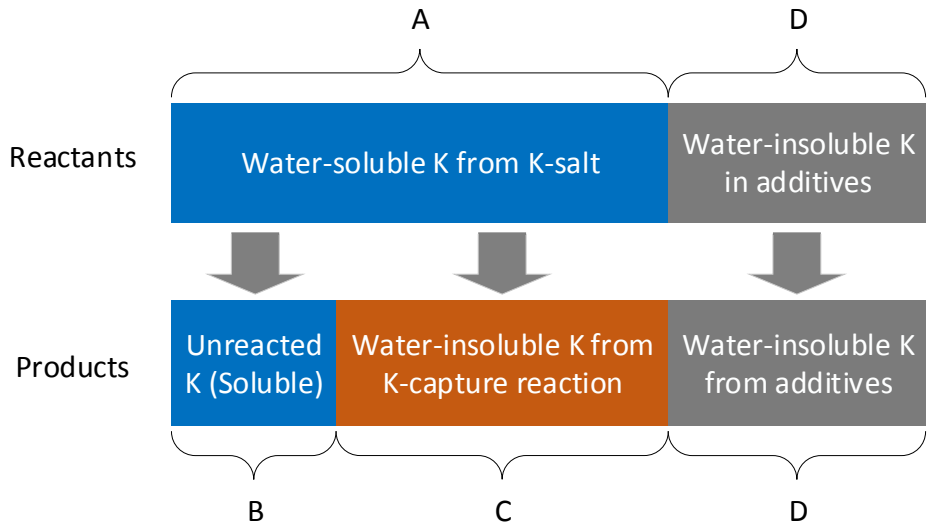

Figure 2-3. Potassium transformations in the K-capture reaction.

As shown in Figure 2-3, potassium in the reactants originated both from the K-salts (KOH, K_2CO_3, KCl and K_2SO_4) and the additives (kaolin, mullite and coal fly ash). The majority of potassium in the reactants was from K-salts, which was water-soluble (part A). The remaining potassium was from additives and it was water-insoluble (part D). During the K-capture reaction, a part of the water-soluble K reacted with additives forming water-insoluble K-aluminosilicate (part C in the products) while the unreacted K-salts remained

water-soluble (part B). The K-conversion (X_K), and K-capture level (C_K) were calculated based on the ICP-OES analysis results of reacted samples as shown in Equation 2.1 and 2.2. Detailed information on calculation method is available in Appendix B.

$$X_K = \frac{C}{A} \times 100\ \% \tag{2.1}$$

$$C_K = \frac{n_{K-salt} M_K X_K}{m_{ad.}} \tag{2.2}$$

In Equation 2.1, C is the amount of water-insoluble potassium formed by the K-capture reaction, and A is the amount of potassium from K-salts fed into the reactor, as shown in Figure 2-3. n_{Ksalt} (mol) is the molar amount of K-salt fed into the reactor, M_K is the molar mass of K (39 g/mol) and $m_{ad.}$ is the mass of solid additives fed into the reactor (g).

To characterize the mineralogical composition of the reacted solid products, the collected samples were washed with deionized water at room temperature for 24 hours to remove the water-soluble compounds (i.e. the K-salts in the reactant), and then filtered using a 0.4 μm membrane. Subsequently, the water-washed solid samples were subjected to X-ray diffractometry (XRD) analysis. The XRD spectra were determined with a Huber diffractometer with characteristic Cu Kα radiation and operation conditions of 40 kV and 40 mA. The wave length was 1.54056 Å. The identification of the main crystalline phase was performed with the JADE 6.0 software package (MDI Livermore, CA) and the diffraction database of PDF2-2004.

2.4 Equilibrium Calculations

To understand the transformation of K-salts without additives at high temperature, global equilibrium calculations at the same conditions as the K-salt vaporization experiments were conducted. To make a comparison of the experimental K-conversion (X_K) and K-capture level (C_K) relative to equilibrium, global equilibrium calculations were carried out at corresponding conditions. The calculations were performed using the Equilibrium module of the software FactSage 7.0. The databases of FactPS, FToxid, FTsalt and FTpulp were employed for the calculations. Information about the different databases can be found in literatures.[149, 150] Detailed information on the equilibrium calculation can be found in Appendix C.

3 Potassium Capture by Kaolin, Part 1: KOH

Abstract: The reaction of gaseous KOH with kaolin and mullite powder at suspension-fired conditions was studied by entrained flow reactor (EFR) experiments. A water based slurry containing kaolin/mullite and KOH was fed into the reactor and the reacted solid samples were analyzed to quantify the K-capture level. The effect of reaction temperature, K-concentration in the flue gas, the molar ratio of K/(Al+Si) in reactants, gas residence time, and kaolin particle size on K-capture reaction was systematically investigated. Corresponding equilibrium calculations were conducted with FactSage 7.0. The experimental results showed that kaolin reached almost full conversion to K-aluminosilicates at suspension-fired conditions at 1100-1450 °C for a residence time of 1.2 s and a particle size of D_{50} = 5.47 μm. The amount of potassium captured by kaolin generally followed the equilibrium at temperatures above 1100 °C, but lower conversion was observed at 800 °C and 900 °C. Crystalline kaliophilite ($KAlSiO_4$) was formed at higher temperatures (1300 °C and 1450 °C), whereas, amorphous K-aluminosilicate was formed at lower temperatures. Coarse kaolin (D_{50} = 13.48 μm) captured KOH less effectively than normal (D_{50} = 5.47 μm) and fine (D_{50} = 3.51 μm) kaolin powder at 1100 °C and 1300 °C. The difference was less significant at 900 °C. Mullite generated from kaolin captured KOH less effectively than kaolin at temperatures below 1100 °C. However, at 1300 °C and 1450 °C, the amount of potassium captured by mullite became comparable to that of kaolin.

3.1 Introduction

Suspension-fired boilers (also called pulverized fuel combustion boilers) are increasingly used for production of power and heat from biomass.[7, 67] Combustion of biomass in suspension-fired boilers can produce renewable, CO_2-neutral electricity with a higher electrical efficiency compared with grate-fired boilers.[4] However, during the combustion process of biomass, significant amounts of K-species, such as KOH, KCl and K_2SO_4, are released to gas phase in the boiler chamber, and this leads to deposit formation, corrosion[19,

[34, 39, 151-156] as well as de-activation of SCR (Selective Catalytic Reduction) catalysts.[29, 30, 54, 55, 57, 157] Ash deposition and corrosion problems may be mitigated by reducing the steam temperature in super heater and re-heater tubes. However, this will cause a reduced electrical efficiency of power plants.[4, 11, 16, 18, 27]

To minimize the ash related problems in biomass combustion, different treatments and processing technologies have been developed, including use of alkali scavenging additives,[14, 83, 85, 86, 96, 136, 140, 158] co-combustion with other biofuels or fossil fuels,[119, 120, 159-161] utilizing effective deposit removal techniques,[63] and a combination of different thermo-chemical processes.[65, 66] Among these, using additives is a promising option, primarily due to its high effectiveness and low requirements for boilers.

The basic principle of additive addition is that the additives are injected to boilers to react with the problematic gaseous K-salts (such as KOH and KCl), forming K-species (such as K-aluminosilicates, or K-sulfates) with low corrosivity and high melting temperatures.[12, 14, 59, 67, 82, 85, 87, 107, 128, 140, 158, 162, 163] Biomass firing additives can generally be categorized into Al-Si based, S-based, and P/Ca-based, according to the major elements present in the additives.[67-69, 82, 106, 129]

Kaolin[60, 90, 93, 98, 164] and coal fly ash[93] are typical Al-Si based additives for biomass combustion and have been studied in laboratory-scale experiments. In addition, coal fly ash has been utilized in full-scale biomass suspension-fired boilers in Denmark, and has been shown to have the capacity to significantly remedy deposition and corrosion problems.[12, 14] The mineralogical composition of coal fly ash is complex, including mainly mineral phases such as quartz, mullite, kaolinite, illite, siderite, etc.[115, 118] Among these mineral phases, kaolinite is one of the most effective minerals for K-capture.[165] Kaolinite is a layered aluminosilicate mineral with chemical formula of $Al_2Si_2O_5(OH)_4$. Kaolin is a kind of clay that is rich in kaolinite. Investigating the K-capture reaction by kaolin is important for obtaining an improved understanding of K-capture by coal fly ash.

Kaolin undergoes complex transformation when being heated up. Above 450 °C, kaolin transfers into metakaolin via a dehydroxylation reaction as shown in reaction R 3.1.[98] Metakaolin is a type of amorphous aluminosilicate that reacts effectively with gaseous K-salts.[98] Metakaolin further transforms into spinel structure and amorphous SiO_2 when it is heated to above 980 °C, see reaction R 3.2. Mullite starts to form at around 1100 °C, and its amount increases with temperature and time, according to reaction R 3.3.[100] At temperatures above 1400 °C, needle shaped mullite grains are formed, and the size and the aspect ratio of the mullite grains increase with increasing calcination temperature.[100]

Generally, compared to metakaolin, mullite is believed to be less reactive for alkali capture.[93] Thus the transformation of kaolin at high temperatures may influence the K-capture reaction. To achieve the best K-capture results, kaolin should be injected into boilers at an optimal temperature window.

$$Al_2Si_2O_5(OH)_4\ (kaolin) \rightarrow Al_2O_3 \cdot 2SiO_2\ (metakaolin) + 2H_2O\ (g) \quad \text{(R 3.1)}$$

$$Al_2O_3 \cdot 2SiO_2(metakaolin) \rightarrow Al_2O_3 \cdot SiO_2\ (spinel) + SiO_2(amorphous) \quad \text{(R 3.2)}$$

$$3\ (Al_2O_3 \cdot SiO_2)\ (spinel) + 3\ SiO_2(amorphous) \rightarrow 3Al_2O_3 \cdot 2SiO_2\ (mullite) + 4\ SiO_2(amorphous) \quad \text{(R 3.3)}$$

Alkali-capture, especially the Na-capture reaction by kaolin has been widely studied primarily due to its application for cleaning Na-species from hot flue gases in Combined Cycle Gas Turbine (CCGT) power plants[76, 79, 101] and for dealing with ash-related problems in combustion of Na-rich low rank coals in power plant boilers.[75, 96, 102, 103, 166] However, when it comes to biomass combustion, K-capture reaction is of greater concern, but it has been studied to a less extent.[98]

Gas phase release and speciation of potassium depends on many factors including combustion conditions, fuel ash transformation chemistry, etc. In the combustion of biomass with high K but low Cl and S contents, KOH(g) is the dominant K-species in the high temperature flue gas.[21, 167] When S and Cl are available, KCl and K_2SO_4 would be formed during the combustion process, but at high temperature, KCl and K_2SO_4 can also transfer into KOH in the presence of water.[98]

KOH is a troublesome K-species and the main reactions involved for kaolin/metakaolin to capture KOH are shown in reaction R 3.4 and R 3.5.[21] The two main products are kalsilite ($KAlSiO_4$) and leucite ($KAlSi_2O_6$) with melting temperatures above 1600 °C and 1500 °C, respectively. Therefore, the melt-induced slagging and corrosion in biomass-fired boilers could be significantly mitigated by the use of kaolin.[4, 27, 168] However, the kinetics and detailed knowledge on the KOH-capture reaction by kaolin is still limited, especially, for suspension combustion.

$$Al_2O_3 \cdot 2SiO_2(metakaolin) + 2KOH \rightarrow 2KAlSiO_4\ (kalsilite) + H_2O \quad \text{(R 3.4)}$$

$$Al_2O_3 \cdot 2SiO_2(metakaolin) + 2KOH + 2SiO_2 \rightarrow 2KAlSi_2O_6\ (leucite) + H_2O \quad \text{(R 3.5)}$$

To the author's knowledge, the only literature available on alkali-capture by dispersed kaolin particles at suspension-fired conditions is the experimental study by Wendt and co-

workers[75, 92, 97] done in a 17-kW down-flow combustor which simulated the conditions in suspension-fired boilers. A sodium acetate solution was injected in the reactor to produce a Na vapor. The effect of temperature, residence time as well as the presence of sulfur and chlorine on the Na-capture reaction was studied. Results showed that the rate of NaOH adsorption was higher than that of NaCl, and they proposed that NaOH is the only reacting species in both cases. However, whether the kinetics of Na and K capture by kaolin are the same has not been established.[93]

Gaseous KOH capture by kaolin pellets (around 1 mm) in a fixed bed was studied by Steenari and co-workers.[98, 112, 113] They found that kaolin captured KCl more effectively than KOH, indicating that KCl and KOH can both react directly with kaolin. The KOH concentration was very low in these studies, with a typical KOH-concentration of 1.1 ppm, which is far below the K-concentration in biomass suspension-fired boilers.[151]

The degree of conversion of kaolin to K-aluminosilicates may be limited by equilibrium constrains. In addition, the rate of reaction may be limited by the external and internal diffusion of the gaseous potassium species, and by the reaction kinetics. Typically, a decreased kaolin particle size and/or an increased residence time lead to an increased conversion to the products.

At suspension-fired conditions, the reaction between gaseous KOH and dispersed kaolin particles may be affected by the local temperature, the additive particle size and composition, and the reaction time. Understanding the influence of different parameters on the K-capture reaction is crucial and helpful for providing recommendations for optimal utilization of kaolin and coal fly ash in full-scale boilers.

The objective of this work is to develop a method to study the K-capture reactions by solid additives at well-controlled suspension-fired conditions, and to systematically investigate the impact of different parameters on the K-capture reaction by solid additives, such as reaction temperature, K-concentration/molar ratio of K/(Al+Si) in the reactant, kaolin particle size, gas residence time and the high temperature transformation of kaolin. The potassium capture reaction using kaolin was studied in this chapter and Chapter 4. This chapter focuses on the KOH capture by kaolin, and Chapter 4 focuses on the K-capture reaction by kaolin using KCl, K_2CO_3 and K_2SO_4.

3.2 Experimental

The KOH capture experiments by kaolin were carried out in the DTU entrained flow reactor (EFR) which has been described in Chapter 2. Two sets of experiments were conducted: KOH evaporation experiments, and KOH-capture experiments using kaolin and mullite. The experimental conditions are summarized in Table 3-1.

Table 3-1. Experimental conditions in the Entrained Flow Reactor (EFR).

Experimental series	Additives	Temp./°C	Gas residence time/s	K-concentration /ppmv	K/(Al+Si)
(A) KOH evaporation experiments	No additive	800	1.2	500	No Al, Si
		900			
		1100			
		1300			
		1450			
(B) KOH-capture by kaolin (impact of K-concentration)	normal kaolin (D_{50} = 5.47 μm)	1100	1.2	50	0.048
				250	0.240
				500	0.481
				750	0.721
				1000	0.961
(C) KOH-capture by kaolin (impact of temperature)	normal kaolin (D_{50} = 5.47 μm)	800	1.2	50, 500	0.048, 0.481
		900			
		1100			
		1300*			
		1450			
(D) KOH-capture by kaolin (impact of residence time)	normal kaolin (D_{50} = 5.47 μm)	800, 1100	0.7	500	0.481
			1.2		
			1.5		
			1.9		
(E) KOH-capture by kaolin (impact of kaolin particle size)	fine kaolin (D_{50} = 3.51 μm)	900, 1100, 1300	1.2	500	0.481
	normal kaolin (D_{50} = 5.47 μm)	800, 900, 1100, 1300*, 1450			
	coarse kaolin (D_{50} = 13.48 μm)	900, 1100, 1300			
(F) KOH-capture by mullite	Mullite (D_{50} = 5.90 μm)	800, 900, 1100, 1300, 1450	1.2	500	0.471

Note: *Experiments were repeated.

In the KOH evaporation experiments (series (A) in Table 3-1), KOH solution was injected into the EFR without solid additives, to study the evaporation and transformation behavior of KOH at high temperature. The concentration of KOH in the flue gas was kept at 500 ppmv. The mass of solid samples collected in the cyclone and filter were weighted to study the vaporization of KOH. Additionally, the collected solid samples were analyzed with XRD to determine the transformation of KOH at high temperatures.

In the KOH-capture experiments (experiment series B-F in Table 3-1), a slurry containing both KOH and kaolin/mullite was injected into the EFR. In all the KOH-capture experiments, the concentration of kaolin in the flue gas was kept constant, while the amount of KOH in the feeding slurry was adjusted. Thereby, the concentration of KOH in the flue gas was changed consequently. The KOH-concentration (K-concentration in Table 2) in the flue gas was changed from 50 ppmv to 1000 ppmv, and the molar ratio of K/(Al+Si) in reactants was changed from 0.048 to 0.961 correspondingly.

3.3 Results and discussion

3.3.1 Evaporation and transformation of KOH in the EFR

Equilibrium calculations as well as EFR experiments were conducted to investigate the evaporation and transformation of KOH at high temperatures. The mass fractions of the collected solid products in cyclone and filter are shown in Figure 3-1 (A). The results of corresponding equilibrium calculations are shown in Figure 3-1 (B).

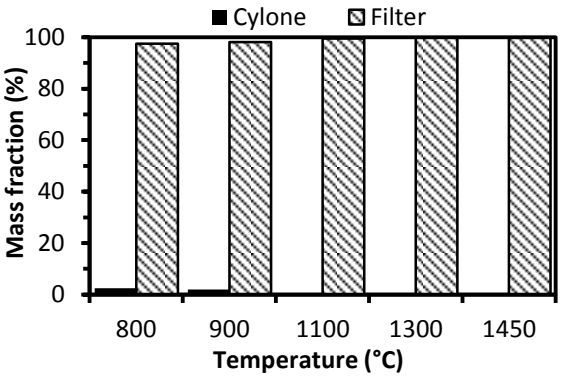

(A) EFR experiments

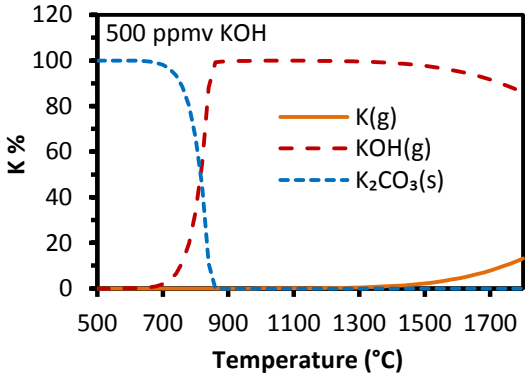

(B) Equilibrium calculation

Figure 3-1. (A) Mass distribution of solid samples collected in cyclone and filter from KOH evaporation experiments; (B) Equilibrium calculation results of KOH evaporation under conditions of experimental series A of Table 3-1.

In the EFR sampling system, the large particles were collected in the cyclone, while the aerosols were collected in the filter. When the K-salts were completely vaporized in the reactor and then cooled down in the extraction probe, aerosols would form and all solid products would be collected in the filter. If some of the salt particles generated from evaporation of slurry droplets were not fully vaporized, both aerosols and some larger particles would be present, resulting in some solid material being collected also by the cyclone. The experimental data in Figure 3-1 (A) indicate that a complete vaporization of KOH was obtained at 1100 °C. At 800 and 900 °C, the mass fraction of samples collected in the cyclone was 2.0 % and 1.5 %, respectively, indicating that a small amount of KOH not evaporated. This is in agreement with the equilibrium calculations (Figure 3-1 (B)), which predicted that the majority of KOH appeared as vapor at temperatures above 820 °C.

XRD analysis of the solid samples collected from the KOH evaporation experiments showed that $K_2CO_3 \cdot 1.5H_2O$ is the only product. The is probably because, during cooling, gaseous or condensed KOH reacts with CO_2 to form K_2CO_3, which then absorbs moisture from the air forming $K_2CO_3 \cdot 1.5H_2O$.

3.3.2 Representativeness of solid product samples

The solid products from the EFR experiments, including samples from the sampling probe, cyclone and filter, were carefully collected. For each experiment, the collected solid products corresponded to about 58 % to 75 % of the theoretical amount solid samples extracted by the probe. The rest were lost, mainly by deposition on the inner wall of the reactor tube.[169]

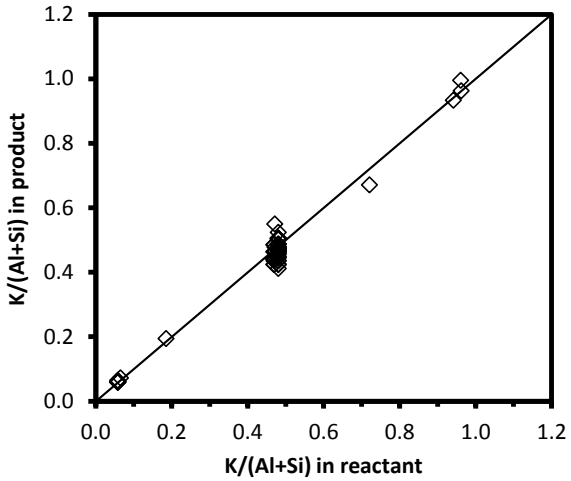

Figure 3-2. Comparison of K/(Al+Si) in collected solid products and that of fed reactants.

Therefore, in order to be able to determine the conversion degree of the reaction based on the collected solid product samples, the representativeness of the collected solid product

samples were checked. This was done by comparing the molar ratio of K/(Al+Si) in the products with that of the fed reactants. The results based on ICP-OES analysis are shown in Figure 3-2. The molar ratios of K/(Al+Si) in the collected solid samples are nearly identical to those of the reactants, implying that the solid product samples are representative.

3.3.3 Evolution of kaolin in the EFR

Slurries of normal kaolin (D_{50} = 5.47 μm) without and with KOH were fed into the EFR at 1300 °C, where the residence time was 1.2 s. XRD and SEM-EDX were utilized to study the mineralogical and morphological evolutions of kaolin during the reaction with KOH. The XRD spectra of the raw kaolin, the dehydroxylated kaolin (i.e. product of kaolin fed into the EFR without KOH), mullite, and the water-washed KOH-captured kaolin samples are compared in Figure 3-3.

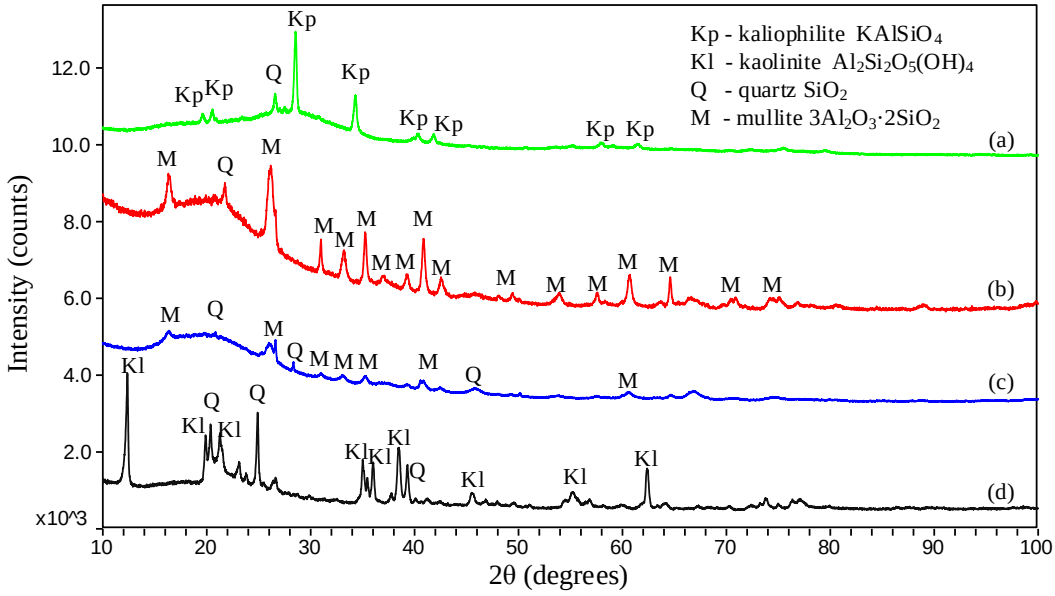

Figure 3-3. XRD spectra of raw, dehydroxylated, KOH-reacted kaolin. (a) 500 ppmv KOH-reacted kaolin; (b) mullite (1100 °C, 24 hours); (c) dehydroxylated kaolin; (d) raw kaolin. For sample (a) and (c), reaction temperature in the EFR was 1300 °C, and the gas residence time was 1.2 s.

The results show that only mullite and quartz were detected in the dehydroxylated kaolin (Figure 3-3 c); no kaolinite was detected. This reveals that at 1300 °C, with a residence time of 1.2 s, all kaolinite from raw kaolin has decomposed completely. However, the peaks corresponding to mullite of the dehydroxylated kaolin are obviously weaker compared to the peaks of the mullite powder (Figure 3-3 b). This shows that not all the decomposed

kaolinite was converted to crystalline mullite with some remaining as amorphous species, like metakaolin and amorphous silica.[100] In the water washed KOH-reacted kaolin (Figure 3-3 a), crystalline kaliophilite ($KAlSiO_4$) was detected, as the reaction product of kaolin and KOH at high temperatures (1300 °C) in the EFR.

The SEM images of raw kaolin, the dehydroxylated kaolin and water-washed KOH-reacted kaolin are compared in Figure 3-4. It is seen that raw kaolin particles are all in a form of an irregular flaky shape, while the dehydroxylated kaolin particles are slightly more spherical but kept the original inner flaky structure. The flaky structure indicates that no significant melting took place at 1300 °C, in agreement with the reported mullite melting point of 1830 °C.[170] For the KOH-reacted kaolin sample, some spherical particles with smooth surface were observed, showing the particles experienced melting in the EFR. Since the kaliophilite ($KAlSiO_4$) detected in the KOH-reacted solid product has a melting point of 1800 °C,[97] it is mostly likely some amorphous products with low melting point were formed as well.

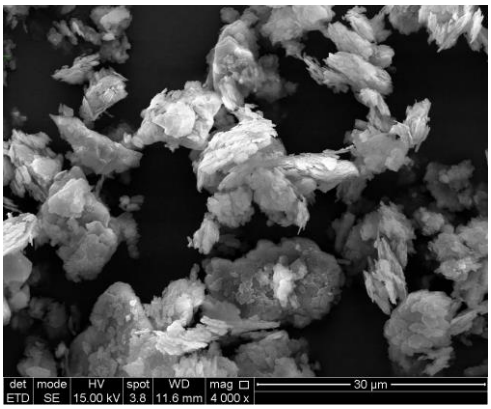

(A) Raw kaolin

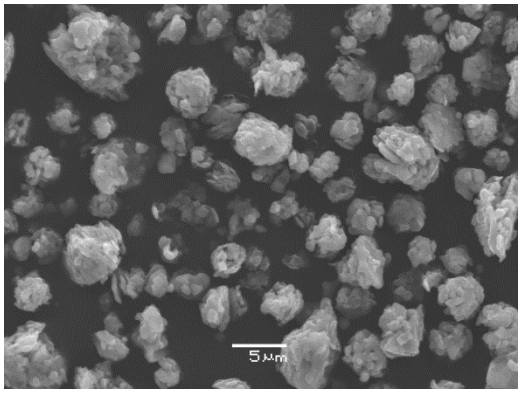

(B) Dehydroxylated kaolin

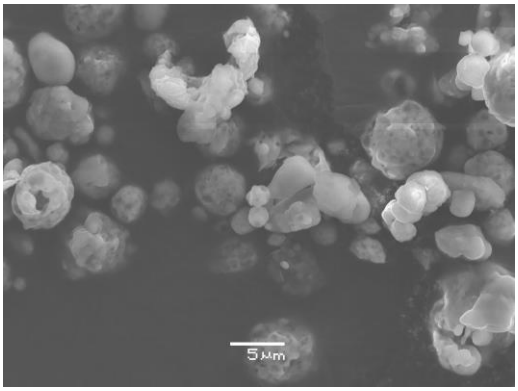

(C) KOH-reacted kaolin

Figure 3-4. (A) SEM images of raw kaolin; (B) dehydroxylated kaolin (without KOH fed at 1300 °C, residence time was 1.2 s); and (C) water-washed KOH-reacted kaolin (500 ppmv KOH by kaolin at 1300 °C, residence time was 1.2 s, K/(Al+Si) in reactant is 0.481).

Water-washed KOH-reacted kaolin (Figure 3-4 (C)) was analyzed with SEM-EDX to get the elemental composition. The result shows that the molar ratio of K:Al:Si is 1:1.18:1.37, i.e., with extra Si compared to the chemical formula of kaliophilite ($KAlSiO_4$). This is attributed to the presence of quartz (SiO_2), which was also detected with the XRD analysis. It could also be due to the formation of some amorphous Si-species, which cannot be detected by XRD analysis.

3.3.4 KOH capture by kaolin

3.3.4.1 Equilibrium calculations

Equilibrium calculations were carried out for the same conditions as in the EFR, but with a wider temperature range from 500 °C to 1800 °C. The influence of both the KOH concentration and thereby the molar K/(Al+Si) ratio in the reactants, and the reaction temperature was studied by the calculations. A summary of the equilibrium calculation results is shown in Table 3. The detailed results are available in Appendix C.

The results in Table 3-2 indicate that the main K-aluminosilicate species formed from the reaction between KOH and kaolin varies with the molar ratio of K/(Al+Si) in the input. At 800-1450 °C, with 50 ppmv KOH, sanidine ($KAlSi_3O_8$) is the main aluminosilicate product with K:Al:Si = 1:1:3; With 250 ppmv KOH, both sanidine ($KAlSi_3O_8$) and leucite ($KAlSi_2O_6$) are major K-aluminosilicates; while with 500-1000 ppmv KOH, kaliophilite ($KAlSiO_4$) with K:Al:Si = 1:1:1 became the dominating K-aluminosilicate.

Table 3-2. Summary of the equilibrium calculation results of KOH capture by kaolin.

Input conditions	Temp. /°C	K-species appearing	Al-con.	Si-con.	K-con.	K-capture/(g K/g kaolin)
50 ppmv KOH, K/(Al+Si) = 0.048	800	100 % $KAlSi_3O_8$	9 %	23 %	100 %	0.023
	900	100 % $KAlSi_3O_8$	9 %	23 %	100 %	0.023
	1100	100 % $KAlSi_3O_8$	9 %	23 %	100 %	0.023
	1300	100 % $KAlSi_3O_8$	9 %	23 %	100 %	0.023
	1450	99 % $KAlSi_3O_8$ + 1 % KOH	9 %	23 %	99 %	0.022
250 ppmv KOH, K/(Al+Si) = 0.240	800	25 % $KAlSi_3O_8$ + 75 % $KAlSi_2O_6$	49 %	98 %	100 %	0.129
	900	25 % $KAlSi_3O_8$ + 75 % $KAlSi_2O_6$	49 %	98 %	100 %	0.129
	1100	24 % $KAlSi_3O_8$ + 76 % $KAlSi_2O_6$	49 %	97 %	100 %	0.129
	1300	20 % $KAlSi_3O_8$ + 80 % $KAlSi_2O_6$	49 %	96 %	100 %	0.128
	1450	22 % $KAlSi_3O_8$ + 77 % $KAlSi_2O_6$	49 %	96 %	99 %	0.128
500 ppmv KOH, K/(Al+Si) = 0.481	800	92 % $KAlSiO_4$ + 6 % $KAlSi_2O_6$	100 %	98 %	98 %	0.264
	900	91 % $KAlSiO_4$ + 7 % $KAlSi_2O_6$ + 1 % KOH	100 %	99 %	98 %	0.264
	1100	91 % $KAlSiO_4$ + 7 % $KAlSi_2O_6$ + 2 % KOH	100 %	99 %	98 %	0.263
	1300	82 % $KAlSiO_4$ + 12 % $KAlSi_2O_6$ + 6 % KOH	95 %	100 %	94 %	0.252
	1450	50 % $KAlSiO_4$ + 28 % $KAlSi_2O_6$ + 21 % KOH	79 %	100 %	78 %	0.209
750 ppmv KOH, K/(Al+Si) = 0.721	800	57 % $KAlSiO_4$ + 8 % $KAlO_2$ + 31 % K_2SiO_3 + 3 % KOH	88 %	78 %	57 %	0.231
	900	63 % $KAlSiO_4$ + 1 % $KAlO_2$ + 18 % K_2SiO_3 + 16 % KOH	98 %	87 %	63 %	0.258
	1100	65 % $KAlSiO_4$ + 8 % $K_2Si_2O_5$ + 27 % KOH	100 %	89 %	65 %	0.263
	1300	57 % $KAlSiO_4$ + 8 % $KAlSi_2O_6$ + 35 % KOH	100 %	100 %	65 %	0.263
	1450	57 % $KAlSiO_4$ + 8 % $KAlSi_2O_6$ + 35 % KOH	100 %	100 %	65 %	0.263
1000 ppmv KOH, K/(Al+Si) = 0.961	800	29 % $KAlSiO_4$ + 19 % $KAlO_2$ + 49 % K_2SiO_3 + 3 % KOH	61 %	55 %	29 %	0.161
	900	35 % $KAlSiO_4$ + 13 % $KAlO_2$ + 38 % K_2SiO_3 + 14 % KOH	73 %	65 %	35 %	0.191
	1100	48 % $KAlSiO_4$ + 11 % K_2SiO_3 + 41 % KOH	100 %	89 %	48 %	0.264
	1300	43 % $KAlSiO_4$ + 6 % $KAlSi_2O_6$ + 52 % KOH	100 %	100 %	48 %	0.264
	1450	43 % $KAlSiO_4$ + 6 % $KAlSi_2O_6$ + 51 % KOH + 1 % K	100 %	100 %	48 %	0.264

3.3.4.2 Impact of the potassium concentration

The experimental K-capture level (C_K) and K-conversion (X_K) are compared with the estimations from equilibrium calculations in Figure 3-5. The KOH-concentration in the flue gas varied from 50 ppmv to 1000 ppmv, while the reaction temperature was kept constant at 1100 °C. The experimental data followed a similar trend but was slightly lower as compared to the equilibrium prediction. When the KOH concentration increased from 50 ppmv to 500 ppmv, the K-capture level (C_K) by kaolin increased from 0.022 g K/ (g kaolin) to 0.227 g K/ (g kaolin). However, no obvious increase of C_K is observed when the KOH concentration increased further to 750 and 1000 ppmv. This is probably because the active compound in kaolin has been fully converted into K-aluminosilicates, while the increased KOH remained unreacted. The equilibrium constrain can explain the decrease of K-conversion (X_K). X_K decreased slightly from 95.8 % to 84.6 % when the KOH concentration increased from 50 ppmv to 500 ppmv, while X_K decreased sharply when the KOH concentration increased from 500 ppmv to 1000 ppmv as shown in Figure 3-5 (B).

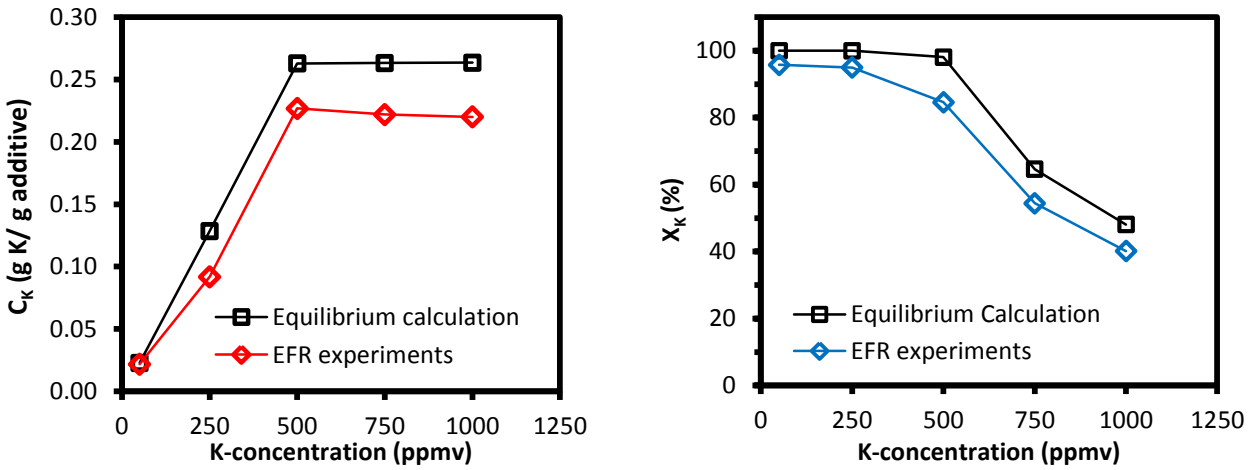

(A) K-capture level (C_K) (B) K-conversion (X_K)

Figure 3-5. K-capture level (C_K) and K-conversion (X_K) of KOH-capture by normal kaolin (D_{50} = 5.47 μm) at different KOH concentrations from 50 ppmv to 1000 ppmv (molar K/(Al+Si) ratio in reactants varied from 0.048 to 0.961). Reaction temperature was 1100 °C and gas residence time was 1.2 s.

The XRD spectra of the water-washed KOH-reacted kaolin at 50, 250 and 500 ppmv KOH are compared in Figure 3-6. The spectra at 750 ppmv and 1000 ppmv were similar to that at 500 ppmv and are not included. The results show that in the 50 ppmv-KOH product, only quartz and mullite were detected as the main crystalline phases. No crystalline K-aluminosilicate was detected in the sample, although sanidine ($KAlSi_3O_8$) was predicted by

the equilibrium calculations as shown in Table 3-2. This is probably because the concentration of K-aluminosilicates is low and/or they remained in an amorphous state, which cannot be detected. The 250 ppmv KOH spectrum shows that leucite ($KAlSi_2O_6$) with a molar ratio of K:Al:Si = 1:1:2 was the main K-aluminosilicate, while kaliophilite ($KAlSiO_4$) with a molar ratio of K:Al:Si = 1:1:1 became the main K-aluminosilicate at 500 ppmv KOH. The XRD analysis results generally agree with the equilibrium calculations shown in Table 3-2.

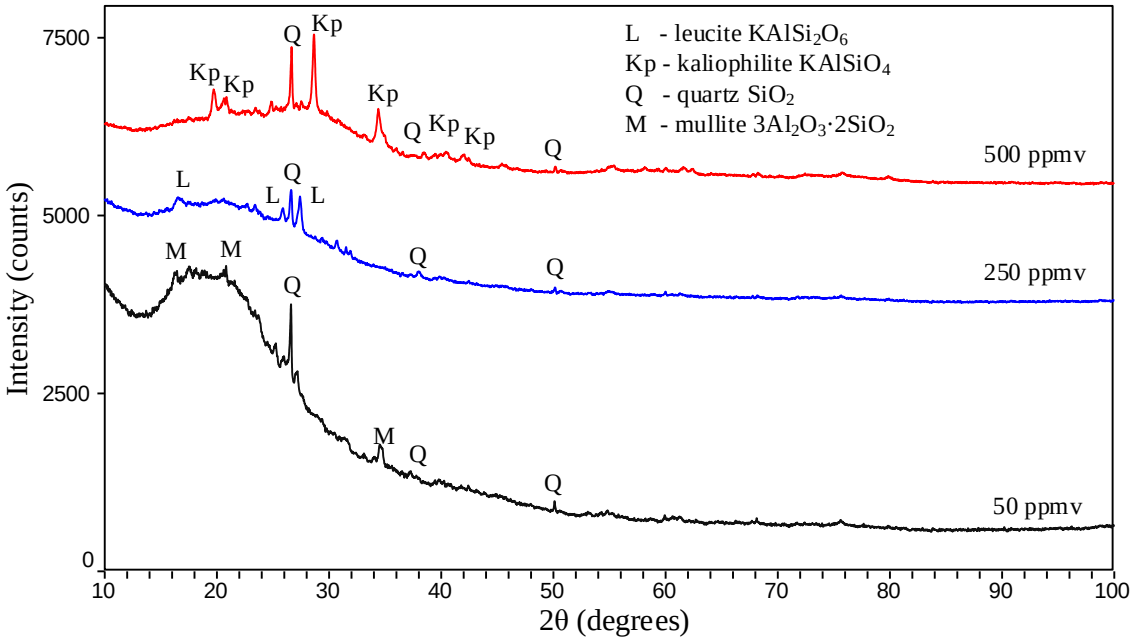

Figure 3-6. XRD spectra of water-washed KOH-reacted kaolin at 50, 250 and 500 ppmv KOH. The reaction temperature was 1100 °C, the molar ratio of K/(Al+Si) was 0.048, 0.240 and 0.481 and the gas residence time was 1.2 s.

3.3.4.3 Impact of reaction temperature

The K-capture level (C_K) and K-conversion (X_K) obtained at different reaction temperatures (800-1450 °C) and two different KOH concentrations (50 ppmv and 500 ppmv) were compared with the equilibrium calculation results in Figure 3-7. Figure 3-7 (A) and (B) show that, at 500 ppmv KOH, the K-capture level (C_K) increased from 0.166 g K/(g kaolin) to 0.241 g K/(g kaolin) by 43.6 %, when the reaction temperature increased from 800 °C to 1300 °C. The K-conversion (X_K) increased from 62.1 % to 89.1 %, correspondingly. However, when the temperature was increased further to 1450 °C, C_K and X_K decreased to 0.198 g K/(g kaolin) and 74.0 % respectively. This is caused by a change in the equilibrium products with a decreased amount of kaliophilite ($KAlSiO_4$) and an increased amount of leucite

($KAlSi_2O_6$) at high temperatures. At 1300 °C and 1450 °C, the K-capture level (C_K) is close to the equilibrium calculation value. At 1100 °C and below, the K-capture levels (C_K) are below the equilibrium levels, implying the process is kinetic controlled.

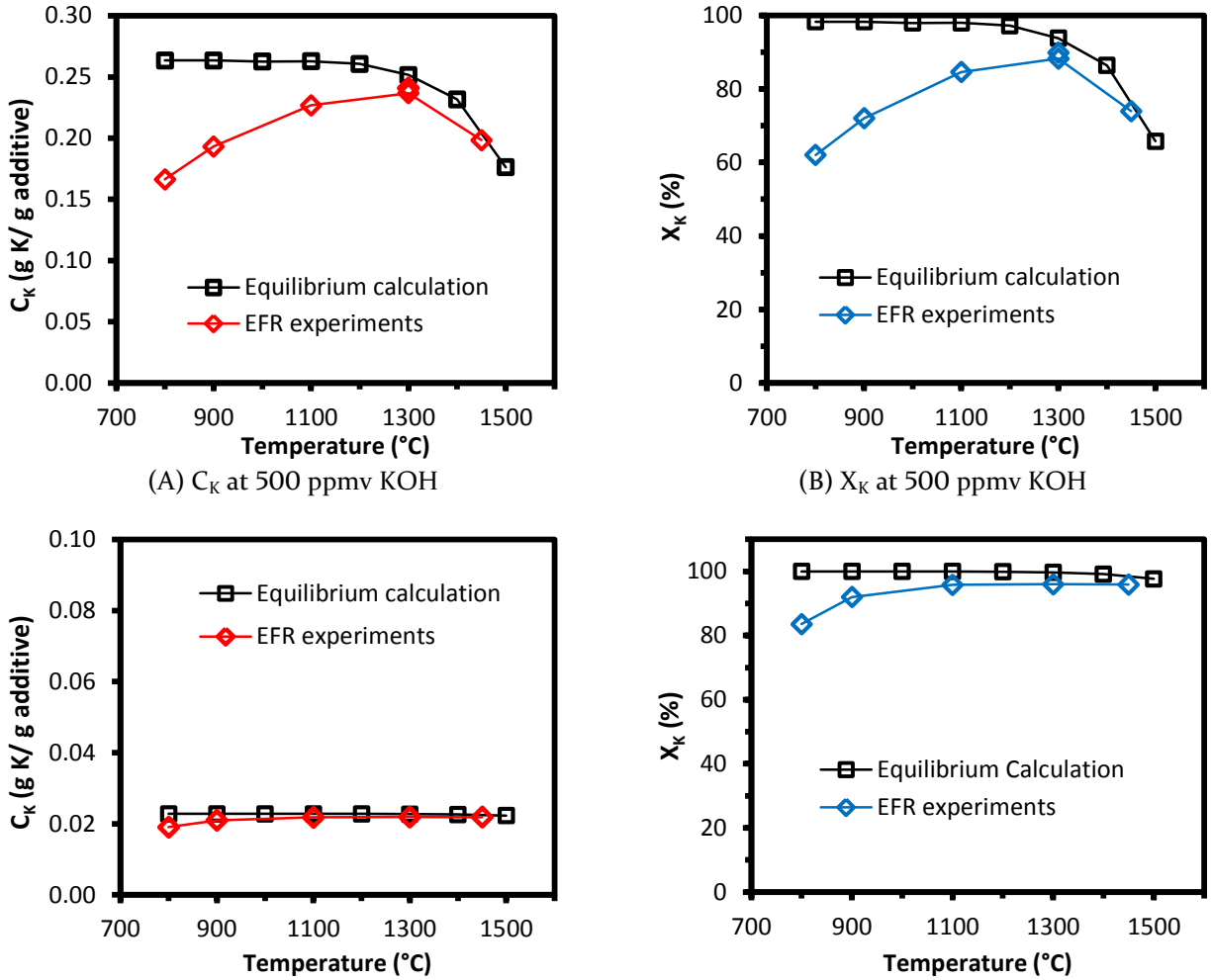

(A) C_K at 500 ppmv KOH

(B) X_K at 500 ppmv KOH

(C) C_K at 50 ppmv KOH

(D) X_K at 50 ppmv KOH

Figure 3-7. K-capture level (C_K) and K-conversion (X_K) of KOH capture by normal kaolin (D_{50} = 5.47 μm) at temperatures from 800 to 1450 °C. KOH-concentration was 500 ppmv, and molar K/(Al+Si) ratio was 0.481 in (A) and (B); KOH-concentration was 50 ppmv, molar K/(Al+Si) ratio was 0.048 in (C) and (D). Gas residence time was 1.2 s for all experiments, and equilibrium calculation results included for comparison.

Figure 3-7 (C) and (D) show that at 50 ppmv KOH, the K-capture level (C_K) was predicted to be 0.023 g K/(g additive), by the equilibrium calculations, and the predicted K-conversion (X_K) was higher than 99.2 % through the whole temperature range. At temperatures above 1100 °C, the experimental C_K and X_K were close to the equilibrium calculations. At 800 °C and 900 °C, the experimental result is slightly lower than the value predicted by the

equilibrium calculations. The only K-aluminosilicate predicted by the calculations is sanidine ($KAlSi_3O_8$) with a molar ratio of K:Al:Si = 1:1:3.

The water-washed 500 ppmv KOH-reacted kaolin samples were subjected to XRD analysis, with the spectra shown in Figure 3-8. It shows that with the temperature increased from 800 to 1450 °C, the peaks of kaliophilite ($KAlSiO_4$) increased significantly. The results indicate that either kaliophilite was generated in larger quantities or that it became more crystalline with the increasing temperature or due to a faster cooling rate in the sampling system. No other crystalline K-aluminosilicate product was detected, although leucite ($KAlSi_2O_6$) was also predicted by the equilibrium calculations. The formation of kaliophilite was also observed in experimental studies by Steenari and her co-workers.[59] Kalsilite ($KAlSiO_4$), a polymorph of kaliophilite was also widely reported in previous studies.[74, 97, 98, 113] At 800 °C and 900 °C, no clear signal of K-aluminosilicate was detected by XRD. This is probably because the formed K-aluminosilicate existed in an amorphous form at lower temperatures. Kaolinite was detected in the 800 and 900 °C solid products, indicating an incomplete dehydroxylation of kaolin at temperatures below 900 °C in the EFR.

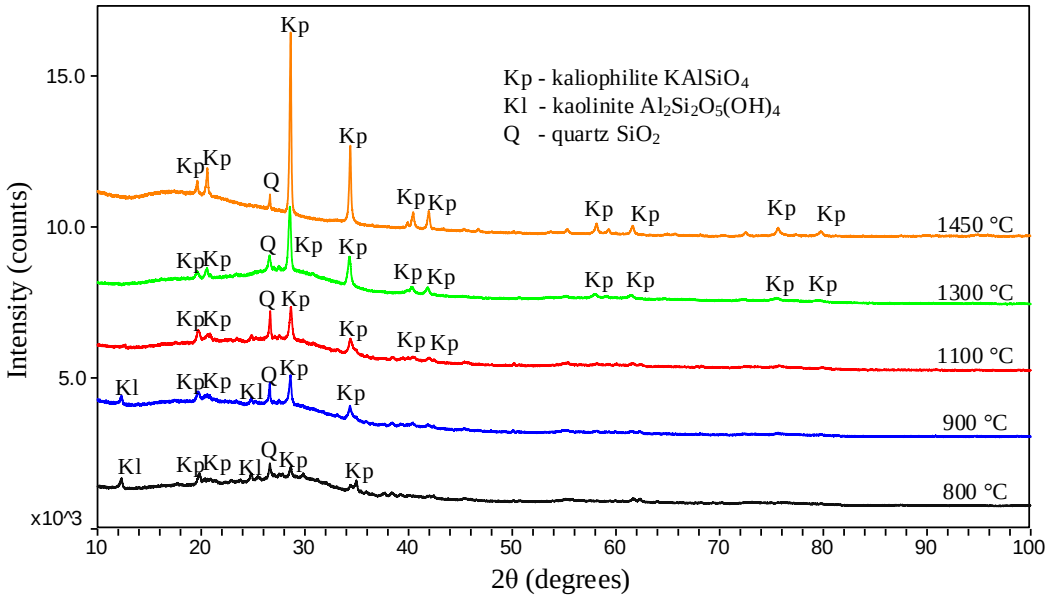

Figure 3-8. XRD spectra of water-washed solid samples from the experiments of KOH capture by normal kaolin (D_{50} = 5.47 μm) at different reaction temperatures, from 800 °C to 1450 °C. KOH concentration was 500 ppmv, (K/(Al+Si) = 0.481) and the gas residence time was 1.2 s.

3.3.4.4 Impact of gas residence time

The impact of gas residence time on the KOH-capture reaction was investigated at 800 °C and 1100 °C. At 800 °C, the gas residence time varied from 1.2 s to 1.9 s, while at 1100 °C, it was changed from 0.7 s to 1.7 s. In all experiments, the KOH-concentration in the flue gas and the molar ratio of K/(Al+Si) in the reactants were kept constant, at 500 ppmv and 0.481, respectively. The experimental results were compared to the equilibrium calculation results in Figure 3-9.

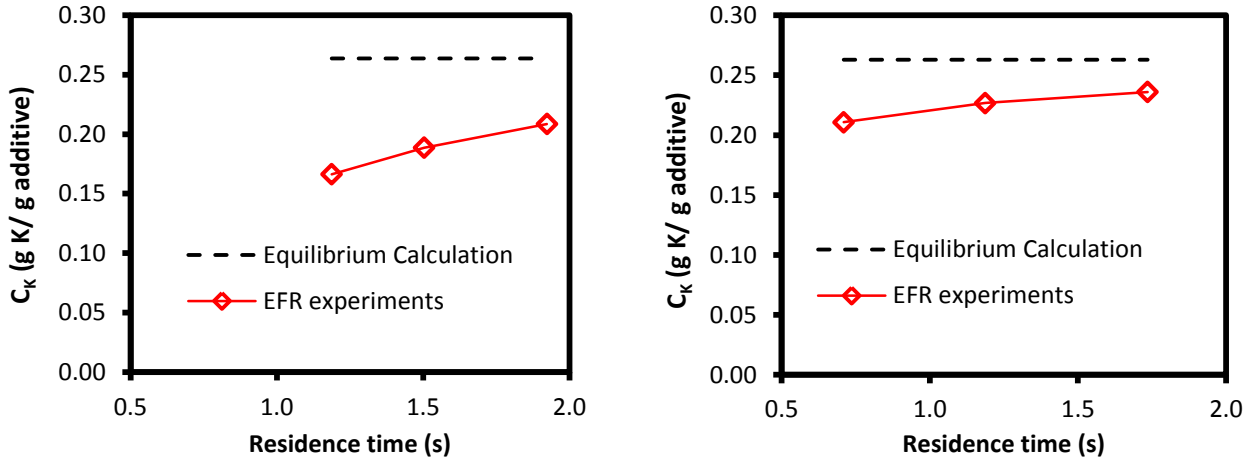

Figure 3-9. K-capture level (C_K) of KOH capture by the normal kaolin (D_{50} = 5.47 µm) at different gas residence times. Reaction temperature was 800 °C (A) and 1100 °C (B) respectively, and the KOH-concentration was 500 ppmv (K/(Al+Si) = 0.481). Equilibrium calculation results are included for comparison.

At 800 °C, as shown in Figure 3-9 (A), when the gas residence time increased from 1.2 s to 1.9 s, K-capture level (C_K) increases by 25.4 % from 0.166 g K/g kaolin to 0.209 g K/g kaolin. However at 1100 °C, when the gas residence time increased from 0.7 s to 1.2 s, C_K increased by 7.6 %, from 0.211 to 0.227 g K/g kaolin. When the gas residence time increased further from 1.2 s to 1.7 s, C_K increased to 0.236 by 4.1 %.

In summary, the KOH-capture reaction by kaolin reached equilibrium at temperatures of 1300 °C and 1450 °C, with a gas residence time of 1.2 s and a kaolin particle size of D_{50} = 5.47 µm. At 1100 °C with a residence time of 1.7 s, the reaction is close to the equilibrium. However, at 800 °C, C_K is obviously further away from the equilibrium even with a longer residence time of 1.9 s, showing that the reaction is more kinetically or diffusion controlled at 800 °C.

3.3.4.5 Impact of kaolin particle size

The K-capture level (C_K) of fine kaolin, normal kaolin and coarse kaolin at 800-1450 °C were compared to the equilibrium calculation results in Figure 3-10. Generally, the results show that at 900-1300 °C fine kaolin and normal kaolin behaved similarly, and C_K did not increase when the D_{50} of kaolin particle size decreased from 5.47 µm to 3.51 µm. For coarse kaolin, C_K is similar as that of normal and fine kaolin at 900 °C. However it became lower than the C_K of normal and fine kaolin at 1100 and 1300 °C. This indicates that the conversion at 1100 and 1300 °C is partly limited by the transport processes, at least for the coarse kaolin. However, at 800 and 900 °C the reaction appears to be kinetically limited.

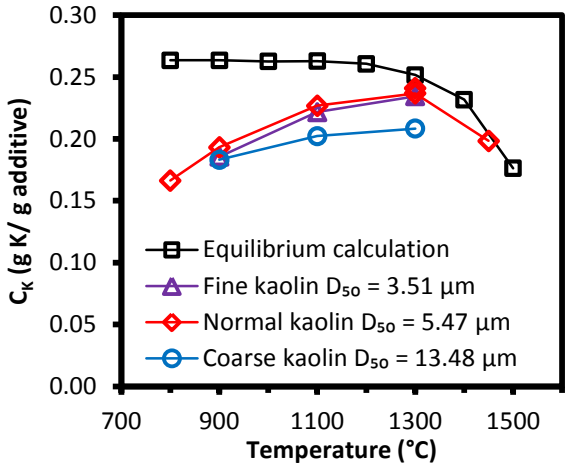

Figure 3-10. K-capture level (C_K) of KOH capture by kaolin of different particle size: fine kaolin (D_{50} = 3.51 µm), normal kaolin (D_{50} = 5.47 µm) and coarse kaolin (D_{50} = 13.48 µm). KOH concentration was 500 ppmv (molar ratio of K/(Al+Si) in reactant was 0.481), and gas residence time was 1.2 s. Equilibrium calculations are included for comparison.

3.3.4.6 KOH capture by mullite

The KOH capture level of mullite (D_{50} = 5.90 µm) was compared with that of normal kaolin (D_{50} = 5.47 µm) in Figure 3-11, at reaction temperatures of 800-1450 °C, gas residence time of 1.2 s and a KOH concentration of 500 ppmv. The EFR experimental results show, that at low temperatures (800-1100 °C), C_K of mullite is much lower than that of kaolin. This is probably partly because the BET surface area of mullite is smaller than that of kaolin (shown in Table 2-1) and thereby limited the internal KOH transport in the particles. On the other hand, the kinetics of the mullite-KOH reaction is probably slower than that of the kaolin-KOH reaction. At 1300 °C and 1450 °C, C_K of mullite increased significantly, and at 1450 °C, the value is close to that of the normal kaolin. This is probably because at high temperatures

(1300 and 1450 °C), the KOH-reacted mullite particles are melted, and the KOH diffusion mechanism changed from a slow gas-solid diffusion to a faster gas-liquid diffusion which improved the transport of KOH inside the mullite particles. A similar phenomenon was observed by Zheng et al., when the KCl capture by mullite pellets was studied in a fixed bed reactor.[93]

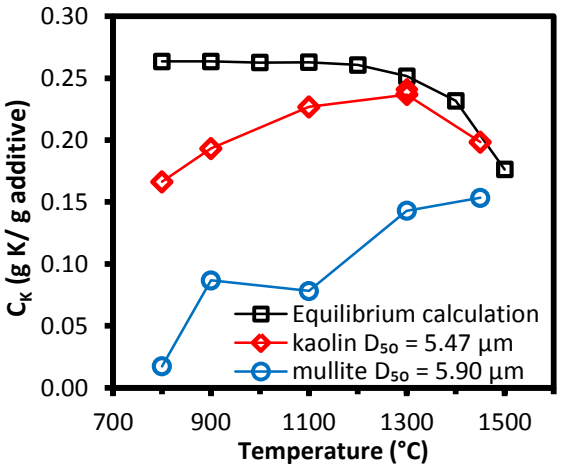

Figure 3-11. Comparison of K-capture level (C_K) of KOH capture by kaolin and mullite. Reaction temperature changed from 800 °C to 1450 °C. KOH concentration was 500 ppmv (K/(Al+Si) = 0.481), and gas residence time was 1.2 s. Equilibrium calculation results for kaolin are included for comparison.

3.4 Conclusions

The impact of different parameters, including the potassium concentration in flue gas (molar ratio of K/(Al+Si) in reactants), the reaction temperature, the residence time, the kaolin particle size, as well as the high temperatures phase transformations of kaolin, on the KOH-capture reaction at suspension fired conditions was investigated. The reaction was studied by performing experiments in an entrained flow reactor and chemical equilibrium calculations.

The K-capture level (C_K) increased significantly when the KOH-concentration increased from 50 to 500 ppmv, corresponding to an increase in the molar K/(Al+Si) ratio from 0.048 to 0.481, whereas no obvious increase was observed when KOH-concentration increased further to 750 ppmv and 1000 ppmv. Leucite ($KAlSi_2O_6$) was formed at 250 ppmv KOH (K/(Al+Si) = 0.240). While at 500 ppmv KOH and above (K/(Al+Si) ≥ 0.481), kaliophilite ($KAlSiO_4$) was formed as the dominant product.

A nearly full conversion of kaolin (D_{50} = 5.47 μm) was obtained without kinetic or transport limitations at temperatures above 1100 °C with the applied conditions (residence time of 1.2 s, and a KOH concentration of 500 ppmv). However, at 800 and 900 °C, the experimental data were considerably lower than the equilibrium predictions, and the K-capture level increased significantly when the gas residence time increased, implying the reaction is probably kinetically controlled. The optimal temperature window for injecting kaolin for K-capture at suspension-fired conditions is 1100-1300 °C. Crystalline kaliophilite ($KAlSiO_4$) was detected by XRD analysis at 1100 °C or above, while at 800 and 900 °C, amorphous K-aluminosilicate was formed.

Fine kaolin powder (D_{50} = 3.51 μm) and normal kaolin powder (D_{50} = 5.47 μm) behaved similarly in terms of K-capture level (C_K), while coarse kaolin (D_{50} = 13.48 μm) showed a considerably smaller K-capture level at 1100 and 1300 °C. This is probably because KOH diffusion into the kaolin particles became a limiting factor for the coarse kaolin at 1100 °C and above. At 900 °C, where the difference was smaller, the reaction is more kinetically controlled and the additive particle size did not influence the reaction significantly with the applied particle sizes.

Mullite captured KOH less effectively compared to kaolin at temperatures below 1100 °C. However C_K of mullite increased significantly at 1300 and 1450 °C. At 1450 °C, the K-capture level of mullite is comparable to that of kaolin.

4 Potassium Capture by Kaolin, Part 2: K_2CO_3, KCl, and K_2SO_4

Abstract: The reaction of kaolin powder with K_2CO_3, KCl and K_2SO_4 at suspension-fired conditions was studied by entrained flow reactor experiments and equilibrium calculations. The influence of reaction temperature, K-concentration in the flue gas, molar ratio of K/(Al+Si) in the reactants, and gas residence time on the reaction was investigated. The results showed that the K-capture level (C_K) of K_2CO_3 and KCl by kaolin generally followed the equilibrium predictions at temperatures above 1100 °C, when using a kaolin particle size of D_{50} = 5.47 µm and a residence time of 1.2 s. This revealed that a nearly full conversion was obtained without kinetic or transport limitations at the conditions applied. At 800 and 900 °C, the measured conversions were lower than the equilibrium predictions, indicating that the reactions were either kinetically or diffusion controlled. The measured C_K of K_2SO_4 by kaolin was much lower than the equilibrium predictions. Kaliophilite ($KAlSiO_4$) product was predicted by the equilibrium calculations of the K_2SO_4 capture reaction; however the XRD analysis results revealed that leucite ($KAlSi_2O_6$) was formed. Compared with the C_K of KOH reacting with kaolin, the C_K of K_2CO_3 was similar, while the C_K value of KCl and K_2SO_4 were both lower.

4.1 Introduction

The Danish government plans to phase out coal from power plants by 2030, mainly through promoting wind energy and replacing coal with biomass in power plants.[171] Suspension-firing of biomass can provide CO_2-neutral electricity with higher efficiency compared to traditional grate-firing.[67] However, ash-related problems have sometimes hampered the utilization of biomass in suspension-fired power plants.

Potassium is present naturally in plant materials and it is the main cause for most ash-related problems,[11, 36, 153, 172] including deposition,[15, 49, 151, 156] corrosion[52, 173] and SCR catalyst deactivation in biomass-fired boilers.[29, 54, 57] During biomass combustion, potassium is released to gas phase in different forms depending on the ash chemistry of the fuels and

combustion conditions. K-species including KOH, K_2CO_3, KCl and K_2SO_4 have been detected in the ash from biomass-fired boilers.[11, 12, 19, 131, 174-177] In the combustion of woody biomass with a low fuel Cl and S content, potassium may appear as K_2CO_3 and KOH in the flue gas.[21] However, when Cl and S are available, like in the case of herbaceous biomass combustion, KCl and K_2SO_4 become the dominant K-containing compounds.[21, 125] KCl and K_2SO_4 have melting temperatures of around 770 °C and 850 °C, respectively. The binary system of KCl and K_2SO_4 may melt at as low as 690 °C forming sticky surface on heat transfer surfaces.[33] The melted K-salts can function as a glue and accelerate the formation of ash deposit. Additionally, the deposited KCl can cause severe corrosion.[28] When the flue gas is cooled down, the condensation of KCl and K_2SO_4 forms aerosols that can poison SCR de-NO_x catalysts and thereby impede the plant NO_x removal system.[29, 54, 57] The efficiency and availability of biomass-fired boilers can be decreased due to problems caused by the potassium-rich biomass ash.[4, 34, 37]

Injecting additives to capture and transfer the volatile potassium species into less corrosive compounds with a higher melting point is an option to reduce biomass ash related challenges.[12, 14, 78, 106] Kaolin and coal fly ash have been identified as effective potassium-capture additives for biomass combustion.[178, 179] Kaolin is a kind of clay that is rich in a layered aluminosilicate mineral – kaolinite ($Al_2Si_2O_5(OH)_4$). Coal fly ash often contains mullite ($3Al_2O_3{\cdot}2SiO_2$) as the main mineral phase.[115] Kaolinite and mullite can react with volatile alkali species and bind alkali in alkali-aluminosilicate species.[12, 74]

When kaolin is heated, it decomposes and transfers into metakaolin above 450 °C.[180, 181] Metakaolin can capture gaseous potassium species such as KOH, KCl and K_2SO_4. Using KCl as an example, metakaolin react with KCl forming K-aluminosilicate, releasing HCl into the gas phase, see reaction R 4.1 and R 4.2.[98, 112, 113] K-aluminosilicate has a higher melting point compared to KOH, KCl and K_2SO_4 and thereby the potassium becomes less problematic for the boiler operation. Coal fly ash with mullite as the main mineral phase, can react with volatile K-species in a similar way as kaolin.[12, 118, 147, 148, 182, 183]

$$Al_2O_3 \cdot 2SiO_2(metakaolin) + 2KCl + H_2O \rightarrow 2KAlSiO_4(kalsilite/kaliophilite) + 2HCl\ (g) \quad \text{(R 4.1)}$$

$$Al_2O_3 \cdot 2SiO_2(metakaolin) + 2SiO_2 + 2KCl + H_2O \rightarrow 2KAlSi_2O_6\ (leucite) + 2HCl(g) \quad \text{(R 4.2)}$$

Kaolin has been tested in a large-scale CFB boilers as an additive to prevent alkali-related problems.[53] With the addition of kaolin, the amount of water soluble K and Cl in the fly ash

was significantly decreased, and the bed agglomeration temperature was increased.[53] Coal fly ash has been commercially utilized in full-scale biomass suspension-fired boilers in Denmark.[12, 14, 184] In order to optimize the use of these additives in biomass suspension-fired boilers, a thorough understanding of the reaction of these additives with different volatile potassium species is wanted.

Alkali capture by kaolin has been studied previously.[74-76, 93, 98, 113] Shadman and co-workers studied the reaction of gaseous NaCl and KCl with kaolin flakes in a fixed bed reactor. [74, 76, 78, 79, 123] The results showed that kaolin captured NaCl and KCl irreversibly through chemical reaction. The reaction was diffusion-influenced under the studied conditions (800 °C, kaolin flakes with a thickness of 0.5 mm, and a residence time of 40 hours). A weight increase of 26.6 % of saturated kaolin flakes was observed by the NaCl-kaolin reaction.[78]

In the study by Zheng et al.,[93] the kinetics of gaseous KCl capture by kaolin pellets with a diameter of 1.5 mm was investigated in a fixed bed reactor. The influence of oxygen content (0-20 %), water content (0-3 vol. %), KCl concentration (0-1600 ppmv), as well as the reaction temperature (900-1500 °C) on the reaction was studied. It was shown that the diffusion of KCl inside the kaolin pellets was the rate-controlling step of the reaction at the studied conditions. The reaction temperature posed a significant impact on the KCl-capture reaction under the studied conditions. The K-capture level of kaolin decreased with exposure temperature up to 1300 °C and then increased with further increasing the exposure temperature to 1500 °C. This is because at 900-1300 °C, sintering of kaolin pellets took place, resulting in a gradual replacement of fast gas diffusion by slow condensed-state diffusion. At temperatures above 1300 °C, a partially molten phase was formed inside the pellets; as a result the liquid diffusion improved the transport of KCl.[93]

In a fixed bed study by Tran et al.,[98, 112, 113] the K-capture reaction by kaolin flakes with a diameter of 0.5-2 mm was studied in a fixed bed reactor equipped with an alkali detector. The reaction temperature was in the range of 750-950 °C. The results revealed that potassium is captured by kaolin not only via chemical adsorption, but also physical adsorption. The comparison of results using KOH, KCl and K_2SO_4 show that the total absorption rate of KCl by kaolin was slightly higher than that of KOH, while the absorption rate of K_2SO_4 was significantly lower than that of KOH and KCl at the studied conditions.

The studies mentioned above were all conducted in fixed bed reactors where kaolin was present in the form of pellets or flakes, and the reaction time was as long as hours. The reaction conditions differ significantly from those in suspension fired boilers, where kaolin particles are well dispersed and the reaction time is only a few seconds.[14, 24] Additionally,

alkali species and kaolin may be exposed to flame temperature as high as 1700 °C.[4, 24] The reaction of K-species with kaolin at suspension-firing conditions takes place between condensed-phase kaolin particles (solid or melted) and the gaseous potassium species.[59, 107] The reaction may be influenced by external and internal diffusion, kinetic limitations and chemical equilibrium.[93, 98] To the authors' knowledge, quantitative study on K-capture by kaolin at suspension-fired conditions is not available, and no previous study is published where the influence of alkali species (KCl, KOH, K_2CO_3 and K_2SO_4) on the reaction with kaolin at suspension-fired conditions is investigated and compared.

Wendt and co-workers studied the gaseous sodium capture reaction by kaolin at suspension fired conditions using a 17-kW down flow combustor. The results showed that the capture rate of NaOH was obviously higher than that of NaCl. They proposed that NaOH was the only reacting species in both cases.[75, 97] However, whether the kinetics of Na-species and K-species capture by kaolin are the same has not been established.

In Chapter 3,[185] we have investigated the reaction between KOH and kaolin at suspension-fired conditions in the temperature range of 800-1450 °C. It was shown that 1 g kaolin reacting with gas phase KOH can capture up to 0.22 g K in the temperature range of 1100-1300 °C, with a kaolin particle size of D_{50} = 5.47 μm and a residence time of 1.2 s. At the applied conditions, the KOH conversion could be reasonably predicted by equilibrium calculations at temperatures above 1100 °C.[185]

The aim of this chapter is to get a thorough understanding of the K-capture reaction by kaolin under suspension-fired conditions so as to minimize or avoid ash-related problems caused by K-species during combustion of K-rich biomass fuels. More specifically, the objective is to understand the influences of the molar ratio of K/(Al+Si) in reactants, K-concentration, reaction temperature and K-species type on the K-capture reaction using kaolin at suspension-firing conditions.

4.2 Experimental

The experiments were conducted in the DTU entrained flow reactor (EFR) which is described in Chapter 2. The experimental conditions are summarized in Table 4-1. Two series of experiments were conducted in the EFR: K-salt vaporization experiments and K-capture experiments using kaolin. The experimental conditions are summarized in Table 4-1. In the K-salt vaporization experiments (series A in Table 4-1), solutions of K_2CO_3, KCl and K_2SO_4 respectively were fed into the EFR without kaolin, to study the vaporization and

transformation of K_2CO_3, KCl and K_2SO_4 at high temperatures. The concentration of KCl was kept at 500 ppmv, while K_2CO_3 and K_2SO_4 were kept at 250 ppmv to maintain the same K-concentration in the flue gas. The solid samples in the cyclone and filter were carefully collected, weighted and stored for further analysis.

Table 4-1. Experimental conditions of the EFR experiments.

Experimental series	K-species	Additives	Temp./°C	Gas residence time/s	K in gas /ppmv	K/(Al+Si)
(A) K-salt vaporization experiments	K_2CO_3	No additive	800, 900, 1100, 1300, 1450	1.2	500	No Al, Si
	KCl					
	K_2SO_4					
(B) K_2CO_3-capture by kaolin (impact of **K-concentration**)	K_2CO_3	kaolin	1100	1.2	50	0.048
					500	0.481
					1000	0.961
(C) K_2CO_3-capture by kaolin (impact of **temperature**)	K_2CO_3	kaolin	800	1.2	500	0.481
			900			
			1100			
			1300			
			1450			
(D) KCl-capture by kaolin (impact of **K-concentration**)	KCl	kaolin	1300	1.0-1.2	50*	0.048
					250*	0.240
					500*	0.481
					750	0.721
					1000	0.961
(E) KCl-capture by kaolin (impact of **temperature**)	KCl	kaolin	800	1.0-1.2	50, 500	0.048, 0.481
			900			
			1100			
			1300*			
			1450			
(F) KCl-capture by kaolin (impact of **residence time**)	KCl	kaolin	1100, 1300	0.6	500	0.481
				0.8		
				1.2		
				1.9		
(G) K_2SO_4-capture by kaolin (impact of **K-concentration**)	K_2SO_4	kaolin	1100	1.2	50	0.048
					500	0.481
					1000	0.961
(H) K_2SO_4-capture by kaolin (impact of **temperature**)	K_2SO_4	kaolin	800	1.2	500	0.481
			900			
			1100			
			1450			

Note: *Experiments were repeated.

In the K-capture experiments (series B-H in Table 4-1), KCl, K_2CO_3 and K_2SO_4 were fed into the EFR together with kaolin, respectively. The impact of K-concentration, molar ratio of

K/(Al+Si) in reactants, reaction temperature, and gas residence time on the K-capture reaction was investigated. In the K-capture experiments, the concentration of kaolin in the flue gas inside the EFR was kept constant. While the concentration of K-salts in the flue gas was varied, and the molar K/(Al+Si) ratio in the reactants changed consequently. The K-concentration in the flue gas was varied from 50 ppmv to 1000 ppmv, and the molar K/(Al+Si) ratio in the reactants changed from 0.048 to 0.961 correspondingly. For each experiment, solid products were carefully collected from the cyclone and filter. The representativeness of the collected solid samples was examined by comparing the molar ratios of K/(Al+Si) in collected solid samples with that of the fed reactants.

4.3 Results and discussion

4.3.1 Vaporization and transformation of K-salts

The vaporization and transformation of K_2CO_3, KCl, and K_2SO_4 at high temperatures may affect the K-capture reaction, and it was studied at the conditions shown in series (A) of Table 4-1. K-species (K_2CO_3, KCl and K_2SO_4) entered into the EFR in a form of slurry droplets. When water in these droplets evaporated, condensed phase K-salts were formed, which could be vaporized to gas phase or stay as condensed phase in the reactor. If all the K-salts are vaporized, aerosols will be formed and captured only by the filter. If the K-salts are not fully vaporized, the condensed K-salts can generate some larger particles being collected by the cyclone. The mass fraction of the solid samples collected in the cyclone and filter is shown in Figure 4-1 (A, B and C). Results of corresponding equilibrium calculations were shown in Figure 4-1 (D, E and F).

For K_2CO_3, the experimental results reveal that, at temperatures ≥ 1100 °C, all solid samples were captured by the filter, implying a complete vaporization was obtained. At 800 °C and 900 °C, 1.6 % and 2.7 % of the product samples was captured by the cyclone, respectively. An increase of CO_2 concentration by 262 ppmv in flue gas was observed at 1100 °C and above, corresponding to a complete decomposition of K_2CO_3 forming KOH and CO_2. This also indicates that the recarbonation of KOH during the gas cooling process is negligible, probably due to the fast cooling rate and the short residence time. At 800 and 900 °C, the CO_2 concentration increased by 122 ppmv and 213 ppmv, showing a decomposition fraction of 48.8 % and 85.2 %, respectively. However, XRD analysis of the collected solid samples showed that $K_2CO_3{\cdot}1.5H_2O$ is the only solid product collected from the K_2CO_3 vaporization experiments. The results imply that, the KOH aerosols collected by the metal filter probably

reacted with CO_2 and moisture during the process of collecting, storage or delivery for XRD analysis, forming $K_2CO_3 \cdot 1.5H_2O$.

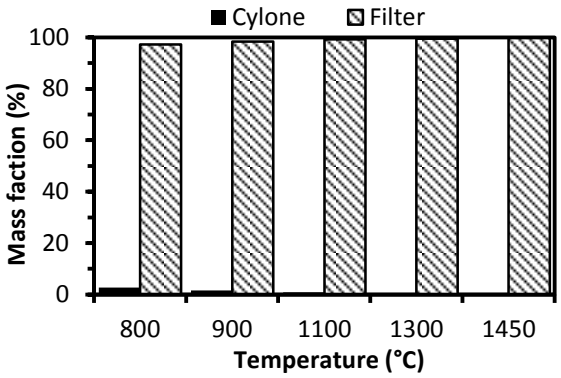

(A) K_2CO_3 vaporization in EFR

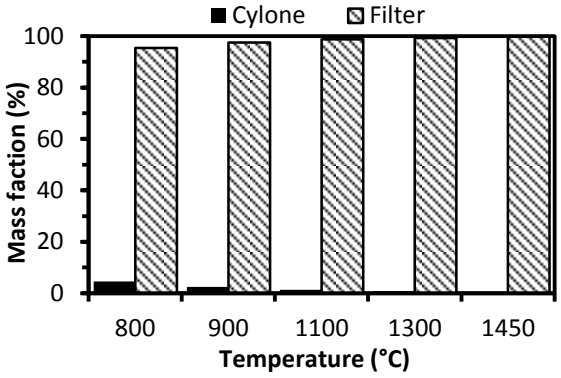

(B) KCl vaporization in EFR

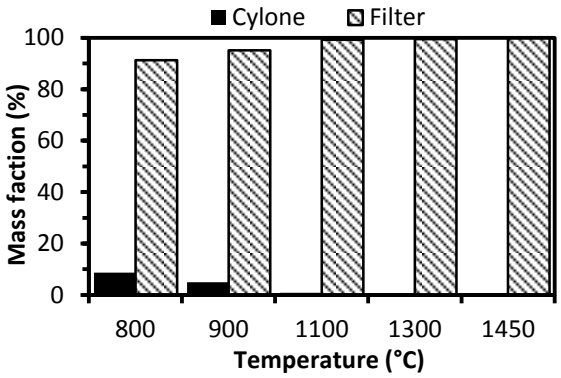

(C) K_2SO_4 vaporization in EFR

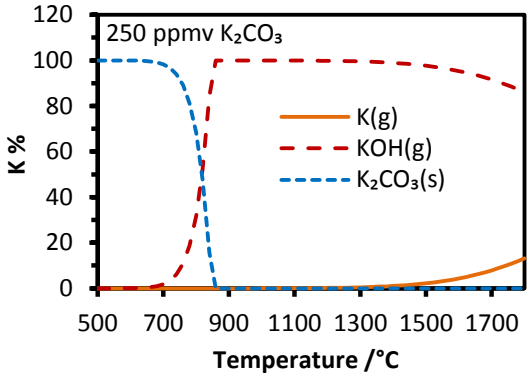

(D) Equilibrium calculation (K_2CO_3)

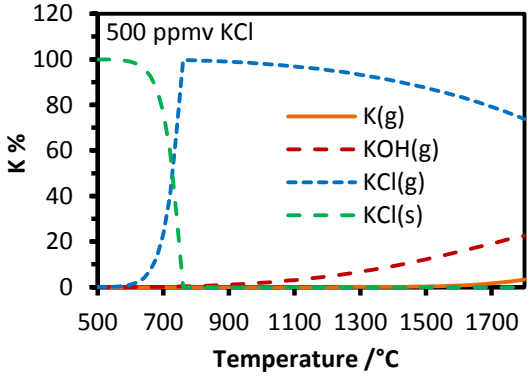

(E) Equilibrium calculation (KCl)

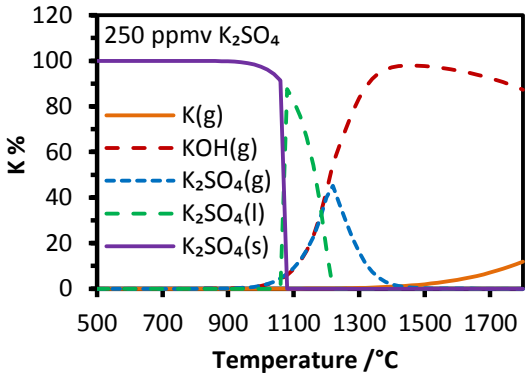

(F) Equilibrium calculation (K_2SO_4)

Figure 4-1. Mass distribution of solid samples collected in the cyclone and filter from K-salt vaporization experiments (A) K_2CO_3 (B) KCl (C) K_2SO_4, and corresponding equilibrium calculation results (D) K_2CO_3 (E) KCl (F) K_2SO_4.

The KCl vaporization experiments show that all samples were collected in the filter at temperatures above 1100 °C, implying a complete vaporization of KCl at 1100 °C. At 800 and 900 °C, 4.6 % and 2.5 % of the product solid samples were collected in the cyclone. The equilibrium calculations on KCl showed that at temperatures above 740 °C, potassium appeared mainly as gaseous KCl. Above 800 °C, some KOH appeared but gaseous KCl

remained the dominant K-species. Solid samples collected from KCl vaporization experiments were analyzed with XRD and showed that all collected products were KCl, with no potassium carbonate or potassium hydrate detected.

The equilibrium calculation results showed that the melting point of K_2SO_4 was 1070 °C, and KOH starts to form at 900 °C. At 900-1070 °C, solid, gaseous K_2SO_4 and gaseous KOH co-existed, while at 1070-1220 °C, liquid, gaseous K_2SO_4 and gaseous KOH co-existed, with gaseous K_2SO_4 being the dominant species. At temperatures 1200-1800 °C, gaseous KOH became the major K-species. The mass distribution of the solid samples collected from K_2SO_4 vaporization experiments is illustrated in Figure 4-1 (C). It shows that more than 99 % of the solid samples were collected from the filter above 1100 °C. However the filter fraction is obviously lower at 800 °C and 900 °C, as 91 % and 95 % respectively, indicating a lower degree of K_2SO_4 vaporization. The XRD analysis of the solid product samples shows that only K_2SO_4 was present, although a decomposition of K_2SO_4 forming KOH and SO_3/SO_2 was predicted by the equilibrium calculations. This is probably because K_2SO_4 was reformed rapidly during the cooling down process. This can also explain the fact that no SO_2 was detected in the flue gas during the K_2SO_4 vaporization experiments.

4.3.2 K_2CO_3 capture by kaolin

4.3.2.1 Equilibrium calculation

The equilibrium calculation results of K_2CO_3 capture by kaolin at 50-1000 ppmv K (25-500 ppmv K_2CO_3) in flue gas showed that the K-capture behavior of K_2CO_3 was the same as that of KOH,[185] so the equilibrium calculation results of K_2CO_3 capture by kaolin is not included in the thesis. Detailed results can be found in Appendix C of the thesis. This is because at high temperatures, K_2CO_3 decomposed forming KOH and CO_2, and then the formed KOH reacted with kaolin.

4.3.2.2 Impact of potassium concentration

The experimental results of K_2CO_3 capture by kaolin at different K-concentrations at 1100 °C are compared with the equilibrium calculation results in Figure 4-2. The experimental C_K and X_K generally followed the equilibrium predictions. The C_K increased from 0.019 g K/(g additive) to 0.216 g K/(g additive) when the K_2CO_3 concentration increased from 25 ppmv to 250 ppmv (molar ratio of K/(Al+Si) in reactants changed from 0.048 to 0.481), with X_K staying almost constant, at around 82.0 %. When the concentration of K_2CO_3 increased further to 375 ppmv (K/(Al+Si) = 0.721) and 500 ppmv (K/(Al+Si) = 0.961), C_K did not

increase compared to that at 250 ppmv K_2CO_3. At the same time, X_K decreased from 80.6 % to 40.8 %, indicating that more K_2CO_3 stayed unreacted with kaolin. This is probably because, as indicated by the equilibrium calculation, a complete conversion of kaolin to K-aluminosilicate has taken place, at 250 ppmv K_2CO_3. Thereby, the increased K_2CO_3 was not captured by kaolin forming K-aluminosilicates at 375 and 500 ppmv K_2CO_3.

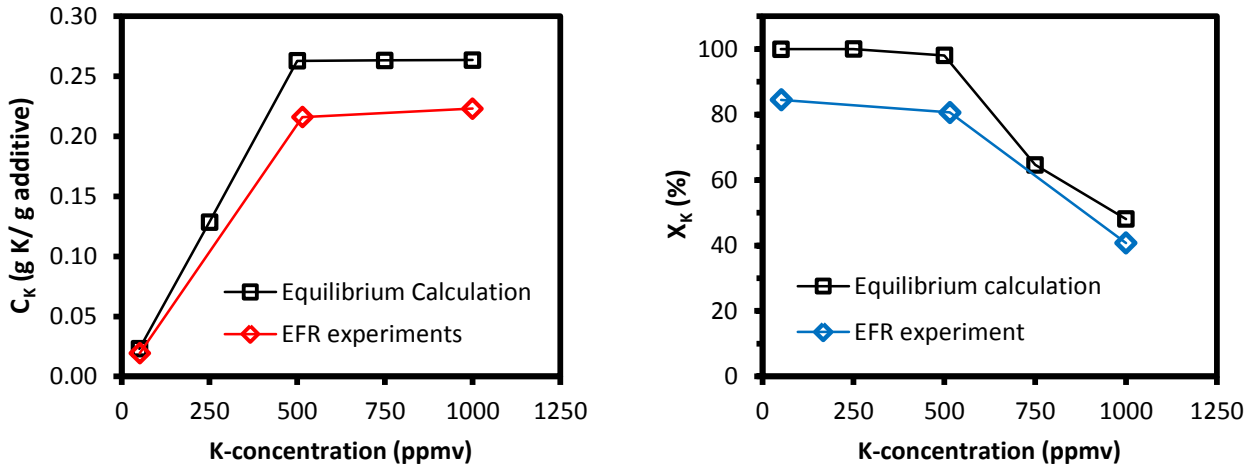

(A) K-capture level (C_K) (B) K-conversion (X_K)

Figure 4-2. K-capture level (C_K) and K conversion (X_K) of K_2CO_3-capture by kaolin at K_2CO_3 concentration varied from 25 ppmv to 500 ppmv (molar ratio of K/(Al+Si) in reactants changed from 0.048 to 0.961). Reaction temperature was 1100 °C. Gas residence time was 1.2 s. Equilibrium calculation results were included for comparison.

4.3.2.3 Impact of reaction temperature

The influence of reaction temperature on the K_2CO_3-capture reaction by kaolin was investigated experimentally at 800-1450 °C. The K_2CO_3 concentration was kept constant at 250 ppmv (500 ppmv K in flue gas), with a gas residence time of 1.2 s. The experimental C_K and X_K are compared with the equilibrium calculation results in Figure 4-3. It is seen that C_K increased from 0.159 g K/(g additive) to 0.231 g K/(g additive) by 31.1 %, when the reaction temperature increased from 800 °C to 1300 °C. Simultaneously, X_K increased from 59.3 % to 86.1 %. Whereas, when the reaction temperature increased further to 1450 °C, the C_K and X_K decreased slightly to 0.204 g K/(g additive) and 66.1 %, respectively. This is likely due to the change of reaction products. Equilibrium calculation suggests a decreased formation of kaliophilite ($KAlSiO_4$) and an increased formation of leucite ($KAlSi_2O_6$) at 1450 °C. However, leucite was not detected by XRD in the 1450 °C sample, probably because some amorphous K-species with K:Al:Si = 1:1:2 was formed. Considering the results on KOH-capture by kaolin

in Chapter 3,[185] 900-1300 °C is a preferable temperature window for KOH and K_2CO_3 capture by kaolin.

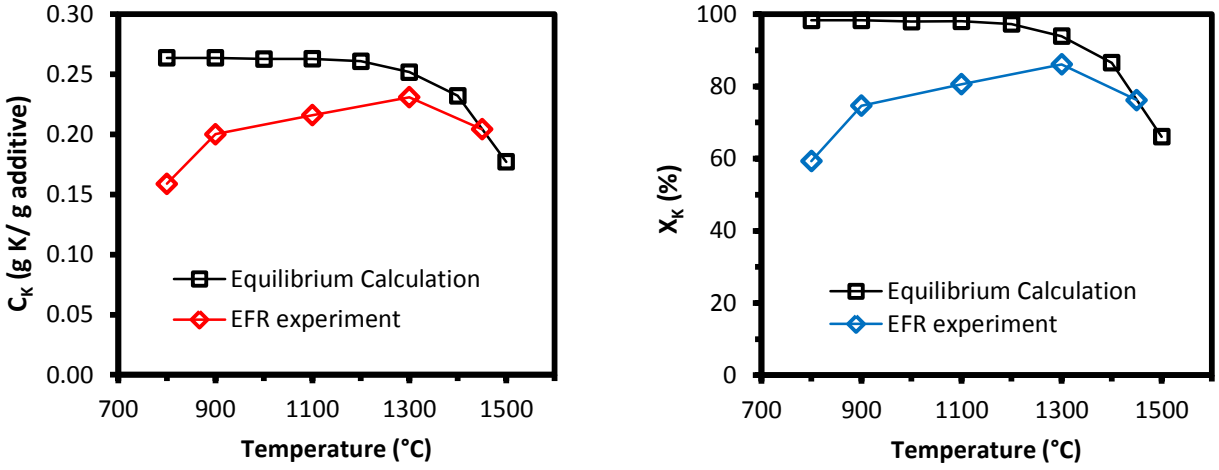

(A) K-capture level (C_K) (B) K-conversion (X_K)

Figure 4-3. K-capture level (C_K) and K-conversion (X_K) of K_2CO_3 capture by kaolin at different temperatures (800-1450 °C). K_2CO_3 concentration was 250 ppmv (K-concentration was 500 ppmv), molar ratio of K/(Al+Si) in reactants was 0.481, residence time was 1.2 s. Equilibrium calculation results are included for comparison.

4.3.3 KCl capture by kaolin

4.3.3.1 Equilibrium calculation

The results of equilibrium calculations of KCl capture by kaolin at different temperatures and KCl-concentrations were summarized in Table 4-2. Detailed results of the equilibrium calculation are available in Appendix C. The type of the K-aluminosilicate products formed varied with the molar K/(Al+Si) ratio in the reactants. As shown in Table 4-2, with a molar ratio of K/(Al+Si) = 0.048 (50 ppmv KCl), the main K-aluminosilicate product was sanidine ($KAlSi_3O_8$) with a molar K:Al:Si ratio of 1:1:3. As the molar K/(Al+Si) ratio in reactants increased to 0.240 (250 ppmv KCl), leucite ($KAlSi_2O_6$) with a molar K:Al:Si ratio of 1:1:2, became the dominant K-aluminosilicate with some sanidine ($KAlSi_3O_8$) co-existing. When the molar ratio of K/(Al+Si) in reactants increased to 0.481 or higher (≥ 500 ppmv KCl), kaliophilite ($KAlSiO_4$) with a molar K:Al:Si ratio of 1:1:1 was predicted at the lower temperature range (800-900 °C), while at high temperatures (1100-1450 °C), leucite ($KAlSi_2O_6$) remained the dominant K-aluminosilicate.

4.3.3.2 Impact of potassium concentration

The impact of KCl concentration on the KCl-capture reaction by kaolin was investigated by EFR experiments using 50-1000 ppmv KCl at a reactor temperature of 1300 °C. The experimental C_K and X_K are compared with the equilibrium calculation results in Figure 4-4. The trend of the experimental C_K and X_K generally followed the equilibrium calculation data at 1300 °C. The C_K increased significantly from 0.020 g K/(g additive) to 0.131 g K/(g additive), when the KCl-concentration increased from 50 to 500 ppmv (K/(Al+Si) increased from 0.048 to 0.481 correspondingly). However, when the KCl-concentration increased further to 750 ppmv and 1000 ppmv (with a K/(Al+Si) molar ratio of 0.721 and 0.961, respectively), C_K did not increase. On the other hand, X_K decreased significantly from 90.1 % to about 25.3 % when the KCl-concentration increased from 50 ppmv to 1000 ppmv. This is probably because all the free Si has been consumed forming K-aluminosilicate at 500 ppmv KCl, with no Si available for further KCl capture. According to the equilibrium calculation, the main product of the KCl-kaolin reaction is leucite ($KAlSi_2O_6$), and the K-capture level is limited by the availability of Si. The formation of leucite was confirmed by the XRD analysis results, see Figure 4-6.

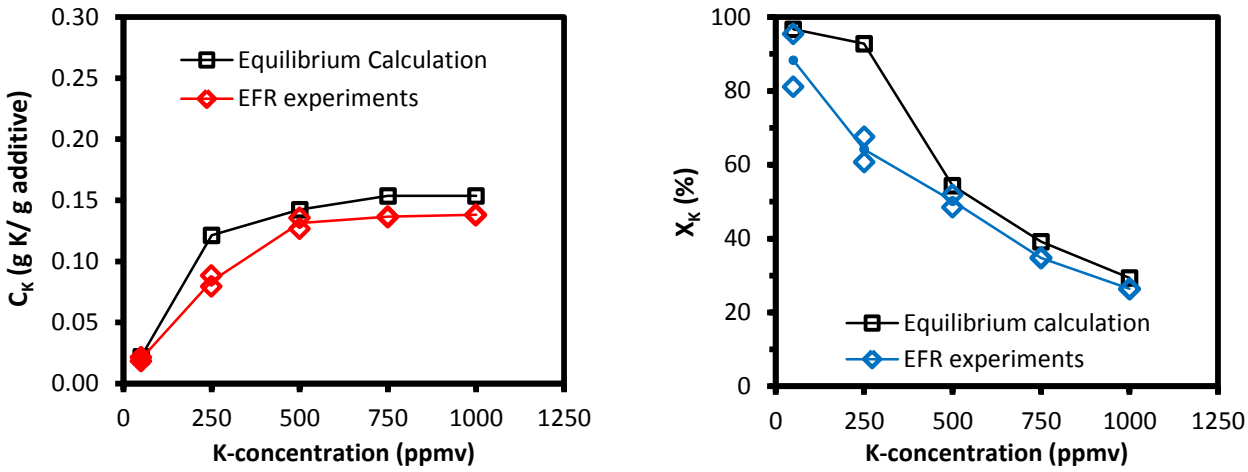

(A) K-capture level (C_K) (B) K-conversion (X_K)

Figure 4-4. K-capture level (C_K) and K-conversion (X_K) of KCl capture by kaolin at 50-1000 ppmv KCl, the corresponding molar K/(Al+Si) ratio varied from 0.048 to 0.961, reaction temperature was 1300 °C. Equilibrium calculation results are included for comparison.、

4.3.3.3 Impact of reaction temperature

To investigate the influence of reaction temperature on the KCl-capture reaction, experiments were conducted at temperatures from 800 °C to 1450 °C. In all experiments, the KCl concentration in flue gas was 500 ppmv, corresponding to a molar K/(Al+Si) ratio of

0.481 in reactants. The gas residence time was 1.2 s. The experimental results are compared to the equilibrium calculation results in Figure 4-5.

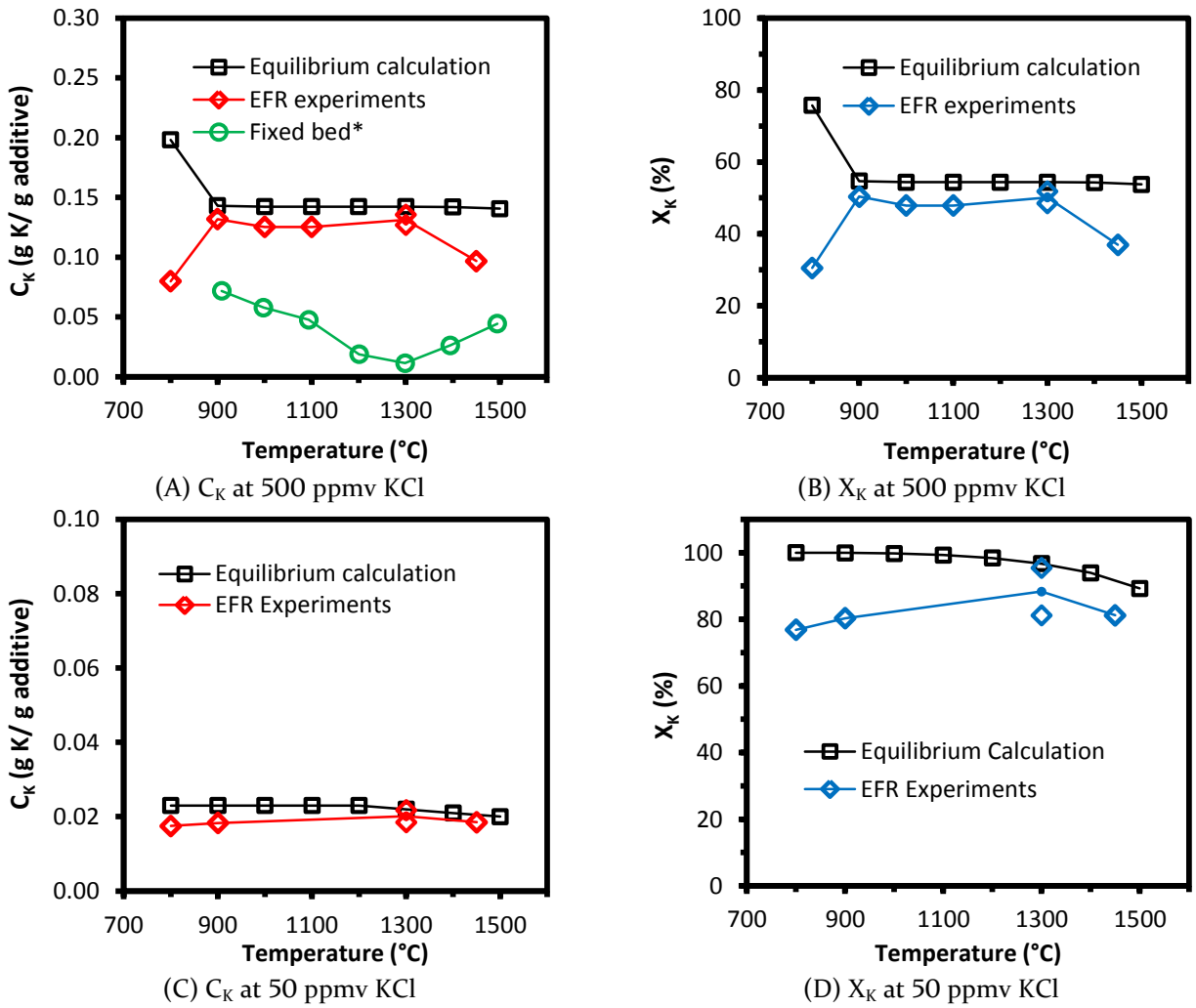

(A) C_K at 500 ppmv KCl

(B) X_K at 500 ppmv KCl

(C) C_K at 50 ppmv KCl

(D) X_K at 50 ppmv KCl

Figure 4-5. C_K (K-capture level) and X_K (K-conversion) of KCl capture by kaolin at different temperatures (800-1450 °C). KCl-concentration was 500 ppmv in (A) and (B), and it was 50 ppmv in (C) and (D). *Fixed bed data was calculated from literature (1100 °C, 1000 ppmv KCl, residence time was 1 hour).[93]

As shown in Figure 4-5 (A) and (B), at 500 ppmv KCl, the K-capture level (C_K) was close to the equilibrium prediction and stayed steady at about 0.142 g K/(g additive) at temperatures from 900 °C to 1300 °C. The K-conversion (X_K) was also steady at about 55.0 %. The C_K and X_K of KCl were lower than that of KOH-kaolin reaction (C_K of KOH was 0.193-0.241 g K/(g additive), and X_K was 72.1-90.0 %). This could be explained that kaliophilite ($KAlSiO_4$) was detected by XRD in the KOH-reacted kaolin, while leucite ($KAlSi_2O_6$) was detected in the KCl-reacted kaolin (Figure 4-6). The formation of leucite ($KAlSi_2O_6$) consumed more Si than kaliophilite ($KAlSiO_4$).

At 800 °C and 1450 °C, C_K was obviously lower than that at 900-1300 °C. At 800 °C, the reaction is probably kinetically controlled and do not reach the equilibrium state. Additionally, the incomplete vaporization of KCl at 800 °C, may also contribute to the lower KCl conversion. At 1450 °C, the decrease of C_K may be due to an increased transformation of kaolinite into mullite and amorphous silica,[98] which are less reactive towards KCl.[93]

In Figure 4-5 (A), C_K was also compared with the results from a study using a fixed bed reactor where cylindrical kaolin pellets of diameter of 1.5 mm were utilized for KCl capture.[93] The C_K values obtained in the fixed bed reactor are obviously lower than that in the EFR experiments, although the reaction time in the fixed bed reactor (about 1 hour) was much longer than that in the EFR (about 1 second). One possible reason is that in the fixed bed reactor, probably, it was actually mullite that reacted with KCl due to a long residence time of up to 1 hour and the high temperature. Another possible reason is that kaolin was in the shape of pellets with a diameter of 1.5 mm, where the reaction was strongly controlled by internal diffusion. Another difference is that the results from fixed bed reactor have an opposite temperature-dependence trend comparing to that of the EFR. This is presumably because the controlling mechanisms in the two reactors are different. In the fixed bed experiments, the reaction was controlled by internal diffusion as mentioned above. Thus C_K decreased from 900 °C to 1300 °C, due to the increased sintering degree of kaolin pellets. However, C_K increased again when temperature was further increased to 1400 °C and 1500 °C, due to the enhanced internal diffusion caused by melting of kaolin pellets.[93] However, in the EFR, the reaction was mainly equilibrium controlled at 900-1300 °C. In summary, the favorable temperature window for KCl-capture by kaolin is 900-1300 °C.

Figure 4-5 (C) and (D) show that at 50 ppmv KCl, the experimental X_K and C_K were almost constant, and they generally followed the equilibrium predictions. The C_K was about 0.021 g K/(g additive) with about 80.2 % KCl captured by kaolin forming water-insoluble K-aluminosilicate.

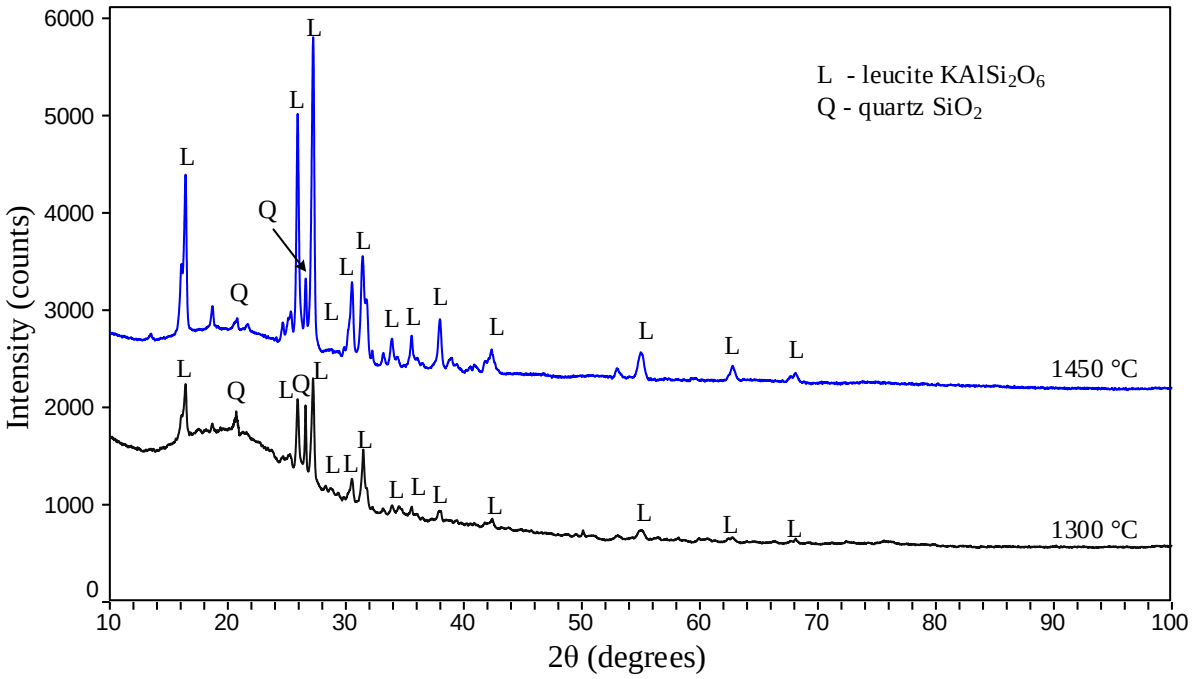

Figure 4-6. XRD spectra of water-washed KCl-reacted kaolin samples at 1300 °C and 1450 °C, KCl concentration in flue gas was 500 ppmv, molar K/(Al+Si) ratio in reactants was 0.481, gas residence time was about 1.0 s.

The XRD spectra of water-washed KCl-reacted kaolin samples at 1300 °C and 1450 °C are compared in Figure 4-6. The results show that leucite ($KAlSi_2O_6$) was formed by the KCl-kaolin reaction at 1300 °C and 1450 °C. At 1450 °C, peaks of leucite are much stronger than that at 1300 °C. However, the ICP-OES analysis results showed than more leucite was formed at 1300 °C than experiments at 1450 °C. This indicates that a large amount of amorphous K-aluminosilicate was probably present at 1300 °C, and the leucite formed at 1450 °C was much more crystalline.

4.3.3.4 Impact of gas residence time

The impact of gas residence time on the KCl-capture reaction was studied at 1100 °C and 1300 °C, respectively. The KCl concentration in the flue gas was kept constant at 500 ppmv, with K/(Al+Si) = 0.481. The C_K and X_K results are shown in Figure 4-7.

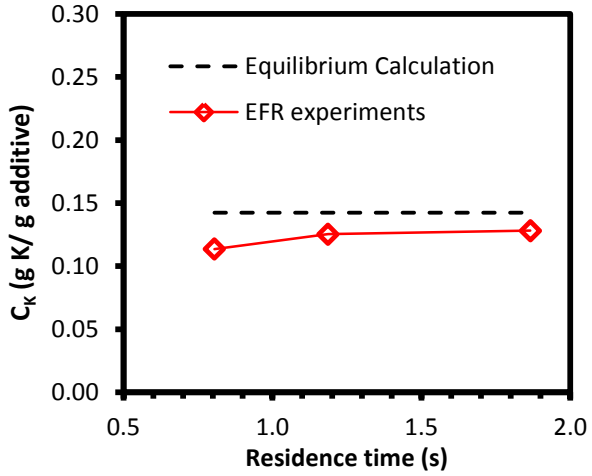

(A) K-capture level (C_K) at 1100 °C

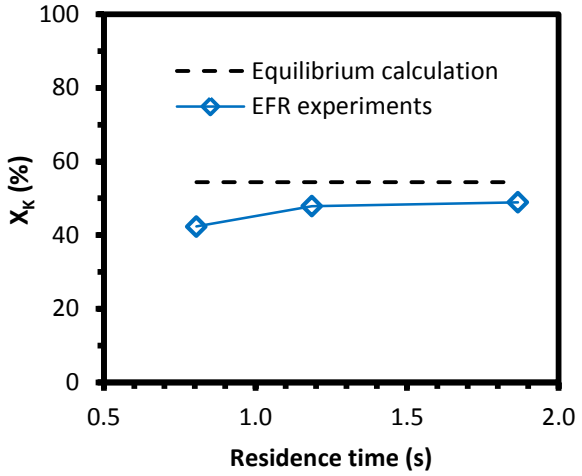

(B) K-conversion (X_K) at 1100 °C

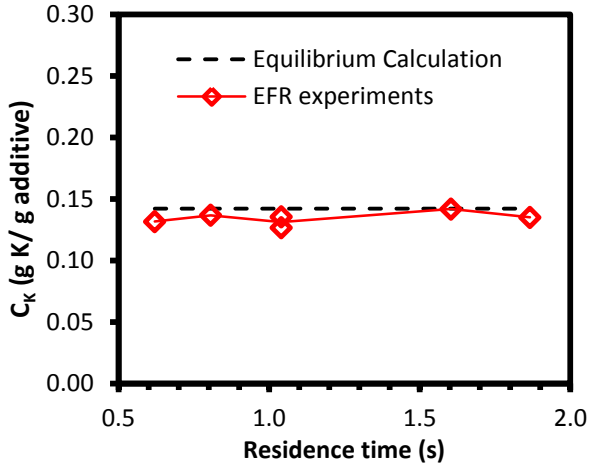

(C) K-capture level (C_K) at 1300 °C

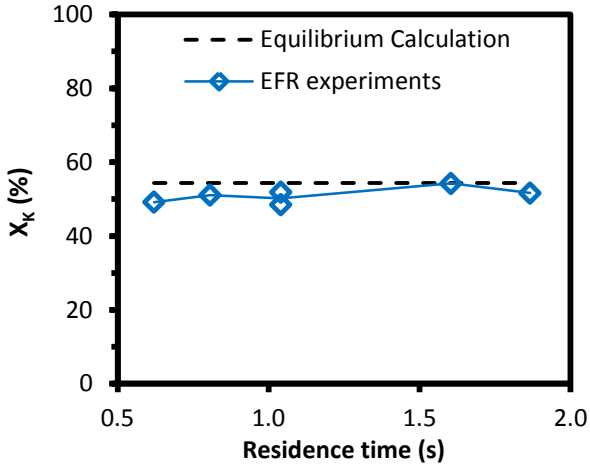

(D) K-conversion (X_K) at 1300 °C

Figure 4-7. K-capture level (C_K) and K-conversion (X_K) of KCl capture by kaolin at different gas residence time. KCl concentration in flue gas was 500 ppmv, (molar K/(Al+Si) ratio in reactants was 0.481). Reaction temperature was 1100 °C and 1300 °C.

The results in Figure 4-7 (A) and (B) show that at 1100 °C when the gas residence time increased from 0.8 s to 1.2 s, the C_K increased from 0.114 g K/(g additive) to 0.128 g K/(g additive) by 12.3 %. The X_K increased from 42.4 % to 49.0 %. This indicates that at 1100 °C, with a gas residence time below 1.2 s, the K-capture reaction is to some degree limited by kinetics or diffusion.

The results at 1300 °C show that the value of C_K and X_K did not change when the residence time increased from 0.6 s to 1.9 s and the number was close to the equilibrium prediction, implying that the KCl-capture reaction was at equilibrium. The results imply that at 1300 °C, with kaolin particles of D_{50} = 5.47 μm, it took very short time (≤ 0.6 s) for the KCl-capture reaction to reach equilibrium.

4.3.4 K_2SO_4 capture by kaolin

4.3.4.1 Equilibrium Calculation

The equilibrium calculation results of K_2SO_4 capture by kaolin at 25-500 ppmv K_2SO_4 (K-concentration was 50 ppmv to 1000 ppmv) are summarized in Table 4-3. Detailed results of the equilibrium calculation are available in Appendix C. The type and amount of K-aluminosilicate formed changed with the molar ratio of K/(Al+Si) in reactants (K_2SO_4 concentration in flue gas). At 25 ppmv K_2SO_4 (molar ratio of K/(Al+Si) = 0.048), sanidine ($KAlSi_3O_8$) is predicted to be the main K-aluminosilicate product, with K:Al:Si = 1:1:3. At 125 ppmv K_2SO_4 (molar ratio of K/(Al+Si) = 0.240), leucite ($KAlSi_2O_6$) became the main K-aluminosilicate product, with sanidine ($KAlSi_3O_8$) co-existing. At 250, 375 and 500 ppmv K_2SO_4, (molar ratio of K/(Al+Si) ≥ 0.481), kaliophilite ($KAlSiO_4$) turned to be the main K-aluminosilicate product.

Table 4-2. Results of equilibrium calculations of KCl-capture by kaolin.

Input conditions	Temp. /°C	K-species appearing	Al-con.	Si-con.	K-con.	K-capture/(g K/(g additive))
50 ppmv KCl, K/(Al+Si) =0.048	800	100 % $KAlSi_3O_8$	9 %	24 %	100 %	0.023
	900	100 % $KAlSi_3O_8$	9 %	24 %	100 %	0.023
	1100	99 % $KAlSi_3O_8$ + 1 % KCl	9 %	24 %	99 %	0.023
	1300	97 % $KAlSi_3O_8$ + 3 % KCl	8 %	23 %	97 %	0.022
	1450	92 % $KAlSi_3O_8$ + 7 % KCl + 1 % KOH	8 %	22 %	92 %	0.022
250 ppmv KCl, K/(Al+Si) =0.240	800	21 % $KAlSi_3O_8$ + 79 % $KAlSi_2O_6$	50 %	98 %	100 %	0.131
	900	23 % $KAlSi_3O_8$ + 77 % $KAlSi_2O_6$ + 1 % KCl	50 %	98 %	99 %	0.130
	1100	28 % $KAlSi_3O_8$ + 70 % $KAlSi_2O_6$ + 3 % KCl	49 %	99 %	97 %	0.128
	1300	33 % $KAlSi_3O_8$ + 60 % $KAlSi_2O_6$ + 7 % KCl	46 %	97 %	93 %	0.121
	1450	45 % $KAlSi_3O_8$ + 41 % $KAlSi_2O_6$ + 13 % KCl	43 %	97 %	87 %	0.113
500 ppmv KCl, K/(Al+Si) =0.481	800	33 % $KAlSi_2O_6$ + 43 % $KAlSiO_4$ + 24 % KCl	75 %	100 %	76 %	0.198
	900	54 % $KAlSi_2O_6$ + 1 % $KAlSiO_4$ + 45 % KCl	54 %	100 %	55 %	0.143
	1100	54 % $KAlSi_2O_6$ + 46 % KCl	54 %	100 %	54 %	0.142
	1300	54 % $KAlSi_2O_6$ + 45 % KCl	54 %	100 %	54 %	0.142
	1450	54 % $KAlSi_2O_6$ + 45 % KCl + 1 % KOH	54 %	100 %	54 %	0.142
750 ppmv KCl, K/(Al+Si) =0.721	800	10 % $KAlSi_2O_6$ + 56 % $KAlSiO_4$ + 35 % KCl	98 %	100 %	65 %	0.256
	900	22 % $KAlSi_2O_6$ + 32 % $KAlSiO_4$ + 47 % KCl	80 %	100 %	53 %	0.209
	1100	38 % $KAlSi_2O_6$ + 62 % KCl	56 %	100 %	38 %	0.147
	1300	37 % $KAlSi_2O_6$ + 62 % KCl	56 %	100 %	37 %	0.147
	1450	37 % $KAlSi_2O_6$ + 61 % KCl + 1 % KOH	56 %	100 %	37 %	0.147
1000 ppmv KCl, K/(Al+Si) =0.961	800	4 % $KAlSi_2O_6$ + 47 % $KAlSiO_4$ + 49 % KCl	100 %	100 %	50 %	0.263
	900	6 % $KAlSi_2O_6$ + 42 % $KAlSiO_4$ + 52 % KCl	95 %	100 %	48 %	0.251
	1100	27 % $KAlSi_2O_6$ + 73 % KCl	54 %	100 %	27 %	0.142
	1300	27 % $KAlSi_2O_6$ + 72 % KCl + 1 % KOH	54 %	100 %	27 %	0.142
	1450	27 % $KAlSi_2O_6$ + 71 % KCl + 1 % KOH	54 %	100 %	27 %	0.142

Table 4-3. Equilibrium calculation results of K_2SO_4-capture by kaolin.

Input conditions	Temp. /°C	K-species appearing	Al-con.	Si-con.	K-con.	K-capture/(g K/(g additive))
25 ppmv K_2SO_4, K/(Al+Si) = 0.048	800	100 % $KAlSi_3O_8$	10 %	28 %	100 %	0.027
	900	100 % $KAlSi_3O_8$	10 %	28 %	100 %	0.027
	1100	100 % $KAlSi_3O_8$	10 %	28 %	100 %	0.027
	1300	100 % $KAlSi_3O_8$	10 %	28 %	100 %	0.027
	1450	99 % $KAlSi_3O_8$ + 1 % KOH	10 %	28 %	99 %	0.026
125 ppmv K_2SO_4, K/(Al+Si) = 0.240	800	92 % $KAlSi_2O_6$ + 8 % $KAlSi_3O_8$	51 %	98 %	100 %	0.134
	900	92 % $KAlSi_2O_6$ + 8 % $KAlSi_3O_8$	51 %	98 %	100 %	0.134
	1100	93 % $KAlSi_2O_6$ + 7 % $KAlSi_3O_8$	51 %	97 %	100 %	0.134
	1300	93 % $KAlSi_2O_6$ + 7 % $KAlSi_3O_8$	51 %	96 %	100 %	0.134
	1450	94 % $KAlSi_2O_6$ + 5 % $KAlSi_3O_8$	51 %	96 %	100 %	0.133
250 ppmv K_2SO_4, K/(Al+Si) = 0.481	800	53 % $KAlSi_2O_6$ + 47 % K_2SO_4	54 %	100 %	53 %	0.142
	900	53 % $KAlSi_2O_6$ + 47 % K_2SO_4	54 %	100 %	53 %	0.142
	1100	7 % $KAlSi_2O_6$ + 90 % % $KAlSiO_4$ + 1 % KOH	100 %	99 %	98 %	0.262
	1300	13 % $KAlSi_2O_6$ + 80 % % $KAlSiO_4$ + 6 % KOH	95 %	100 %	93 %	0.250
	1450	31 % $KAlSi_2O_6$ + 44 % % $KAlSiO_4$ + 24 % KOH	76 %	100 %	75 %	0.201
375 ppmv K_2SO_4, K/(Al+Si) = 0.721	800	35 % $KAlSi_2O_6$ + 65 % K_2SO_4	54 %	99 %	35 %	0.141
	900	35 % $KAlSi_2O_6$ + 65 % K_2SO_4	54 %	100 %	35 %	0.142
	1100	5 % $KAlSi_2O_6$ + 61 % % $KAlSiO_4$ + 33 % K_2SO_4 + 2 % KOH	100 %	100 %	65 %	0.263
	1300	5 % $KAlSi_2O_6$ + 61 % % $KAlSiO_4$ + 5 % K_2SO_4 + 29 % KOH	100 %	100 %	65 %	0.263
	1450	5 % $KAlSi_2O_6$ + 61 % % $KAlSiO_4$ + 34 % KOH	100 %	100 %	65 %	0.263
500 ppmv K_2SO_4, K/(Al+Si) = 0.961	800	26 % $KAlSi_2O_6$ + 74 % K_2SO_4	54 %	100 %	26 %	0.141
	900	26 % $KAlSi_2O_6$ + 74 % K_2SO_4	54 %	100 %	26 %	0.142
	1100	4 % $KAlSi_2O_6$ + 45% % $KAlSiO_4$ + 50 % K_2SO_4 + 1 % KOH	100 %	100 %	49 %	0.263
	1300	4 % $KAlSi_2O_6$ + 45% % $KAlSiO_4$ + 14 % K_2SO_4 + 36 % KOH	100 %	100 %	49 %	0.263
	1450	4 % $KAlSi_2O_6$ + 45% % $KAlSiO_4$ + 1 % K_2SO_4 + 49 % KOH	100 %	100 %	49 %	0.263

4.3.4.2 Impact of potassium concentration

The experimental K-capture level (C_K) and K-conversion (X_K) at 25-500 ppmv K_2SO_4 (50-1000 ppmv K) were compared with the equilibrium calculation results in Figure 4-8. Generally, the experimental C_K and X_K were obviously lower than the equilibrium data, although they followed a similar trend. The experimental C_K increased from 0.018 g K/(g additive) to 0.115 g K/(g additive), when the K_2SO_4-concentration in flue gas increased from 25 ppmv to 250 ppmv. At the same time, the experimental X_K decreased from 68.0 % to 42.7 % correspondingly. As K_2SO_4-concentration increased further to 500 ppmv (K/(Al+Si) = 0.961), the C_K did not increase, while X_K decreased significantly to 21.7 %.

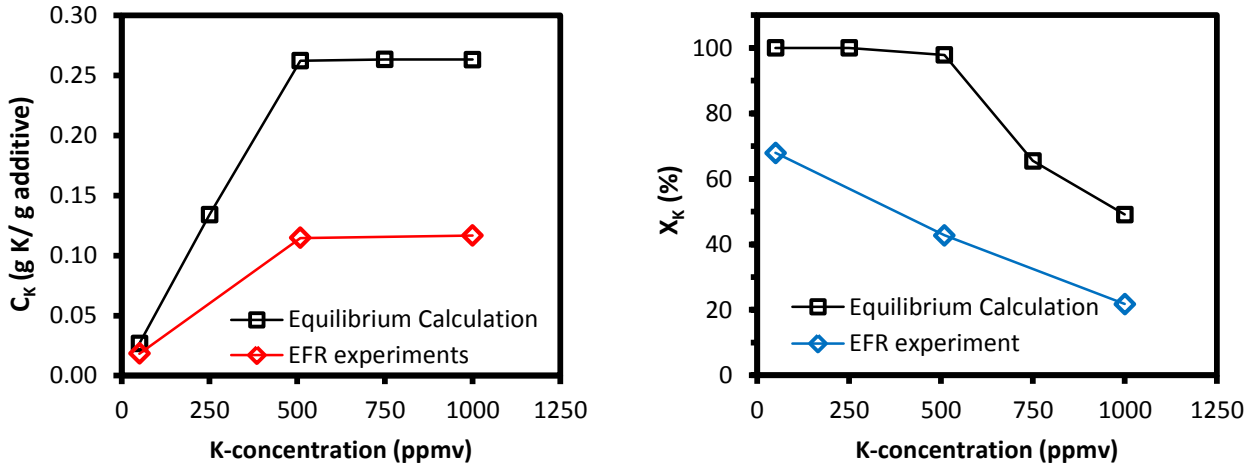

(A) K-capture level (C_K) (B) K-conversion (X_K)

Figure 4-8. C_K (K-capture level) and X_K (K-conversion) of K_2SO_4 capture by kaolin at 25-500 ppmv K_2SO_4 (50-1000 ppmv K) in flue gas (molar ratio of K/(Al+Si) in reactants varied from 0.048 to 0.961). Reaction temperature was 1100 °C. Gas residence time was 1.2 s. Equilibrium calculation results were included for comparison.

4.3.4.3 Impact of reaction temperature

The experimental C_K and X_K of K_2SO_4-capture by kaolin at different reaction temperatures from 800-1450 °C are compared with the equilibrium predictions in Figure 4-9. The results show that the experimental data did not follow the equilibrium predicted trend, and the experimental C_K and X_K were obviously lower than the equilibrium values. The experimental C_K and X_K increased significantly when the reaction temperature increased from 800 °C to 1100 °C. However, when the reaction temperature increased further to 1450 °C, the experimental C_K and X_K decreased slightly. This is because at temperatures below 1100 °C, the reaction was kinetically controlled, and the incomplete vaporization of K_2SO_4 at low temperatures also inhibited the conversion of K_2SO_4. At 1450 °C, the transformation of

kaolin into mullite became significant, and the formed mullite is less reactive towards K_2SO_4.[93, 186] In summary, K_2SO_4 may be capture by kaolin most effectively at 900-1300 °C.

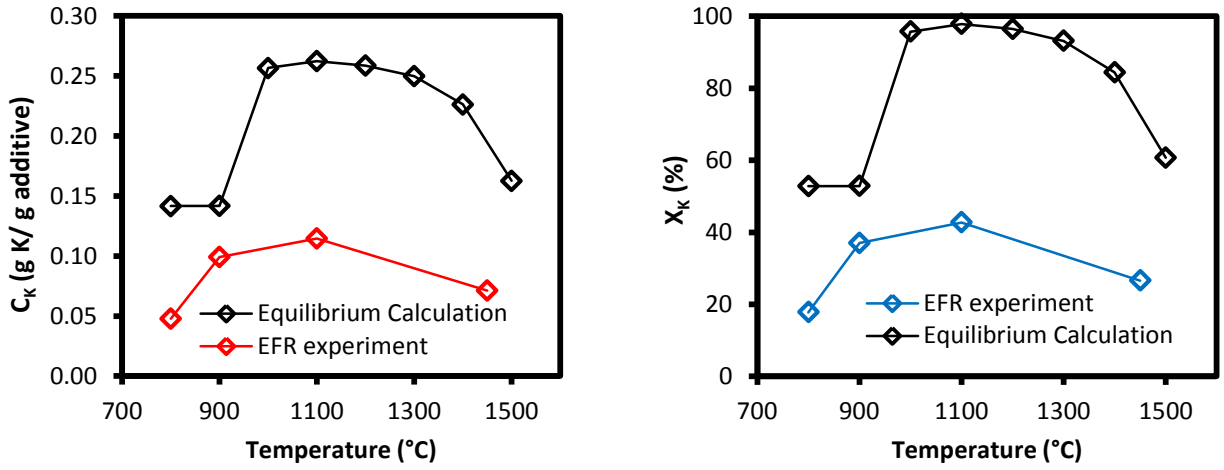

(A) K-capture level (C_K) (B) K-conversion (X_K)

Figure 4-9. K-capture level (C_K) and K-conversion (X_K) of K_2SO_4 capture by kaolin at 800-1450 °C. K_2SO_4 concentration was 250 ppmv (500 ppmv K). Residence time was 1.2 s. Equilibrium calculation results are included for comparison.

It is remarkable that the experimental C_K and X_K of K_2SO_4 are so much lower than the equilibrium predictions. But interestingly they were reasonably similar to the levels found for KCl, although the equilibrium predicted C_K and X_K for K_2SO_4 is considerably higher than that of KCl.

Kaliophilite ($KAlSiO_4$) was predicted as the main K-aluminosilicate product at 1100°C and 500 ppmv K (250 ppmv K_2SO_4) for K_2SO_4-capture reaction by kaolin. However, the XRD analysis results show that leucite ($KAlSi_2O_6$) was detected instead of kaliophilite ($KAlSiO_4$), see Figure 4-10. Thereby the equilibrium product of K_2SO_4 capture by kaolin was wrongly predicted and the reaction product of K_2SO_4 capture by kaolin was the same as KCl.

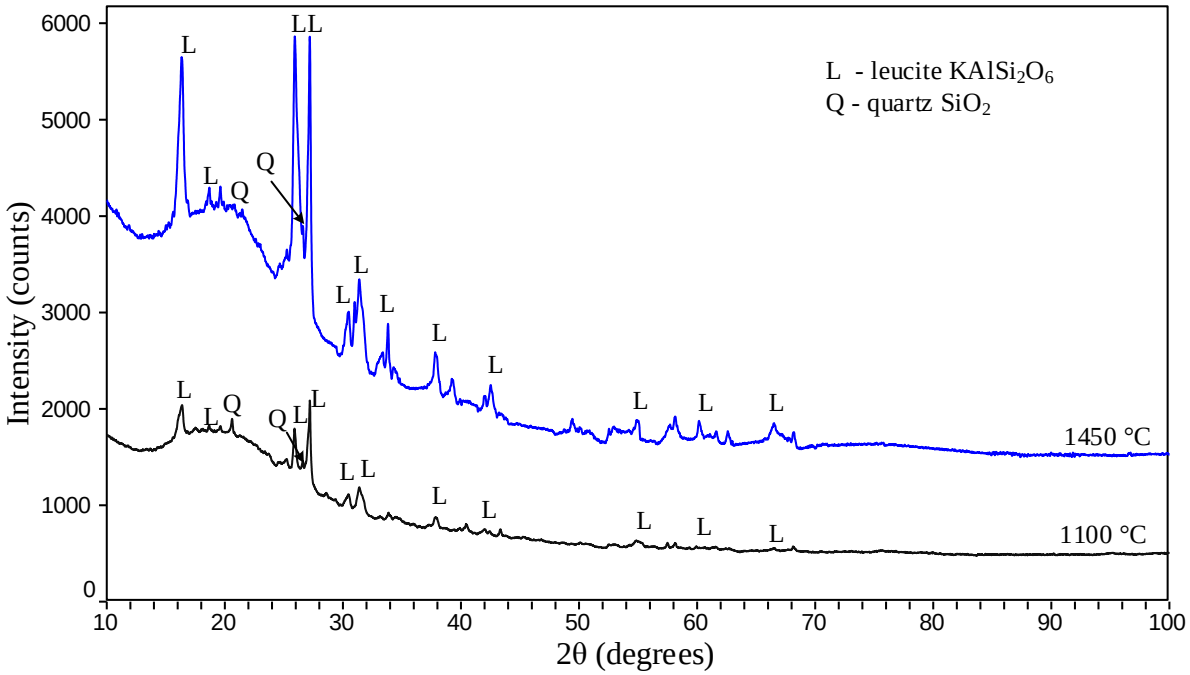

Figure 4-10. XRD spectra of water-washed K_2SO_4-reacted kaolin at 1100 °C and 1450 °C. K_2SO_4 concentration was 250 ppmv (500 ppmv K) in flue gas. Molar K/(Al+Si) ratio in reactants was 0.481. Gas residence time was 1.2 s.

4.3.5 Comparison of different K-species

The experimental results of using different K-species, including KOH, K_2CO_3, KCl and K_2SO_4, to react with kaolin at different K-concentration and different temperatures are compared in Figure 4-11. In Figure 4-11 (A), the experiments of KOH, K_2CO_3 and K_2SO_4 were all conducted at 1100 °C, while the KCl experiments were conducted at 1300 °C. However, the EFR experimental results (shown in Figure 4-5 (A)) indicate that KCl-capture by kaolin behaved similarly at 1100 °C and 1300 °C, so the results are still comparable.

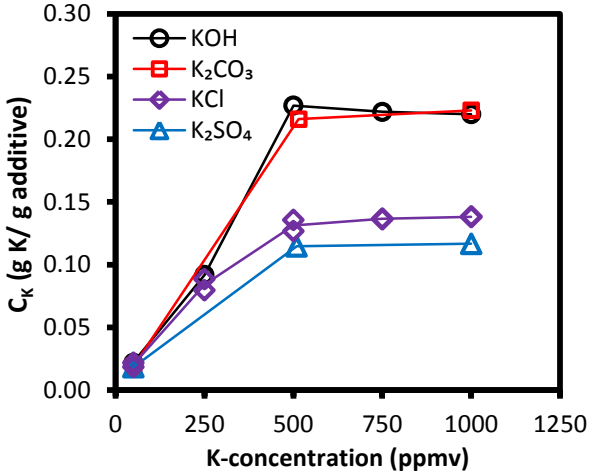

(A) C_K at different K-concentrations

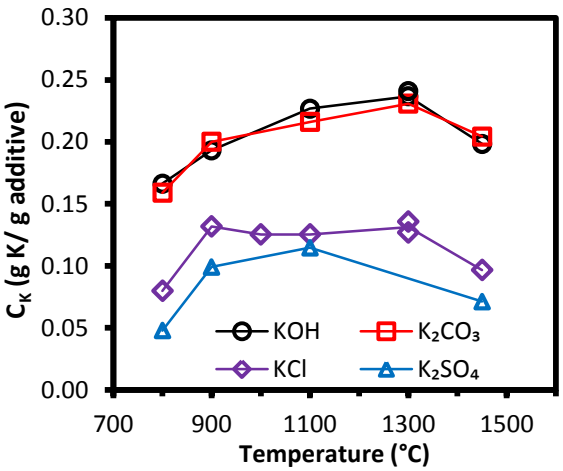

(B) C_K at different temperatures

Figure 4-11. Comparison of KOH, K_2CO_3, KCl, and K_2SO_4 capture by kaolin at different K-concentrations and temperatures. In (A), KOH, K_2CO_3 and K_2SO_4 experiments were at 1100 °C, KCl experiments were at 1300 °C. In (B), K-concentration was 500 ppmv for all experiments.

The results show that KCl and K_2SO_4 were captured in a similar way, while KOH and K_2CO_3 behaved similarly. This is probably because the reaction between K_2CO_3 and kaolin took place according to reaction R 4.3, R 4.4 and R 4.5. K_2CO_3 firstly decomposed into KOH and CO_2, and then the formed KOH reacted with kaolin forming K-aluminosilicate. The decomposition of K_2CO_3 has been observed in the K_2CO_3 vaporization and transformation experiments, which has been discussed in section 4.3.3.1.

$$K_2CO_3 + H_2O \rightarrow 2KOH + CO_2(g) \quad \text{(R 4.3)}$$

$$Al_2O_3 \cdot 2SiO_2 + 2KOH \rightarrow 2KAlSiO_4\ (kaliophilite) + 2H_2O \quad \text{(R 4.4)}$$

$$Al_2O_3 \cdot 2SiO_2 + 2SiO_2 + 2KOH \rightarrow 2KAlSi_2O_6\ (leucite) + 2H_2O \quad \text{(R 4.5)}$$

Another important result is that at 500 ppmv K in flue gas and above, KCl and K_2SO_4 are captured by kaolin less effectively compared to KOH or K_2CO_3. Although the equilibrium calculation predicted a similar K-capture level for K_2SO_4 and K_2CO_3 capture by kaolin at temperatures above 1100 °C. One reason is that at 500 ppmv K and above, kaliophilite ($KAlSiO_4$) was formed as product from KOH and K_2CO_3 capture reaction, while leucite ($KAlSi_2O_6$) existed as the main K-aluminosilicate product from KCl and K_2SO_4 capture experiments, which has been confirmed by the XRD analysis. More Si was consumed in the KCl and K_2SO_4 capture reaction due to the formation of leucite ($KAlSi_2O_6$). Another reason is that the presence of HCl and SO_2 in KCl and K_2SO_4 capture reactions inhibited the K-

capture reaction by kaolin, similar phenomena was observed in a previous sodium capture study.[75] The results indicate that more Al-Si based additive shall be used in boilers if Cl-rich fuels are fired and all K shall be converted to K-aluminosilicate. Additionally, an Al-Si additive with a relatively higher content of Si (like Si-rich coal fly ash) seems more suitable for K-capture when burning Cl-rich biomass fuels.

The results also show that kaolin captured KCl slightly more effectively than K_2SO_4. This may be good for the situation of co-firing straw and coal where KCl and K_2SO_4 both exist, since Al and Si from the co-fired coal can destroy the corrosive KCl more effectively, and the less corrosive K_2SO_4 is captured at a lower level.

4.4 Conclusions

A thorough understanding of the K-capture reaction by kaolin under suspension-fired conditions is wanted to mitigate alkali-related problems in biomass combustion boilers. The reaction of KOH, K_2CO_3, KCl and K_2SO_4 with kaolin was studied by entrained flow reactor experiments and equilibrium calculations. The influence of molar ratio of K/(Al+Si) in reactants, K-concentration in flue gas, reaction temperature, K-species type, and residence time on the K-capture reaction was investigated.

The experimental results of using different K-concentrations show that for KCl at 1300 °C, and for KOH, K_2CO_3 and K_2SO_4 at 1100 °C, the K-capture level (C_K) increased when the K-concentration increased from 50 ppmv to 500 ppmv (molar ratio K/(Al+Si) increased from 0.048 to 0.481). But it did not increase, when the K-concentration increased further to 750 and 1000 ppmv (molar ratio of K/(Al+Si) in reactants was 0.721 and 0.961), probably because all active compounds in kaolin had already been converted forming K-aluminosilicates.

For KCl, KOH and K_2CO_3, C_K and X_K generally followed the equilibrium predictions at temperatures above 1100 °C, when applying a kaolin particle size of D_{50} = 5.47 μm and a residence time of 1.2 s. However, at lower temperatures (800 °C and 900 °C), the reactions were probably kinetically controlled, and the measured K-capture level was lower than the equilibrium predictions. For K_2SO_4, the measured C_K was significantly lower than the equilibrium predictions even at temperatures above 1100 °C. This is most likely because kaliophilite ($KAlSiO_4$) was predicted by the equilibrium calculations, but XRD analysis revealed that leucite ($KAlSi_2O_6$) was formed from the reaction. The KCl-capture experiments conducted with different residence times show that, at 1100 °C, the K-capture level increased

slightly with residence time, indicating a kinetically limited reaction at this temperature. However, at 1300 °C, C_K reached the equilibrium level at a residence time as short as 0.6 s.

Experiments using different K-species show that, K_2CO_3 behaved the same as KOH in terms of being captured by kaolin at suspension-fired conditions. KCl and K_2SO_4 behaved similarly, but they were captured less effectively than KOH and K_2CO_3. The study indicates that the main product of the KCl and K_2SO_4 reactions with kaolin when excess potassium is available are leucite ($KAlSi_2O_6$), while kaliophilite ($KAlSiO_4$) is mainly formed when KOH and K_2CO_3 reacted with kaolin with excess potassium available. The maximum obtainable K-capture level (C_K) for KCl and K_2SO_4 was approximately 0.12 g K/g kaolin while for KOH and K_2CO_3 a maximum capture level of approximately 0.24 g K/g kaolin could be obtained. The results imply that more kaolin shall be used in boilers if Cl-rich fuels are fired and all K shall be converted to K-aluminosilicate. In addition, an Al-Si additive with a relatively higher content of Si (like Si-rich coal fly ash) may be more effective for K-capture when burning Cl-rich biomass fuels.

5 Potassium Capture by Coal Fly Ash, Part 1: KOH

Abstract: The KOH-capture reaction by coal fly ash at suspension-fired conditions was studied through entrained flow reactor (EFR) experiments and chemical equilibrium calculations. The influence of KOH-concentration (50-1000 ppmv), reaction temperature (800-1450 °C), and coal fly ash particle size (D_{50} = 6.03-33.70 μm) on the reaction was investigated. The results revealed that, at 50 ppmv KOH (molar ratio of K/(Al+Si) = 0.048 of feed), the measured K-capture level (C_K) of coal fly ash was comparable to the equilibrium prediction, while at 250 ppmv KOH and above, the measured data were lower than chemical equilibrium. Similar to the KOH-kaolin reaction reported in Chapter 3, leucite ($KAlSi_2O_6$) and kaliophilite ($KAlSiO_4$) were formed from the KOH-coal fly ash reaction. However, coal fly ash captured KOH less effectively compared to kaolin at 250 ppmv KOH and above. Studies at different temperatures showed that, at 800 °C, the KOH-coal fly ash reaction was probably kinetically controlled. At 900-1300 °C it was diffusion limited, while at 1450 °C, it was equilibrium limited to some extent. At 500 ppmv KOH (molar ratio of K/(Al+Si) = 0.481), and a gas residence time of 1.2 s, 0.063 g K/(g additive) and 0.087 g K/(g additive) was captured by coal fly ash (D_{50} = 10.20 μm) at 900 and 1450 °C, respectively. Experiments with coal fly ash of different particle sizes showed that a higher K-capture level were obtained using finer particle sizes, indicating some internal diffusion control of the process.

5.1 Introduction

Existing coal suspension-fired boilers have been converted to biomass combustion to increase the share of renewable power and district heat production in Denmark.[12, 14] Compared to traditional biomass grate-fired power plants, biomass suspension-fired power plants have higher efficiency, and they can compensate for the fluctuations of the wind power production.[67] However, the alkali elements (mainly K) in biomass fuels to a high degree evaporates during combustion in PF (pulverized fuel) boilers,[18, 43, 153, 187] and are present in the gas phase as KOH, KCl or K_2SO_4.[22, 24, 63] When the flue gas is cooling down,

these K-compounds condense and may form sticky deposit on super-heater and re-heater tubes, resulting in accelerated deposit formation as well as corrosion. Additionally, K-salt aerosols formed from nucleation and condensation of gaseous K-species can deteriorate the performance of de-NO_x SCR catalyst through physical deposition and chemical poisoning.[30, 56, 57, 188]

One option to deal with these alkali-induced problems is to inject additives that can react with volatile alkali species to form less problematic compounds with higher melting points. Various additives have been investigated, and they can largely be categorized into four groups: Al-Si based,[67, 76, 93, 98, 189] S-based,[51, 53, 130] P-based [140] and Ca-based,[137] according to the major elements that are present in the additives.[67, 68] Among the different additives, coal fly ash was the only one that has been commercially utilized in full-scale suspension-fired boilers due to its low cost and high effectiveness.[12, 14, 184]

Coal fly ash is a solid residue from combustion of coal. Approximately 500 million tons of coal fly ash are produced worldwide each year.[115] Coal fly ash could be an environmental concern if not handled properly.[115] The mineralogical composition of coal fly ash is quite complex, depending on the parental coal and the combustion technology. The dominant mineral phases include quartz, mullite, illite and siderite.[147] The effectiveness of coal fly ash in capturing volatile K-species from biomass has been observed in co-combustion of coal and biomass.[121, 190, 191]

The K-capture reaction by coal fly ash was studied by Wu and co-workers in a full-scale biomass suspension-fired boiler.[12, 14] The impact of injection of coal fly ash in different amounts on the deposition behavior, deposit composition and the formation of aerosols was investigated. With the addition of coal fly ash, the amount of aerosols formed was greatly suppressed, with its composition changed from K-S-Cl rich to Ca-P-Si rich.[14] The composition of the ash deposit is also significantly influenced. The amount of K_2SO_4 in inner layer deposit collected from high temperature flue gas (1300 °C) was greatly reduced. KCl, KOH, and K_2CO_3 in the inner layer of the deposit completely disappeared, when adding coal fly ash. The large outer deposit also transferred from K-Ca-Si rich to Si-Al rich, resulting in an easier and more frequent removal of the deposits. In the deposits formed at low temperature flue gas (800 °C), KCl disappeared, and the content of KOH and K_2CO_3 was significantly decreased. The corrosion risk was considerably decreased consequently. However, because of the complexity of the full-scale system, no quantitative data such as the potassium capture amount of per unit of coal fly ash could be obtained.

Quantitative and detailed study on K-capture reaction by coal fly ash at high-temperature conditions is still rare. To the authors' knowledge, the only two quantitative studies on K-capture by coal fly ash were both conducted in fixed bed reactors, where coal fly ash pellets with a diameter of 1.5 mm or piles of coal ash were utilized.[93, 122] However, the residence time of coal fly ash in these fixed bed reactors was in an order of hours, significantly larger than that of biomass suspension-fired boilers, where coal fly ash particles only stay a few seconds in the flue gas.[12, 14]

The objective of this work is to study quantitatively the K-capture behavior of coal fly ash at well-controlled conditions in suspension, and to understand the influence of reaction conditions. Potassium capture by coal fly ash at suspension-fired conditions was studied in this chapter and Chapter 6. This chapter focuses on the KOH capture by coal fly ash, while Chapter 6 deals with capture of K_2CO_3, KCl and K_2SO_4 by coal fly ash.

5.2 Experimental

The KOH capture experiments by coal fly ash were conducted in the DTU entrained flow reactor (EFR) which has been described in Chapter 2. Experimental conditions of the KOH capture experiments by coal fly ashes are summarized in Table 5-1. The influence of the KOH-concentration, the molar ratio of K/(Al+Si) in reactants, the reaction temperature and the fly ash particle size on the KOH-capture reaction were investigated.

In the experimental series (A) of Table 5-1, the concentration of coal fly ash in the feeding slurry was kept constant while the fraction of KOH was varied, to investigate the effect of KOH concentration in flue gas (50-1000 ppmv) and the molar ratio of K/(Al+Si) in reactants (0.048-0.961).

In series (B), the impact of temperature on the reaction was investigated. Two different KOH concentrations in the flue gas were studied: 50 and 500 ppmv.

In series (C), the influence of coal fly ash particle size on the K-capture reaction was studied by feeding ASV2 coal fly ashes with different particle sizes: the grinded ASV2 coal fly ash (D_{50} = 6.03 μm), ASV2CFA0-32 μm (D_{50} = 10.20 μm) and ASV2CFA 32-45 μm (D_{50} = 33.70 μm) into the EFR. The results were also compared with data from Chapter 3 where the KOH capture by kaolin and mullite was investigated. The gas residence time in the reactor was kept at 1.2 s in all the experiments.

Table 5-1. Conditions of the experiments in the Entrained Flow Reactor (EFR).

Experimental series	K-species	additives	D_{50} of additives /μm	Temp./ ℃	Gas residence time/s	K in gas /ppmv	K/(Al+Si)
(A) KOH-capture by CFA (impact of **K-concentration**)	KOH	ASV2CFA0-32	10.20	1300	1.2	50	0.048
						250	0.240
						500	0.481
						750	0.721
						1000	0.961
(B) KOH-capture by CFA (impact of **temperature**)	KOH	ASV2CFA0-32	10.20	800	1.2	50, 500	0.481
				900			
				1100			
				1300			
				1450			
(C) KOH-capture by CFA (impact of **CFA particle size**)	KOH	ASV2CFAGR	6.03	1300	1.2	500	0.481
		ASV2CFA0-32	10.20				
	KOH	AMVCFA0-32	33.70				

5.3 Results and discussion

5.3.1 Representativeness of solid product samples

Although the solid samples obtained from the sampling system (sampling tube, cyclone, and filter) were carefully collected, the mass balance for each experiment only closed within about 58-75 %. The difference was due to the deposition on the inner wall of the reactor tube and other places. The calculation of K-capture level (C_K) and K-conversion (X_K) was based on the assumption that the collected samples are representative. The representativeness was examined by comparing the molar ratio of K/(Al+Si) in products with that of the fed reactants. The result basing on ICP-OES analysis is shown in Figure 5-1. It reveals that the molar ratio of K/(Al+Si) in the collected solid samples is close to that of fed reactants, suggesting that the solid samples are representative.

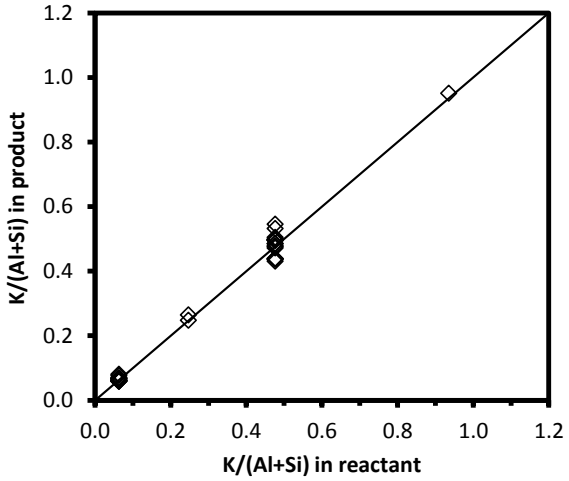

Figure 5-1. Comparison of K/(Al+Si) in collected solid products and reactants fed into the EFR using coal fly ash as the additive.

5.3.2 KOH capture by coal fly ash

5.3.2.1 Equilibrium calculation

The equilibrium calculation results of KOH capture by ASV2CFA0-32 at different temperatures (800-1450 °C) and KOH concentrations (50-1000 ppmv) are summarized in Table 5-2. More detailed results can be found in Appendix D.

The calculations indicate that the type of the K-aluminosilicates formed from the KOH-capture reaction changes with the K-concentration or the molar ratio of K/(Al+Si) in reactants. At 50 ppmv KOH (molar K/(Al+Si) in reactant was 0.048), sanidine ($KAlSi_3O_8$) with K:Al:Si = 1:1:3 was predicted as the main K-aluminosilicate product through the whole temperature range, 800-1450 °C. When the KOH concentration increased to 250 ppmv, leucite ($KAlSi_2O_6$) with a molar ratio of K:Al:Si = 1:1:2, became the dominant K-aluminosilicate. At 500, 750 and 1000 ppmv KOH, kaliophilite ($KAlSiO_4$) with a molar ratio of K:Al:Si = 1:1:1 was the main K-aluminosilicate product.

5.3.2.2 Impact of KOH concentration

The measured K-capture level (C_K) and K-conversion (X_K) of KOH capture by ASV2CFA0-32 at different KOH concentrations (50-1000 ppmv) and 1300 °C are compared with equilibrium calculations in Figure 5-2. For 50 ppmv KOH, the measured C_K (0.022 g K/(g additive)) and X_K (95 %) of ASV2CFA0-32 are close to the equilibrium values. However, the experimental C_K and X_K become remarkably lower than the equilibrium data at 250 ppmv KOH and above. As the KOH-concentration in the flue gas increased from 50 ppmv to 500

ppmv, although the K-capture level (C_K) increased considerably from 0.022 g K/(g additive) to 0.074 g K/(g additive), K-conversion (X_K) decreased sharply from 95 % to 32 %. With a further increase of KOH concentration to 750 and 1000 ppmv, no obvious increase of C_K was observed, and the K-conversion (X_K) dropped to 16 % at 1000 ppmv, showing that most KOH remained unreacted in this case. The difference between equilibrium data and experimental data implied that only part of the coal fly ash participated in the K-capture reaction.

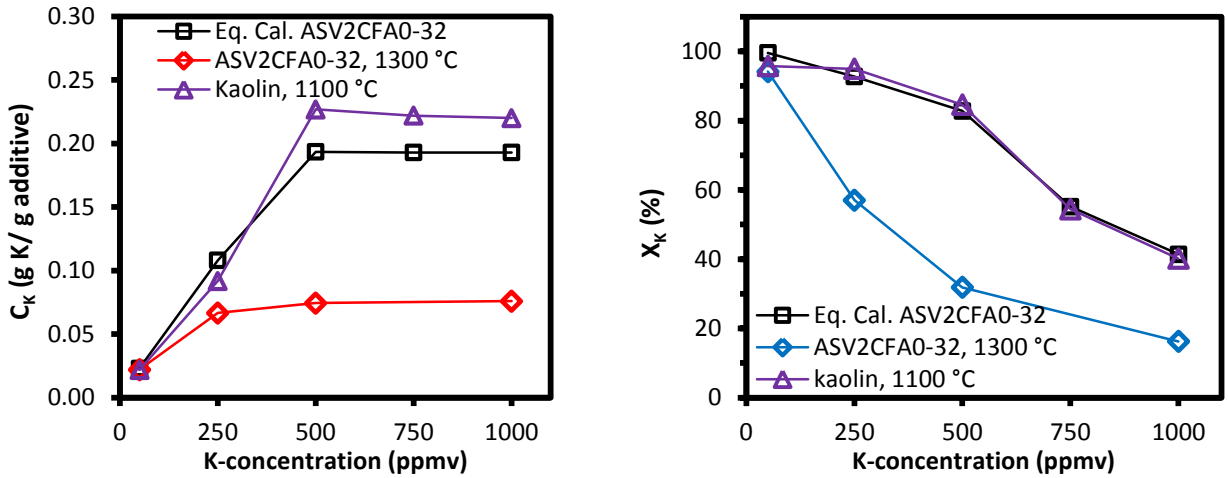

(A) K-capture level (C_K) (B) K-conversion (X_K)

Figure 5-2. K-capture level (C_K) and K-conversion (X_K) of KOH-capture by ASV2CFA0-32 and kaolin (D_{50} = 5.47μm) at KOH concentrations from 50 to 1000 ppmv. Molar ratio of K/(Al+Si) in reactants varied from 0.048 to 0.961. Reaction temperature for ASV2CFA0-32 was 1300 °C and reaction temperature of kaolin was 1100 °C; Gas residence time was 1.2 s. Equilibrium calculation results of KOH capture by ASV2CFA0-32 are included for comparison.[185]

Table 5-2. Equilibrium calculation results of KOH capture by coal fly ash (ASV2CFA0-32 μm).

Input conditions	Temp. /°C	K-species appearing	Al-con.	Si-con.	K-con.	K-capture/(g K/(g additive))
50 ppmv KOH, K/(Al+Si) =0.048	800	100 % $KAlSi_3O_8$	12 %	24 %	100 %	0.023
	900	100 % $KAlSi_3O_8$	12 %	24 %	100 %	0.023
	1100	100 % $KAlSi_3O_8$	12 %	24 %	100 %	0.023
	1300	100 % $KAlSi_3O_8$	12 %	24 %	100 %	0.023
	1450	98 % $KAlSi_3O_8$ + 1 % KOH+ 1 % KCl	12 %	24 %	98 %	0.023
250 ppmv KOH, K/(Al+Si) =0.240	800	100 % $KAlSi_2O_6$	60 %	81 %	100 %	0.117
	900	100 % $KAlSi_2O_6$	60 %	80 %	100 %	0.116
	1100	98 % $KAlSi_2O_6$ + 1 % KOH	60 %	80 %	98 %	0.115
	1300	93 % $KAlSi_2O_6$ + 6 % KOH	56 %	75 %	93 %	0.108
	1450	93 % $KAlSi_2O_6$ + 6 % KOH	56 %	75 %	93 %	0.109
500 ppmv KOH, K/(Al+Si) =0.481	800	72 % $KAlSiO_4$ + 10 % $KAlSi_2O_6$	100 %	75 %	83 %	0.193
	900	71 % $KAlSiO_4$ + 12 % $KAlSi_2O_6$ + 2 % KOH	100 %	77 %	83 %	0.193
	1100	55 % $KAlSiO_4$ + 28 % $KAlSi_2O_6$ + 15 % KOH	100 %	89 %	83 %	0.193
	1300	55 % $KAlSiO_4$ + 28 % $KAlSi_2O_6$ + 16 % KOH	100 %	90 %	83 %	0.193
	1450	57 % $KAlSi_2O_6$ + 42 % KOH	69 %	92 %	57 %	0.133
750 ppmv KOH, K/(Al+Si) =0.721	800	55 % $KAlSiO_4$ + 41 % K_2SiO_3 + 2 % KOH	100 %	67 %	55 %	0.193
	900	55 % $KAlSiO_4$ + 36 % K_2SiO_3 + 2 % $K_2Si_2O_5$+ 4 % KOH	100 %	67 %	55 %	0.193
	1100	55 % $KAlSiO_4$ + 18 % $K_2Si_2O_5$+ 24 % KOH	100 %	67 %	55 %	0.193
	1300	36 % $KAlSiO_4$ + 19 % $KAlSi_2O_6$ + 44 % KOH	100 %	90 %	55 %	0.193
	1450	29 % $KAlSiO_4$ + 23 % $KAlSi_2O_6$ + 47 % KOH	94 %	91 %	52 %	0.181
1000 ppmv KOH, K/(Al+Si) =0.961	800	32 % $KAlSiO_4$ + 9 % $KAlO_2$ + 52 % K_2SiO_3 + 4 % KOH	78 %	52 %	32 %	0.151
	900	41 % $KAlSiO_4$ + 1 % $KAlO_2$ + 36 % K_2SiO_3 + 21 % KOH	99 %	66 %	41 %	0.191
	1100	41 % $KAlSiO_4$ + 15 % $K_2Si_2O_5$ + 41 % KOH	100 %	67 %	41 %	0.193
	1300	27 % $KAlSiO_4$ + 14 % $KAlSi_2O_6$ + 58 % KOH	100 %	90 %	41 %	0.193
	1450	27 % $KAlSiO_4$ + 14 % $KAlSi_2O_6$ + 58 % KOH + 1 % K	100 %	90 %	41 %	0.193

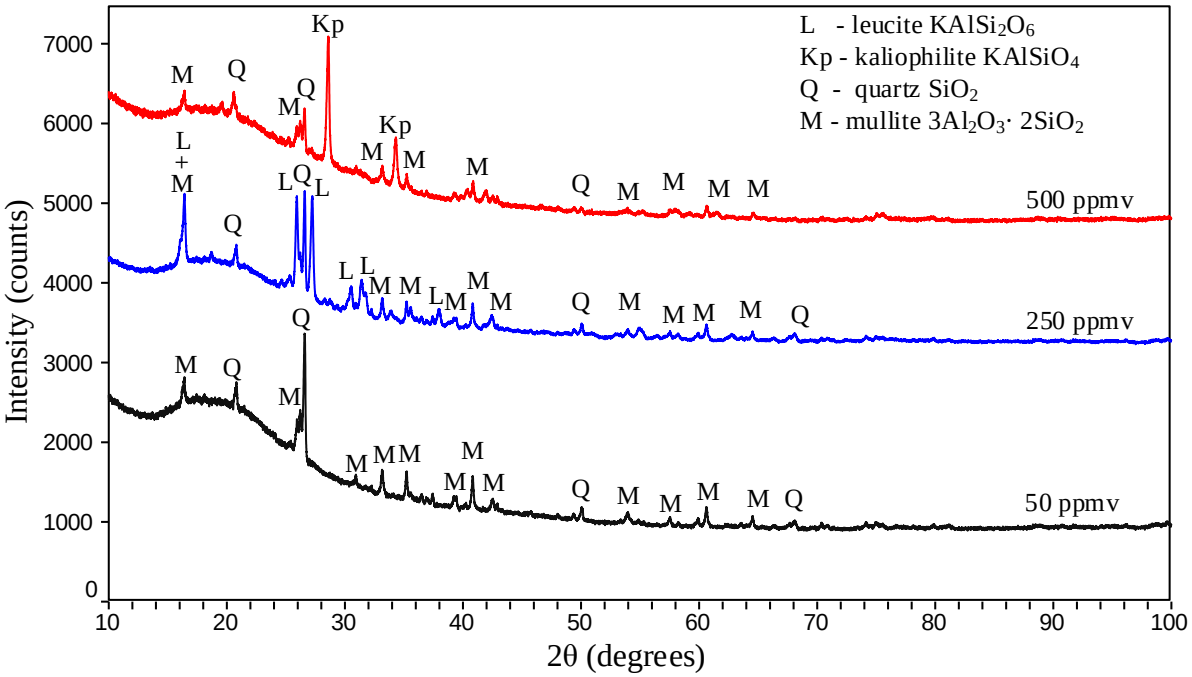

Figure 5-3. XRD spectra of water-washed KOH-reacted ASV2CFA0-32 at 50 ppmv, 250 ppmv and 500 ppmv KOH. The reaction temperature was 1300 °C, the molar ratio of K/(Al+Si) in the reactants was varied form 0.048, 0.240 and 0.481 and the gas residence time was 1.2 s.

Also, the measured C_K and X_K of KOH reaction with kaolin from Chapter 3[185] are included for comparison in Figure 5-2. The experiments of KOH capture by kaolin were conducted at 1100 °C, while the experiments with ASV2CFA0-32 were conducted at 1300 °C. Although the reaction temperature was different, the results are still comparable, because the K-capture behavior of kaolin at 1100 °C and 1300 °C is similar according to the results in Chapter 3.[185] The results show that the measured C_K and X_K of ASV2CFA0-32 were considerably lower than that of kaolin. There may be several reasons for the lower efficiency of the coal fly ash compared to kaolin. One possible reason is that the main mineral phase of coal fly ash, mullite, is less reactive towards potassium than kaolin and metakaolin. Another possible reason is that the BET surface area of ASV2CFA0-32 (8.04 m^2/g) is smaller than that of kaolin (12.70 m^2/g), and the median diameter of ASV2CFA0-32 (10.20 μm) is larger than that of kaolin (5.47 μm). Consequently, there were fewer active sites for KOH-capture in ASV2CFA0-32 [185]. In addition, diffusion limitations for KOH inside the coal fly ash particles may have also played a role, resulting in an incomplete consumption of mullite in the case of coal fly ash. The incomplete consumption of mullite is supported by the XRD results

shown in Figure 5-3, in which peaks corresponding to mullite were detected in the KOH-reacted coal fly ash.

The XRD spectra of water-washed KOH-reacted ASV2CFA0-32 at 50 ppmv, 250 ppmv and 500 ppmv KOH are compared in Figure 5-3. At 50 ppmv KOH, only mullite and quartz originated from the raw coal fly ash were detected. No crystalline K-aluminosilicate was detected, although sanidine ($KAlSi_3O_8$) was predicted by the equilibrium calculations. This is probably because either the content of K-aluminosilicate in the products was too low to be detected, or amorphous K-aluminosilicates were formed which cannot be detected by XRD. In the 250 ppmv sample, leucite ($KAlSi_2O_6$) was detected as the main K-aluminosilicate product. In the 500 ppmv sample, kaliophilite ($KAlSiO_4$) was present as the dominant K-aluminosilicate. The type of K-aluminosilicates detected by XRD, generally agrees with the equilibrium results as shown in Table 5-2. Notably, mullite was detected in all the three KOH-reacted coal fly ash samples, showing that part of the mullite remained unreacted in those samples. This is different from what was observed in the study of KOH capture by kaolin, where a full conversion of kaolin to K-aluminosilicate was observed and no mullite was detected in the product samples at 500 ppmv KOH and above with a reaction temperature of 1100 °C.[185]

5.3.2.3 Impact of reaction temperature

The measured K-capture level (C_K) and K-conversion (X_K) of KOH capture by ASV2CFA0-32 at different reaction temperatures (800-1450 °C) are compared with the equilibrium calculation results in Figure 5-4. KOH concentrations of 50 ppmv and 500 ppmv in the flue gas were studied. The C_K and X_K of KOH capture by kaolin at the same conditions [185] are included as well for comparison. As shown in Figure 5-4 (A) and (B), at 500 ppmv KOH, the measured C_K and X_K of KOH capture by ASV2CFA0-32 were both significantly lower than equilibrium data. At 800 °C, the K-capture level (C_K) was only 0.025 g K/(g additive), with 11 % of KOH captured as K-aluminosilicate. When the temperature increased to 900 °C, C_K increased significantly to 0.063 g K/(g additive), with 27 % of KOH converted to K-aluminosilicate. At temperatures of 900-1100 °C, the C_K stayed constant. However, when the reaction temperature increased further to 1300 °C and 1450 °C, C_K increased by 38 % reaching 0.087 g K/(g additive), with 37 % of fed KOH chemically bonded by coal fly ash as K-aluminosilicate at 1450 °C.

At 50 ppmv KOH, the measured C_K and X_K of ASV2CFA0-32 were close to the equilibrium predictions; see Figure 5-4 (C) and (D). The C_K and X_K were both constant and independent

of the reaction temperature in the temperature range of 900-1300 °C. The C_K was around 0.019 g K/(g additive), with about 94 % KOH converted to K-aluminosilicate.

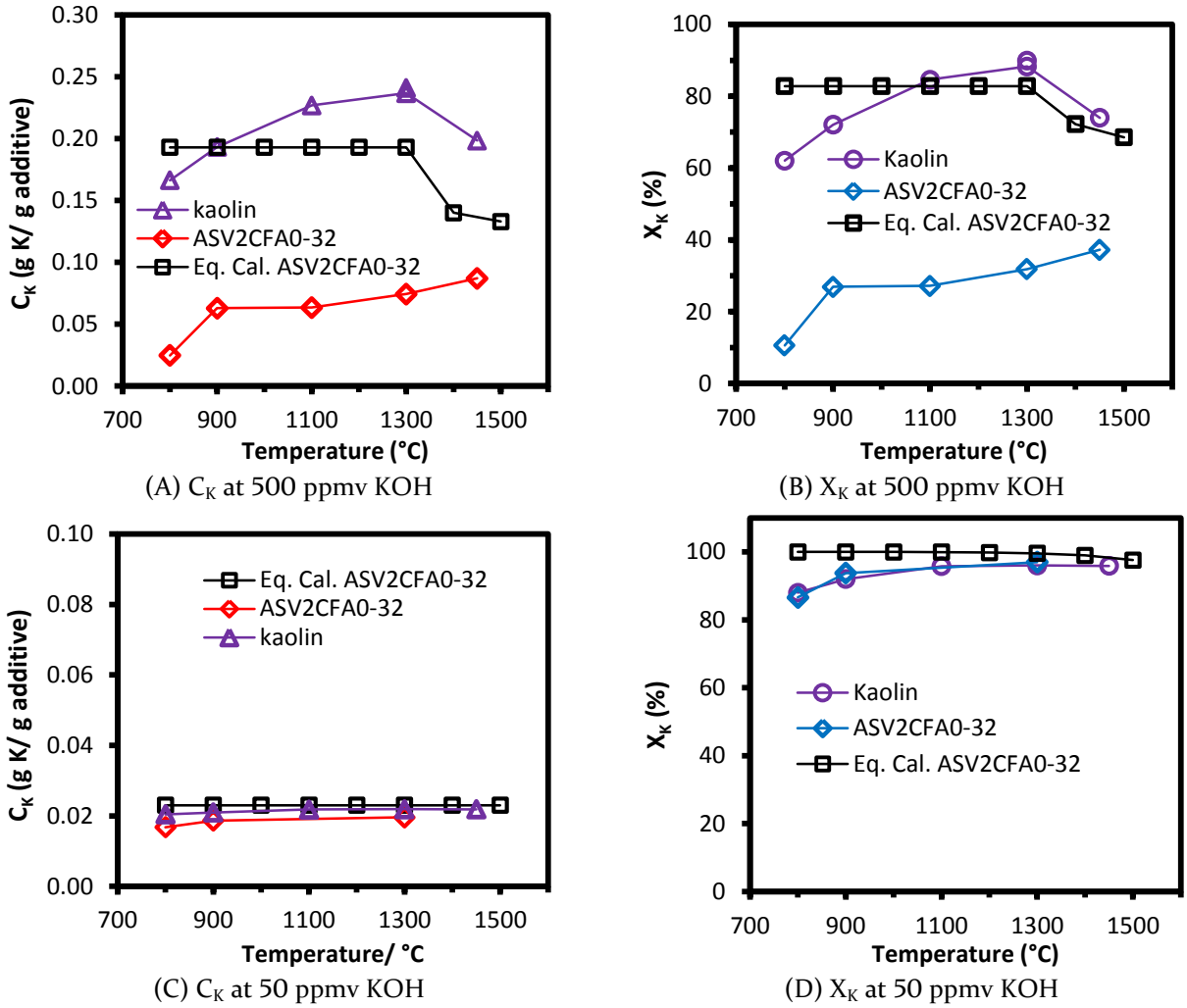

(A) C_K at 500 ppmv KOH

(B) X_K at 500 ppmv KOH

(C) C_K at 50 ppmv KOH

(D) X_K at 50 ppmv KOH

Figure 5-4. Comparison of K-capture level (C_K) and K-conversion (X_K) of KOH capture by ASV2CFA0-32 and kaolin (D_{50} = 5.47μm) at temperatures from 800 to 1450 °C. The KOH concentration was 500 ppmv (molar ratio of K/(Al+Si) = 0.481) in (A) and (B). KOH concentration was 50 ppmv, and molar ratio of K/(Al+Si) = 0.048 in (C) and (D). Gas residence time was 1.2 s, and equilibrium calculation results of KOH capture by ASV2CFA0-32 are included for comparison.[185]

Comparison of results of KOH-ASV2CFA0-32 and KOH-kaolin in Figure 5-4 shows that, at 500 ppmv KOH, the C_K and X_K of ASV2CFA0-32 were considerably lower than that of kaolin, showing that coal fly ash (ASV2CFA0-32) captures KOH less effectively in this case. Additionally, the trend of the C_K and X_K of kaolin and ASV2CFA0-32 at 500 ppmv was obviously different. For kaolin, C_K and X_K firstly increased and then decreased when the reaction temperature was changed from 800 °C to 1450 °C, reaching a peak at 1300 °C. The

C_K and X_K of ASV2CFA0-32 increased sharply when the temperature increased from 800 °C to 900 °C, and it stayed constant at 900-1100 °C. When the reaction temperature increased further to 1300 °C and 1450 °C, they increased again, probably because the melting of the coal fly ash particles accelerated the internal diffusion of KOH. However, at 50 ppmv KOH, the C_K and X_K of ASV2CFA0-32 were comparable to that of kaolin. The trend at different temperatures of the two additives (kaolin and ASV2CFA) was also the same.

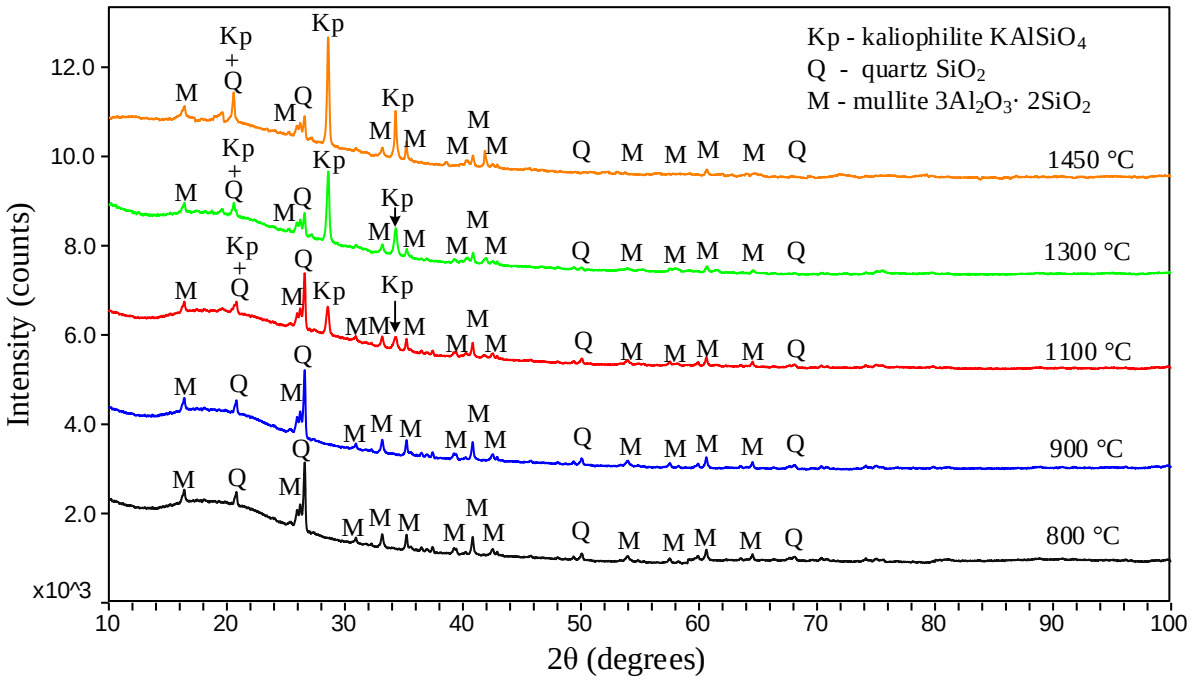

Figure 5-5. XRD spectra of water washed KOH-reacted ASV2CFA0-32 samples at different temperatures (800-1450 °C). The KOH-concentration was 500 ppmv, with molar ratio of K/(Al+Si) in reactants of 0.481. Gas residence time was 1.2 s.

The XRD spectra of water-washed 500 ppmv KOH-reacted coal fly ash at different temperatures (800-1450 °C) are compared in Figure 5-5. At 800 °C and 900 °C, only mullite and quartz were detected in the samples and the spectra were almost the same as that of the parental coal fly ash, implying that the formed K-aluminosilicate remained in amorphous phase, or that the concentration of crystalline phase was too low to be detected. In the 1100 °C sample, crystalline kaliophilite ($KAlSiO_4$) was detected. When the reaction temperature increased further to 1300 °C and 1450 °C, the peaks of kaliophilite ($KAlSiO_4$) became stronger, indicating that more crystalline kaliophilite ($KAlSiO_4$) was formed. Notably, mullite and quartz were detected in all the product samples, showing an incomplete conversion of the coal fly ash (ASV2CFA). This supports the results that the measured K-capture level (C_K) and K-conversion (X_K) were considerably lower than those

predicted by equilibrium calculations. According to the results from Chapter 3 on KOH capture by kaolin,[185] a fully conversion of kaolin into K-aluminosilicate was observed. The difference between kaolin and ASV2CFA0-32 indicates that, the controlling mechanisms of KOH-capture reaction by coal fly ash and kaolin in the EFR are different. In the KOH-kaolin system, the reaction was equilibrium limited, while the KOH-coal fly ash reaction was probably diffusion or kinetically controlled.

5.3.2.4 Impact of coal fly ash particle size

The K-capture level (C_K) and K-conversion (X_K) of KOH by ASV2 coal fly ash of different particle sizes are compared in Figure 5-6. At 800 °C, the C_K and X_K of ASV2 coal fly ash of different particle sizes are almost independent of different particle size, probably due to a kinetically controlled reaction at this temperature. When the reaction temperature increased to 900 °C and above, the C_K of the finer coal fly ash (ASV2CFAGR) was significantly higher than that of normal coal fly ash (ASV2CFA0-32). The C_K and X_K of coarse coal fly ash (ASV2CFA32-45) were lower than that of ASV2CFA0-32. This indicates that at 900-1300 °C, the reaction was diffusion-influenced.

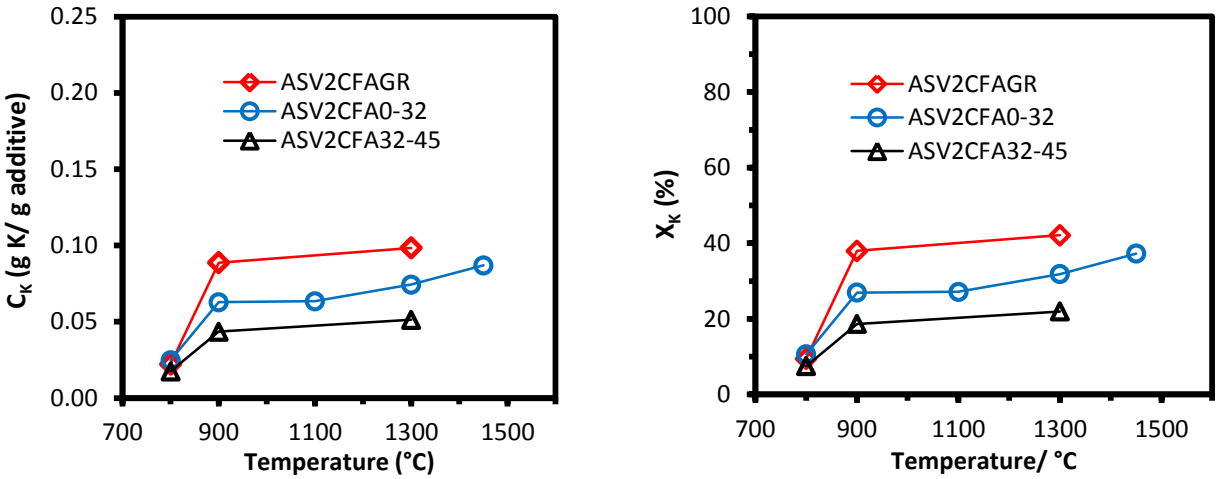

(A) K-capture level (B) K-conversion

Figure 5-6. Comparison of K-capture level (C_K) and K-conversion (X_K) of KOH capture by ASV2 coal fly ash of different particle sizes: ASV2CFAGR with D_{50} = 6.03 μm, ASV2CFA0-32 with D_{50} = 10.20 μm, and ASV2CFA32-45 with D_{50} = 33.70 μm. The reaction temperature was 1300 °C; gas residence time was 1.2 s; KOH concentration in flue gas was 500 ppmv, with molar K/(Al+Si) ratio of 0.481.

5.3.2.5 KOH capture by kaolin, mullite and coal fly ash

The measured K-capture level (C_K) and K-conversion (X_K) of KOH-coal fly ash (ASV2CFA0-32 and ASV2CFAGR) reaction obtained at different temperatures are compared with the experimental results of KOH-kaolin and mullite reaction from Chapter 3[185] in Figure 5-7. The mullite sample was generated by heat treatment of kaolin at 1100 °C for 24 hours [185]. The median diameter D_{50} of ASV2CFAGR (D_{50} = 6.02 μm) was comparable to that of the kaolin (D_{50} = 5.47 μm) and mullite powder (D_{50} = 5.90 μm), while the D_{50} of ASV2CFA0-32 was somewhat larger (10.2 μm). The BET surface area of kaolin (12.7 m^2/g) was higher than those of mullite (5.30 m^2/g) and ASV2CFAGR (9.07 m^2/g). The main mineral phase of the mullite powder and the ASV2 coal fly ash (ASV2CFAGR, ASV2CFA0-32) was mullite, whereas it was kaolinite for kaolin powder.

The results show that at 800 °C, the C_K of ASV2CFA0-32, ASV2CFAGR and mullite was at the same level, about 0.020 g K/(g additive), while the value for kaolin was much higher at 0.167 g K/(g additive). One possible reason is that the BET surface areas of coal fly ash and mullite were smaller than that of kaolin, resulting in a smaller amount of reactive spots and a slower internal diffusion of KOH. Another possible reason is that the kinetics of the KOH-capture reaction by mullite and kaolinite are different and it is probably slower for mullite than that of kaolinite or metakaolin. Considering that the BET surface area and median diameter D_{50} of ASV2CFAGR were comparable to those of kaolin but that the C_K of kaolin was still considerably higher than that of ASV2CFAGR, the difference of the kinetics of KOH-capture by kaolinite and mullite might be the main reason for the observed difference of C_K at 800 °C.

In the temperature range 900-1300 °C, the C_K of coal fly ashes, mullite and kaolin all increased with increasing temperature, but the C_K of coal fly ash and mullite was both considerably lower than that of kaolin. When the temperature increased further to 1450 °C, the C_K of mullite increased significantly, and it became comparable to that of kaolin. However, there is a less pronounced increase in C_K for the two ASV2 coal fly ashes. At 1450 °C, the relatively lower C_K of the two ASV2 coal fly ashes may be partly due to the equilibrium limit as shown in Figure 5-8, and partly due to internal diffusion limitations. In summary, the KOH-capture reaction by kaolin, mullite and coal fly ash at 800 °C were all kinetically controlled. At 900-1300 °C, KOH capture by mullite and coal fly ash were more diffusion-influenced. At 1450 °C, KOH capture by kaolin, and mullite was limited by equilibrium, while it is diffusion influence for coal fly ash (ASV2CFA0-32 and ASV2CFAGR).

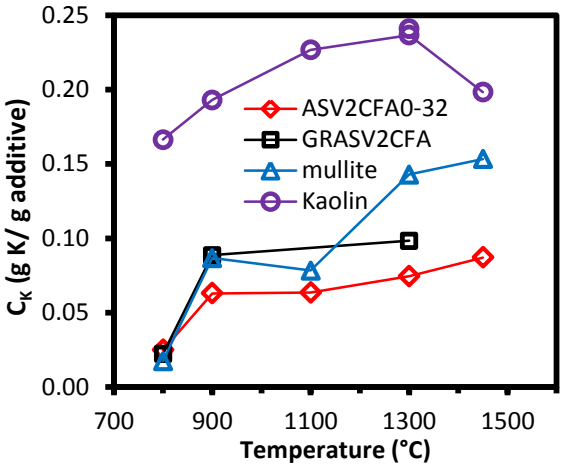

Figure 5-7. Comparison of K-capture level (C_K) and K-conversion (X_K) of ASV2 coal fly ashes of different particle size (ASV2CFA0-32 and ASV2CFAGR), kaolin and mullite. The KOH concentration was 500 ppmv in all experiments, with molar K/(Al+Si) ratio of 0.481. Gas residence time was 1.2 s.

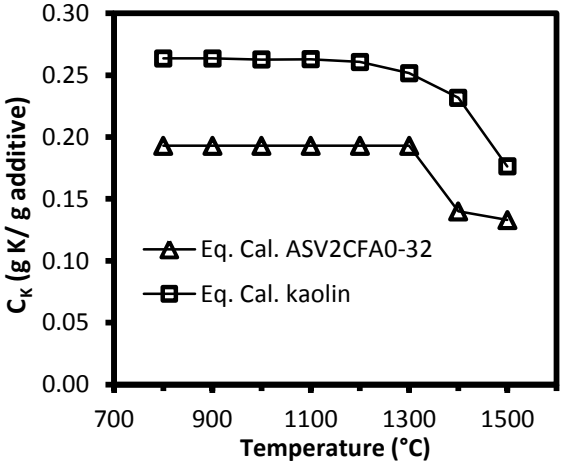

Figure 5-8. Comparison of equilibrium calculated K-capture level (C_K) of KOH capture by kaolin and ASV2CFA0-32. The KOH concentration was 500 ppmv in flue gas, with molar K/(Al+Si) ratio of 0.481.

5.4 Conclusions

The KOH-capture reaction with coal fly ash was studied by entrained flow reactor experiments and equilibrium calculations. The impacts of KOH-concentration, molar ratio

of K/(Al+Si) in reactants, reaction temperature and particle size of coal fly ash were investigated. The results of KOH-capture reaction using coal fly ash was also compared with the results of kaolin and mullite in Chapter 3.[185]

The experimental results at 1300 °C and a gas residence time of 1.2 s, with different KOH concentrations and molar ratio of K/(Al+Si) of the feed showed that, the K-capture level (C_K) of coal fly ash increased with the KOH concentration at 50-500 ppmv KOH (K/(Al+Si) = 0.048-0.481), but did not increase further at a KOH concentration of 750-1000 ppmv. At 50 ppmv KOH, the measured K-capture level (C_K) was comparable to that of equilibrium calculation and the C_K of kaolin from Chapter 3[185]. However, at 250 ppmv KOH and above (molar K/(Al+Si) $\geq$ 0.240), the measured C_K was lower than the equilibrium data. The main alkali product species formed were leucite ($KAlSi_2O_6$) at 250 ppmv, and kaliophilite ($KAlSiO_4$) at 500 ppmv. Although the types of formed K-aluminosilicates (predicted by equilibrium calculations) agreed with those of the KOH-kaolin reaction, coal fly ash captured KOH less effectively at 250 ppmv KOH and above.

At 500 ppmv KOH (K/(Al+Si) = 0.481 in reactants), when the temperature changed from 800 to 1450 °C, C_K of the coal fly ash generally increased from 0.025 g K/(g additive) to 0.087 g K/(g additive). The K-capture level (C_K) was lower than that of kaolin throughout the temperature range studied. At 800 °C, with a particle size of D_{50} = 10.20 μm, the KOH-capture reaction by coal fly ash was probably kinetically controlled. At 900-1300 °C, the reaction conversion level increased with the decreased particle size and was transport limited, but may also be kinetically limited. At 1450 °C the reaction was limited by equilibrium as well. The gradual increase of C_K at 900-1450°C may be caused by the increased internal or external transport of KOH.

At 50 ppmv KOH (K/(Al+Si) = 0.048), which is representative for the gaseous potassium level in wood suspension-fired plants, C_K of coal fly ash (around 0.02 g K/(g additive)) was comparable to the equilibrium data. Results of the reaction between KOH and coal fly ash of different particle sizes at 900-1300 °C showed that, decreasing the coal fly ash particle size from D_{50} = 10.20 μm to D_{50} = 6.03 μm could increase the K-capture level (C_K) from 0.05 to 0.08 g K/(g additive).

6 Potassium Capture by Coal Fly Ash, Part 2: K_2CO_3, KCl, and K_2SO_4

Abstract: The potassium capture behavior of two coal fly ashes at well-controlled suspension-fired conditions was investigated through entrained flow reactor (EFR) experiments and chemical equilibrium calculations. The impact of local reaction conditions, i.e., K-speciation (K_2CO_3, KCl or K_2SO_4), K-concentration in flue gas, molar K/(Al+Si) ratio in reactants, reaction temperature, and coal ash type on the reaction was studied. The results show that the K-capture level of coal fly ash at a K-concentration of 500 ppmv was considerably lower than the equilibrium data as well as that of kaolin.[192] However, at 50 ppmv K, which is close to the typical K level in full-scale wood dust-firing boilers, no obvious difference between kaolin and coal fly ash was observed. Comparison of results for different K-species showed that coal fly ash captured KOH and K_2CO_3 more effectively than KCl and K_2SO_4. Additionally, a coal fly ash with higher content of Si and a lower melting point captured KCl more effectively than the reference coal fly ash.

6.1 Introduction

Biomass suspension-combustion has a higher electrical efficiency and higher load-flexibility compared to traditional grate-fired boilers, but the ash-related problems, including deposition, corrosion and SCR catalyst deactivation, may be more severe [67] than that in grate-fired boilers,[4, 17, 22-24, 26, 156, 187, 193] due to a higher concentration of fly ash in the flue gas.[4] Potassium originating from biomass is the primary cause for the ash-related problems. Potassium may be present as KOH, KCl, K_2SO_4 in the flue gas or other forms depending on the fuel composition, ash transformation chemistry, combustion conditions, etc.[22] In combustion of woody biomass with low chlorine and sulfur concentrations, potassium exists in the flue gas in the boiler chamber mainly as gaseous KOH.[14, 21] When firing straw or other chlorine-rich biomass, chlorine facilitates the release of potassium, and KCl becomes the main K-species in the high temperature flue gas. Apart from accelerating deposit formation and SCR catalyst deactivation, severe corrosion is also attributed to KCl.[28-30, 152, 194] When firing bio-fuels

containing sulfur, K_2SO_4 is formed as another K-compound.[193] The binary system of KCl and K_2SO_4 may melt at temperatures as low as 690 °C,[33] forming a sticky surface on super-heaters and boiler surfaces, which results in accelerated fouling and slagging.

Various methods have been developed to overcome these ash-related problems in biomass-fired boilers, including use of additives,[59, 68, 82, 83, 140, 158, 178] co-firing,[121] leaching,[61, 62, 195, 196] and application of anti-corrosion coating or materials.[197, 198] Kaolin and coal fly ash are effective additives which can chemically capture K-species forming K-aluminosilicates with higher melting points.

Coal fly ash is the only additive that has been commercially utilized in full-scale biomass suspension-fired boilers for K-capture.[12, 14] In a full-scale boiler measuring campaign conducted by Wu and co-workers,[12] the influence of the addition of coal fly ash on the transformation of potassium, the deposition behavior, the deposit composition and the formation of sub-micrometer aerosols was systematically investigated.[12, 14] The amount of aerosols formed was greatly suppressed, with the composition of the aerosols changed from K-S-Cl rich to Ca-P-Si rich[14] when adding coal fly ash. The large outer deposit changed from K-Ca-Si rich to Si-Al rich, resulting in an easier and more frequent removal of the deposits.[12] However, due to the complexity of full-scale boiler combustion and the inevitable variation of conditions (bulk chemistry of fuel, load of boiler, etc.), it is almost impossible to conduct well-controlled quantitative studies on the K-capture reaction of coal fly ash in full-scale boilers.

Some lab-scale experiments have been carried out to alleviate these problems.[93, 122] Zheng et al. studied the KCl capture behavior of coal fly ash pellets in a fixed bed reactor,[93] where two types of coal ash were utilized: bituminous coal ash and lignite coal ash. The influences of parent coal type, the reaction temperature, and the K-concentration on the reaction were investigated. The results were also compared with that of kaolin,[192] showing that bituminous coal ash with a high content of Al and Si behaved similarly to kaolin and captured KCl effectively. However, the lignite coal ash pellets, which were rich in Ca and Mg, only captured negligible amounts of potassium.[93]

In another fixed bed reactor study, Liu et al.[122] investigated the KCl capture reaction by bituminous coal fly ash (70-100 μm) which were paved in a stainless steel wires holder.[122] The impact of reaction temperature, KCl-concentration and the reaction atmosphere was investigated. The results indicated that 900 °C was the optimal K-capture temperature for the investigated coal fly ash. In addition, a reducing

atmosphere and the presence of water vapor promoted the K-capture capability of the coal fly ash.[122]

Through these fixed bed studies, important data on K-capture by coal fly ash were obtained. However, the reaction conditions in the fixed bed reactors are obviously different from those in full-scale suspension-fired boilers.[93] In the fixed bed reactors, coal ash was usually in the form of pellets, flakes, piles or paved in holders, causing the reaction with gaseous K-species to be influenced by internal diffusion.[74, 78, 93] In suspension-fired boilers, coal ash particles are well-dispersed in the flue gas, having a size smaller than 100 μm, and the controlling mechanism can be quite different. The K-capture reaction under suspension-fired conditions can be limited by thermal equilibrium, mass transfer, or chemical kinetics. Additionally, local reaction temperature, gas atmosphere, additive particle size, additive composition and reaction time also impact upon the K-capture reaction by coal fly ash.[93, 98, 114] However, knowledge on the K-capture reaction of coal ash is limited, and quantitative experimental results on K-capture by coal fly ash at suspension-fired conditions are still not available. Understanding the reaction as well as its relation to local parameters is desirable to achieve an optimal performance of added coal fly ash and model development.

The objective of this chapter is to study the K-capture reaction by coal fly ash at suspension-fired conditions. The impacts of coal ash type, ash particle size, K-species type, K-concentration, and reaction temperature on the K-capture reaction were investigated. This chapter and Chapter 5 studied the potassium capture by coal fly ash. Chapter 5 focused on the KOH capture reaction by coal fly ash,[199] and this chapter addresses the reaction of coal fly ash with KCl, K_2CO_3 and K_2SO_4.

6.2 Experimental

The K-capture experiments using coal fly ash were carried out in the DTU entrained flow reactor (EFR), which has been described in Chapter 2. Three different K-species (KCl, K_2CO_3 and K_2SO_4) and two types of coal fly ash (ASV2 and AMV) were utilized. The influence of local parameters on the reaction was investigated by preforming EFR experiments under the experimental conditions summarized in Table 6-1. In series (A) of Table 6-1, the coal fly ash concentration in flue gas was constant, while the KCl concentration in flue gas was varied from 50 ppmv to 750 ppmv. The corresponding molar K/(Al+Si) ratio in reactants changed from 0.048 to 0.721. In experimental series (B) and (C) the KCl-concentration was kept constant, but the reaction temperature

was changed from 800 °C to 1450 °C to study the influence of temperature on the KCl capture reaction using ASV2 and AMV coal fly ashes. The K_2CO_3 and K_2SO_4 capturing behavior by coal fly ash was investigated in experimental series (D) and (E) of Table 6-1.

Table 6-1. Experimental conditions of K-capture using coal fly ashes.

Experimental series	K-species	Additives	Temp./°C	Gas residence time/s	K in gas /ppmv	K/(Al+Si)
(A) KCl-capture by ASV2CFA0-32 (impact of **K-concentration**)	KCl	ASV2CFA 0-32	1300	1.2	50*	0.048
					250	0.240
					500*	0.481
					750	0.721
(B) KCl-capture by ASV2CFA0-32 (impact of **temperature**)	KCl	ASV2CFA 0-32	800	1.2	50, 500	0.048, 0.481
			900			
			1100			
			1300			
			1450			
(C) KCl-capture by AMVCFA0-32 (impact of **temperature**)	KCl	AMVCFA 0-32	800	1.2	500	0.481
			900			
			1100			
			1300			
			1450			
(D) K_2CO_3-capture by ASV2CFA0-32 (impact of **temperature**)	K_2CO_3	ASV2CFA 0-32	800	1.2	500	0.481
			900			
			1300			
(E) K_2SO_4-capture by ASV2CFA0-32 (impact of **temperature**)	K_2SO_4	ASV2CFA 0-32	800	1.2	500	0.481
			900			
			1300*			

*Experiments were repeated.

6.3 Results and discussion

6.3.1 KCl capture by coal fly ash

6.3.1.1 Equilibrium calculations

Equilibrium calculation results of KCl capture by ASV2CFA0-32 at 50-1000 ppmv KCl and 800-1450 °C were summarized in Table 6-2. Detailed results of the equilibrium calculations are available in Appendix D. The results show that the type of K-aluminosilicate formed from the K-capture reaction varied with the changing KCl-concentration and the corresponding molar ratio of K/(Al+Si) in reactants. At 50

ppmv KCl (molar K/(Al+Si) ratio in reactant was 0.048), sanidine ($KAlSi_3O_8$) was the main K-aluminosilicate. When the KCl concentration increased to 250 ppmv and 500 ppmv, leucite ($KAlSi_2O_6$) was predicted to be the dominant K-aluminosilicate at 1100-1450 °C. At 800-900 °C, kaliophilite ($KAlSiO_4$) and leucite ($KAlSi_2O_6$) co-existed in the solid products. The equilibrium K-capture level (C_K) of coal fly ash increased when the KCl concentration changed from 50 ppmv to 500 ppmv. However, when the KCl concentration was increased further to 750 and 1000 ppmv, no further increase of C_K was observed.

6.3.1.2 Impact of KCl concentration

To investigate the KCl-capture behavior of coal fly ash at different KCl concentrations, experiments were conducted at 50 ppmv to 750 ppmv KCl, where the molar ratio of K/(Al+Si) in reactants changed from 0.048 to 0.721, correspondingly. The experimental results and equilibrium calculation data are compared in Figure 6-1. Results of KCl-capture by kaolin from Chapter 4[192] were also included for comparison.

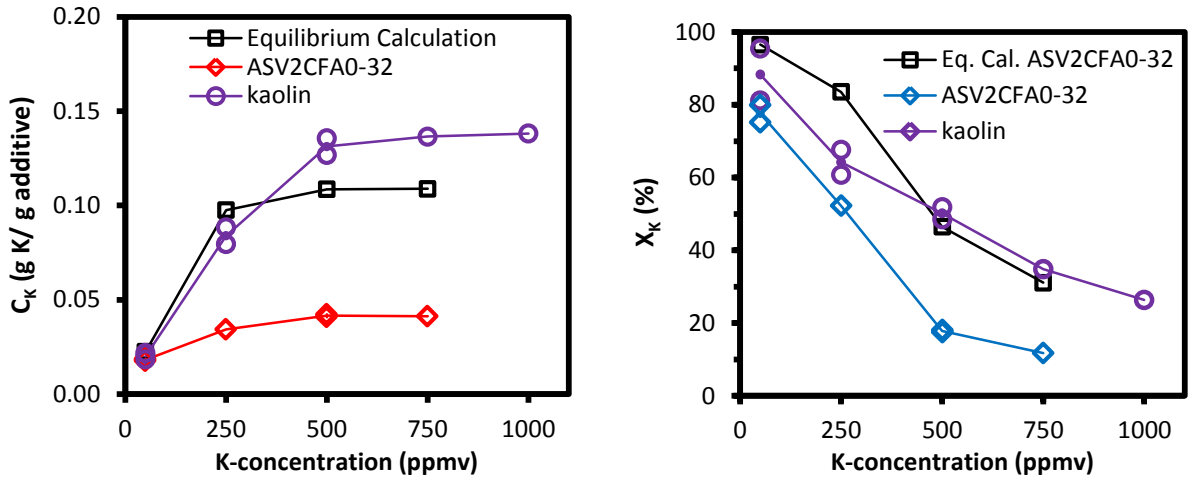

Figure 6-1. K-capture level (C_K) and K-conversion (X_K) of KCl capture by ASV2CFA0-32 at different KCl concentration from 50 ppmv to 750 ppmv (molar ratio of K/(Al+Si) changed from 0.048 to 0.721). Reaction temperature was 1300 °C, and gas residence time was 1.2 s. Experimental data of KCl capture by kaolin from Chapter 4[192] and equilibrium calculation data of KCl capture by ASV2CFA0-32 were included for comparison.

Table 6-2. Equilibrium calculation results of KCl capture by ASV2CFA0-32.

Input conditions	Temp. /°C	K-species appearing	Al-con.	Si-con.	K-con.	K-capture/(g K/(g additive))
50 ppmv KCl, K/(Al+Si) =0.048	800	100 % $KAlSi_3O_8$	12 %	24 %	100 %	0.023
	900	100 % $KAlSi_3O_8$	12 %	24 %	100 %	0.023
	1100	99 % $KAlSi_3O_8$ + 1 % KCl	12 %	24 %	99 %	0.023
	1300	97 % $KAlSi_3O_8$ + 3 % KCl	12 %	23 %	97 %	0.023
	1450	92 % $KAlSi_3O_8$ + 7 % KCl + 1 % KOH	11 %	22 %	92 %	0.021
250 ppmv KCl, K/(Al+Si) =0.240	800	95 % $KAlSi_2O_6$ + 5 % KCl	57 %	77 %	95 %	0.111
	900	94 % $KAlSi_2O_6$ + 6 % KCl	57 %	76 %	94 %	0.110
	1100	89 % $KAlSi_2O_6$ + 11 % KCl	54 %	72 %	89 %	0.104
	1300	84 % $KAlSi_2O_6$ + 16 % KCl	50 %	68 %	84 %	0.098
	1450	81 % $KAlSi_2O_6$ + 18 % KCl + 1 % KOH	49 %	66 %	81 %	0.095
500 ppmv KCl, K/(Al+Si) =0.481	800	6 % $KAlSiO_4$ + 51 % $KAlSi_2O_6$ + 40 % KCl	69 %	88 %	57 %	0.134
	900	55 % $KAlSi_2O_6$ + 45 % KCl	66 %	88 %	55 %	0.128
	1100	47 % $KAlSi_2O_6$ + 53 % KCl	57 %	76 %	47 %	0.110
	1300	46 % $KAlSi_2O_6$ + 53 % KCl + 1 % KOH	56 %	75 %	46 %	0.109
	1450	45 % $KAlSi_2O_6$ + 54 % KCl + 1 % KOH	54 %	72 %	45 %	0.104
750 ppmv KCl, K/(Al+Si) =0.721	800	33 % $KAlSiO_4$ + 19 % $KAlSi_2O_6$ + 46 % KCl	95 %	72 %	52 %	0.184
	900	3 % $KAlSiO_4$ + 35 % $KAlSi_2O_6$ + 63 % KCl	68 %	73 %	37 %	0.131
	1100	33 % $KAlSi_2O_6$ + 67 % KCl	59 %	65 %	33 %	0.114
	1300	31 % $KAlSi_2O_6$ + 68 % KCl + 1 % KOH	56 %	62 %	31 %	0.109
	1450	31 % $KAlSi_2O_6$ + 67 % KCl + 2 % KOH	56 %	62 %	31 %	0.109
1000 ppmv KCl, K/(Al+Si) =0.961	800	29 % $KAlSiO_4$ + 19 % $KAlSi_2O_6$ + 57 % KCl	100 %	87 %	41 %	0.193
	900	16 % $KAlSiO_4$ + 19 % $KAlSi_2O_6$ + 65 % KCl	84 %	87 %	35 %	0.162
	1100	25 % $KAlSi_2O_6$ + 75 % KCl	60 %	81 %	25 %	0.116
	1300	25 % $KAlSi_2O_6$ + 75 % KCl + 1 % KOH	56 %	75 %	23 %	0.109
	1450	23 % $KAlSi_2O_6$ + 75 % KCl + 2 % KOH	56 %	75 %	23 %	0.109

It is seen from Figure 6-1, that the measured K-capture level (C_K) of ASV2CFA0-32 increased from 0.019 g K/(g additive) to 0.041 g K/(g additive), when the KCl concentration increased from 50 ppmv to 500 ppmv. Measured K-conversion (X_K) of ASV2CFA0-32 decreased from 80.0 % to 17.5 % correspondingly. However, when the KCl-concentration increased further to 750 ppmv and 1000 ppmv, C_K did not increase, with X_K decreased further to 11.7 %. Comparing to the equilibrium calculation results, the measured C_K and X_K was considerably lower. This implied that the KCl-ASV2CFA0-32 reaction was far from reaching chemical equilibrium probably due to internal diffusion limitations of KCl.

Comparing the C_K and X_K of ASV2CFA0-32 with kaolin[192] in Figure 6-1, at 250 ppmv KCl and above, the experimental C_K and X_K of ASV2CFA0-32 were remarkably lower than that of kaolin.[192] The lower BET surface area (8.04 m^2/g) and the relatively bigger particle size (D_{50} = 10.20 μm) of ASV2CFA0-32 compared with kaolin (BET surface area = 12.70 m^2/g, D_{50} = 5.47 μm) was one possible reason; another possible reason being the lower reactivity of mullite in coal fly ash towards potassium, compared to kaolinite.[93] At 50 ppmv KCl, the measured C_K and X_K of ASV2CFA0-32 were comparable to those of kaolin[192] at the same molar ration of K/(Al+Si) in reactants. The result indicated that at low K-concentrations, 50 ppmv, which is representative for the gaseous potassium level in practical wood suspension-fired plants,[12, 13, 49, 151] the K-capture capacity of kaolin and coal fly ash is similar. This is probably because at lower K/(Al+Si), the mullite in the surface layer of coal fly ash particles is probably sufficient for capturing the low amount of potassium, therefore the reaction is less influenced by the internal diffusion of KCl.

The XRD results of water-washed KCl-reacted ASV2CFA0-32 are shown in Figure 6-2. In the 50 ppmv KCl-reacted ash sample, no crystalline K-aluminosilicate was detected, although sanidine ($KAlSi_3O_8$) was predicted by the equilibrium calculations (Table 6-2). This is probably because K-aluminosilicate products existed in amorphous phase or its content was too low to be detected. Leucite ($KAlSi_2O_6$) was detected both in the 250 ppmv and 500 ppmv KCl-reacted ash samples. This agrees with the equilibrium prediction shown in Table 6-2. Additionally, the types of K-aluminosilicate detected also agree with what was observed in KCl-kaolin reaction in Chapter 4.[192] Notably, in addition to K-aluminosilicate, mullite ($3Al_2O_3{\cdot}2SiO_2$) and quartz (SiO_2) were also detected in all the KCl-reacted ash samples, indicating that some mullite and quartz originating from the parental coal fly ash remained unreacted. This is presumably the reason why the measured K-capture level (C_K) of ASV2CFA0-32 was remarkably lower than the equilibrium prediction.

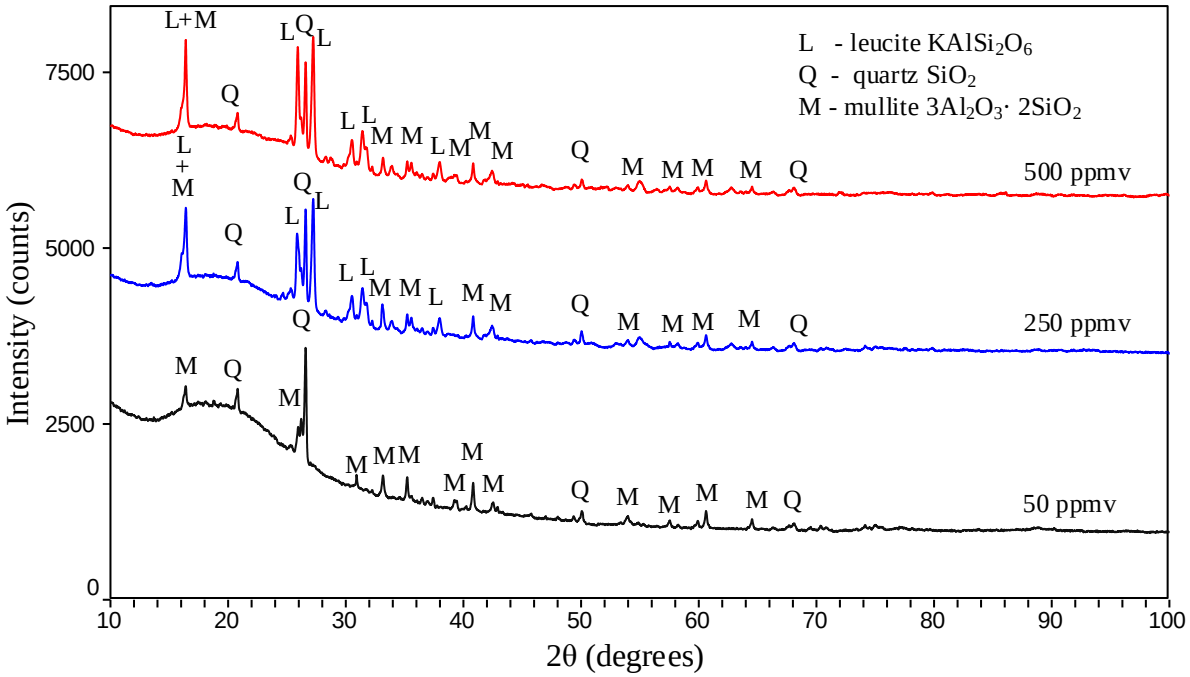

Figure 6-2. XRD spectra of water-washed KCl-reacted ASV2CFA0-32 at 50 ppmv, 250 ppmv and 500 ppmv KCl in flue gas. The reaction temperature in the EFR was 1300 °C. The molar ratio of K/(Al+Si) in the reactants changed from 0.048 to 0.961. Gas residence time was 1.2 s.

6.3.1.3 Impact of reaction temperature

The K-capture level (C_K) and K-conversion (X_K) of KCl capture by ASV2CFA0-32 and AMVCFA0-32 at different temperatures were shown in Figure 6-3 and Figure 6-4, respectively. For ASV2CFA0-32, experiments were conducted at 50 ppmv and 500 ppmv KCl. For AMVCFA0-32, experiments were only conducted in the case of 500 ppmv KCl. For all experiments, the gas residence time was kept constant at 1.2 s.

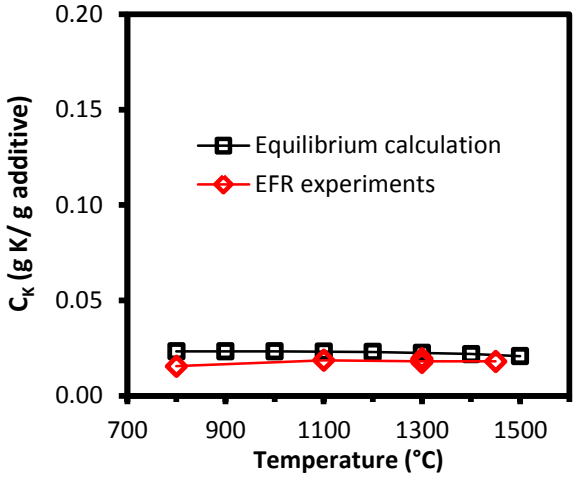

(A) K-capture level at 50 ppmv KCl

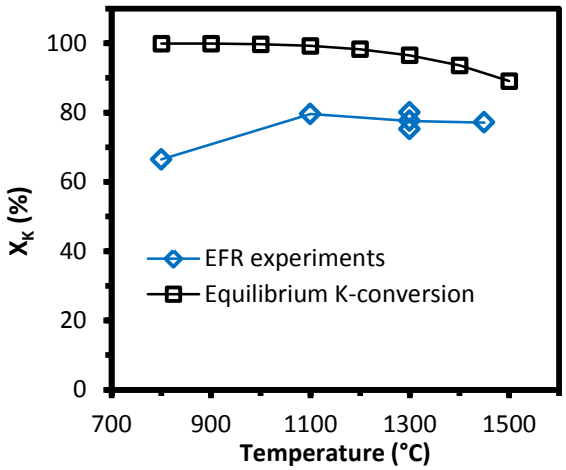

(B) K-conversion at 50 ppmv KCl

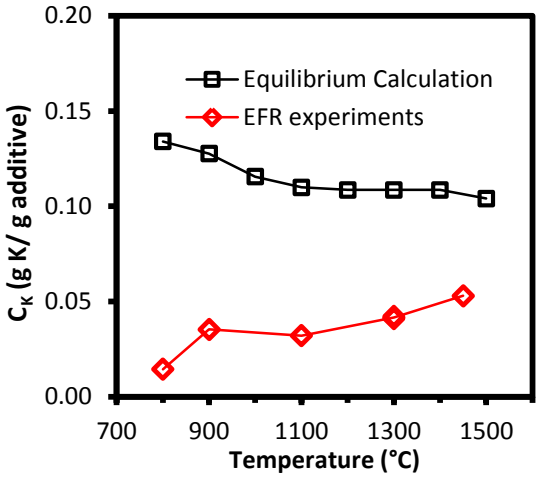

(C) K-capture level at 500 ppmv KCl

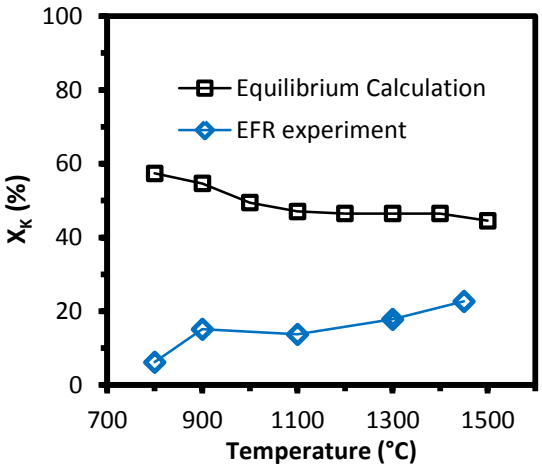

(D) K-conversion at 500 ppmv KCl

Figure 6-3. K-capture level (C_K) and K-conversion (X_K) of KCl-capture by ASV2CFA0-32 at different temperatures (800-1450 °C). In (A) and (B) KCl-concentration was 50 ppmv (molar ratio of K/(Al+Si) = 0.048). In (C) and (D) KCl-concentration was 500 ppmv (molar ratio of K/(Al+Si) = 0.481). Gas residence time was 1.2 s. Equilibrium calculation results are included for comparison.

As shown in Figure 6-3(A) and (B), at 50 ppmv KCl, the measured C_K and X_K of ASV2CFA0-32 were close to the equilibrium calculation data and no obvious change of C_K was observed within the studied temperature range (800-1450 °C). C_K was around 0.018 g K/(g additive), with about 80 % of the potassium fed captured by coal fly ash.

Figure 6-3(C) and (D) show that, at 800 °C and 500 ppmv, the measured C_K is fairly low (0.015 g K/(g additive)). However, when the reaction temperature increased to 900 and 1100 °C, the experimental C_K increased significantly to 0.035 g K/(g additive). This is because, at 800 °C, the KCl-coal fly ash reaction was probably kinetically controlled, and it was less kinetically influenced at 900-1100 °C. As the reaction temperature increased further

to 1300 and 1450 °C, C_K increased gradually to 0.053 g K/(g additive). However, the experimental C_K and X_K were both obviously lower than the equilibrium predictions. Noticing the vaporization degree of KCl (500 ppmv) at different temperatures from 800 to 1450 °C in the EFR was similar (95.4-99.7%). The increase of C_K at 900-1450 °C, especially at 1300 and 1450 °C, is probably due to the melting of coal ash particles (deformation temperature of ASV2CFA0-32 was 1280 °C), which enhanced the KCl diffusion inside the particle (D_{50} = 10.20 μm). A similar phenomenon was observed in the KCl capture experiments using AMVCFA0-32, as discussed below.

Another interesting result in Figure 6-3 is that, at 800 °C, C_K of 500 ppmv KCl (0.015 g K/(g additive)) is comparable to that of 50 ppmv KCl (0.014 g K/(g additive)). It shows that, at 800 °C, increasing the KCl-concentration from 50 to 500 ppmv did not elevate the amount of potassium captured by coal fly ash under the studied condition. This is probably because the reaction at 800 °C was kinetically controlled and the KCl concentration did not to a large degree influence the reaction.

The experimental C_K and X_K for KCl-capture by AMVCFA0-32 are shown in Figure 6-4 (A) and (B). The trend of C_K and X_K of AMVCFA0-32 was similar to that of ASV2CFA0-32. At 800 °C, C_K was as low as 0.015 g K/(g additive), and it increased to around 0.030 g K/(g additive) at 900 and 1100 °C. When the temperature increased further to 1300 and 1450 °C, C_K increased considerably to 0.069 g K/(g additive).

The experimental C_K for KCl capture by bituminous coal fly ash pellets (diameter of 1.5 mm in a fixed bed reactor) from literature[93] is included in Figure 6-4 (A) for comparison. The KCl concentration in the fixed bed reactor was 1000 ppmv, and the residence time was 1 hour, i.e., much longer than that in the EFR (1.2 s) of this study. It is seen that C_K in the fixed bed reactor from literature was considerably higher than that in the EFR at 800-1100 °C. This is because the longer residence time in the fixed bed reactor favored the reaction and more Al and Si from coal fly ash participated in the KCl capture reaction. However, at 1300 °C, the C_K in fixed bed and EFR became comparable despite the difference in residence time and KCl concentration. Possibly this is because the melting of the ash particles at high temperature (1300 °C and 1450 °C) made the reaction in the EFR less diffusion-influenced.

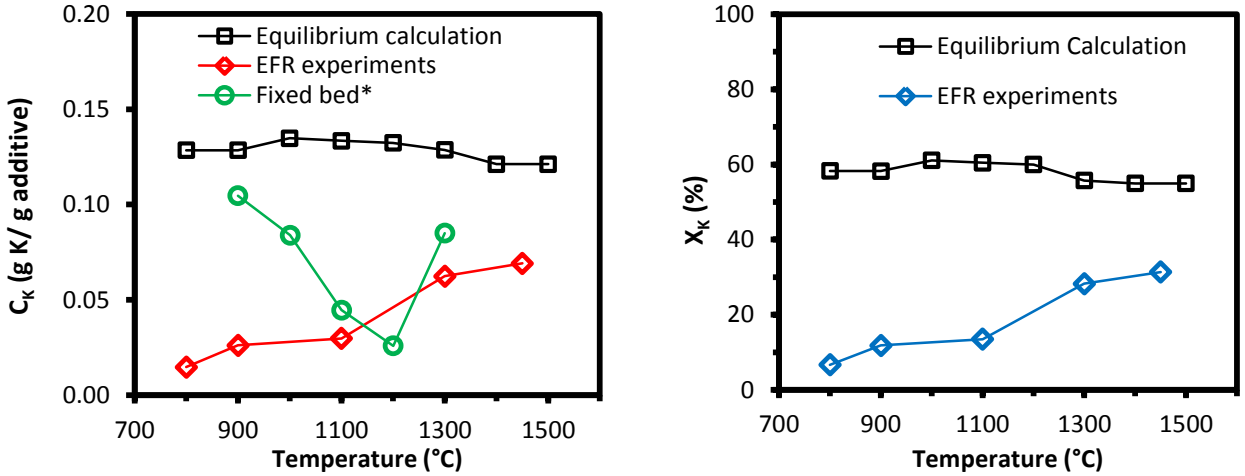

(A) K-capture level of AMVCFA0-32 (B) K-conversion of AMVCFA0-32

Figure 6-4. KCl capture by AMVCFA0-32 at different temperatures (800 °C - 1450 °C). KCl-concentration was 500 ppmv with molar ratio of K/(Al+Si) = 0.481 in reactants. Gas residence time was 1.2 s. Equilibrium calculation results and fixed bed reactor data* (bituminous coal ash pellets with diameter of 1.5 mm, 1100 °C, 1000 ppmv KCl, residence time was 1 hour) calculated from literature[93] are included for comparison.

6.3.1.4 Impact of coal fly ash type

The measured C_K of the two ashes (ASV2CFA0-32 and AMVCFA0-32) as well as that of kaolin from Chapter 4[192] are compared in Figure 6-5. Below 1100 °C, C_K and X_K of ASV2CFA0-32 and AMVCFA0-32 were similar, whereas at 1300 °C and 1450 °C, AMVCFA0-32 captured KCl more effectively than ASV2CFA0-32, despite its higher content of K and Na. One possible reason is that the melting point of AMVCFA0-32 is lower than ASV2CFA0-32, as shown in Table 2-1. The melting presumably facilitates diffusion of KCl inside the fly ash particles. Similar phenomena, that the K-capture amount by coal fly ash increased at 1200 °C and above, was observed by Zheng in a fixed bed study of KCl capture by coal fly ash pellets.[93] Another possible reason is that the Si concentration in AMVCFA0-32 is higher than that in ASV2CFA0-32. The higher Si content facilitated the formation of leucite ($KAlSi_2O_6$) (K:Al:Si = 1:1:2) in the KCl-coal fly ash reaction.

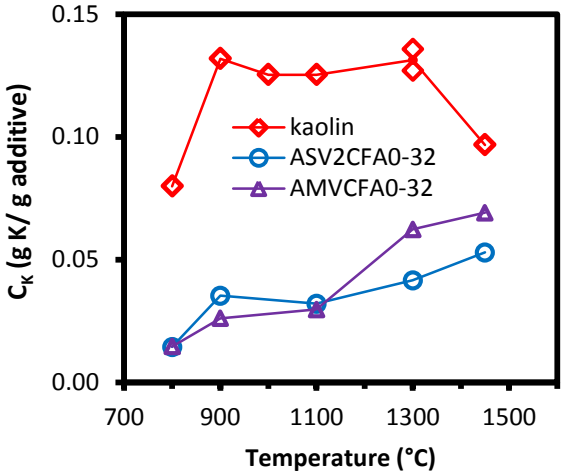

Figure 6-5. Comparison of C_K of KCl capture by ASV2CFA0-32, AMVCFA0-32 and kaolin[192] at different temperature. KCl-concentration was 500 ppmv with molar ratio of K/(Al+Si) = 0.481, gas residence time was 1.2 s.

6.3.2 K_2CO_3 capture by coal fly ash

6.3.2.1 Equilibrium calculation

Equilibrium calculations of K_2CO_3 capture by ASV2CFA0-32 were conducted with a K_2CO_3 concentration of 250 ppmv (K-concentration in flue gas was 500 ppmv), and reaction temperatures changing from 500 °C to 1800 °C. The equilibrium calculation results are summarized in Table 6-3, and detailed data can be found in Appendix D.

The equilibrium calculation results generally agreed with the prediction for KOH-capture by ASV2CFA0-32 in our Chapter 3.[199] At 250 ppmv K_2CO_3 (K/(Al+Si) = 0.481) and 800-1300 °C, kaliophilite ($KAlSiO_4$) was predicted to be the dominant K-aluminosilicate, together with some (leucite) $KAlSi_2O_6$. At 1450 °C, leucite ($KAlSi_2O_6$) was present as the dominant K-aluminosilicate product. The equilibrium C_K and X_K was constant at 800-1300 °C, and a decreased C_K was predicted at 1450 °C.

6.3.2.2 Impact of reaction temperature

The measured C_K and X_K of K_2CO_3 capture by ASV2CFA0-32 are compared to the equilibrium calculations in Figure 6-6, under the conditions of 800-1300 °C, 250 ppmv K_2CO_3 and a gas residence time of 1.2 s. The experimental C_K and X_K of K_2CO_3 capture by kaolin (D_{50} = 5.47 μm) from Chapter 4[192] were included for comparison. We believe that at the applied temperatures (800°C and above) K_2CO_3 decomposes to KOH that reacts with the coal fly ash.

According to work, the vaporization degree of K_2CO_3 at 800-1450 °C in the EFR was similar (97.3-99.7 %). However, experimental C_K (0.025 g K/(g additive)) at 800 °C was much lower than that at 900 °C (0.056 g K/(g additive)). The significant difference is probably because the reaction was kinetically controlled at 800 °C. When the reaction temperature increased to 1300 °C, C_K increased slightly to 0.070 g K/(g additive). The experimental X_K had the same trend as that of C_K, and it was below 30 % throughout the whole temperature range studied.

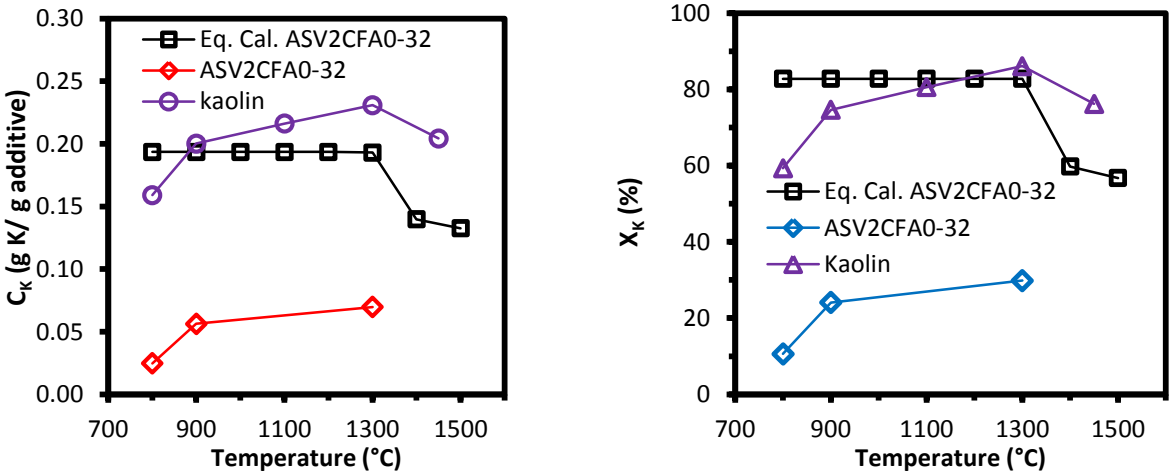

(A) K-capture level C_K (B) K-conversion X_K

Figure 6-6. K-capture level (C_K) and K-conversion (X_K) of K_2CO_3 capture by ASV2CFA0-32 at temperatures from 800 °C to 1300 °C. K_2CO_3 concentration was 250 ppmv, with molar ratio of K/(Al+Si) = 0.481. Gas residence time was 1.2 s. Equilibrium calculation results of K_2CO_3 capture by ASV2CFA0-32, and experimental results of K_2CO_3-capture by kaolin from Chapter 4[192] are included for comparison.

The results also show that the experimental C_K and X_K of ASV2CFA0-32 were significantly lower than that of kaolin[192] and the data predicted by equilibrium. The lower BET surface area of coal fly ash (8.04 m^2/g) than that of kaolin (12.70 m^2/g), and the bigger particle size of ASV2CFA0-32 (D_{50} = 12.70 μm) than that of kaolin (D_{50} = 5.47 μm) may cause some of the difference. Another possible reason is that the main mineral phase in ASV2CFA0-32, mullite, was less active towards K_2CO_3. Additionally, the relatively lower Al content of ASV2CFA0-32 may have contributed to the lower C_K as well.

The XRD spectra of water-washed K_2CO_3-reacted ASV2CFA0-32 at different temperatures were compared in Figure 6-7. In the 1300 °C sample, kaliophilite ($KAlSiO_4$) was detected together with mullite and quartz. However, in the 800 °C and 900 °C samples, no crystalline K-aluminosilicate was detected although the ICP-OES analysis showed that the

experimental C_K at 900 °C was similar as that of 1300 °C. This is probably because, at 900 °C, only amorphous K-aluminosilicate was formed, and it cannot be detected by XRD.

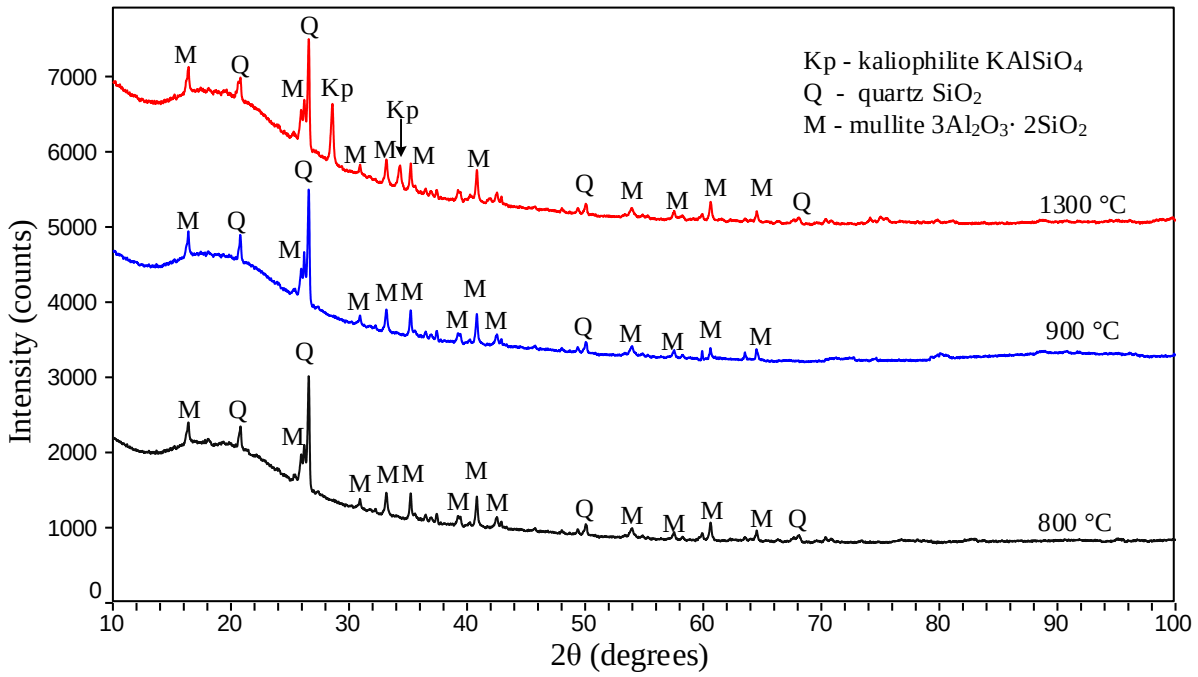

Figure 6-7. XRD spectra of water-washed K_2CO_3-reacted ASV2CFA0-32 coal fly ashes. K_2CO_3 concentration was 250 ppmv; molar K/(Al+Si) in reactants was 0.481. Gas residence time was 1.2 s.

6.3.3 K_2SO_4 capture by coal fly ash

6.3.3.1 Equilibrium calculation

Equilibrium calculations of K_2SO_4 capture by ASV2CFA0-32 were conducted at 250 ppmv K_2SO_4 and a temperature range from 500 °C to 1800 °C. The equilibrium calculation results are summarized in Table 6-4. Detailed results are provided in Appendix D.

The equilibrium calculations show that at 800 °C, 900 °C and 1450 °C, leucite ($KAlSi_2O_6$) was predicted to be the dominant K-aluminosilicate product. At 1100 °C and 1300 °C, kaliophilite ($KAlSiO_4$) was predicted to be present as the main K-aluminosilicate in the product. The calculated C_K firstly increased and then decreased with the increasing temperature in the studied temperature range.

Table 6-3. Summary of the equilibrium calculation results of K_2CO_3 capture by ASV2CFA0-32.

Input conditions	Temp. /°C	K-species appearing	Al-con.	Si-con.	X_K	C_K/(g K/(g additive))
250 ppmv K_2CO_3, K/(Al+Si) = 0.481	800	73 % $KAlSiO_4$ + 10 % $KAlSi_2O_6$	100 %	76 %	83 %	0.194
	900	71 % $KAlSiO_4$ + 12 % $KAlSi_2O_6$ + 2 % KOH	100 %	77 %	83 %	0.194
	1100	55 % $KAlSiO_4$ + 28 % $KAlSi_2O_6$ + 15 % KOH	100 %	90 %	83 %	0.194
	1300	55 % $KAlSiO_4$ + 28 % $KAlSi_2O_6$ + 17 % KOH	100 %	90 %	83 %	0.194
	1450	57 % $KAlSi_2O_6$ + 42 % KOH	69 %	92 %	57 %	0.133

Table 6-4. Summary of the equilibrium calculation results of K_2SO_4 capture by ASV2CFA0-32.

Input conditions	Temp. /°C	K-species appearing	Al-con.	Si-con.	X_K	C_K/(g K/(g additive))
250 ppmv K_2SO_4, K/(Al+Si) = 0.481	800	60 % $KAlSi_2O_6$ + 40 % K_2SO_4	73 %	98 %	60 %	0.141
	900	59 % $KAlSi_2O_6$ + 28 % K_2SO_4	72 %	96 %	59 %	0.139
	1100	54 % $KAlSiO_4$ + 28 % $KAlSi_2O_6$ + 4 % KOH	99 %	89 %	82 %	0.191
	1300	54 % $KAlSiO_4$ + 28 % $KAlSi_2O_6$ + 16 % KOH	100 %	90 %	83 %	0.193
	1450	57 % $KAlSi_2O_6$ + 42 % KOH	69 %	92 %	57 %	0.133

6.3.3.2 Impact of temperature

The experimental C_K and X_K of K_2SO_4 capture by ASV2CFA0-32 are compared with equilibrium calculations as well as the experimental C_K and X_K of K_2SO_4 capture by kaolin [192] in Figure 6-8. At 800 °C, C_K of ASV2CFA0-32 was 0.013 g K/(g additive), with only 5.7 % K_2SO_4 converted into K-aluminosilicate. The low conversion was partly because of an incomplete vaporization of K_2SO_4, and partly because the reaction was slow at 800 °C. At 900 °C and 1300 °C, C_K increased to 0.025 g K/(g additive) and 0.037 g K/(g additive) respectively. However, similar to what was observed for KCl and K_2CO_3 capture by ASV2CFA0-32, the measured C_K and X_K of K_2SO_4 were remarkably lower than the equilibrium data. This is because the fly ash only partly reacted, with some mullite remaining unreacted in products. This was supported by the XRD results shown below.

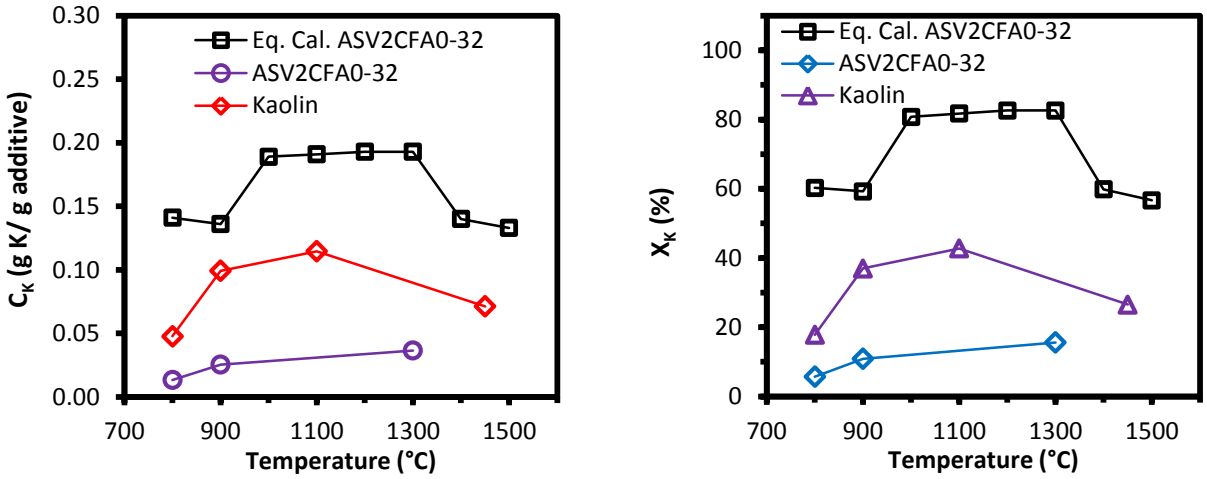

(A) K-capture level (C_K) (B) K-conversion (X_K)

Figure 6-8. K-capture level (C_K) and K-conversion (X_K) of K_2SO_4 capture by ASV2CFA0-32 at temperatures from 800 °C to 1300 °C. K_2SO_4 concentration in flue gas was 250 ppmv, and molar ratio of K/(Al+Si) in reactants was 0.481. Gas residence time was 1.2 s. Equilibrium calculation results of K_2SO_4 capture by ASV2CFA0-32, and experimental C_K of K_2SO_4 capture by kaolin[192] are included for comparison.

The XRD spectra of water-washed K_2SO_4-reacted ASV2 coal fly ash are compared in Figure 6-9. At 800 °C and 900 °C, only mullite and quartz were detected in the products, with no indication of crystalline K-aluminosilicates. In the 1300 °C sample, leucite ($KAlSi_2O_6$) was the only K-aluminosilicate detected, although kaliophilite ($KAlSiO_4$) and leucite ($KAlSi_2O_6$) were predicted to co-exist by the equilibrium calculation. Similar results were observed in the K_2SO_4-kaolin reaction in Chapter 4.[192]

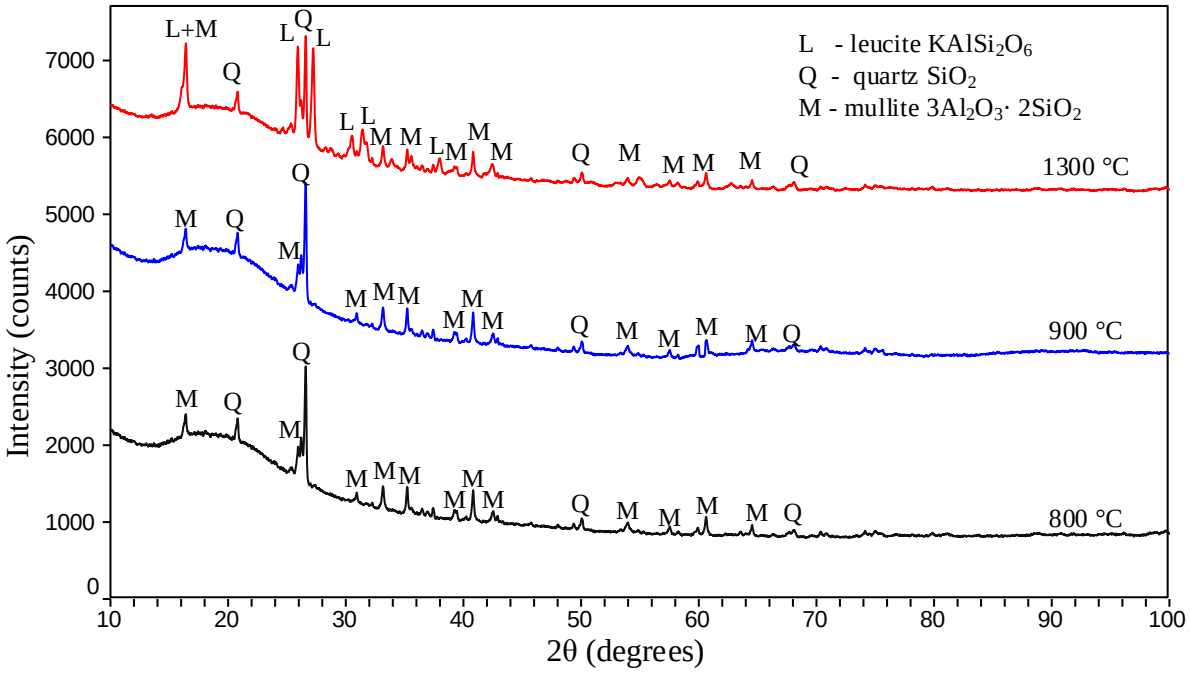

Figure 6-9. XRD spectra of water-washed K_2SO_4-reacted ASV2 coal fly ashes (ASV2CFA0-32) at different temperatures (800, 900 and 1300 °C). K_2SO_4 concentration was 250 ppmv; molar K/(Al+Si) ratio in reactants was 0.481. Gas residence time was 1.2 s.

6.3.4 Comparison of different K-species

Reaction between ASV2CFA0-32 and different K-species (KOH, K_2CO_3, KCl and K_2SO_4) is compared in Figure 6-10. The results of KOH-ASV2CFA0-32 reaction are from Chapter 5.[199] It shows that the K-capture level (C_K) for KOH and K_2CO_3 by ASV2CFA0-32 were very similar (0.05-0.07 g K/(g additive)). We attribute this to a rapid conversion of K_2CO_3 to KOH in the reactor followed by reaction of KOH with ASV2CFA0-32. A similar behavior was observed in Chapter 3 and 4 where KOH and K_2CO_3 capture by kaolin was investigated.[185, 192] The trend of C_K of K_2SO_4 capture by ASV2CFA0-32 at different temperatures generally agreed with that of KCl (C_K = 0.02-0.04 g K/(g additive)). Similar results were also seen in Chapter 4, where KCl and K_2SO_4 capture by kaolin was investigated.[192] ASV2CFA0-32 captured KOH and K_2CO_3 more effectively than KCl and K_2SO_4 in the studied temperature range and K-concentration.

The results imply that in the case of capturing KCl or K_2SO_4, more additives may be needed to achieve a satisfactory K-capture. The reason for this is that at high temperatures the main product of the reaction with KCl or K_2SO_4, is leucite ($KAlSi_2O_6$) while the main product of

reactions with KOH and K_2CO_3 is kaliophilite ($KAlSiO_4$). In addition, coal fly ash with a relatively higher content of Si seems more suitable than coal fly ash with a similar Al and Si contents for K-capture when burning Cl-rich biomass fuels.

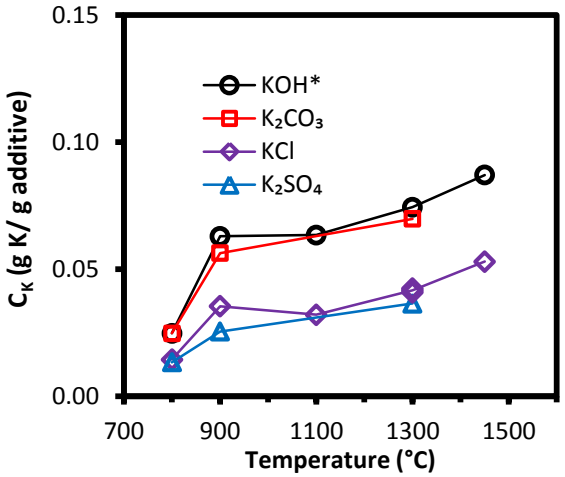

Figure 6-10. Comparison of C_K of K-capture by ASV2CFA0-32 using different K-species (KOH, K_2CO_3, KCl and K_2SO_4). The K-concentration was 500 ppmv; molar K/(Al+Si) ratio in reactants was 0.481. Gas residence time was 1.2 s. * Data of KOH capture by ASV2CFA0-32 was from Chapter 5.

6.4 Conclusions

The KCl, K_2CO_3 and K_2SO_4 capture behavior of two coal fly ashes were studied by conducting experiments in an entrained flow reactor and chemical equilibrium calculations. The influence of the type of K-species and K-concentration in flue gas, molar ratio of K/(Al+Si) in reactants, reaction temperature, as well as the type of coal fly ash on the K-capture reaction was systematically investigated.

For KCl at 1300 °C, the K-capture level (C_K) of coal fly ashes increased from 0.02 g K/(g additive) to 0.04 g K/(g additive) when the KCl concentration increased from 50 ppmv to 500 ppmv (molar ratio of K/(Al+Si) in reactants increased from 0.048 to 0.481). However, no increase in C_K was observed when the KCl concentration increased further to 750 ppmv (molar ratio of K/(Al+Si) = 0.721).

At 800 °C, the K-capture reaction was kinetically limited and a relatively low K-capture level (C_K) was observed for all K-species: KOH,[199] KCl, K_2CO_3 and K_2SO_4. At 900 °C and up to 1450 °C, C_K generally increased with increasing reaction temperature for all the applied K-species. Possibly the melting of coal fly ash at high temperature (1300 and 1450 °C)

enhanced the internal diffusion of K-species, which consequently contributed to the increase of C_K. KOH and K_2CO_3 had similar C_K levels of 0.05-0.07 g K/(g additive), and KCl and K_2SO_4 obtained C_K levels of 0.02-0.04 g K/(g additive) in the temperature range from 900 to 1450°C (with a K-concentration of 500 ppmv, molar K/(Al+Si) ratio in reactants of 0.481 and a residence time of 1.2 s). At high temperature (1300 °C) crystalline kaliophilite ($KAlSiO_4$) was detected in K_2CO_3-reacted coal fly ash, and leucite ($KAlSi_2O_6$) were detected in KCl and K_2SO_4-reacted coal fly ashes. In addition, mullite was detected in reacted coal fly ashes by XRD, showing that coal fly ash remained only partially reacted in the product samples.

The C_K and X_K levels of the two investigated coal fly ashes were compared with that of kaolin from Chapter 3 and 4.[185, 192] C_K of the two coal fly ashes was obviously lower than that of kaolin at 500 ppmv K. However, at 50 ppmv K, which is close to the level in full-scale wood suspension-fired boilers, C_K of kaolin and coal fly ash was similar. The AMVCFA0-32 coal ash with a lower melting point and high Si content captured more KCl than ASV2CFA0-32, probably because the internal diffusion of KCl inside the AMV coal ash particles was enhanced by the melting of the coal ash particles, and the high Si content facilitated the formation of leucite ($KAlSi_2O_6$).

7 Implications and Recommendations Regarding Use Additives in PF-Boilers

Kaolin and coal fly ash can be applied as K-capture additives in PF-boilers (pulverized fuel fired boilers). Kaolin is the most effective additive for alkali capture, while coal fly ash is the only additive which has been commercially utilized in full-scale biomass fired PF-boilers. Quantitative study on K-capture by kaolin and coal fly ash was conducted through entrained flow reactor experiments and chemical equilibrium calculations.

Results of the reaction between KOH/KCl and kaolin at different K-concentration showed that the K-capture level (C_K) of kaolin increased significantly when K concentration increased from 50 to 500 ppmv (molar K/(Al+Si) ratio in reactants increased from 0.048 to 0.481). However, no obvious increase of C_K was obtained when K-concentration increased further to 750 ppmv and 1000 ppmv. Similar trend was observed for the reaction between KOH/KCl and coal fly ash. The difference between kaolin and coal fly ash is that, at 250 ppmv K and above, the C_K of coal fly ash was considerably lower than that of kaolin. The smaller BET surface area, larger particle size and the less reactive mullite of coal fly ash probably contributed to this. A full conversion of kaolin to K-aluminosilicate was obtained in the K-capture reaction (residence time is 1.2 s, kaolin particle size D_{50} = 5.47 μm). In the case of coal fly ash, only part of the coal fly ash participated the K-capture reaction.

The trend of C_K for KOH, K_2CO_3, KCl and K_2SO_4 capture as a function of temperature by kaolin were similar. C_K firstly increased and then decreased in the studied temperature range (800-1450 °C), reaching a peak at 1300 °C. The trend of C_K of the four K-specie capture by coal fly ash was different from that of kaolin. It increased with temperature in the whole temperature range (800-1450 °C). The increasing of C_K at 1300-1450 °C of coal fly ash was probably because of an enhanced internal diffusion of K in melted coal fly ash particles at high temperature.

Generally, KCl and K_2SO_4 were captured by kaolin and coal fly ash less effectively than KOH and K_2CO_3. One reason is that leucite ($KAlSi_2O_6$) was formed instead of kaliophilite ($KAlSiO_4$) as the main product in KCl/K_2SO_4 – kaolin/coal fly ash reaction. More Si was

consumed when capturing the same amount of K. Based on the results from this study and the open literature, some recommendations and guidelines for optimal utilization of kaolin and coal fly ash to capture alkali species in PF-boilers are provided.

Influence of additive type

Laboratory entrained flow reactor studies show that, at 500 ppmv (Figure 7-1 (A)), kaolin can capture more than 0.2 g K/(g additive) at 900-1450 °C, if K exists in the form of KOH. Coal fly ash has also shown to be an efficient additive, however, with a lower capacity than kaolin. ASV2CFA0-32 coal fly ash can capture up to 0.1 g K/(g additive) at 1450 °C. The AMVCFA0-32 coal fly ash with lower melting point and higher Si concentration captures more K (0.15 g K/(g additive)). At 50 ppmv (Figure 7-1 (A)), which is comparable to the K-concentration in wood-fired full-scale boilers,[200] the K-capture level of kaolin and coal fly ash was similar, about 0.02 g K/(g additive). C_K was independent of reaction temperature at 50 ppmv KOH. The composition of coal fly ash has a significant influence on its K-capture capability. Bituminous coal ash rich in Al and Si usually can capture K-species more effectively than lignite coal ashes, which are rich in Ca and Mg.[93]

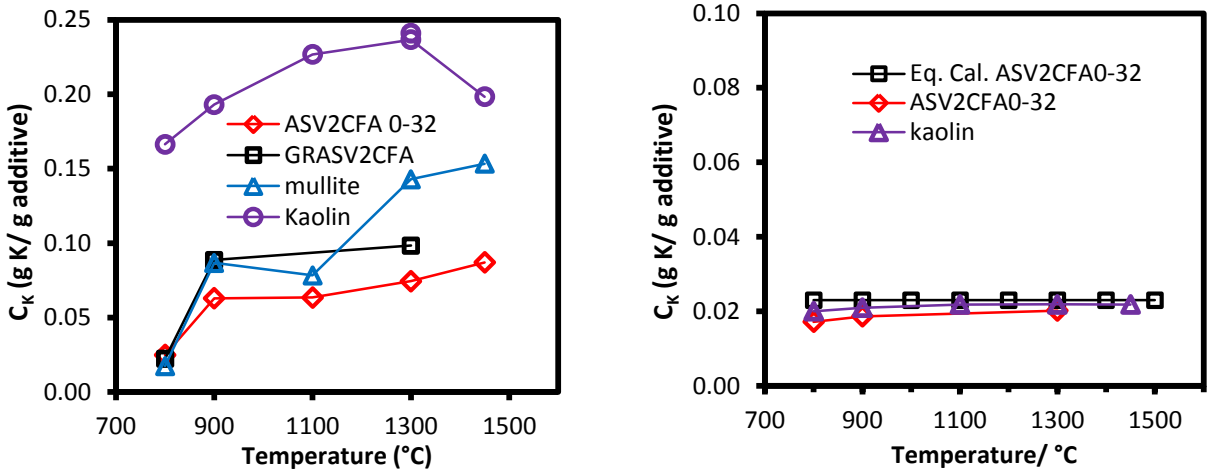

(A) C_K at 500 ppmv KOH (B) C_K at 50 ppmv KOH

Figure 7-1. K-capture level of kaolin, mullite, and coal fly ash. (A) 500 ppmv KOH, molar K/(Al+Si) ratio of 0.481 (B) 50 ppmv KOH, molar K/(Al+Si) ratio of 0.048. Gas residence time was 1.2 s.

Influence of fuel type

Typically, wood pellet fuels contain 0.1 wt. % (dry basis) K and for herbaceous materials as straw, this value is typically 1.0 wt. % (dry basis). This means that the amount of additive needed to make the biomass ash manageable, is much higher for straw, than for wood.

Assuming ideal conditions, with respect to additive particle size, local temperatures, and, full mixing of fuel and additive, a binding capacity of 0.02 g K/(g additive)(coal fly ash) could be achieved. The boiler shall be supplied with a minimum of 50 g coal fly ash, per kg wood fuel, corresponding to a mass input of 5 wt. % coal fly ash compared to the dry fuel input. With this dosage, around 97 % K could be removed from flue gas at 1100 °C and above (Figure 5-4 (D)). Since straw have a factor 10 times higher alkali content, a 10 times higher additive input will be needed. However, such a high additive consumption seems to be economical prohibitive, and to the authors knowledge no straw fired boilers use presently additives to prevent alkali metal induced problems. In addition, when firing biomass containing Cl or S, more additives should be added since kaolin and coal fly ash capture KCl and K_2SO_4 less effectively than KOH and K_2CO_3. When biomass containing Cl was fired, coal fly ash with a higher molar ratio of Si/Al is preferred because $KAlSi_2O_6$ (Si:Al = 2:1) was formed as the main K-aluminosilicate.

Influence of Temperature

The entrained flow reactor results revealed that the temperature that the additives experience has a significant influence on the K-capture capability. To obtain an optimal K-capture behavior, an appropriate injection temperature window should be selected. In the case of utilizing coal fly ash for K-capture, the highest K-capture level was observed at 1300 and 1450 °C, probably due to the melting of coal ash particles and a consequent enhanced internal K diffusion at high temperature.

When using kaolin for K-capture, the optimal temperature different from that of coal fly ash. Metakaolin is more reactive towards potassium than mullite. Consequently, a temperature window where more metakaolin and less mullite are formed, is preferred. According to the experimental results, in the KOH-kaolin system, 1100-1300 °C is the optimal temperature. For KCl-kaolin, 900-1300 °C is the optimal temperature.

Influence of additive particle size

The experimental results of KOH capture by coal fly ash in the entrained flow reactor (EFR) (residence time was 1.2 s) have shown that at 900-1300 °C, the fine fraction of the coal fly ash (D_{50} = 10.20 μm) had a higher K-capture level (0.06 g K/(g additive)) than the coarse fraction (D_{50} = 33.70 μm) (0.04 g K/(g additive)). Grinding the fine fraction to even finer (D_{50} = 6.03 μm) alleviated the K-capture level further to 0.09 g K/(g additive). The results indicate that a mean size of below 10 μm is advantageous, and that with the short residence times available in PF boilers, coal fly ash with a size above 50 μm shall not be applied.

Dosage methods

Additives can be introduced into boilers in different ways and at different positions. They can be directly fed into the boiler chamber above burners through separate nozzles, or they can be premixed with fuels before feeding into the boiler. The injection place influences not only the temperature profile that the additives experiences but also the mixing behavior of additives and fuels. To obtain a complete mixing with the fuel, premixing of the additive with the fuel before entering the boiler seems to be advantageous.

8 Conclusions and Suggestions for Future Work

8.1 Main conclusions

The potassium capture reaction using kaolin and coal fly ash was investigated in this work through EFR experiments and equilibrium calculations. The influence of local parameters, including K-concentration (50-1000 ppmv), K/(Al+Si) molar ratio (0.048-0.961), reaction temperature (800-1450 °C), gas residence time (0.6-1.9 s), additives particle size as well as the type of K-species (KOH, KCl, K_2CO_3, K_2SO_4) on the reaction was studied. The results revealed that kaolin and coal fly ash can capture gaseous K-species effectively under suspension-fired conditions.

For all the four studied K-species, KOH, KCl, K_2CO_3 and K_2SO_4, at 1100 and 1300 °C, the K-capture level (C_K) increased significantly when the K-concentration increased from 50 ppmv to 500 ppmv (molar ratio of K/(Al+Si) varied from 0.048 to 0.961). For KOH and K_2CO_3, A K-capture level higher than 0.2 g K/(g additive) was achieved at 500 ppmv K. For KCl and K_2SO_4, a C_K around 0.1 K/(g additive) was obtained. However, when the K-concentration increased further to 750 ppmv and 1000 ppmv (molar K/(Al+Si) in reactants increased to 0.721 and 0.961), no obvious increase of C_K was obtained. The possible reason is that the reactive compound in kaolin has been completely consumed, leaving the increased K-salts not to be captured. The experimental C_K and X_K (K-capture fraction) closely followed the equilibrium level for KOH, K_2CO_3 and KCl, but, for K_2SO_4, the experimental data was obviously lower compared to equilibrium data. Similar results were observed in the experiments using coal fly ash. Nevertheless, the C_K (0.05 g K/(g additive)) of coal fly ash at 500 ppmv K was considerably lower than that of kaolin (0.2 g K/(g additive)) at the same conditions. At 50 ppmv K, which is close to the conditions prevailing in practical wood suspension-fired boilers, the difference between kaolin and coal fly ash was insignificant.

Temperature influenced the C_K of kaolin, mullite and coal fly ash as well. At 500 ppmv K, when temperature increased from 800 to 1450 °C, C_K of kaolin firstly increased and then

decreased, reaching peak at 1300 °C (0.24 g K/(g additive)). For KOH, KCl and K_2CO_3, the C_K and X_K of kaolin generally followed the equilibrium predictions and obtained a full conversion, at 1100 °C and above (kaolin particle size D_{50} = 5.47 μm, gas residence time was 1.2 s). For K_2SO_4, the measured C_K was lower than the equilibrium predictions. The reason is that kaliophilite ($KAlSiO_4$) was predicted by the global equilibrium calculations in the K_2SO_4-kaolin reaction, but leucite ($KAlSi_2O_6$) was actually detected by XRD. Compared to the results of kaolin, the C_K of mullite and coal fly ash was as low as 0.08 g K/(g additive) at 900 and 1100 °C, but it increased with temperature and reached maximum at 1450 °C. C_K of mullite (0.15 g K/(g additive)) at 1450 °C was only slightly lower than that of kaolin (0.19 g K/(g additive)). Additionally, crystalline kaliophilite ($KAlSiO_4$) or leucite ($KAlSi_2O_6$) were detected in the 1300 °C and 1450 °C samples, while amorphous K-aluminosilicate was formed at lower temperatures. Comparison of C_K of different coal fly ashes showed that Al-Si rich coal fly ash with a relatively lower melting point is favorable for K-capture reaction. At 1450 °C, a potassium capture level of 0.07 g K/(g additive) was achieved using AMVCFA0-32, while it was 0.05 g K/(g additive) for ASV2CFA0-32 which has a higher melting point. Especially, coal fly ash with a higher Si content is preferred for K-capture when burning Cl-rich fuels.

Results of K-capture by kaolin and coal fly ash of different particle sizes showed that. At 1300 °C, fine kaolin (D_{50} = 3.51 μm) and normal kaolin (D_{50} = 5.47 μm) captured similar amount of potassium, higher than 0.24 g K/(g additive), while a lower C_K of about 0.20 g K/(g additive) was observed for coarse kaolin (D_{50} = 13.48 μm). Results of KOH capture by coal fly ash of different particle sizes showed that the fine coal fly ash fraction with D_{50} of 10.20 μm has a higher K-capture capability (0.07 g K/(g additive)) than that of the coarse fraction with D_{50} of 33.70 μm (0.05 g K/(g additive)). The grinded coal fly ash (D_{50} = 3.51 μm) has an even higher K-capture level.

Results of KOH-capture by kaolin at different residence time revealed that the KOH-kaolin reaction reached equilibrium at 1300 and 1450 °C, with a gas residence time of 1.2 s and a kaolin particle size of D_{50} = 5.47 μm. However, at 800 °C, it was obviously below the equilibrium value even with a longer residence time of 1.9 s, showing that the reaction was more kinetically or diffusion controlled at 800 °C. Similar results were observed for KCl capture by kaolin.

8.2 Suggestions for future work

The reaction of gaseous K-species with kaolin and coal fly ash under well-controlled suspension fired conditions has been quantitatively investigated. A general understanding of the influence of local parameters on the reaction was obtained. However, some further work could be done to improve the knowledge, and aim to get an optimal result using Al-Si-based additives to capture K-species in biomass combustion. A few suggestions which may aid future study in this area are listed below:

- *Additional study on K-capture under real biomass combustion conditions*

  All the experiments in this work were performed using pure chemicals, such as KOH, KCl, K_2CO_3 and K_2SO_4, in order to get well-controlled conditions. Alkali specie in real biomass combustion could be a mixture of various K-salts, Na-salts as well as some heavy metal species. There could be competition between different species. Experiments using real biomass could provide better understanding of the practical process inside boilers.

- *Further study on the reaction using coal fly ash especially the internal diffusion.*

  The results of K-capture by coal fly ash show that the reaction was influence by internal diffusion. Investigation of the diffusion process and impact of coal fly ash properties on the K-diffusion process and thereby the reaction could provide deeper understanding of the K-capture behavior of coal fly ash.

- *The developed method can also be used for studying other additives*

  Except for kaolin and coal fly ash, other K-capture species like S-base additive, P-Ca based additives can also be experimentally studied using this setup. The equilibrium calculation method can also be utilized for the study of other K-capture species.

- *Influence of additive addition on deposit formation and aerosol formation*

  A deposit probe could be employed in the EFR to study the effect of addition of kaolin and coal fly ash on the deposition formation behavior. The amount of aerosols formed could be measured using an impactor to study the influence additive addition on the aerosol formation.

- *Model could be developed basing on experimental data*

Although the global equilibrium calculation can well-predict the K-capture reaction using kaolin at high temperature. The reaction at lower temperature and the K-capture reaction using coal fly ash cannot be well predicted by the equilibrium calculation. A model developed basing on the experimental results could be helpful for biomass combustion industry.

References

(1) NASA Graphic: The relentless rise of carbon dioxide. https: //climate. nasa. gov/ climate resources

(2) CO_2-Earth National Oceanic and Atmospheric Administration (NOAA-US) Daily and Weekly CO_2. Https: //www. CO_2. Earth/ weekly-CO_2

(3) Climate Interactive Overview of the UN Climate Pledge Analysis. https : //www. climate interactive. org/ programs/ scoreboard/

(4) Frandsen, F. J. Ash Formation, Deposition and Corrosion When Utilizing Straw for Heat and Power Production. Doctoral Thesis, Technical University of Denmark, **2011**.

(5) Demirbas, A. *Potential applications of renewable energy sources, biomass combustion problems in boiler power systems and combustion related environmental issues*, *Prog. Energy Combust. Sci.* **2005**, 31, 171-192.

(6) Gross, R.; Leach, M.; Bauen, A. *Progress in renewable energy*, *Environment International* **2003**, 29, 105-122.

(7) Hupa, M. *Ash-Related Issues in Fluidized-Bed Combustion of Biomasses: Recent Research Highlights*, *Energy Fuels* **2012**, 26, 4-14.

(8) Nussbaumer, T. *Combustion and Co-combustion of Biomass: Fundamentals, Technologies, and Primary Measures for Emission Reduction*, *Energy Fuels* **2003**, 17, 1510-1521.

(9) Demirbas, A. *Combustion characteristics of different biomass fuels*, *Prog. Energy Combust. Sci.* **2004**, 30, 219-230.

(10) Williams, A.; Pourkashanian, M.; Jones, J. M. *Combustion of pulverised coal and biomass*, *Prog. Energy Combust. Sci.* **2001**, 27, 587-610.

(11) Frandsen, F. J. *Utilizing biomass and waste for power production—a decade of contributing to the understanding, interpretation and analysis of deposits and corrosion products*, *Fuel* **2005**, 84, 1277-1294.

(12) Wu, H.; Bashir, M. S.; Jensen, P. A.; Sander, B.; Glarborg, P. *Impact of coal fly ash addition on ash transformation and deposition in a full-scale wood suspension-firing boiler*, *Fuel* **2013**, 113, 632-643.

(13) Wu, H.; Bashir, M. S.; Jensen, P. A. *Full-scale ash deposition measurements at Avedøre Power Plant unit 2 during suspension-firing of wood with and without coal ash addition*, Technical University of Denmark: Denmark, 2012.

(14) Damoe, A. J.; Wu, H.; Frandsen, F. J.; Glarborg, P.; Sander, B. *Impact of Coal Fly Ash Addition on Combustion Aerosols (PM 2.5) from Full-Scale Suspension-Firing of Pulverized Wood*, *Energy Fuels* **2014**, 28, 3217-3223.

(15) Baxter, L. L. *Ash deposition during biomass and coal combustion: A mechanistic approach*, *Biomass Bioenergy* **1993**, 4, 85-102.

(16) Knudsen, J. N.; Jensen, P. A.; Dam-Johansen, K. *Transformation and Release to the Gas Phase of Cl, K, and S during Combustion of Annual Biomass*, *Energy Fuels* **2004**, 18, 1385-1399.

(17) Vassilev, S. V.; Baxter, D.; Andersen, L. K.; Vassileva, C. G.; Morgan, T. J. *An overview of the organic and inorganic phase composition of biomass*, *Fuel* **2012**, 94, 1-33.

(18) Dayton, D. C.; French, R. J.; Milne, T. A. *Direct Observation of Alkali Vapor Release during Biomass Combustion and Gasification. 1. Application of Molecular Beam/Mass Spectrometry to Switchgrass Combustion*, *Energy Fuels* **1995**, 9, 855-865.

(19) Wang, G.; Shen, L.; Sheng, C. *Characterization of Biomass Ashes from Power Plants Firing Agricultural Residues*, *Energy Fuels* **2012**, 26, 102-111.

(20) Khan, A. A.; de Jong, W.; Jansens, P. J.; Spliethoff, H. *Biomass combustion in fluidized bed boilers: Potential problems and remedies*, *Fuel Process. Technol.* **2009**, 90, 21-50.

(21) Niu, Y.; Tan, H.; Hui, S. e. *Ash-related issues during biomass combustion: Alkali-induced slagging, silicate melt-induced slagging (ash fusion), agglomeration, corrosion, ash utilization, and related countermeasures*, *Prog. Energy Combust. Sci.* **2016**, 52, 1-61.

(22) Johansen, J. M.; Aho, M.; Paakkinen, K.; Taipale, R.; Egsgaard, H.; Jakobsen, J. G.; Frandsen, F. J.; Glarborg, P. *Release of K, Cl, and S during combustion and co-combustion with wood of high-chlorine biomass in bench and pilot scale fuel beds*, *Proc. Combust. Inst.* **2013**, 34, 2363-2372.

(23) Vassilev, S. V.; Baxter, D.; Andersen, L. K.; Vassileva, C. G. *An overview of the chemical composition of biomass*, *Fuel* **2010**, 89, 913-933.

(24) Damoe, A. J.; Jensen, P. A.; Frandsen, F. J.; Wu, H.; Glarborg, P. *Fly Ash Formation during Suspension Firing of Biomass: Effects of Residence Time and Fuel Type*, *Energy Fuels* **2017**, 31, 555-570.

(25) Bartels, M.; Lin, W.; Nijenhuis, J.; Kapteijn, F.; van Ommen, J. R. *Agglomeration in fluidized beds at high temperatures: Mechanisms, detection and prevention*, *Prog. Energy Combust. Sci.* **2008**, 34, 633-666.

(26) Anicic, B.; Lin, W.; Dam-Johansen, K.; Wu, H. *Agglomeration mechanism in biomass fluidized bed combustion – Reaction between potassium carbonate and silica sand*, *Fuel Process. Technol.* **2018**, 173, 182-190.

(27) Nielsen, H. P.; Frandsen, F. J.; Dam-Johansen, K. *Lab-Scale Investigations of High-Temperature Corrosion Phenomena in Straw-Fired Boilers*, *Energy Fuels* **1999**, 13, 1114-1121.

(28) Nielsen, H. P.; Frandsen, F. J.; Dam-Johansen, K.; Baxter, L. L. *The implications of chlorine-associated corrosion on the operation of biomass-fired boilers*, *Prog. Energy Combust. Sci.* **2000**, 26, 283-298.

(29) Zheng, Y.; Jensen, A. D.; Johnsson, J. E.; Thøgersen, J. R. *Deactivation of V_2O_5-WO_3-TiO_2 SCR catalyst at biomass fired power plants: Elucidation of mechanisms by lab- and pilot-scale experiments*, *Appl. Catal., B: Environ.* **2008**, 83, 186-194.

(30) Zheng, Y.; Jensen, A. D.; Johnsson, J. E. *Deactivation of V_2O_5-WO_3-TiO_2 SCR catalyst at a biomass-fired combined heat and power plant*, *Appl. Catal., B: Environ.* **2005**, 60, 253-264.

(31) Khodayari, R.; Andersson, C.; Odenbrand, C. U.; Andersson, L. H. Deactivation and regeneration of SCR catalysts used in bio fuel power plants, *5th European Conference on Industrial Furnaces and Boilers In Industrial furnaces and boilers*, Portugal, **2000**.

(32) Saidur, R.; Abdelaziz, E. A.; Demirbas, A.; Hossain, M. S.; Mekhilef, S. *A review on biomass as a fuel for boilers*, *Renewable and Sustainable Energy Reviews* **2011**, 15, 2262-2289.

(33) Lindberg, D.; Backman, R.; Chartrand, P. *Thermodynamic evaluation and optimization of the ($NaCl+Na_2SO_4+Na_2CO_3+KCl+K_2SO_4+K_2CO_3$) system*, *The Journal of Chemical Thermodynamics* **2007**, 39, 1001-1021.

(34) Skrifvars, B.-J.; Laurén, T.; Hupa, M.; Korbee, R.; Ljung, P. *Ash behaviour in a pulverized wood fired boiler—a case study*, *Fuel* **2004**, 83, 1371-1379.

(35) Vassilev, S. V.; Baxter, D.; Andersen, L. K.; Vassileva, C. G. *An overview of the composition and application of biomass ash. Part 1. Phase–mineral and chemical composition and classification*, *Fuel* **2013**, 105, 40-76.

(36) Hansen, S. B.; Jensen, P. A.; Frandsen, F. J.; Wu, H.; Bashir, M. S.; Wadenbäck, J.; Sander, B.; Glarborg, P. *Deposit Probe Measurements in Large Biomass-Fired Grate Boilers and Pulverized-Fuel Boilers*, *Energy Fuels* **2014**, 28, 3539-3555.

(37) Bashir, M. S.; Jensen, P. A.; Frandsen, F.; Wedel, S.; Dam-Johansen, K.; Wadenbäck, J.; Pedersen, S. T. *Ash transformation and deposit build-up during biomass suspension and grate firing: Full-scale experimental studies*, *Fuel Process. Technol.* **2012**, 97, 93-106.

(38) Kaufmann, H.; Nussbaumer, T.; Baxter, L.; Yang, N. *Deposit formation on a single cylinder during combustion of herbaceous biomass*, *Fuel* **2000**, 79, 141-151.

(39) Andersen, K. H.; Frandsen, F. J.; Hansen, P. F. B.; Wieck-Hansen, K.; Rasmussen, I.; Overgaard, P.; Dam-Johansen, K. *Deposit Formation in a 150 MW_e Utility PF-Boiler during Co-combustion of Coal and Straw*, *Energy Fuels* **2000**, 14, 765-780.

(40) Steenari, B. M.; Lindqvist, O.; Langer, V. *Ash sintering and deposit formation in PFBC*, *Fuel* **1998**, 77, 407-417.

(41) Michelsen, H. P.; Frandsen, F.; Dam-Johansen, K.; Larsen, O. H. *Deposition and high temperature corrosion in a 10 MW straw fired boiler*, *Fuel Process. Technol.* **1998**, 54, 95-108.

(42) Jenkins, B. M.; Baxter, L. L.; Miles, T. R. *Combustion properties of biomass*, *Fuel Process. Technol.* **1998**, 54, 17-46.

(43) Christensen, K. A.; Stenholm, M.; Livbjerg, H. *The formation of submicron aerosol particles, HCl and SO_2 in straw-fired boilers*, *J. Aerosol Sci* **1998**, 29, 421-444.

(44) Jensen, P. A.; Stenholm, M.; Hald, P. *Deposition Investigation in Straw-Fired Boilers*, *Energy Fuels* **1997**, 11, 1048-1055.

(45) Wright, I. G.; Krause, H. H. *Assessment of factors affecting boiler tube lifetime in waste-fired steam generators: new opportunities for research and technology development*, Golden, Colorado, 1996.

(46) Valero, A.; Cortés, C. *Ash fouling in coal-fired utility boilers. Monitoring and optimization of on-load cleaning*, *Prog. Energy Combust. Sci.* **1996**, 22, 189-200.

(47) Miles, T. R.; Baxter, L. L.; Bryers, R. W.; Jenkins, B. M.; Oden, L. L. *Boiler deposits from firing biomass fuels*, *Biomass Bioenergy* **1996**, 10, 125-138.

(48) Bryers, R. W. *Fireside slagging, fouling, and high-temperature corrosion of heat-transfer surface due to impurities in steam-raising fuels*, *Prog. Energy Combust. Sci.* **1996**, 22, 29-120.

(49) Bashir, M. S.; Jensen, P. A.; Frandsen, F. J.; Wedel, S.; Dam-johansen, K.; Wadenbäck, J. *Suspension-Firing of Biomass. Part 2: Boiler Measurements of Ash Deposit Shedding*, *Energy Fuels* **2012**.

(50) Zbogar, A.; Frandsen, F.; Jensen, P. A.; Glarborg, P. *Shedding of ash deposits*, *Prog. Energy Combust. Sci.* **2009**, 35, 31-56.

(51) Zeuthen, J. H.; Jensen, P. A.; Jensen, J. P.; Livbjerg, H. *Aerosol Formation during the Combustion of Straw with Addition of Sorbents*, *Energy Fuels* **2007**, 21, 699-709.

(52) Okoro, S. C.; Montgomery, M.; Frandsen, F. J.; Pantleon, K. *High Temperature Corrosion under Laboratory Conditions Simulating Biomass-Firing: A Comprehensive Characterization of Corrosion Products*, *Energy Fuels* **2014**, 28, 6447-6458.

(53) Davidsson, K. O.; Steenari, B. M.; Eskilsson, D. *Kaolin Addition during Biomass Combustion in a 35 MW Circulating Fluidized-Bed Boiler*, *Energy Fuels* **2007**, 21, 1959-1966.

(54) Kling, Å.; Andersson, C.; Myringer, Å.; Eskilsson, D.; Järås, S. G. *Alkali deactivation of high-dust SCR catalysts used for NOx reduction exposed to flue gas from 100MW-scale biofuel and peat fired boilers: Influence of flue gas composition*, *Appl. Catal., B: Environ.* **2007**, 69, 240-251.

(55) Kling, A.; Andersson, C.; Myringer, A.; Eskilsson, D.; Jaras, S. *Alkali deactivation of high-dust SCR catalysts used for NOx reduction exposed to flue gas from 100MW-scale biofuel and peat fired boilers: Influence of flue gas composition*, *Appl. Catal., B: Environ.* **2007**, 69, 240-251.

(56) Castellino, F.; Rasmussen, S. B.; Jensen, A. D.; Johnsson, J. E.; Fehrmann, R. *Deactivation of vanadia-based commercial SCR catalysts by polyphosphoric acids*, *Appl. Catal., B: Environ.* **2008**, 83, 110-122.

(57) Zheng, Y.; Jensen, A. D.; Johnsson, J. E. *Laboratory Investigation of Selective Catalytic Reduction Catalysts: Deactivation by Potassium Compounds and Catalyst Regeneration*, *Ind. Eng. Chem. Res.* **2004**, 43, 941-947.

(58) Wieck-Hansen, K.; Overgaard, P.; Larsen, O. H. *Cofiring coal and straw in a 150 MWe power boiler experiences*, *Biomass Bioenergy* **2000**, 19, 395-409.

(59) Steenari, B. M.; Lindqvist, O. *High-temperature reactions of straw ash and the anti-sintering additives kaolin and dolomite*, *Biomass Bioenergy* **1998**, 14, 67-76.

(60) Aho, M.; Silvennoinen, J. *Preventing chlorine deposition on heat transfer surfaces with aluminium–silicon rich biomass residue and additive*, *Fuel* **2004**, 83, 1299-1305.

(61) Jenkins, B. M.; Bakker, R. R.; Wei, J. B. *On the properties of washed straw*, *Biomass Bioenergy* **1996**, 10, 177-200.

(62) Turn, S.; Kinoshita, C.; Ishimura, D.; Jenkins, B.; Zhou, J. *Leaching of Alkalis in Biomass Using Banagrass as a Prototype Herbaceous Species*, National Renewable Energy Laboratory: California, 2003.

(63) Yin, C.; Rosendahl, L. A.; Kær, S. K. *Grate-firing of biomass for heat and power production*, *Prog. Energy Combust. Sci.* **2008**, 34, 725-754.

(64) Wang, J.; Yuan, Y.; Chi, Z.; Zhang, G. *Development and application of anti-fouling ceramic coating for high-sodium coal-fired boilers*, *Journal of the Energy Institute* **2017**.

(65) Jensen, P. A.; Sander, B.; Dam-Johansen, K. *Pretreatment of straw for power production by pyrolysis and char wash*, *Biomass Bioenergy* **2001**, 20, 431-446.

(66) Llorente, M. J. F.; Arocas, P. D.; Nebot, L. G.; García, J. E. C. *The effect of the addition of chemical materials on the sintering of biomass ash*, *Fuel* **2008**, 87, 2651-2658.

(67) Wu, H.; Glarborg, P.; Frandsen, F. J.; Dam-Johansen, K.; Jensen, P. A. *Dust-Firing of Straw and Additives: Ash Chemistry and Deposition Behavior*, *Energy Fuels* **2011**, 25, 2862-2873.

(68) Wang, L.; Hustad, J. E.; Skreiberg, Ø.; Skjevrak, G.; Grønli, M. *A Critical Review on Additives to Reduce Ash Related Operation Problems in Biomass Combustion Applications*, *Energy Procedia* **2012**, 20, 20-29.

(69) Turn, S. Q.; Kinoshita, C. M.; Ishimura, D. M.; Zhou, J.; Hiraki, T. T.; Masutani, S. M. *A review of sorbent materials for fixed bed alkali getter systems in biomass gasifier combined cycle power generation applications*, *J. Inst. Energy* **1999**, 71, 163-177.

(70) Lee, S. H. D.; Swift, W. M.; Johnson, I. Regeneration of Activated Bauxite Used as a Granular Sorbent for Removing Gaseous Alkali Metal Compounds from Hot Flue Gas, *25th Annual International Gas Turbine Conference and Products Show*, New Orleans, LA, **1980**.

(71) Lee, S. H. D.; Johnson, I. *Removal of Gaseous Alkali Metal Compounds from Hot Flue Gas by Particulate Sorbents*, *Journal of Engineering for Power* **1980**, 102, 397-402.

(72) Luthra, K. L.; LeBlanc, O. H. *Adsorption of sodium chloride and potassium chloride on alumina at 800-900.degree.C*, *The Journal of Physical Chemistry* **1984**, 88, 1896-1901.

(73) Bachovchin, D. M.; Alvin, M. A.; DeZubay, E. A.; Mulik, P. R. *Study of high temperature removal of alkali of a pressurized gasification system: Final report*, Westinghouse Electric Corp.: United States, 1986.

(74) Punjak, W. A.; Shadman, F. *Aluminosilicate sorbents for control of alkali vapors during coal combustion and gasification*, *Energy Fuels* **1988**, 2, 702-708.

(75) Mwabe, P. O.; Wendt, J. O. L. Mechanisms governing trace sodium capture by kaolinite in a downflow combustor, *26th Symposium on Combustion*, Napoli Italy, **1996**.

(76) Uberoi, M.; Punjak, W. A.; Shadman, F. *The kinetics and mechanism of alkali removal from flue gases by solid sorbents*, *Prog. Energy Combust. Sci.* **1990**, 16, 205-211.

(77) Zhang, Z.; Scharer, J. M.; Moo-Young, M. *Mathematical model for aerobic culture of a recombinant yeast*, *Bioprocess. Eng.* **1997**, 17, 235-240.

(78) Punjak, W. A.; Uberoi, M.; Shadman, F. *High-temperature adsorption of alkali vapors on solid sorbents*, *AlChE J.* **1989**, 35, 1186-1194.

(79) Shadman, F.; Punjak, W. A. *Thermochemistry of alkali interactions with refractory adsorbents*, *Thermochim. Acta* **1988**, 131, 141-152.

(80) Lee, S. H. D.; Henry, R. F.; Myles, K. M. *Removal of Alkali Vapors by a Fixed Granular-Bed Sorber Using Activated Bauxite as a Sorbent*, **1985**.

(81) Mulik, P. R.; Alvin, M. A.; Yannopoulos, L. N.; Ahmed, M. M.; Ciliberti, D. F. High Temperature Removal of Alkali and Particulates in Pressurized Gasification Systems, *Gas Turbine Conference & Products Show*, Houston, Texas, **1981**.

(82) Aho, M.; Vainikka, P.; Taipale, R.; Yrjas, P. *Effective new chemicals to prevent corrosion due to chlorine in power plant superheaters*, *Fuel* **2008**, 87, 647-654.

(83) Davidsson, K. O.; Åmand, L. E.; Steenari, B. M.; Elled, A. L.; Eskilsson, D.; Leckner, B. *Countermeasures against alkali-related problems during combustion of biomass in a circulating fluidized bed boiler*, *Chem. Eng. Sci.* **2008**, 63, 5314-5329.

(84) Kassman, H.; Bäfver, L.; Åmand, L.-E. *The importance of SO_2 and SO_3 for sulphation of gaseous KCl – An experimental investigation in a biomass fired CFB boiler*, *Combust. Flame* **2010**, 157, 1649-1657.

(85) Tobiasen, L.; Skytte, R.; Pedersen, L. S.; Pedersen, S. T.; Lindberg, M. A. *Deposit characteristic after injection of additives to a Danish straw-fired suspension boiler*, *Fuel Process. Technol.* **2007**, 88, 1108-1117.

(86) Boström, D.; Grimm, A.; Boman, C.; Björnbom, E.; Öhman, M. *Influence of Kaolin and Calcite Additives on Ash Transformations in Small-Scale Combustion of Oat*, *Energy Fuels* **2009**, 23, 5184-5190.

(87) Bäfver, L. S.; Rönnbäck, M.; Leckner, B.; Claesson, F.; Tullin, C. *Particle emission from combustion of oat grain and its potential reduction by addition of limestone or kaolin*, *Fuel Process. Technol.* **2009**, 90, 353-359.

(88) Öhman, M.; Nordin, A. *The Role of Kaolin in Prevention of Bed Agglomeration during Fluidized Bed Combustion of Biomass Fuels*, *Energy Fuels* **2000**, 14, 618-624.

(89) Broström, M.; Kassman, H.; Helgesson, A.; Berg, M.; Andersson, C.; Backman, R.; Nordin, A. *Sulfation of corrosive alkali chlorides by ammonium sulfate in a biomass fired CFB boiler*, *Fuel Process. Technol.* **2007**, 88, 1171-1177.

(90) Öhman, M.; Boström, D.; Nordin, A.; Hedman, H. *Effect of Kaolin and Limestone Addition on Slag Formation during Combustion of Wood Fuels*, *Energy Fuels* **2004**, 18, 1370-1376.

(91) Linak, W. P.; Srivastava, R. K.; Wendt, J. O. L. *Sorbent capture of nickel, lead, and cadmium in a laboratory swirl flame incinerator*, *Combust. Flame* **1995**, 100, 241-250.

(92) Gale, T. K.; Wendt, J. O. L. *High-temperature interactions between multiple-metals and kaolinite*, *Combust. Flame* **2002**, 131, 299-307.

(93) Zheng, Y.; Jensen, P. A.; Jensen, A. D. *A kinetic study of gaseous potassium capture by coal minerals in a high temperature fixed-bed reactor*, *Fuel* **2008**, 87, 3304-3312.

(94) Scandrett, L. A.; Clift, R. *The thermodynamics of alkali removal from coal derived gases*, *J. Inst. Energy* **1984**, 57, 391-397.

(95) Pettersson, A.; Åmand, L.-E.; Steenari, B.-M. *Chemical fractionation for the characterisation of fly ashes from co-combustion of biofuels using different methods for alkali reduction*, *Fuel* **2009**, 88, 1758-1772.

(96) Kyi, S.; Chadwick, B. L. *Screening of potential mineral additives for use as fouling preventatives in Victorian brown coal combustion*, *Fuel* **1999**, 78, 845-855.

(97) Mwabe, P. O. Mechanisms governing alkali metal capture by kaolinite in a downflow combustor. Ph.D. Thesis, The University of Arizona, **1993**.

(98) Tran, K.-Q.; Iisa, K.; Steenari, B.-M.; Lindqvist, O. *A kinetic study of gaseous alkali capture by kaolin in the fixed bed reactor equipped with an alkali detector*, *Fuel* **2005**, 84, 169-175.

(99) Turn, S.; Kinoshita, C.; Ishimura, D.; Zhou, J.; Hiraki, T.; Masutani, S. *Control of Alkali Species in Gasification Systems, Final Report Nrel* **2000**, 1-115.

(100) Chen, C. Y.; Lan, G. S.; Tuan, W. H. *Microstructural evolution of mullite during the sintering of kaolin powder compacts*, *Ceram. Int.* **2000**, 26, 715-720.

(101) Escobar, I.; Oleschko, H.; Wolf, K.-J.; Müller, M. *Alkali removal from hot flue gas by solid sorbents in pressurized pulverized coal combustion*, *Powder Technol.* **2008**, 180, 51-56.

(102) Vuthaluru, H. B.; Vleeskens, J. M.; Wall, T. F. *Reducing fouling from brown coals by sodium-binding additives*, *Fuel Process. Technol.* **1998**, 55, 161-173.

(103) Li, M.; Zhang, Z.; Wu, X.; Fan, J. *Experiment and Mechanism Study on the Effect of Kaolin on Melting Characteristics of Zhundong Coal Ash*, *Energy Fuels* **2016**, 30, 7763-7769.

(104) Wang, L.; Skreiberg, Ø.; Becidan, M.; Li, H. *Investigation of rye straw ash sintering characteristics and the effect of additives*, *Appl. Energy* **2016**, 162, 1195-1204.

(105) Wolf, K. J.; Müller, M.; Hilpert, K.; Singheiser, L. *Alkali Sorption in Second-Generation Pressurized Fluidized-Bed Combustion*, *Energy Fuels* **2004**, 18, 1841-1850.

(106) Wang, L.; Skjevrak, G.; Hustad, J. E.; Skreiberg, Ø. *Investigation of Biomass Ash Sintering Characteristics and the Effect of Additives*, *Energy Fuels* **2014**, 28, 208-218.

(107) Wang, L.; Skreiberg, Ø.; Becidan, M. *Investigation of additives for preventing ash fouling and sintering during barley straw combustion*, *Appl. Therm. Eng.* **2014**, 70, 1262-1269.

(108) Uberoi, M.; Shadman, F. *Sorbents for removal of Lead compounds from hot flue gases*, *AlChE J.* **1990**, 36, 307-309.

(109) Uberoi, M. High-temperature removal of metal vapors by solid sorbents. Ph.D. Thesis, University of Arizona, **1990**.

(110) Scotto, M. V.; Uberoi, M.; Peterson, T. W.; Shadman, F.; Wendt, J. O. L. *Metal capture by sorbents in combustion processes*, *Fuel Process. Technol.* **1994**, 39, 357-372.

(111) Uberoi, M.; Shadman, F. *High-temperature removal of cadmium compounds using solid sorbents*, *Environmental Science & Technology* **1991**, 25, 1285-1289.

(112) Tran, Q. K.; Steenari, B.-M.; Iisa, K.; Lindqvist, O. *Capture of Potassium and Cadmium by Kaolin in Oxidizing and Reducing Atmospheres*, *Energy Fuels* **2004**, 18, 1870-1876.

(113) Tran, K.-Q.; Iisa, K.; Hagström, M.; Steenari, B.-M.; Lindqvist, O.; Pettersson, J. B. C. *On the application of surface ionization detector for the study of alkali capture by kaolin in a fixed bed reactor*, *Fuel* **2004**, 83, 807-812.

(114) Aho, M.; Ferrer, E. *Importance of coal ash composition in protecting the boiler against chlorine deposition during combustion of chlorine-rich biomass*, *Fuel* **2005**, 84, 201-212.

(115) Ahmaruzzaman, M. *A review on the utilization of fly ash*, *Prog. Energy Combust. Sci.* **2010**, 36, 327-363.

(116) Wall, T. F.; Lowe, A.; Wibberley, L. J.; McC. Stewart, I. *Mineral matter in coal and the thermal performance of large boilers*, *Prog. Energy Combust. Sci.* **1979**, 5, 1-29.

(117) Bryers, R. W. *Fireside slagging, fouling, and high-temperature corrosion of heat-transfer surface due to impurities in steam-raising fuels*, *Prog. Energy Combust. Sci.* **1996**.

(118) Chen, Y.; Wang, G.; Sheng, C. *Comparison of Particle Size Evolution during Pulverized Coal Combustion in O_2/CO_2 and O_2/N_2 Atmospheres*, *Energy Fuels* **2013**, 28, 136-145.

(119) Wu, H.; Glarborg, P.; Frandsen, F. J.; Dam-Johansen, K.; Jensen, P. A.; Sander, B. *Co-combustion of pulverized coal and solid recovered fuel in an entrained flow reactor – General combustion and ash behaviour*, *Fuel* **2011**, 90, 1980-1991.

(120) Savolainen, K. *Co-firing of biomass in coal-fired utility boilers*, *Appl. Energy* **2003**, 74, 369-381.

(121) Zheng, Y.; Jensen, P. A.; Jensen, A. D.; Sander, B.; Junker, H. *Ash transformation during co-firing coal and straw*, *Fuel* **2007**, 86, 1008-1020.

(122) Liu, Y.; Duan, X.; Cao, X.; Che, D.; Liu, K. *Experimental study on adsorption of potassium vapor in flue gas by coal ash*, *Powder Technol.* **2017**, 318, 170-176.

(123) Punjak, W. A. High temperature interactions of alkali vapors with solids during coal combusiton and gasification. Ph.D. Thesis, The University of Arizona, **1988**.

(124) Wu, H.; Jespersen, J. B.; Frandsen, F. J.; Glarborg, P.; Aho, M.; Paakkinen, K.; Taipale, R. *Modeling of ferric sulfate decomposition and sulfation of potassium chloride during grate-firing of biomass*, *AlChE J.* **2013**, 59, 4314-4324.

(125) Glarborg, P.; Marshall, P. *Mechanism and modeling of the formation of gaseous alkali sulfates*, *Combust. Flame* **2005**, 141, 22-39.

(126) Hindiyarti, L.; Frandsen, F.; Livbjerg, H.; Glarborg, P.; Marshall, P. *An exploratory study of alkali sulfate aerosol formation during biomass combustion*, *Fuel* **2008**, 87, 1591-1600.

(127) Li, B.; Sun, Z.; Li, Z.; Aldén, M.; Jakobsen, J. G.; Hansen, S.; Glarborg, P. *Post-flame gas-phase sulfation of potassium chloride*, *Combust. Flame* **2013**, 160, 959-969.

(128) Wu, H.; Pedersen, M. N.; Jespersen, J. B.; Aho, M.; Roppo, J.; Frandsen, F. J.; Glarborg, P. *Modeling the Use of Sulfate Additives for Potassium Chloride Destruction in Biomass Combustion*, *Energy Fuels* **2014**, 28, 199-207.

(129) Aho, M.; Paakkinen, K.; Taipale, R. *Destruction of alkali chlorides using sulphur and ferric sulphate during grate combustion of corn stover and wood chip blends*, *Fuel* **2013**, 103, 562-569.

(130) Iisa, K.; Lu, Y.; Salmenoja, K. *Sulfation of Potassium Chloride at Combustion Conditions*, *Energy Fuels* **1999**, 13, 1184-1190.

(131) Sippula, O.; Lind, T.; Jokiniemi, J. *Effects of chlorine and sulphur on particle formation in wood combustion performed in a laboratory scale reactor*, *Fuel* **2008**, 87, 2425-2436.

(132) Yilmaz, A.; Hindiyarti, L.; Jensen, A. D.; Glarborg, P.; Marshall, P. *Thermal Dissociation of SO_3 at 1000–1400 K*, *J. Phys. Chem.* **2006**, 110, 6654-6659.

(133) Sengeløv, L. W.; Hansen, T. B.; Bartolomé, C.; Wu, H.; Pedersen, K. H.; Frandsen, F. J.; Jensen, A. D.; Glarborg, P. *Sulfation of Condensed Potassium Chloride by SO_2*, *Energy Fuels* **2013**, 27, 3283-3289.

(134) Kassman, H.; Broström, M.; Berg, M.; Åmand, L.-E. *Measures to reduce chlorine in deposits: Application in a large-scale circulating fluidised bed boiler firing biomass*, *Fuel* **2011**, 90, 1325-1334.

(135) Henderson, P.; Szakálos, P.; Pettersson, R.; Andersson, C.; Högberg, J. *Reducing superheater corrosion in wood-fired boilers*, *Mater. Corros.* **2006**, 57, 128-134.

(136) Kassman, H.; Pettersson, J.; Steenari, B.-M.; Åmand, L.-E. *Two strategies to reduce gaseous KCl and chlorine in deposits during biomass combustion - injection of ammonium sulphate and co-combustion with peat*, *Fuel Process. Technol.* **2013**, 105, 170-180.

(137) Wu, H.; Castro, M.; Jensen, P. A.; Frandsen, F. J.; Glarborg, P.; Dam-Johansen, K.; Røkke, M.; Lundtorp, K. *Release and Transformation of Inorganic Elements in Combustion of a High-Phosphorus Fuel*, *Energy Fuels* **2011**, 25, 2874-2886.

(138) Grimm, A.; Skoglund, N.; Boström, D.; Öhman, M. *Bed Agglomeration Characteristics in Fluidized Quartz Bed Combustion of Phosphorus-Rich Biomass Fuels*, *Energy Fuels* **2011**, 25, 937-947.

(139) Eriksson, G.; Grimm, A.; Skoglund, N.; Boström, D.; Öhman, M. *Combustion and fuel characterisation of wheat distillers dried grain with solubles (DDGS) and possible combustion applications*, *Fuel* **2012**, 102, 208-220.

(140) De Fusco, L.; Boucquey, A.; Blondeau, J.; Jeanmart, H.; Contino, F. *Fouling propensity of high-phosphorus solid fuels: Predictive criteria and ash deposits characterisation of sunflower hulls with P/Ca-additives in a drop tube furnace*, *Fuel* **2016**, 170, 16-26.

(141) Lindström, E.; Sandström, M.; Boström, D.; Öhman, M. *Slagging Characteristics during Combustion of Cereal Grains Rich in Phosphorus*, *Energy Fuels* **2007**, 21, 710-717.

(142) Gilbe, C.; Öhman, M.; Lindström, E.; Boström, D.; Backman, R.; Samuelsson, R.; Burvall, J. *Slagging Characteristics during Residential Combustion of Biomass Pellets*, *Energy Fuels* **2008**, 22, 3536-3543.

(143) Li, H.; Han, K.; Wang, Q.; Lu, C. *Influence of Ammonium Phosphates on Gaseous Potassium Release and Ash-Forming Characteristics during Combustion of Biomass*, *Energy Fuels* **2015**, 29, 2555-2563.

(144) Grimm, A. Experimental studies of ash transformation processes in combustion of phosphorus-rich biomass fuels. Ph.D. Thesis, Luleå University of Technology, **2012**.

(145) Izquierdo, M.; Querol, X. *Leaching behaviour of elements from coal combustion fly ash: An overview*, *International Journal of Coal Geology* **2012**, 94, 54-66.

(146) Kim, A. G.; Kazonich, G.; Dahlberg, M. *Relative Solubility of Cations in Class F Fly Ash*, *Environmental Science & Technology* **2003**, 37, 4507-4511.

(147) Blissett, R. S.; Rowson, N. A. *A review of the multi-component utilisation of coal fly ash*, *Fuel* **2012**, 97, 1-23.

(148) Vassilev, S. V.; Vassileva, C. G. *A new approach for the classification of coal fly ashes based on their origin, composition, properties, and behaviour*, *Fuel* **2007**, 86, 1490-1512.

(149) Bale, C. W.; Chartrand, P.; Degterov, S. A.; Eriksson, G.; Hack, K.; Ben Mahfoud, R.; Melançon, J.; Pelton, A. D.; Petersen, S. *FactSage thermochemical software and databases*, *Calphad.* **2002**, 26, 189-228.

(150) Bale, C. W.; Bélisle, E.; Chartrand, P.; Decterov, S. A.; Eriksson, G.; Hack, K.; Jung, I. H.; Kang, Y. B.; Melançon, J.; Pelton, A. D.; Robelin, C.; Petersen, S. *FactSage thermochemical software and databases — recent developments*, *Calphad.* **2009**, 33, 295-311.

(151) Bashir, M. S.; Jensen, P. A.; Frandsen, F. J.; Wedel, S.; Dam-johansen, K.; Wadenbäck, J.; Pedersen, S. T. *Suspension-Firing of Biomass . Part 1 : Full-Scale Measurements of Ash Deposit Build-up*, *Energy Fuels* **2012**, 26, 2317-2330.

(152) Hansen, L. A.; Nielsen, H. P.; Frandsen, F. J.; Dam-Johansen, K.; Hørlyck, S.; Karlsson, A. *Influence of deposit formation on corrosion at a straw-fired boiler*, *Fuel Process. Technol.* **2000**, 64, 189-209.

(153) Gao, X.; Yani, S.; Wu, H. *Emission of Inorganic PM_{10} during the Combustion of Spent Biomass from Mallee Leaf Steam Distillation*, *Energy Fuels* **2015**, 29, 5171-5175.

(154) Niu, Y.; Zhu, Y.; Tan, H.; Hui, S.; Jing, Z.; Xu, W. *Investigations on biomass slagging in utility boiler: Criterion numbers and slagging growth mechanisms*, *Fuel Process. Technol.* **2014**, 128, 499-508.

(155) Wang, Q.; Yao, H.; Yu, D.; Dai, L.; Xu, M. *Emission Behavior of Particulate Matter during Co-combustion of Coal and Biomass in a Drop Tube Furnace*, *Energy Fuels* **2007**, 21, 513-516.

(156) Laxminarayan, Y.; Jensen, P. A.; Wu, H.; Frandsen, F. J.; Sander, B.; Glarborg, P. *Deposit Shedding in Biomass-Fired Boilers: Shear Adhesion Strength Measurements*, *Energy Fuels* **2017**, 31, 8733-8741.

(157) Castellino, F.; Jensen, A. D.; Johnsson, J. E.; Fehrmann, R. *Influence of reaction products of K-getter fuel additives on commercial vanadia-based SCR catalysts*, *Appl. Catal., B: Environ.* **2009**, 86, 206-215.

(158) Wang, L.; Skjevrak, G.; Hustad, J. E.; Grønli, M.; Skreiberg, Ø. *Effects of additives on barley straw and husk ashes sintering characteristics*, *Energy Procedia* **2012**, 20, 30-39.

(159) Sami, M.; Annamalai, K.; Wooldridge, M. *Co-firing of coal and biomass fuel blends*, *Prog. Energy Combust. Sci.* **2001**, 27, 171-214.

(160) Wu, H.; Glarborg, P.; Frandsen, F. J.; Dam-Johansen, K.; Jensen, P. A.; Sander, B. *Trace elements in co-combustion of solid recovered fuel and coal*, *Fuel Process. Technol.* **2013**, 105, 212-221.

(161) Wu, H. Co-combustion of Fossil Fuels and Waste. Ph.D. Thesis, Technical University of Denmark, **2011**.

(162) Si, J.; Liu, X.; Xu, M.; Sheng, L.; Zhou, Z.; Wang, C.; Zhang, Y.; Seo, Y.-C. *Effect of kaolin additive on $PM_{2.5}$ reduction during pulverized coal combustion: Importance of sodium and its occurrence in coal*, *Appl. Energy* **2014**, 114, 434-444.

(163) Wibberley, L. J.; Wall, T. F. *Alkali-ash reactions and deposit formation in pulverized-coal-fired boilers: experimental aspects of sodium silicate formation and the formation of deposits*, *Fuel* **1982**, 61, 93-99.

(164) De Fusco, L.; Defoort, F.; Rajczyk, R.; Jeanmart, H.; Blondeau, J.; Contino, F. *Ash Characterization of Four Residual Wood Fuels in a 100 kW_{th} Circulating Fluidized Bed Reactor Including the Use of Kaolin and Halloysite Additives*, *Energy Fuels* **2016**, 30, 8304-8315.

(165) Aho, M. *Reduction of chlorine deposition in FB boilers with aluminium-containing additives*, *Fuel* **2001**, 80, 1943-1951.

(166) Chen, Y.; Xu, Y.; Sheng, C. *Behavior of Na and its capture by adding kaolin during devolatilization, combustion and gasification of Zhundong coal*, *Proc. CSEE* **2016**, 36, 4396-4410.

(167) Wei, X.; Schnell, U.; Hein, K. *Behaviour of gaseous chlorine and alkali metals during biomass thermal utilisation*, *Fuel* **2005**, 84, 841-848.

(168) Michelsen, H. P. Deposition and high-temperature corrosion in biomass-fired boilers. Ph.D. Thesis, Technical University of Denmark, **1998**.

(169) Theis, M.; Mueller, C.; Skrifvars, B.-J.; Hupa, M.; Tran, H. *Deposition behaviour of model biofuel ash in mixtures with quartz sand. Part 1: Experimental data*, *Fuel* **2006**, 85, 1970-1978.

(170) Schneider, H.; Schreuer, J.; Hildmann, B. *Structure and properties of mullite—A review*, *J. Eur. Ceram. Soc.* **2008**, 28, 329-344.

(171) The Danish Government. *Our Future Energy*: Denmark, **2011**.

(172) Sander, B. *Properties of Danish biofuels and the requirements for power production*, *Biomass Bioenergy* **1997**, 12, 177-183.

(173) Sandberg, J.; Karlsson, C.; Fdhila, R. B. *A 7-year long measurement period investigating the correlation of corrosion, deposit and fuel in a biomass fired circulated fluidized bed boiler*, *Appl. Energy* **2011**, 88, 99-110.

(174) Jensen, P. A.; Frandsen, F. J.; Hansen, J.; Dam-Johansen, K.; Henriksen, N.; Hörlyck, S. *SEM Investigation of Superheater Deposits from Biomass-Fired Boilers*, *Energy Fuels* **2004**, 18, 378-384.

(175) Baxter, L. L.; Miles, T. R.; Jenkins, B. M.; Milne, T.; Dayton, D.; Bryers, R. W.; Oden, L. L. *The behavior of inorganic material in biomass-fired power boilers: field and laboratory experiences*, *Fuel Process. Technol.* **1998**, 54, 47-78.

(176) Wiinikka, H.; Gebart, R.; Boman, C.; Boström, D.; Nordin, A.; Öhman, M. *High-temperature aerosol formation in wood pellets flames: Spatially resolved measurements*, *Combust. Flame* **2006**, 147, 278-293.

(177) Blomberg, T. *Which are the right test conditions for the simulation of high temperature alkali corrosion in biomass combustion?*, *Mater. Corros.* **2006**, 57, 170-175.

(178) Xu, L.; Liu, J.; Kang, Y.; Miao, Y.; Ren, W.; Wang, T. *Safely Burning High Alkali Coal with Kaolin Additive in a Pulverized Fuel Boiler*, *Energy Fuels* **2014**, 28, 5640-5648.

(179) Liao, Y.; Wu, S.; Chen, T.; Cao, Y.; Ma, X. *The Alkali Metal Characteristic During Biomass Combustion with Additives*, *Energy Procedia* **2015**, 75, 124-129.

(180) Wang, M. R.; Jia, D. C.; He, P. G.; Zhou, Y. *Influence of calcination temperature of kaolin on the structure and properties of final geopolymer*, *Mater. Lett.* **2010**, 64, 2551-2554.

(181) Insley, H.; Ewell, R. H. *Thermal behavior of the kaolin minerals*, *J. Res. Natl. Bur. Stand* **1935**, 14, 615-27.

(182) Yao, Z. T.; Ji, X. S.; Sarker, P. K.; Tang, J. H.; Ge, L. Q.; Xia, M. S.; Xi, Y. Q. *A comprehensive review on the applications of coal fly ash*, *Earth-Science Reviews* **2015**, 141, 105-121.

(183) Shaheen, S. M.; Hooda, P. S.; Tsadilas, C. D. *Opportunities and challenges in the use of coal fly ash for soil improvements – A review*, *Journal of Environmental Management* **2014**, 145, 249-267.

(184) Bashir, M. S. Characterization and Quantification of Deposit Build-up and Removal in Straw Suspension-Fired Boilers. Ph.D. Thesis, Technical University of Denmark, **2012**.

(185) Wang, G.; Jensen, P. A.; Wu, H.; Frandsen, F. J.; Sander, B.; Glarborg, P. *Potassium Capture by Kaolin, Part 1: KOH*, *Energy Fuels* **2018**, 32, 1851-1862.

(186) Gale, T. K.; Wendt, J. O. L. *Mechanisms and Models Describing Sodium and Lead Scavenging by a Kaolinite Aerosol at High Temperatures*, *Aerosol Sci. Technol.* **2003**, 37, 865-876.

(187) Vassilev, S. V.; Baxter, D.; Andersen, L. K.; Vassileva, C. G. *An overview of the composition and application of biomass ash*, *Fuel* **2013**, 105, 19-39.

(188) Castellino, F.; Jensen, A. D.; Johnsson, J. E.; Fehrmann, R. *Influence of reaction products of K-getter fuel additives on commercial vanadia-based SCR catalysts Part I. Potassium phosphate*, *Appl. Catal., B: Environ.* **2009**, 86, 196-205.

(189) Wang, L.; Becidan, M.; Skreiberg, Ø. *Sintering Behavior of Agricultural Residues Ashes and Effects of Additives*, *Energy Fuels* **2012**, 26, 5917-5929.

(190) Wei, X.; Lopez, C.; von Puttkamer, T.; Schnell, U.; Unterberger, S.; Hein, K. R. G. *Assessment of Chlorine–Alkali–Mineral Interactions during Co-Combustion of Coal and Straw*, *Energy Fuels* **2002**, 16, 1095-1108.

(191) Dayton, D. C.; Belle-Oudry, D.; Nordin, A. *Effect of Coal Minerals on Chlorine and Alkali Metals Released during Biomass/Coal Cofiring*, *Energy Fuels* **1999**, 13, 1203-1211.

(192) Wang, G.; Jensen, P. A.; Wu, H.; Frandsen, F. J.; Sander, B.; Glarborg, P. *Potassium Capture by Kaolin, Part 2: K_2CO_3, KCl and K_2SO_4*, *Energy Fuels* **2018**, 32, 3566-3578.

(193) Li, L.; Yu, C.; Huang, F.; Bai, J.; Fang, M.; Luo, Z. *Study on the Deposits Derived from a Biomass Circulating Fluidized-Bed Boiler*, *Energy Fuels* **2012**, 26, 6008-6014.

(194) Nielsen, H. *Deposition of potassium salts on heat transfer surfaces in straw-fired boilers: a pilot-scale study*, *Fuel* **2000**, 79, 131-139.

(195) Dayton, D. C.; Jenkins, B. M.; Turn, S. Q.; Bakker, R. R.; Williams, R. B.; Belle-Oudry, D.; Hill, L. M. *Release of Inorganic Constituents from Leached Biomass during Thermal Conversion*, *Energy Fuels* **1999**, 13, 860-870.

(196) Davidsson, K. O.; Korsgren, J. G.; Pettersson, J. B. C.; Jäglid, U. *The effects of fuel washing techniques on alkali release from biomass*, *Fuel* **2002**, 81, 137-142.

(197) Oksa, M.; Auerkari, P.; Salonen, J.; Varis, T. *Nickel-based HVOF coatings promoting high temperature corrosion resistance of biomass-fired power plant boilers*, *Fuel Process. Technol.* **2014**, 125, 236-245.

(198) Uusitalo, M. A.; Vuoristo, P. M. J.; Mäntylä, T. A. *High temperature corrosion of coatings and boiler steels below chlorine-containing salt deposits*, *Corros. Sci.* **2004**, 46, 1311-1331.

(199) Wang, G.; Jensen, P. A.; Wu, H.; Frandsen, F. J.; Laxminarayan, Y.; Sander, B.; Glarborg, P. *Potassium Captrue by Coal Fly Ash. Part 1: KOH*, *Fuel* **2018**, Submitted.

(200) Bashir, M. S.; Jensen, P. A.; Frandsen, F.; Wedel, S.; Dam-johansen, K. Suspension-firing of wood with coal ash addition : Probe measurements of ash deposit build-up at Avedøre Power Plant (AVV2). **2012**.

Appendixes

Appendix A Development of liquid feeding system of the EFR

Instead of feeding solid K-species directly into the reactor, K-species and additives, like kaolin, mullite and coal fly ash, were mixed with deionized water, to make a homogeneous slurry. The slurry was subsequently fed into the reactor through a liquid feeding system. The development of the liquid feeding system as well as commissioning this system was summarized in this appendix.

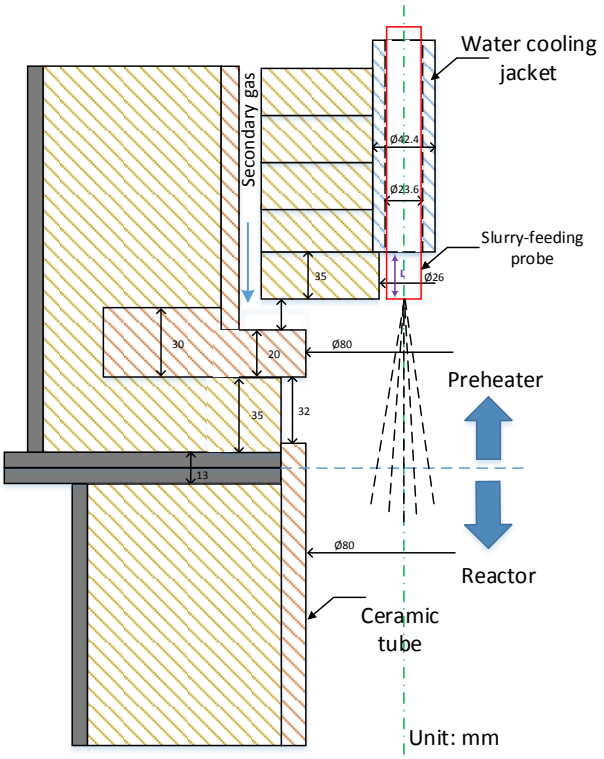

Figure A-1. Water cooling slurry-feeding probe in the EFR.

The inner structure of the EFR is shown in Figure A-1. There are two heating elements in the EFR preheater for preheating secondary gas. As shown in Figure A-1, the tip of the feeding probe is consequently exposed to high temperature flue gas, and the salt and additives from feeding slurry may deposit gradually on the tip of the feeding probe forming plug (Figure A-2) and finally causing ineffective atomizing of the solution or slurry as well as feeding instability. Another reason contributing to the instability of feeding rate is that the additives

(kaolin and coal fly ash) may deposit inside the tube connecting the peristaltic pump and the slurry-feeding probe.

Figure A-2. Plugging of feeding probe after feeding KCl solution for about 22 min.

To solve the instability of the feeding rate, two methods were employed:

- Adjust the position of the slurry-feeding probe. The original position of the feeding probe was shown in Figure A-1. As the purple letter "L" shown, the distance from the tip of the feeding probe to the water cooling jacket is 35 mm. In the following tests, the position parameter was changed to see its influence on the feeding stability. When the tip of the feeding probe is higher than the tip of the water cooling jacket, the "L" has a minus value, for example in Test 2 as shown below.
- Changing the tube connecting the peristaltic pump and the feeding probe with a thinner one (Figure A-3). At the same feeding rate, in thinner tube the flow rate of slurry is higher, which can significantly reduce the deposition of solid additives.

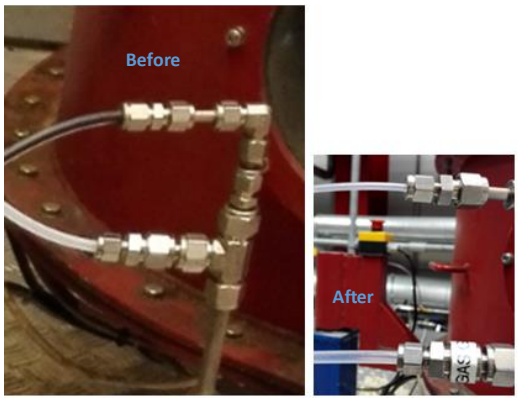

Figure A-3. Tube connecting peristaltic pump and feeding probe (changed before and after).

Feeding rate stability tests were carried out at 1300 °C with preheater zone A at 800 °C and zone B at 1100 °C. 5 wt. % ethanol aqueous solution, 5 wt. % KCl + 5 wt. % ethanol aqueous

solution and 10 wt. % kaolin + 5 wt. % KCl + 5 wt. % ethanol aqueous slurry were fed separately during tests.

Test 1: Original position (L = 35 mm), thick tube

KCl solution was utilized in this test. The figure below shows the CO_2 concentration recorded when feeding KCl solution into the EFR. As can be seen, the CO_2 concentration fluctuated significantly, from 1000 ppmv to 5800 ppmv. In this situation, the concentration of KCl vapor varied a lot, and the samples cannot be used to study the influence of KCl concentration on the KCl capture reaction.

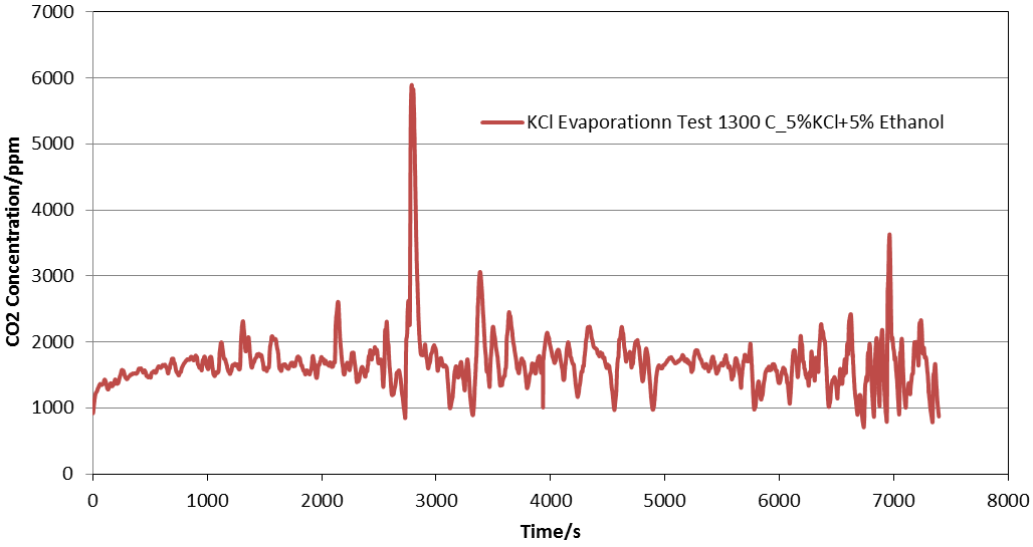

Figure A-4. CO_2 concentration during Test 1(L = 35 mm, thick tube).

Test 2: Feeding probe moved up (L = - 15 mm), thick tube

In Test 2, the feeding probe was move up by 5 cm to avoid the direct exposure to the high temperature flue gas (L = -15 mm). The test included four stages as shown in Figure A-5. In stage 1, 5 wt. % ethanol aqueous solution was fed into the reactor. In this stage, slight and periodical fluctuation of CO_2 concentration was observed. The fluctuation is due to periodical movement of two wipers of the peristaltic pump as shown in Figure A-6.

In stage 2, feeding of ethanol solution was stopped and the CO_2 concentration dropped immediately. In stage 3, KCl solution was pumped into the reactor and the residual ethanol solution was flushed out of the probe. So in stage 3 KCl-solution had not been fed into the reactor. The CO_2 concentration remained steady at the same level as in stage 2. In stage 4, KCl solution was fed into the reactor. The CO_2 concentration measured began to fluctuate and as time passed by, the fluctuation range increased significantly from less than 40 ppmv to more than 500 ppmv.

Comparing to Test 1, the feeding stability in test 2 had been improved significantly but still not satisfied. In this test the value of L is minus meaning the feeding probe is in the water-cooling jacket, which could result of deposit formation at the out let of the water jacket. In the following test the probe was move out the water-cooling jacket and keep L ≥ 0.

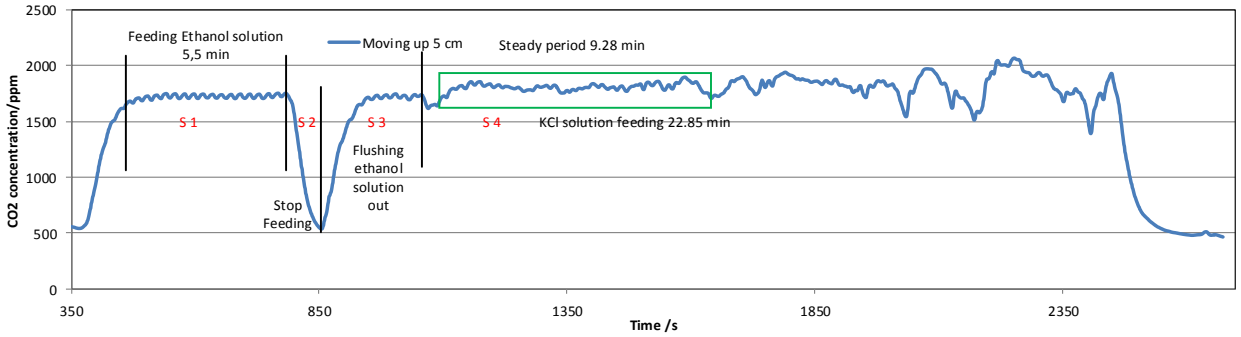

Figure A-5. CO_2 concentration during Test 2 (L = -15 mm, thick tube).

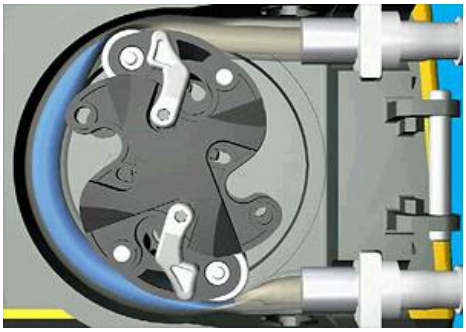

Figure A-6. Structure of peristaltic pump.

Test 3. Feeding probe moved up (L=25 mm), thick tube

In Test 3 the slurry-feeding probe is moved up from the original position by 10 mm (L = 25 mm). KCl solution without kaolin or coal fly ash was fed into the EFR in this test. As shown in Figure A-7, comparing to Test 2, the CO_2 concentration fluctuation can stay in an acceptable range for a certain period, approximately 12 mins.

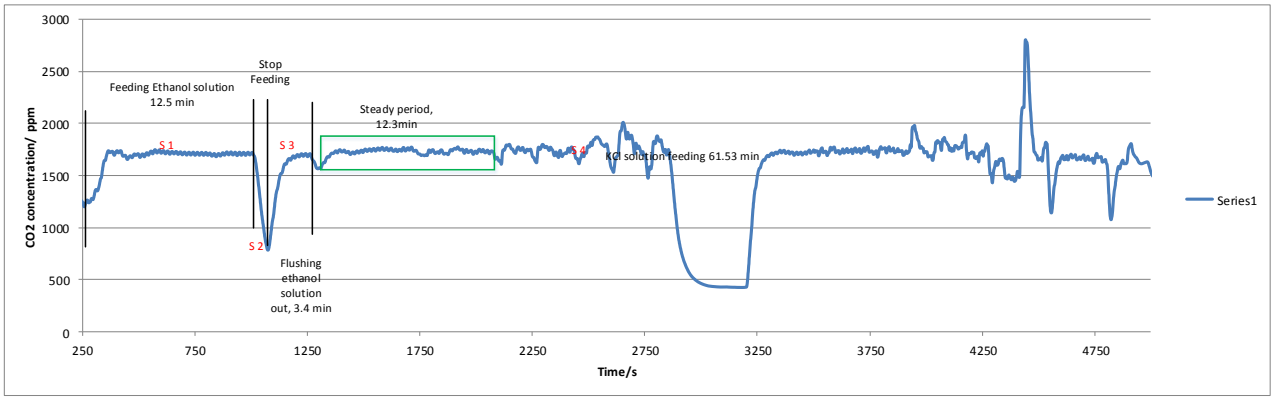

Figure A-7. CO_2 concentration during Test 3 (L = 25 mm), thick tube.

Test 4: Feeding probe moved up (L=25 mm), thin tube

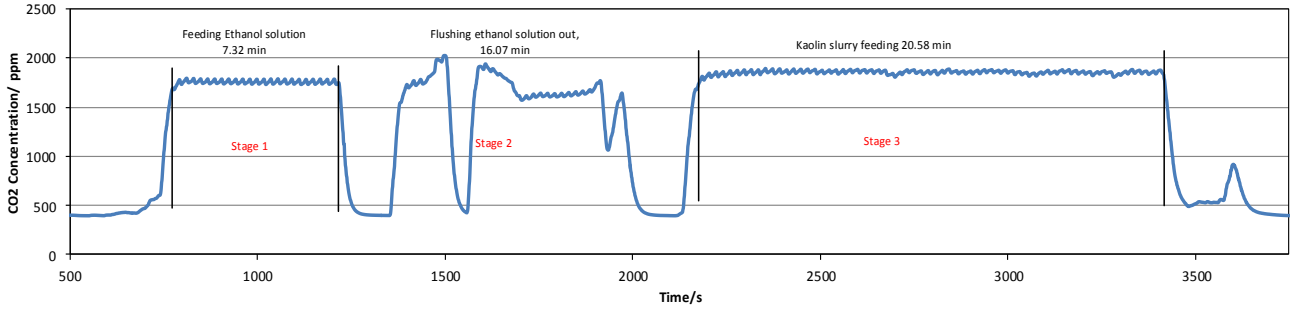

Figure A-8. CO_2 concentration during Test 4 (L = 25mm), thinner tube.

Figure A-9. No clog was observed at the outlet of feeding probe used in Test 4.

In this test, the feeding probe was moved up from the original position by 10 mm (L = 25 mm), and the tube connecting the peristaltic pump and the feeding probe was changed to a thin tube with inner diameter of about 1 mm. Kaolin slurry consisted of 10 wt. % kaolin, 5 wt. % KCl, 5 wt. % ethanol and 80 wt. % water was utilized in this test. The results show

that the feeding stability was considerably improved. At the end of the test, the feeding probe was taken out and examined. As show in Figure A-9, no clog was formed at the outlet of the feeding probe.

Test 5: Repeat Test 4 (at gage pressure of 1-3 mbar).

In this test the pressure of the EFR is kept slightly higher than the atmospheric pressure (1-3 mbar) to check the carbon balance of the system. Other parameters of Test 5 were the same as Test 4. As shown in Figure A-10 no obvious fluctuation is observed during the test.

During the ethanol feeding period, CO_2 concentration was calculated to be 1801 ppmv, while the average of measured CO_2 concentration was 1770 ppmv, which was 1.67 % lower than the calculated number. During kaolin slurry feeding, CO_2 concentration was calculated to be 1957 ppmv, while the average of the measured CO_2 concentration was 1913 ppmv, which was 2.2 % lower than the calculated value. The results show that the measured CO_2 concentrations generally agreed with the calculated numbers, indicating an acceptable carbon balance during the EFR experiments.

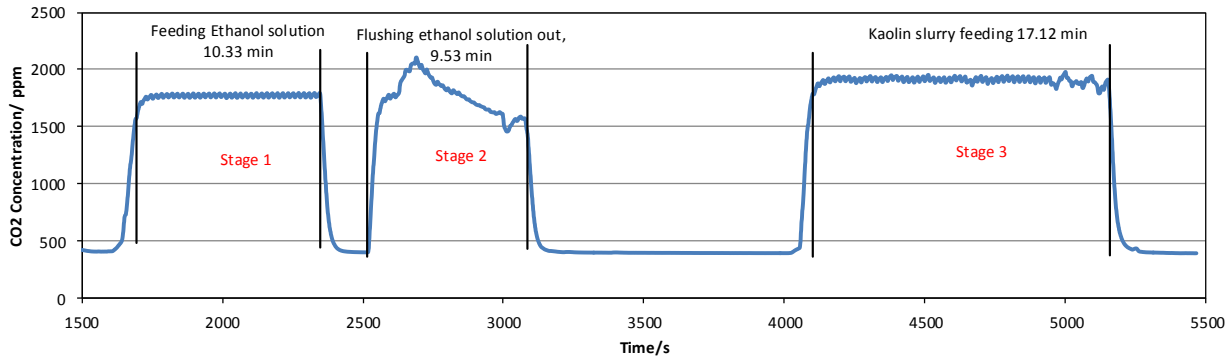

Figure A-10. CO_2 concentration during Test 5.

Appendix B Quantification method of experimental X_K and C_K

Two parameters were defined to quantify the amount of potassium captured by solid additives (kaolin, mullite and coal fly ash): the K-conversion (X_K), and the K-capture level (C_K). X_K is the percentage (%) of input K-salts chemically captured by solid additives forming water-insoluble K-aluminosilicate. C_K is the mass of potassium captured by 1 g of solid additive (g K/(g additive)).

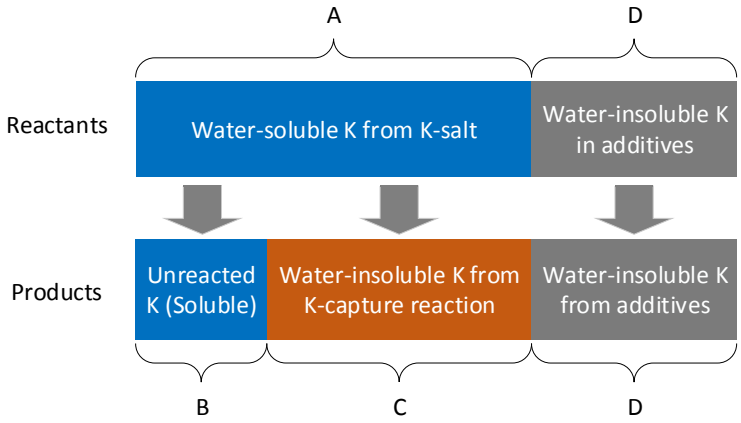

Figure B-1. Potassium transformations in the K-capture reaction.

The transformation of potassium in the reaction system is illustrated in Figure B-1. The water-insoluble K in the products originated from two different sources: Part C was formed from the reaction between K-salts and solid additives, while part D in reactants was from the solid additives. The reacted solid samples collected from the Entrained Flow Reactor (EFR) experiments were subjected to ICP-OES analysis. The concentration of water soluble potassium (part B) and total potassium (part B+C+D) were analyzed. The concentration of water-insoluble potassium (C+D) was calculated consequently. However, part C and D need to be calculated based on the composition of the reactants and the products. The calculation was based on the following assumptions:

The solid samples collected are representative, i.e., the samples collected and those not collected has the same constituents (the molar ratio of K/(Al+Si) in reactants and in products are almost identical, implying the collected products were representative);

Potassium that exists in solid feed additives are water-insoluble (Concentration in kaolin is low and it mainly stays in the form of K-aluminosilicates which is water-insoluble);

The K-conversion (X_K) was calculated according to Equation B-1.

$$X_K = \frac{C}{A} = \frac{A-B}{A} = \frac{\frac{A}{A+D} - \frac{B}{A+D}}{\frac{A}{A+D}} = \frac{Y_F - Y_P}{Y_F} \times 100\% \quad \text{(B-1)}$$

Where Y_F and Y_P are the molar ratio of water soluble K to total K in fed reactants and collected products respectively. Y_F was calculated based on the constituents of slurry and potassium concentration in utilized additives, while Y_P was calculated based on the ICP-OES result of collected solid samples.

The K-capture level (C_K) was calculated according to Equation B-2.

$$C_K = \frac{n_{K-salt}\, M_K X_K}{m_{ad.}} \quad \text{(B-2)}$$

Where n_{K-salt} is the molar amount of K-salt in reactants (mol). M_K is the molar mass of potassium (g/mol). X_K was the K-conversion (%); m_{ad} is the mass of additives (kaolin or mullite) in reactants (g).

Appendix C Equilibrium calculation of K-capture by kaolin

To provide a theoretical analysis of the experimental results, global equilibrium calculations were carried out. The comparison of the results from equilibrium calculations and experiments may shed light upon how far the EFR reaction system is from equilibrium and provide information for understanding the EFR experimental results.

The global equilibrium calculation was performed using the Equilibrium module of the thermochemical software FactSage 7.0. The Equilibrium module is the Gibbs energy minimization work horse of FactSage. It can calculate the concentration of different chemical species when specified elements or compounds react or partially react and reach a state of chemical equilibrium.[149, 150] In this study the databases of FactPS, FToxid, FTsalt and FTpulp were employed for the calculation. FactPS is the data base for pure substance, and it contains data for over 4777 compounds. FToxid is the oxide database for slags, glasses, minerals, ceramics and refractories, etc. FTsalt data base is the salt date base, which contains data for pure salt and salt solutions formed among various combinations of 20 common cations. FTpulp is the pulp and paper database, which contains data for the pulp and paper industry and data on corrosion and combustion in recovery boilers.[149] In the calculations, slag options in solution phases were not checked. Therefore no slag was included in the calculation.

Equilibrium calculations were conducted at 50, 250, 500, 750, and 1000 ppmv K in the flue gas. Molar K/(Al+Si) ratio in reactants varied from 0.048 to 0.961 correspondingly. The reaction temperature was changed from 500 °C to 1800 °C. Similar to the experimental results, the equilibrium K-conversion ($X_{Keq.}$) and equilibrium K-capture level ($C_{Keq.}$) were calculated basing on the equilibrium calculation data. Additionally, the equilibrium Al-conversion ($X_{Aleq.}$) and equilibrium Si-conversion ($X_{Aleq.}$) were calculated as well.

The K-containing products in the equilibrium calculations were categorized into two groups: K-aluminosilicates and other K-containing compounds. The total molar amount of K, Al and Si in the equilibrium calculation system was n_{Kt}, n_{Alt} and n_{Sit}, respectively. The molar amount of K, Al and Si in K-aluminosilicate products was n_{Kals}, n_{Alals} and n_{Sials}, respectively. The mass of additives in the equilibrium calculation system was $m_{ad.eq}$. The equilibrium K-conversion ($X_{Keq.}$), Al-conversion ($X_{Aleq.}$), Si-conversion ($X_{Sieq.}$) and equilibrium K-capture level ($C_{Keq.}$) was calculated as shown in Equation (C-1), (C-2), (C-3) and (C-4).

$$X_{Keq.} = \frac{n_{Kals}}{n_{Kt}} \times 100\ \% \quad \text{(C-1)}$$

$$X_{Aleq.} = \frac{n_{Alals}}{n_{Alt}} \times 100\ \% \quad \text{(C-2)}$$

$$X_{Sieq.} = \frac{n_{Sials}}{n_{Sit}} \times 100\ \% \quad \text{(C-3)}$$

$$C_{Keq.} = \frac{n_{Kt} M_K X_{Keq.}}{m_{ad.eq.}} \quad \text{(C-4)}$$

Where,

$X_{Keq.}$, $X_{Aleq.}$ and $X_{Sieq.}$ - the equilibrium calculated K-conversion, Al-conversion and Si-conversion (%);

$C_{Keq.}$ - the equilibrium calculated K-capture level;

n_{Kals}, n_{Alals}, n_{Sials} - the molar amount of K, Al and Si contained in the equilibrium calculated product K-aluminosilicates;

n_{Kt}, n_{Alt} and n_{Sit} - the total molar amount of K, Al and Si in the equilibrium calculation system;

M_K - the molar mass of K;

$m_{ad.eq.}$ - the mass of additives entered into the equilibrium calculation system;

Equilibrium calculations were conducted at 50, 250, 500 and 1000 ppmv K in the flue gas. Molar K/(Al+Si) ratio in reactants varied from 0.048 to 0.961 correspondingly. The reaction temperature was changed from 500 °C to 1800 °C. The equilibrium calculation results of KOH, K_2CO_3, KCl and K_2SO_4 capture by kaolin are summarized in Figure C-1 to C-4. The primary Y-axis (left Y-axis) of each figure is the percentage of different K-containing compounds or the percentage of conversion of K, Al or Si to K-aluminosilicates. The secondary Y-axis (right Y-axis) is the K-capture level (C_K - the mass of K captured by 1 g kaolin). In all the figures, gaseous K-containing compounds are represented with non-filled markers; liquid compounds are represented with pattern filled markers; solid compounds are represented with solid filled markers. The percentage of K, Al and Si conversion and the K-capture level were represented with dash lines.

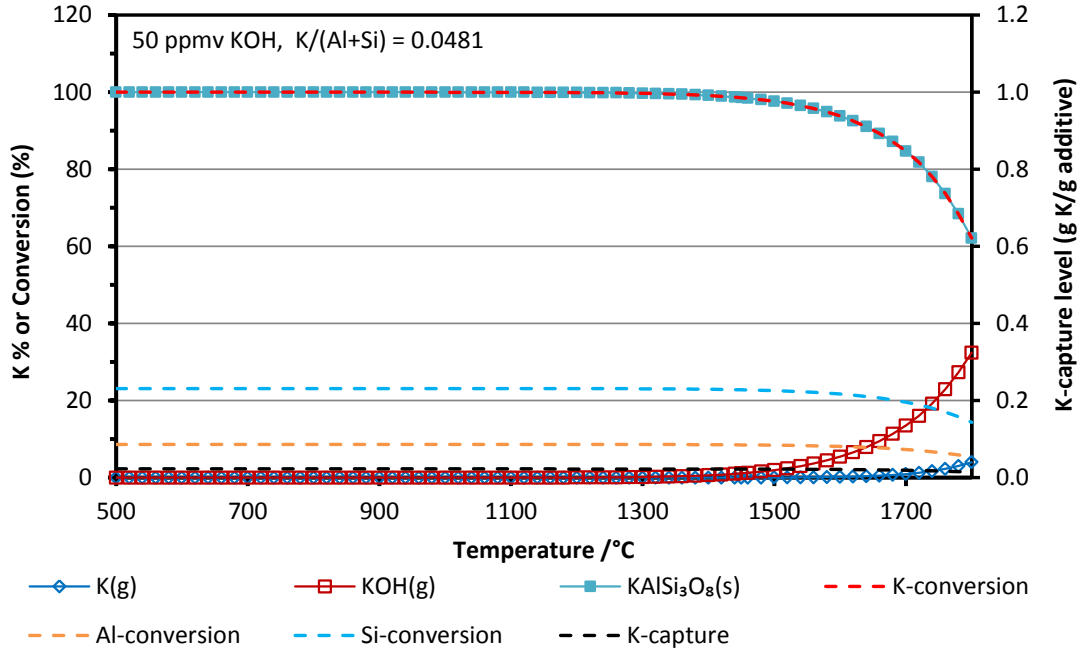

(A) 50 ppmv KOH, K/(Al+Si) =0.048

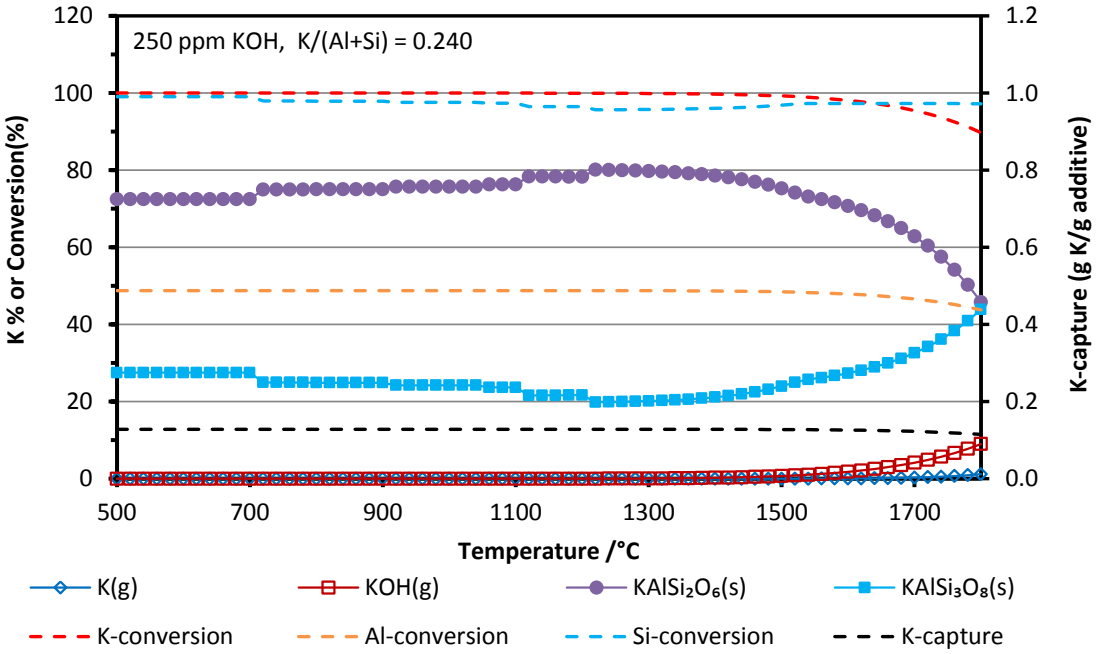

(B) 250 ppmv KOH, K/(Al+Si) =0.240

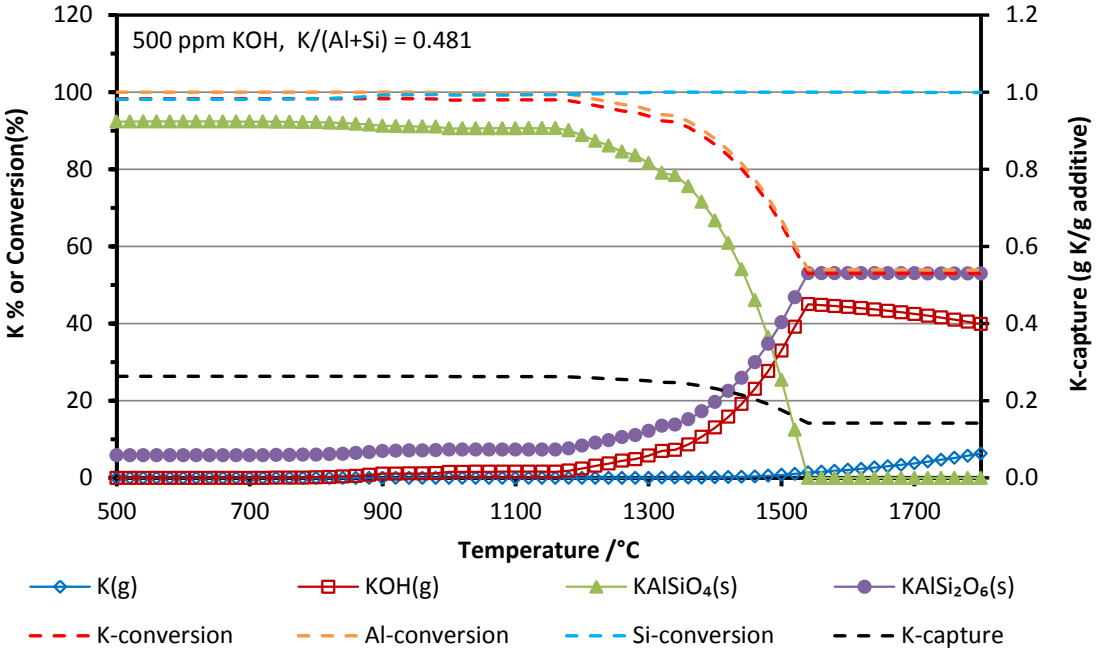

(C) 500 ppmv KOH, K/(Al+Si) =0.481

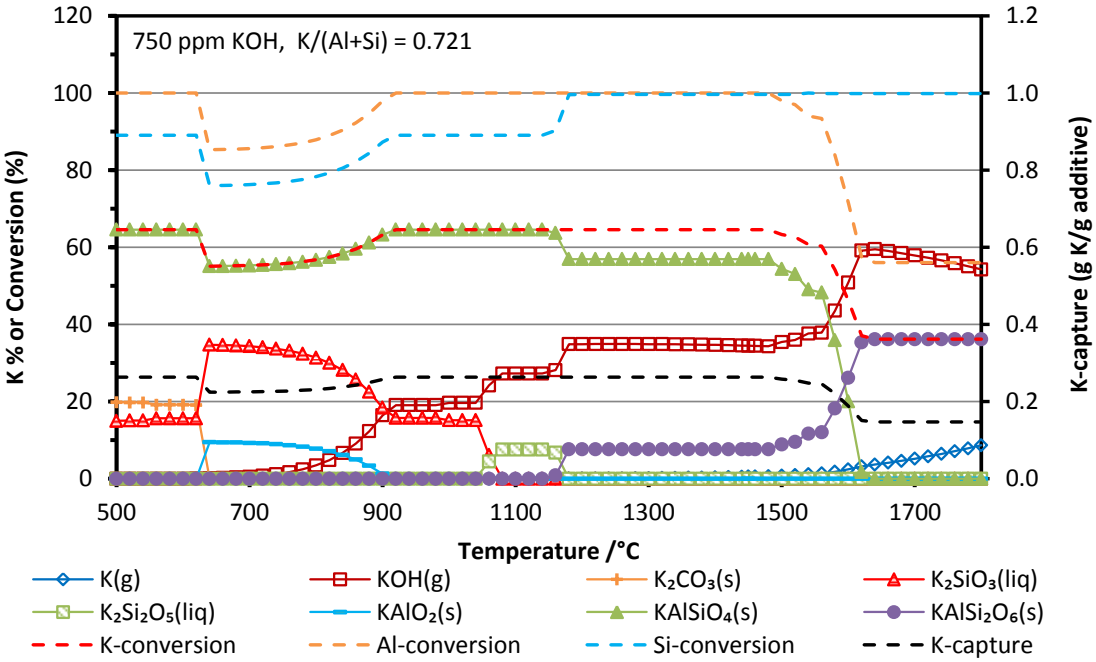

(D) 750 ppmv KOH, K/(Al+Si) =0.721

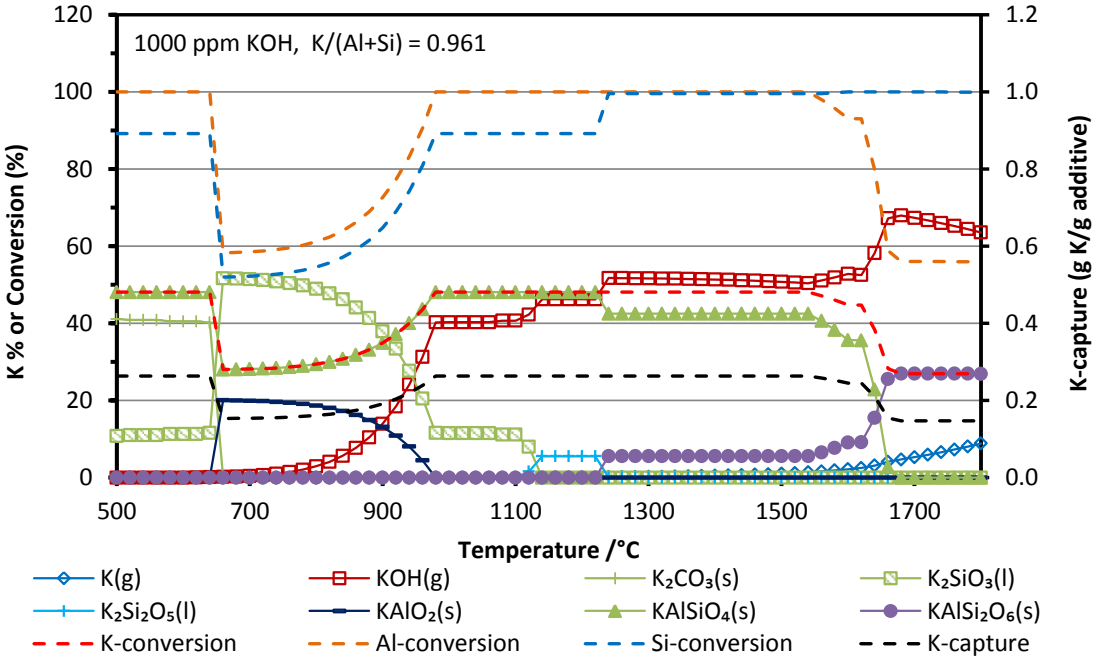

(E) 1000 ppmv KOH, K/(Al+Si) =0.961

Figure C-1. Equilibrium calculation results of KOH capture by kaolin.

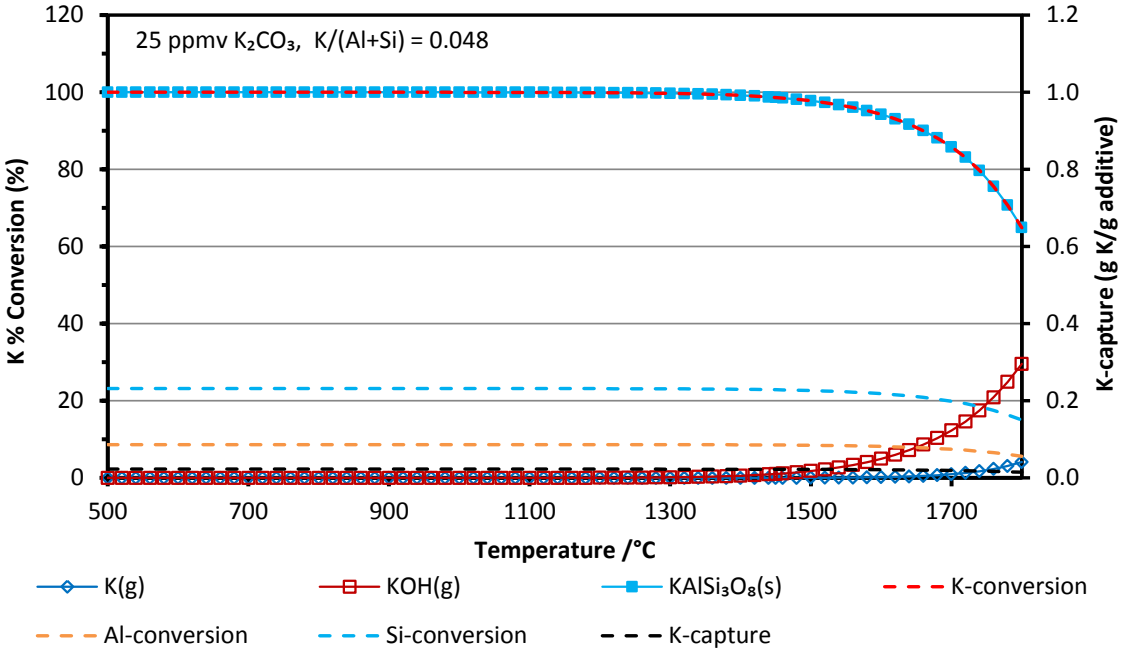

(A) 25 ppmv K_2CO_3, K/(Al+Si) = 0.048

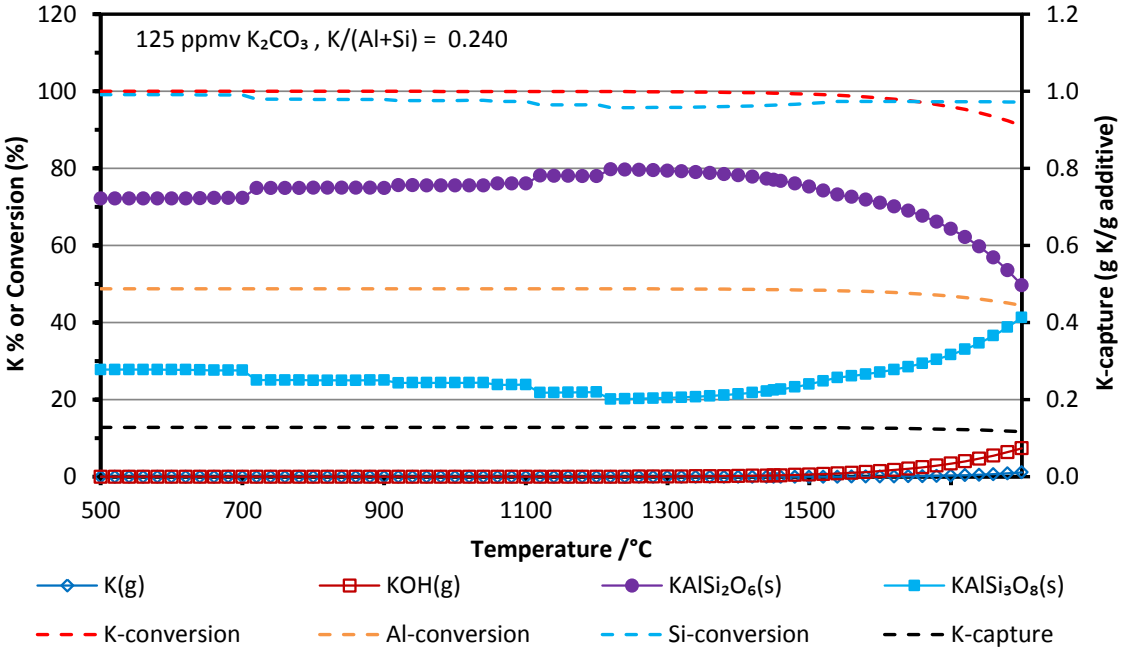

(B) 125 ppmv K_2CO_3, K/(Al+Si) = 0.240

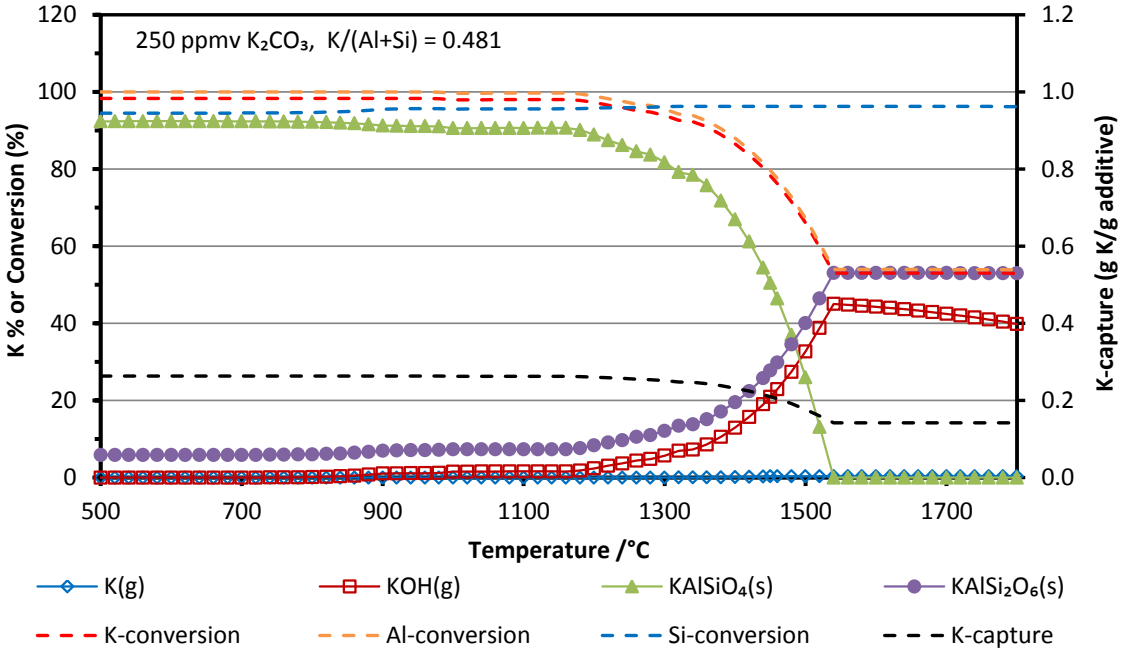

(C) 250 ppmv K_2CO_3, K/(Al+Si) =0.481

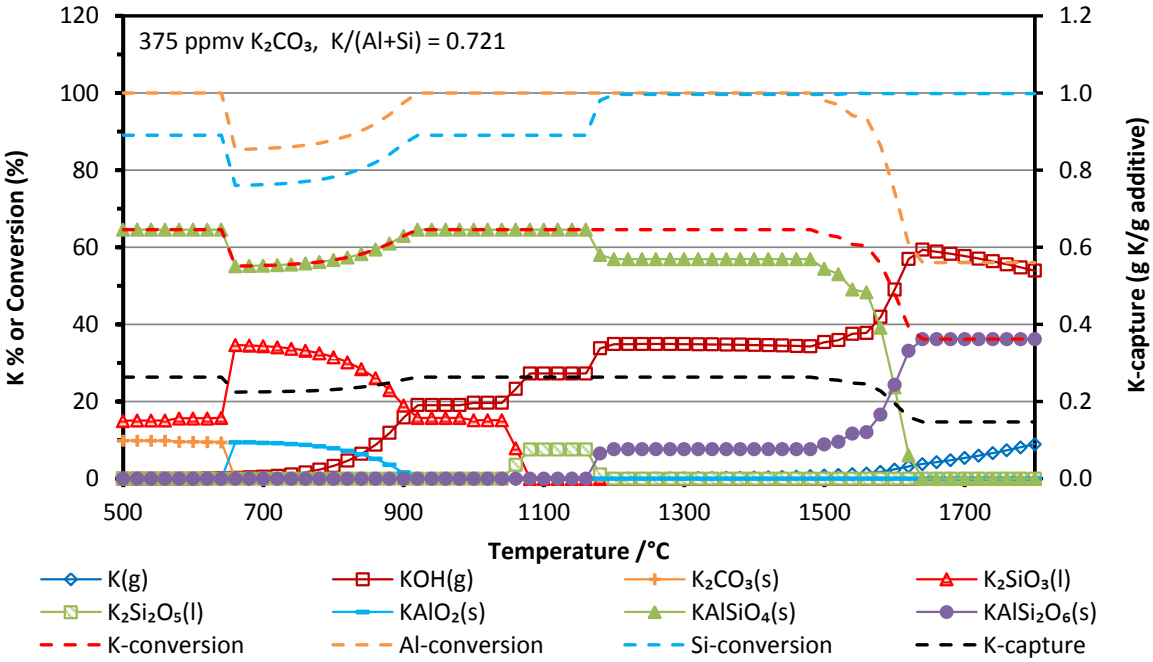

(D) 375 ppmv K_2CO_3, K/(Al+Si) =0.721

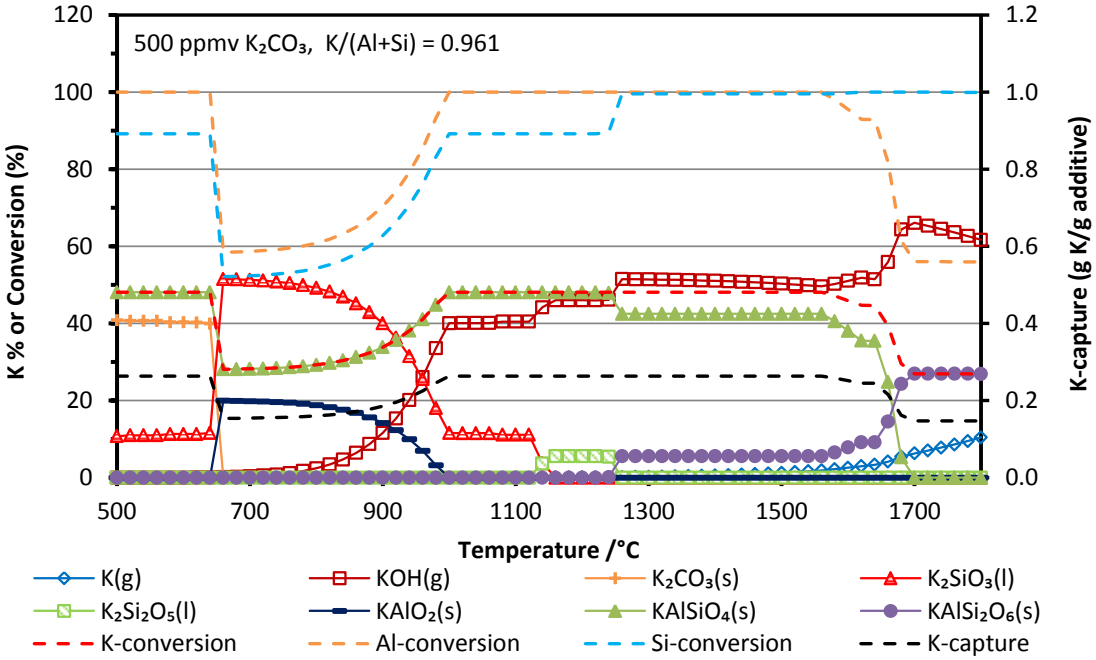

(E) 500 ppmv K_2CO_3, K/(Al+Si) =0.961

Figure C-2. Equilibrium calculation results of K_2CO_3 capture by kaolin.

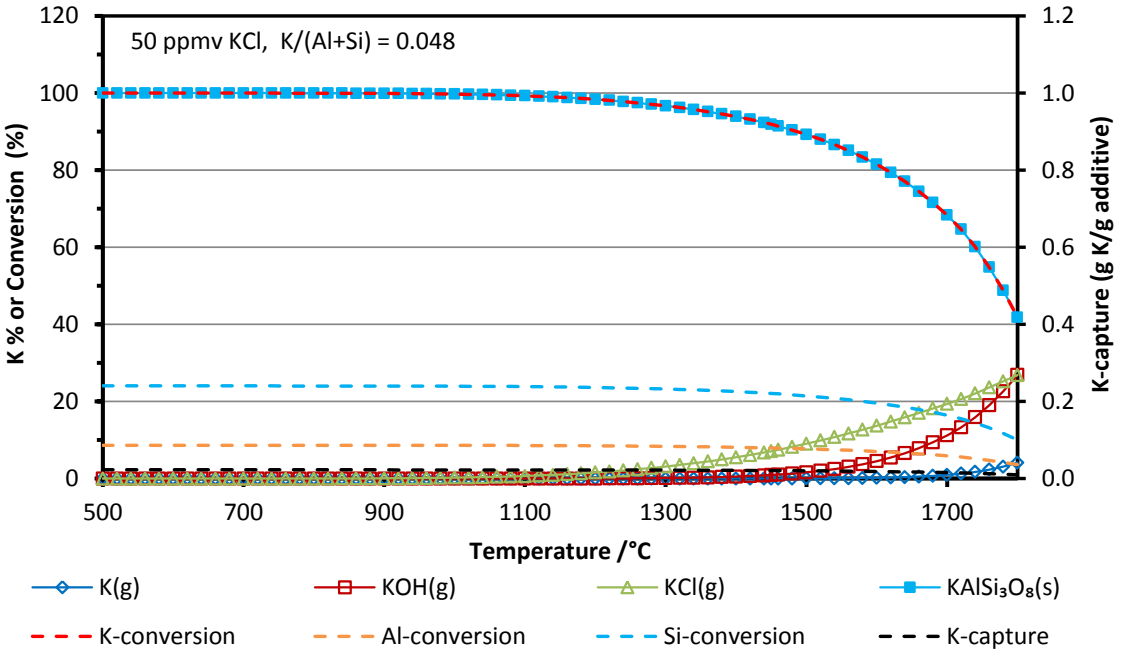

(A) 50 ppmv KCl, K/(Al+Si) =0.048

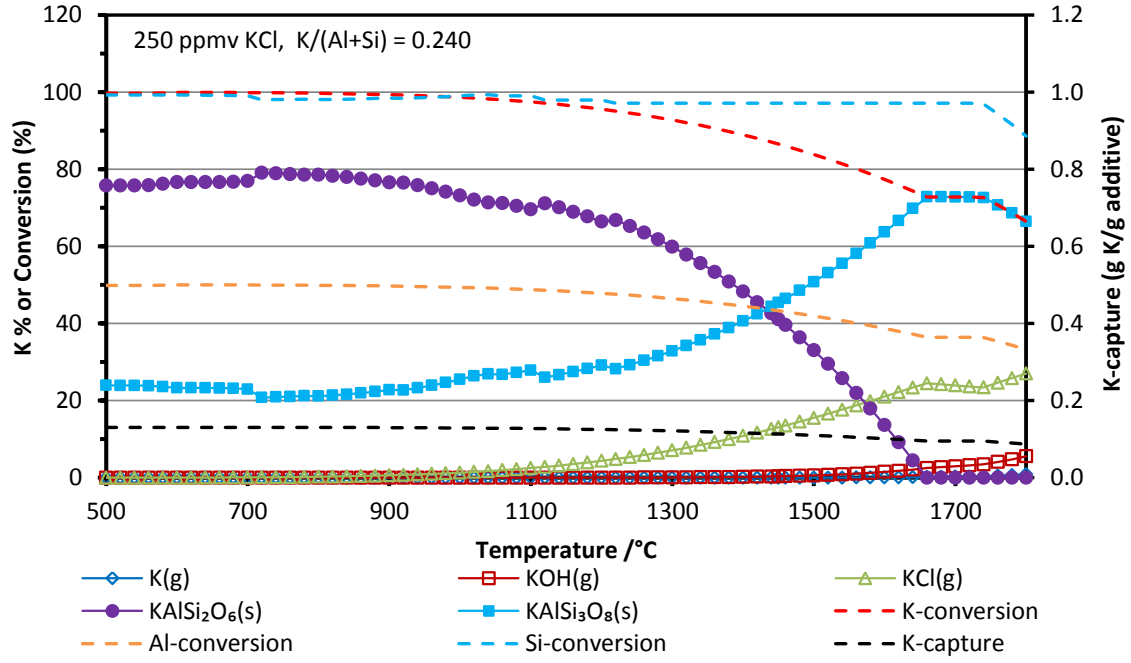

(B) 250 ppmv KCl, K/(Al+Si) =0.240

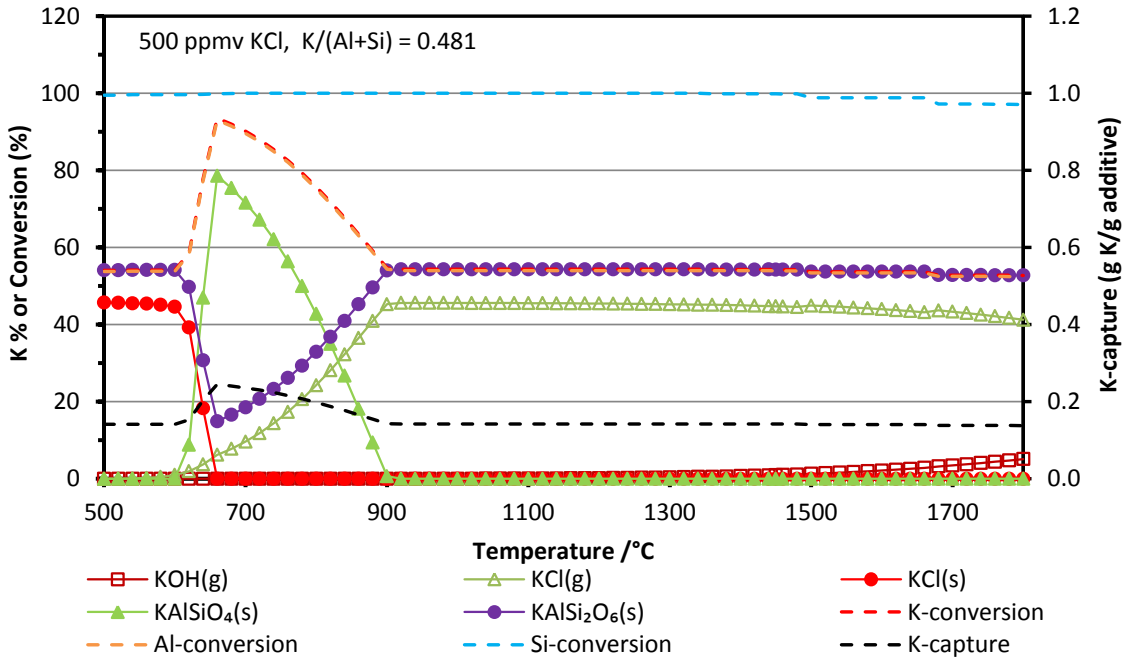

(C) 500 ppmv KCl, K/(Al+Si) =0.481

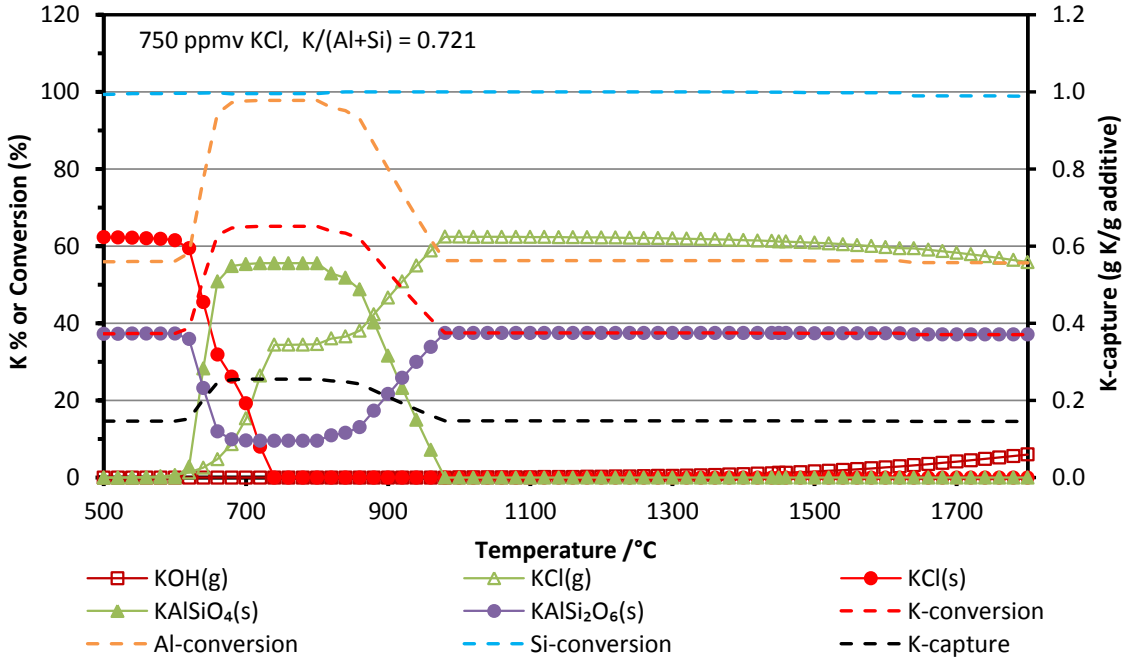

(D) 750 ppmv KCl, K/(Al+Si) =0.721

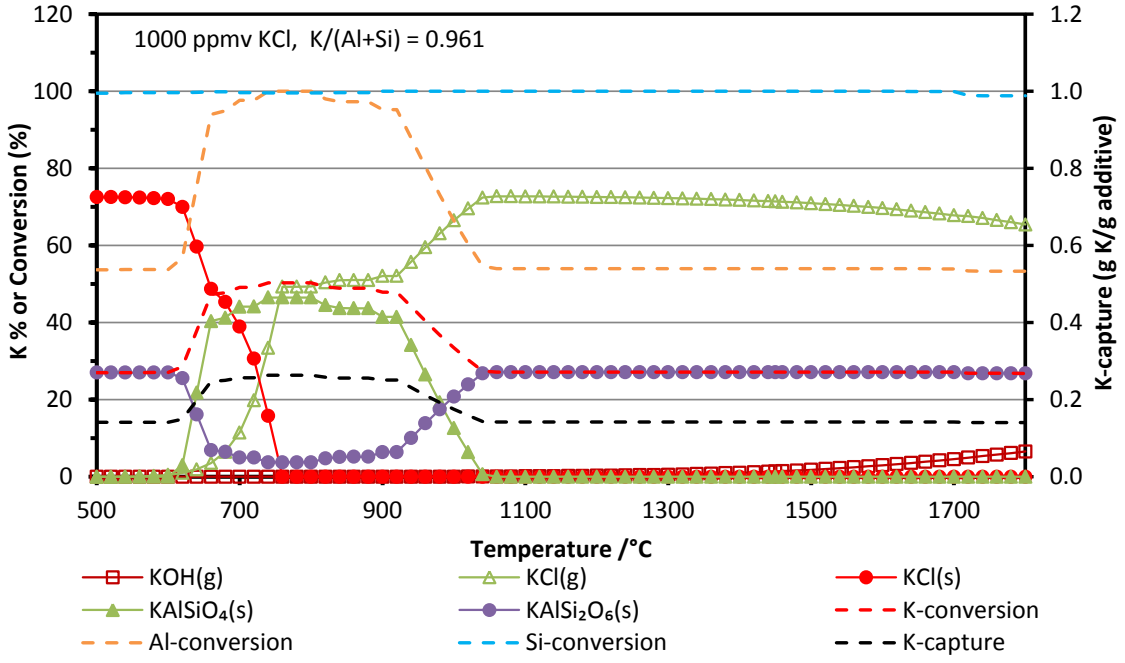

(E) 1000 ppmv KCl, K/(Al+Si) =0.961

Figure C-3. Equilibrium calculation results of KCl capture by kaolin.

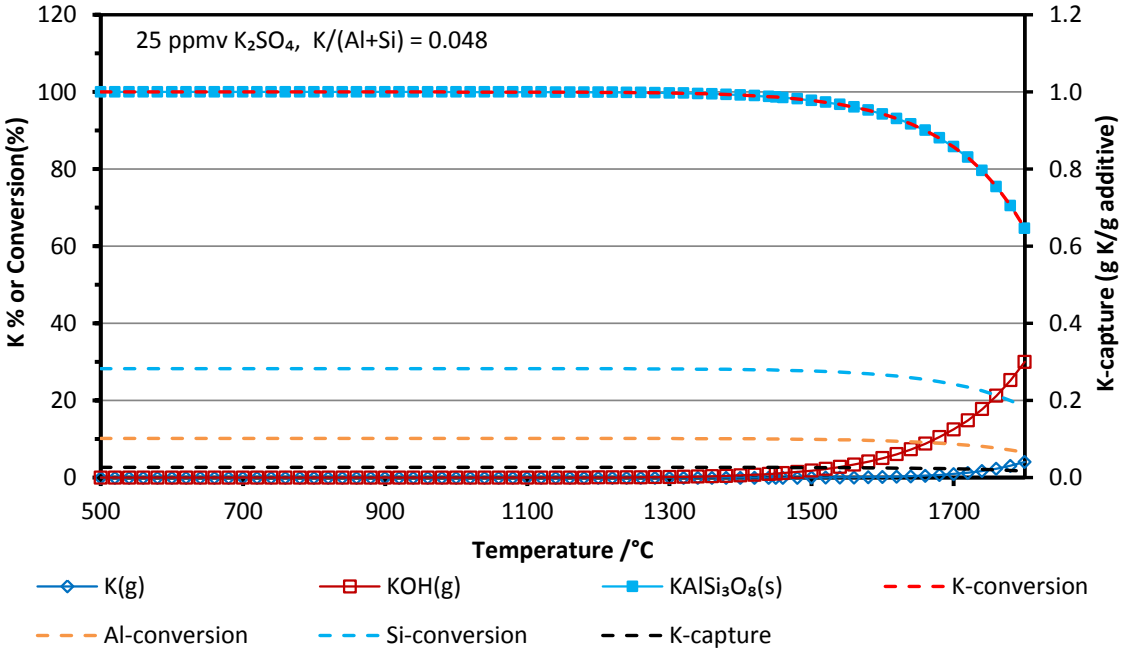

(A) 25 ppmv K_2SO_4, K/(Al+Si) =0.048

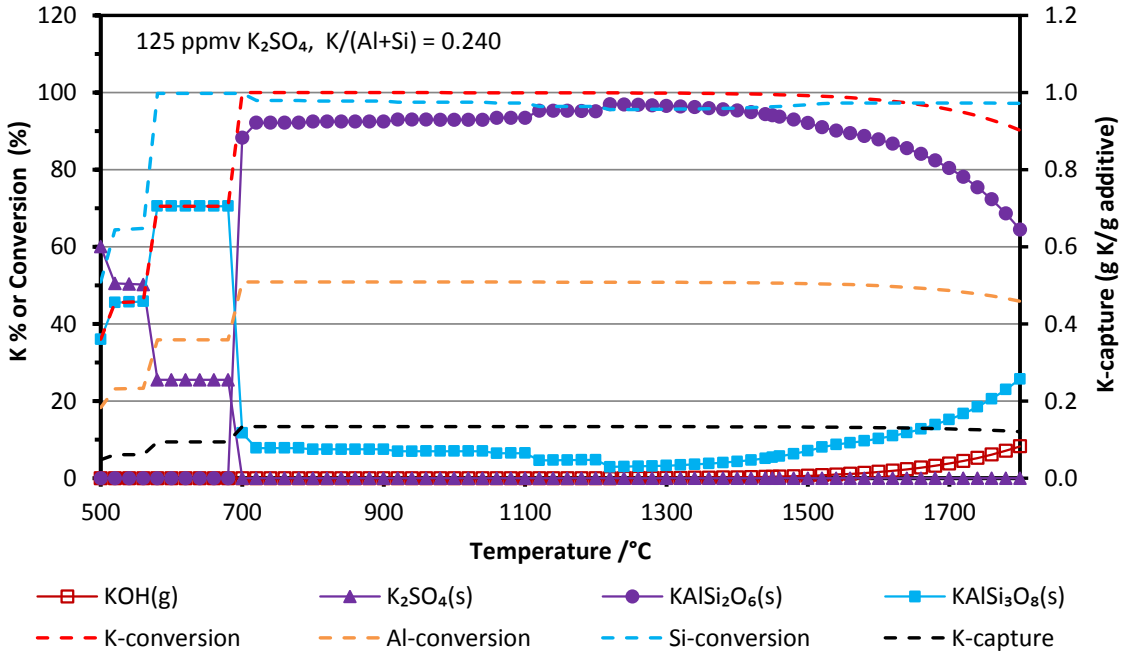

(B) 125 ppmv K_2SO_4, K/(Al+Si) =0.240

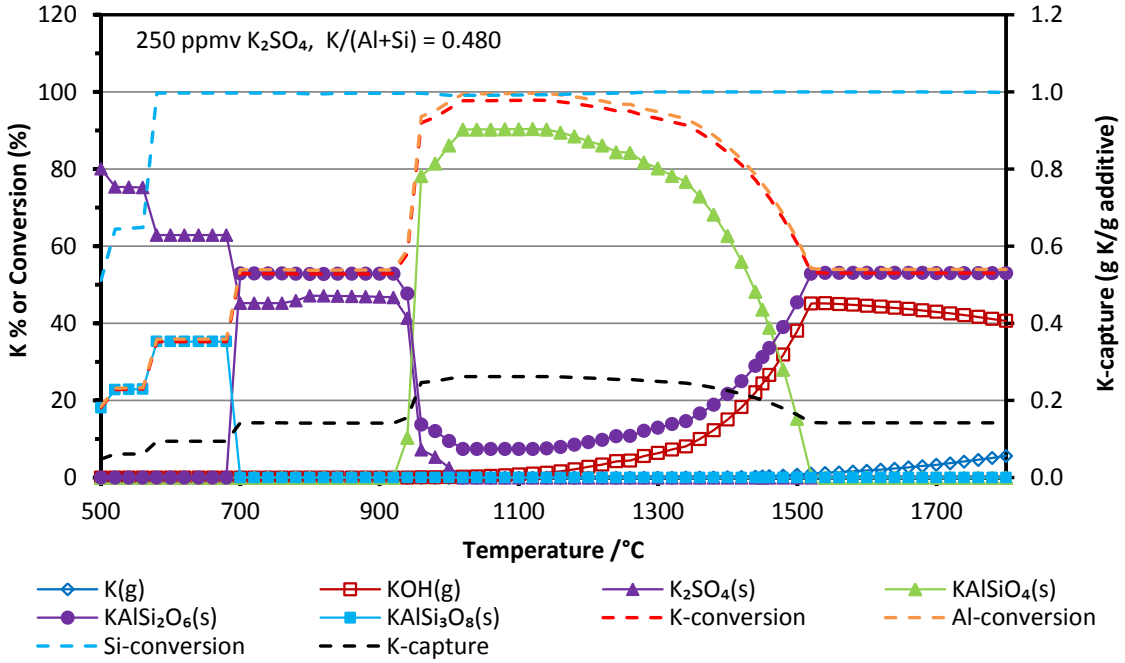

(C) 250 ppmv K_2SO_4, K/(Al+Si) =0.481

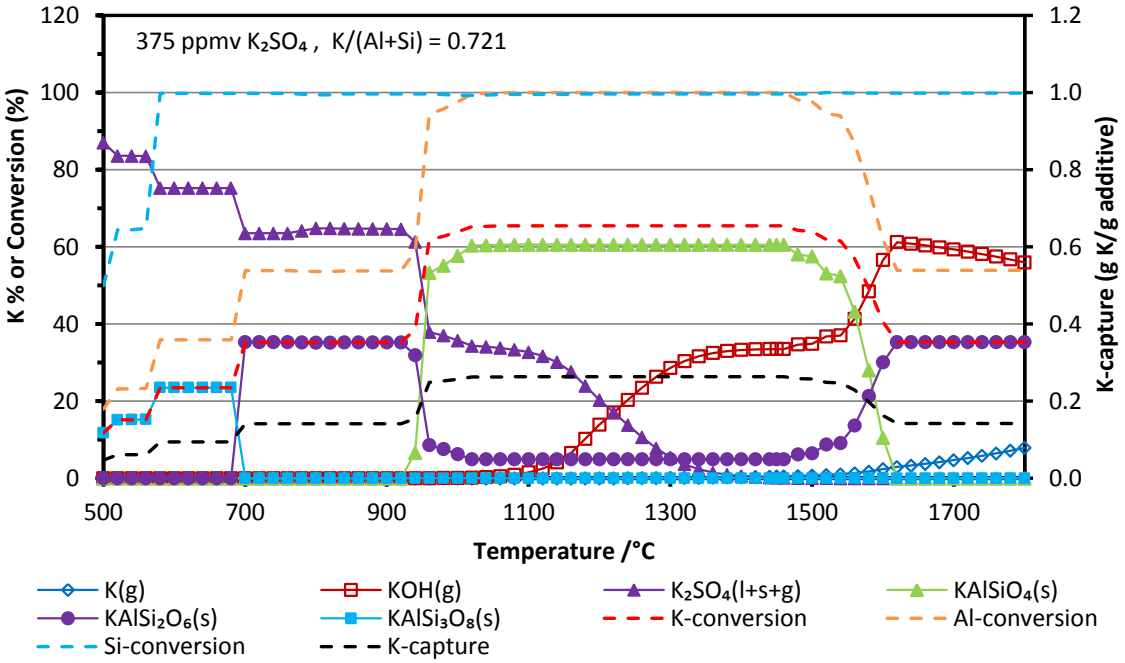

(D) 375 ppmv K_2SO_4, K/(Al+Si) =0.721

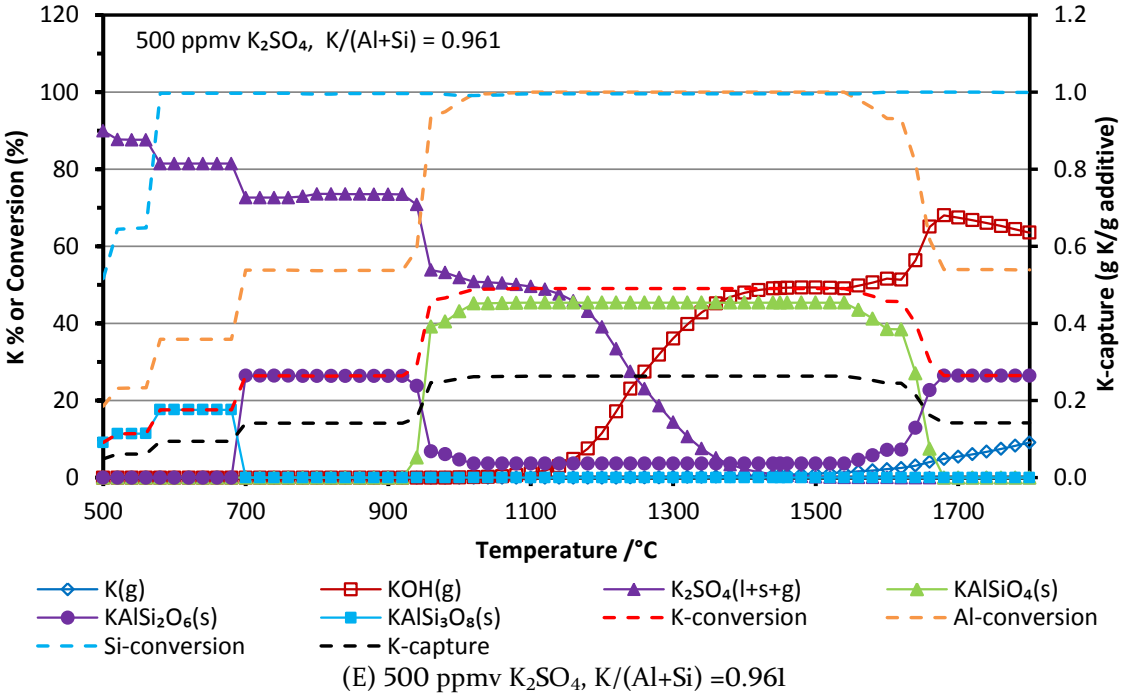

(E) 500 ppmv K_2SO_4, K/(Al+Si) =0.961

Figure C-4. Equilibrium calculation results of K_2SO_4 capture by kaolin.

Appendix D Equilibrium calculation of K-capture by coal fly ash

The equilibrium calculation results of KOH, K_2CO_3, KCl and K_2SO_4 capture by ASV2CFA0-32 (ASV2 coal fly ash 0-32 μm) at different temperature and different K-concentration are illustrated below.

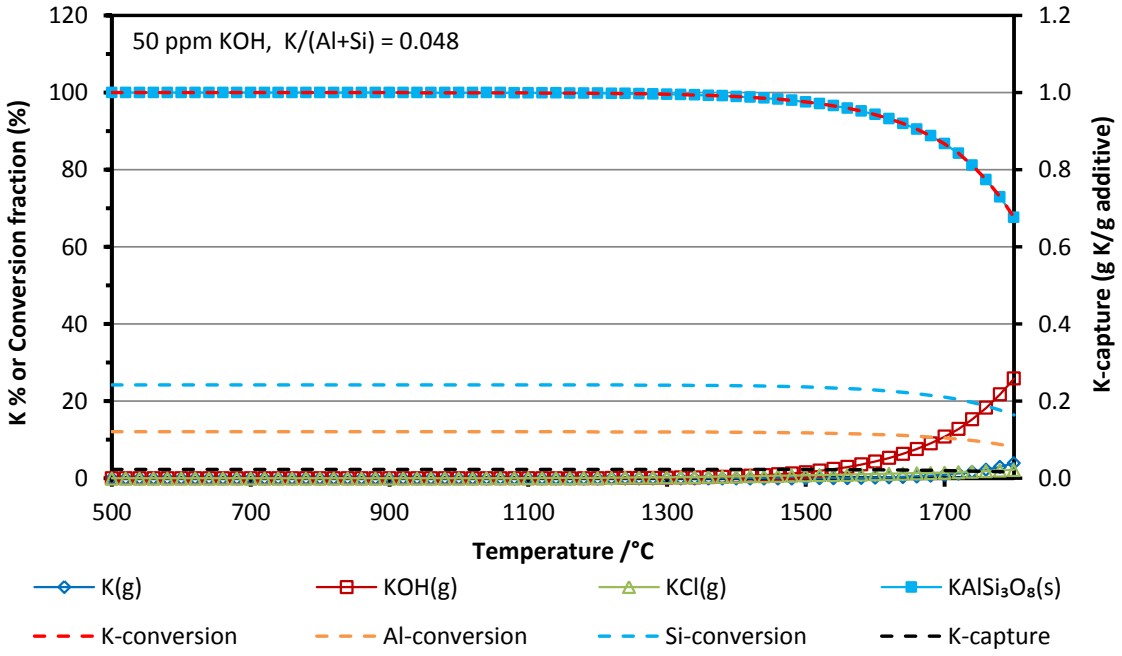

(A) 50 ppm KOH

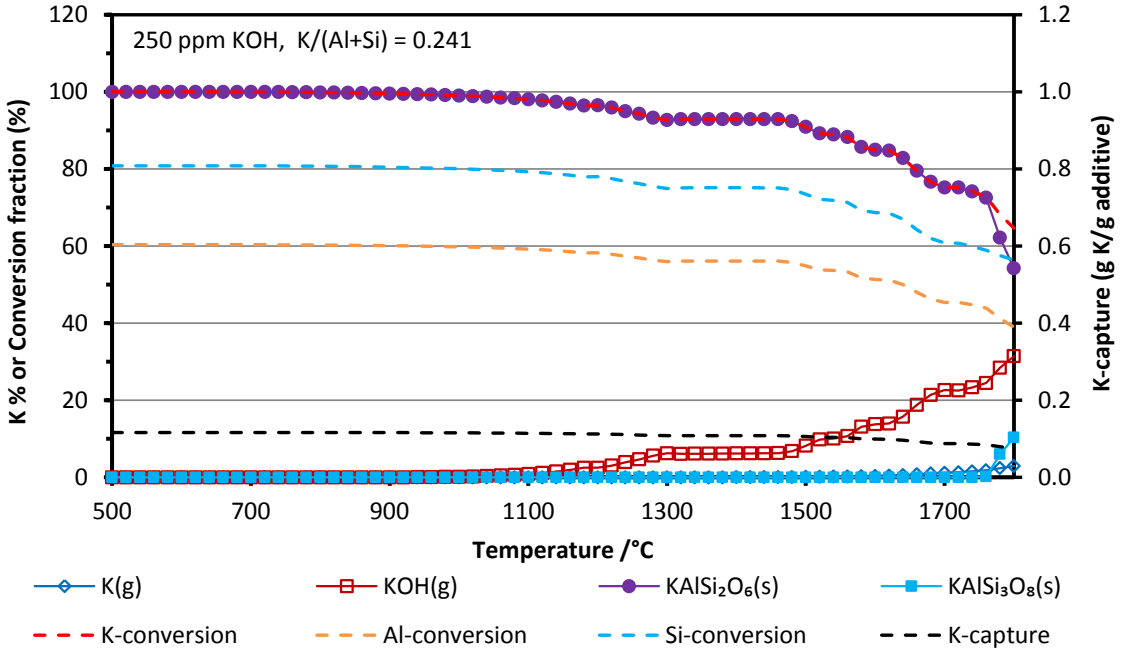

(B) 250 ppm KOH

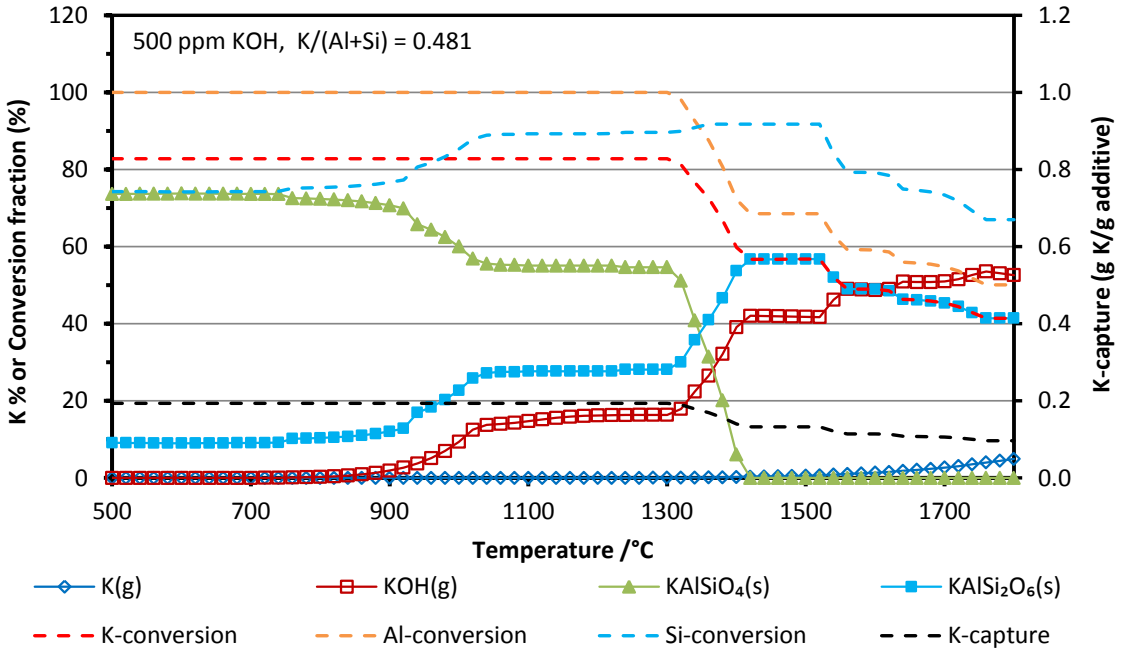

(C) 500 ppm KOH

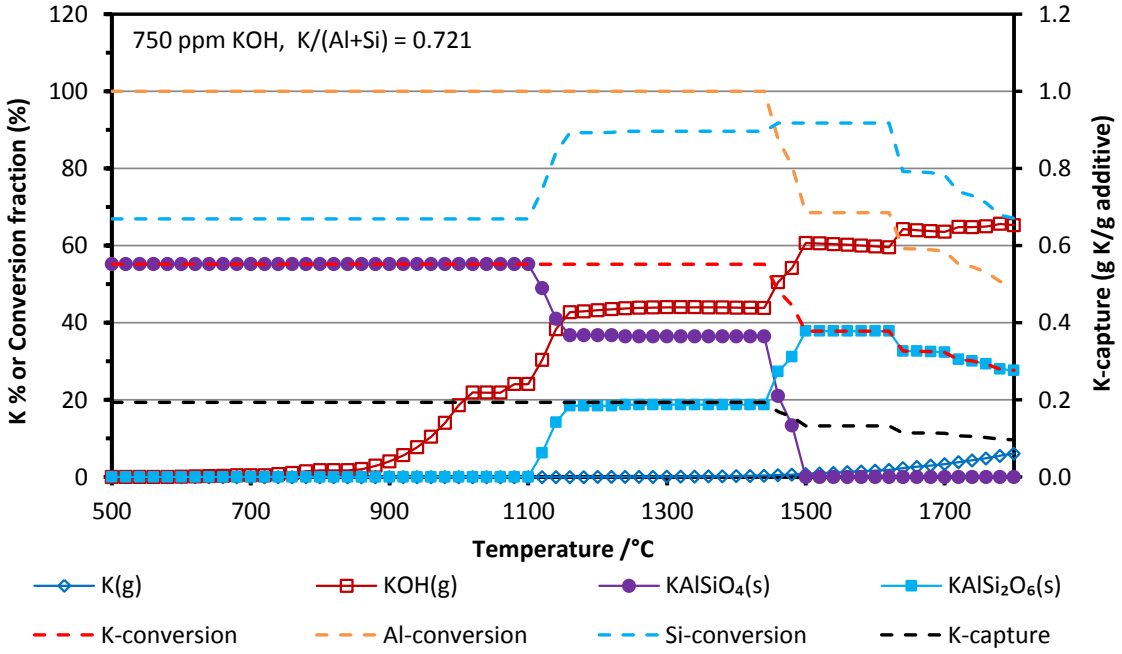

(D) 750 ppm KOH

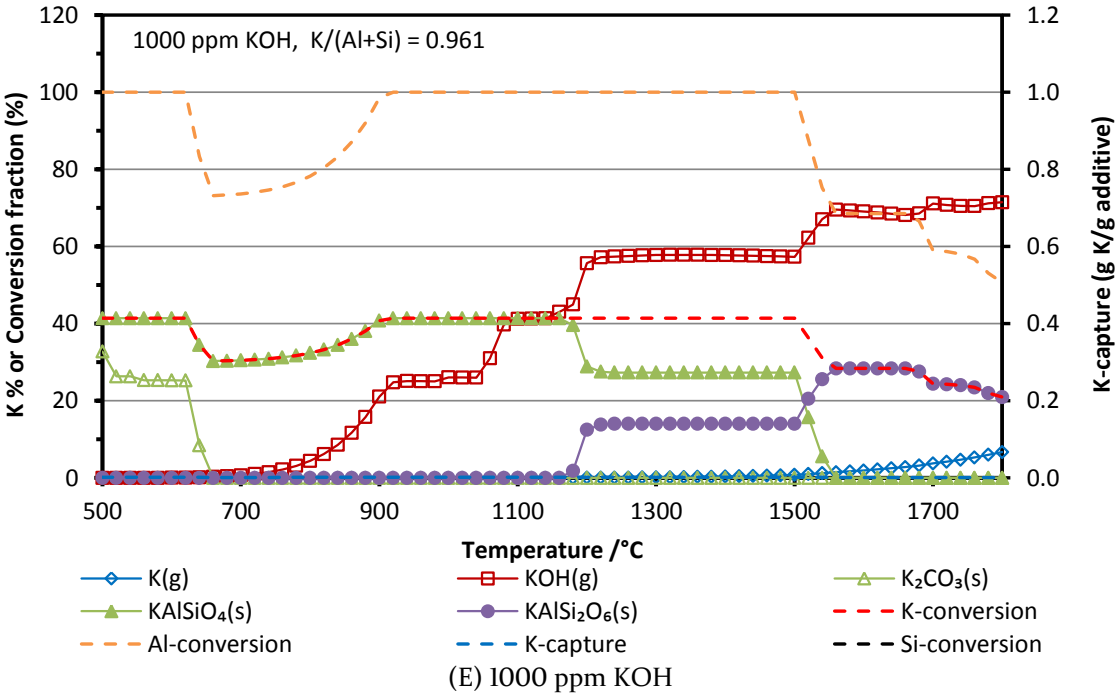

(E) 1000 ppm KOH

Figure D-1. Equilibrium calculation results of KOH capture by ASV2CFA0-32.

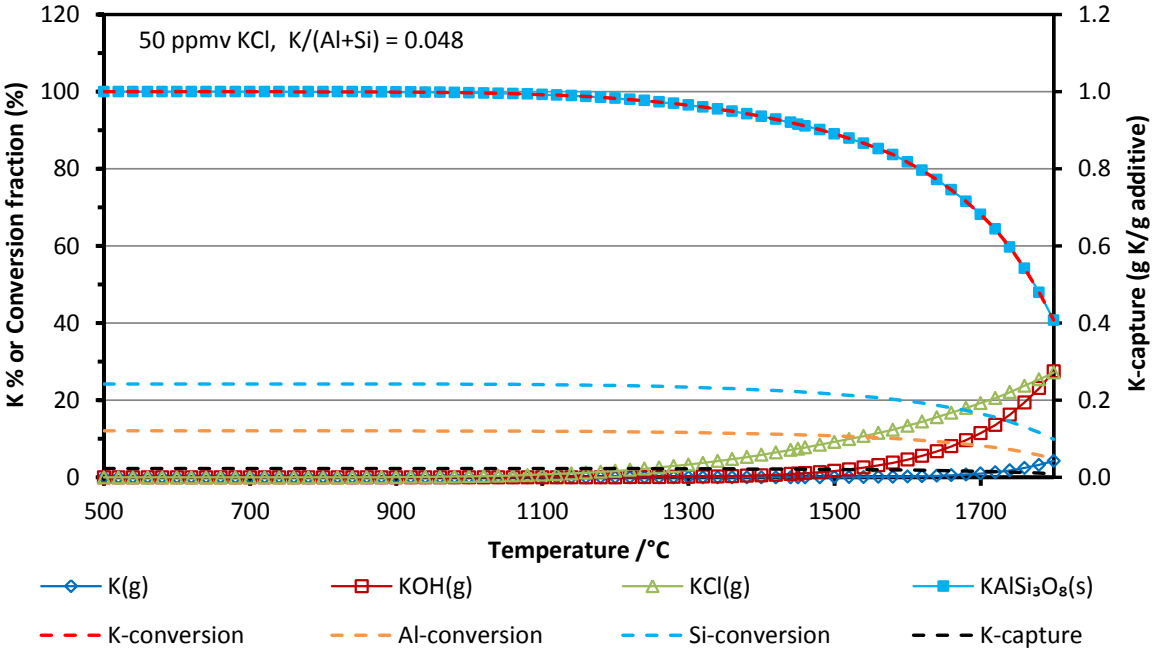

(A) 50 ppmv KCl, K/(Al+Si) =0.048

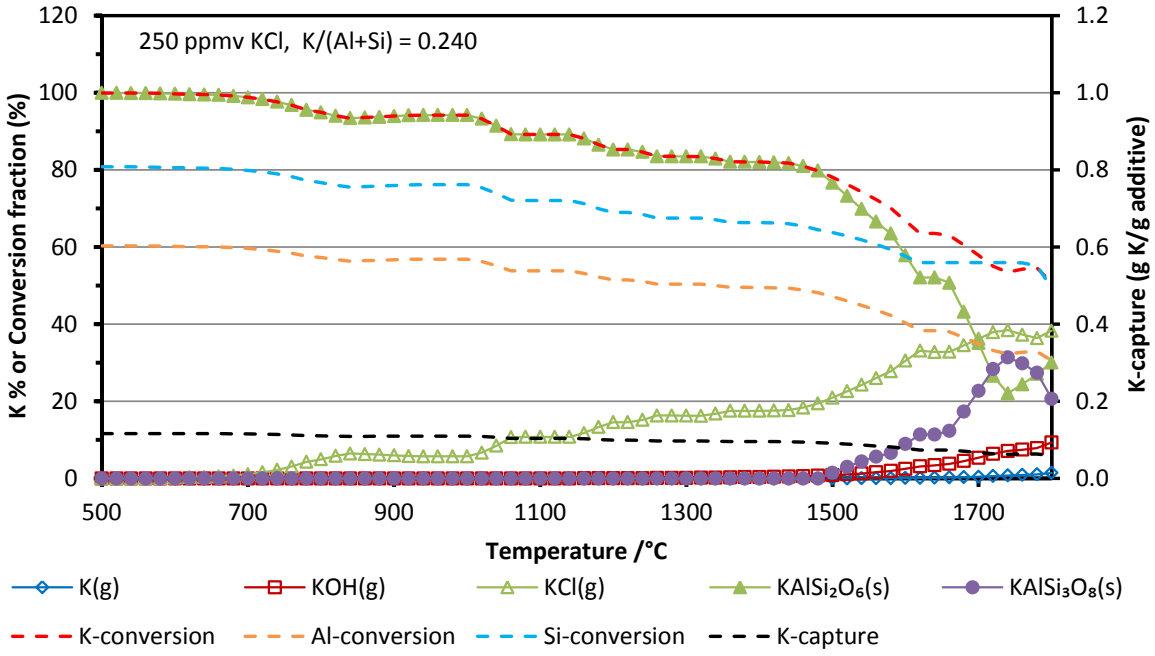

(B) 250 ppmv KCl, K/(Al+Si) =0.240

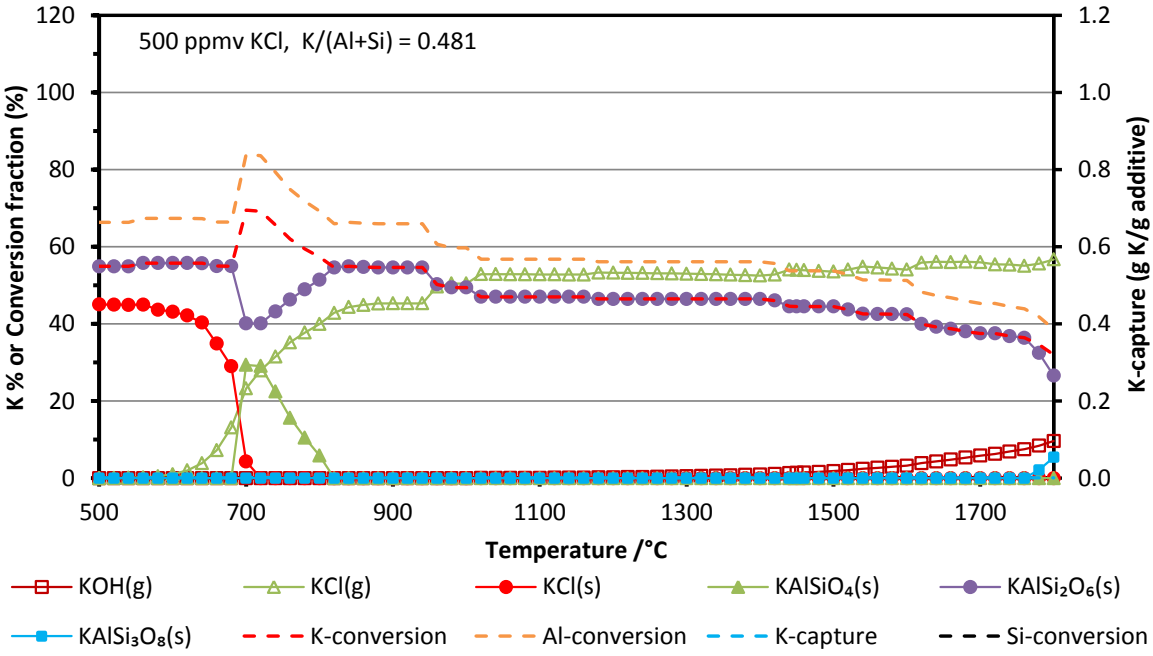

(C) 500 ppmv KCl, K/(Al+Si) =0.481

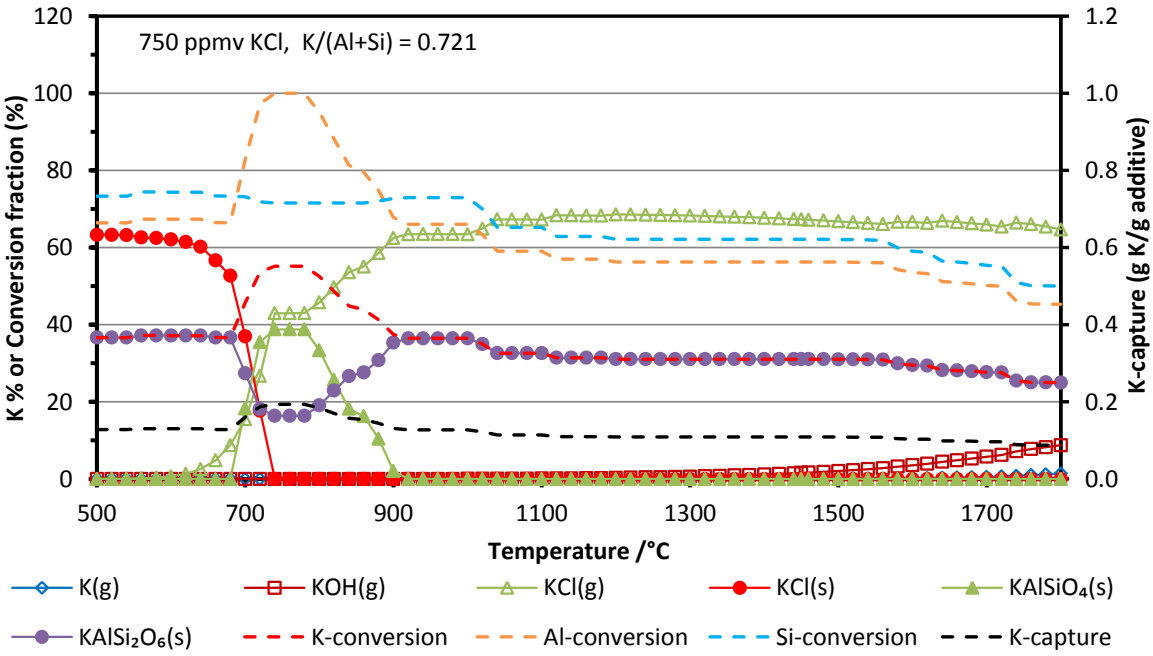

(D) 750 ppmv KCl, K/(Al+Si) =0.721

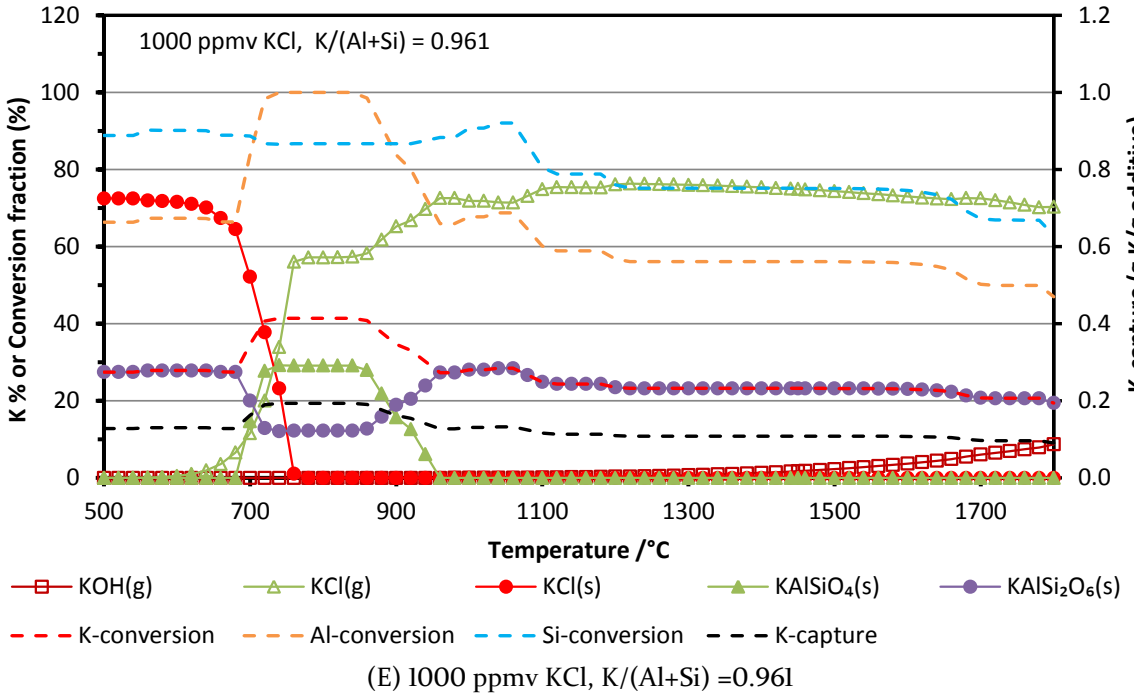

(E) 1000 ppmv KCl, K/(Al+Si) =0.961

Figure D-2. Equilibrium calculation results of KCl capture by ASV2CFA0-32.

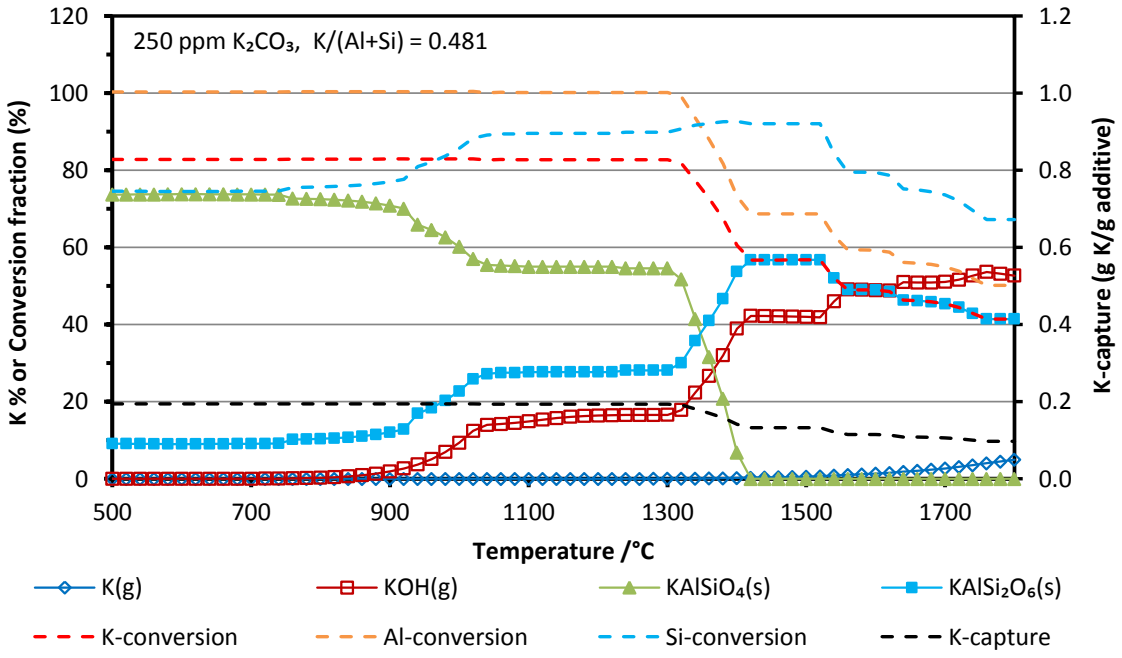

Figure D-3. Equilibrium calculation results of K_2CO_3 capture by ASV2CFA0-32. K_2CO_3 concentration in flue gas was 250 ppmv (K-concentration in flue gas was 500 ppmv).

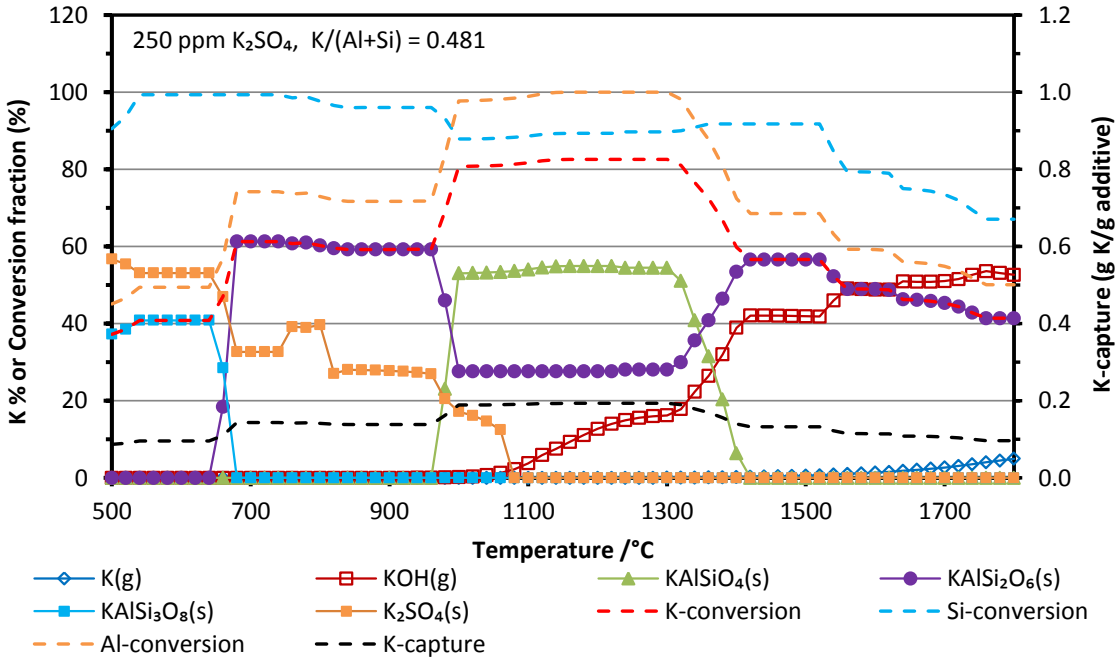

Figure D-4. Equilibrium calculation results of K_2SO_4 capture by ASV2CFA0-32. K_2SO_4 concentration in flue gas was 250 ppmv (K-concentration in flue gas was 500 ppmv).

Department of Chemical and Biochemical Engineering - CHEC
Technical University of Denmark
Søltofts Plads, Building 229
2800 Kgs. Lyngby
Denmark
Phone: +45 45 25 28 00
Web: www.kt.dtu.dk